Development of novel approaches for industrial fermentation of menaquinone-7

A thesis

submitted in fulfilment

of the requirements for the degree of

Doctor of Philosophy

at

The University of Waikato

by

Dinali N. A. Ranmadugala

THE UNIVERSITY OF
WAIKATO
Te Whare Wānanga o Waikato

2018

Abstract

Vitamin K, an anti-haemorrhagic factor discovered by the Danish nutritional biochemist Henrik Carl Peter Dam in 1929, is capable of correcting dietary-induced bleeding disorders in chickens. It is essential for blood coagulation, and therefore must be supplied in the diet. Menaquinones (MK) together with phylloquinone (PK) fall under the common name 'vitamin K'. Recent studies show that dietary intake of menaquinones results in more health benefits than phylloquinone. Menaquinone-7 (MK-7) plays an important role in maintaining human health in the liver, bone and arterial vessels with potential to prevent osteoporosis and cardiovascular diseases as well as cancer. Therefore, MK-7 can be taken as the obvious choice for the prevention of these health complications.

MK-7 is produced industrially by a fermentation process of *Bacillus subtilis* at low concentrations. To date, there have been several attempts to improve MK-7 yield via optimising the fermentation media, genetic mutation of *Bacillus subtilis* and reducing downstream processing steps. Despite this progress, industrial production of MK-7 has been difficult, mainly due to biofilm formation, low MK-7 production by *Bacillus subtilis* and the presence of so many tedious unit operations in the process. As a result, the price of MK-7 is currently US$5 million/kg. It appears worthwhile to develop novel strategies to address the current MK-7 production challenges. The main goal of the current research was, therefore, to develop a novel cost-effective fermentation process by eliminating biofilm formation while enhancing MK-7 production and reducing the fermentation process steps.

In combating biofilm formation in *Bacillus subtilis* fermentation, a major challenge was to adopt strategies which would maintain the viability of the bacterial cells as required by the fermentation process. In this regard, as a first step, a nanobiotechnological approach was taken in which superparamagnetic iron oxide

nanoparticles (Fe_3O_4) were used to decorate *Bacillus subtilis* cells. In comparison to naked iron oxide nanoparticles, iron oxide nanoparticles coated with 3-aminopropyltriethoxysilane (IONs@APTES) significantly reduced the adherence and pellicle biofilm biomass of *Bacillus subtilis* in a concentration-dependent manner without affecting the growth and viability of *Bacillus subtilis*. Further, the research embodied in this thesis also addresses the low MK-7 production by immobilising *Bacillus subtilis* cells using IONs@APTES. Immobilisation of *Bacillus subtilis* cells with IONs@APTES significantly enhanced the MK-7 production, implying that binding of IONs@APTES to *Bacillus subtilis* cells might have changed the state or composition of the cell membranes resulting in enhanced production and secretion of MK-7 to the fermentation medium. In addition to a strategy that minimised bacterial cell attachment and subsequent biofilm formation, the effect of a biofilm detachment strategy was also investigated. As nutrient conditions in the medium can greatly influence biofilm detachment, nutrient components which would interfere with the structural integrity of biofilms and bring about biofilm detachment were investigated by supplementing the medium with salts and urea. In this study the optimum conditions to minimise biofilm formation while maximising MK-7 production was determined by response surface optimisation. These investigations finally led to an optimum fermentation medium for minimum biofilm formation and maximum MK-7 production which consists of 5% (*w*/*v*) yeast extract, 18.9% (*w*/*v*) soy peptone, 5% (*w*/*v*) glycerol, 0.05% (*w*/*v*) K_2HPO_4, 0.32% (*w*/*v*) $CaCl_2$, 0.10% (*w*/*v*) urea and 200 µg/mL IONs@APTES. A ~ 47% reduction in biofilm biomass and ~ 16% increase in MK-7 production was observed after 60 hours of fermentation when the medium was supplemented with 0.32% (*w*/*v*) $CaCl_2$, 0.10% (*w*/*v*) urea and 200 µg/mL IONs@APTES in comparison to the medium without added $CaCl_2$, urea and IONs@APTES. This was found

useful as a non-antibiotic antifouling strategy which would permit the growth and viability of bacterial cells in the fermentation process while minimising biofilm formation and maximising MK-7 production. Using this medium, the feasibility of designing a milking process for enhancing MK-7 productivity was assessed. Initial studies involved selecting biocompatible organic solvent/s for milking MK-7. Milking MK-7 with *n*-hexane proved to be an effective strategy to enhance the total MK-7 production by ~ 1.7-fold in *subtilis* fermentation without compromising the bacterial cell viability in comparison to non-milking conditions. Not only did the total MK-7 increase by ~ 1.7-fold, but the maximum total MK-7 production also reached earlier *i.e*. within 72 hours in comparison to previously recorded liquid state fermentation studies for MK-7 production, which is important from a commercial point of view. In addition, a novel, accurate, reliable and high throughput MK-7 analysis protocol is also presented in the thesis. Hence, by examining and integrating a range of strategies, this thesis provides a feasible approach for industrial production and analysis of MK-7.

Dedication

This dissertation, together with all my academic achievements, are dedicated to my mother, a strong and gentle woman who taught me to trust in God, without whom none of my success would be possible, and to the loving memory of my father for being my guardian throughout my education.

Acknowledgements

My deepest gratitude goes to my chief supervisor, Dr Aydin Berenjian, for giving me the opportunity to conduct this research work and driving me to complete this on time.

I would also like to thank my co-supervisors, Associate Professor Merilyn Manely-Harris and Dr Alireza Ebrahiminezhad, for giving me feedback on my work. Their expertise was an inspiration to succeed and do better in my research. The contribution of Professor Younes Ghasemi and Dr Alireza Ebrahiminezhad by characterising nanoparticles is greatly appreciated.

I am deeply indebted to Ms Helen Turner, Dr Judith Burrows, Dr Barry O'Brien, Dr Megan Grainger, Mrs Jennie Stockdill, Dr Lisa Lee and Mr Daniel Bernstein for their help in my research and for making this journey possible.

I would also like to acknowledge the support of a University of Waikato Doctoral Scholarship over the three years of my study.

A very special thanks go to Ms Cheryl Ward for all her help in referencing and formatting my thesis as well as all the journal articles. I also thank Ms Nikki Crutchly for proofreading my thesis.

My sincere thanks to all my friends at the University of Waikato.

Last but not least, I thank my husband, my mother, and my two daughters for always being with me during the difficult moments during the journey.

Table of Contents

List of Figures

List of Tables

List of Abbreviations

ANOVA	Analysis of Variance
APTES	3-aminopropyltriethoxysilane
βTA	β-2-thienylalanine
CCD	Central Composite face Design
CLSM	Confocal Laser Scanning Microscopy
CVSM	Crystal Violet Staining Method
DAHP	3-deoxy-D-arabino-heptulosonate-7-phosphate
DHNA	1, 4-dihydroxy-2-naphthoate
DLVO	Derjaguin-Landau-Verwey-Overbeek
EPS	Exopolysaccharide
FTIR	Fourier Transformed Infrared spectroscopy
Gla	ɤ- carboxylase glutamate
HNA	1-hydroxy- 2- naphthoic acid
HPLC	High Performance Liquid Chromatography
ION	Iron Oxide Nanoparticle
IONs@APTES	Iron Oxide Nanoparticles coated with APTES
LB	Luria-Bertani
LC-APCI-MS	Liquid Chromatography-Atmospheric Pressure Chemical Ionisation/Mass spectrometry
LSF	Liquid State Fermentation
mFP	*m*-fluoro-D, L-phenylalanine
MK	Menaquinone
MK-7	Menaquinone-7
MK-4	Menaquinone-4
NP	Nanoparticles
NTG	*N*-methyl-*N*-nitro-*N*-nitroso-guanidine
OD	Optical Density
pFP	*p*-fluoro-D, L-phenylalanine
PGA	poly ɤ- glutamate
PK	Phylloquinone
QS	Quorum Sensing
ROS	Reactive Oxygen Species
RSM	Response Surface Methodology

RSD	Relative Standard Deviation
SEM	Scanning Electron microscopy
SSF	Solid State Fermentation
TEM	Transmission Electron Microscopy
VSM	Vibrating Sample Magnetometer
XRD	X-Ray Powder Diffraction

Chapter 1

Introduction

1.1 Motivation

In the recent past, the high demand for MK-7 has proven the importance of the development of novel approaches for MK-7 production. Menaquinones (vitamin K2) comprise a class of therapeutic agents that significantly improve the treatment options for a variety of diseases in addition to their role in blood clotting. MK-7 especially is extensively used as a therapeutic tool for the treatment of cardiovascular diseases (Gast *et al.*, 2009), osteoporosis (Shiraki *et al.*, 2000; Yamaguchi *et al.*, 2000), rheumatoid arthritis (Abdel-Rahman *et al.*, 2015) as well as cancer (Shi *et al.*, 2018). In this regard, there is a positive outlook for MK-7 in the dietary supplement, functional food and beverage industries (Arai, 2007; Sumi, 2004b), and it is reported that the vitamin K market size may witness significant gains over the period of 2016–2024 (Global Market Insights, 2018). MK-7 can be produced via fermentation processes mainly by *Bacillus subtilis* species. Microbial synthesis of MK-7 is, however, influenced by many factors inherent to the process that can affect the yield and operation cost. Often, in liquid state fermentation of MK-7, which is the common cell culture method for the majority of industrial MK-7 bioprocesses, biofilm formation is still a major obstacle for efficient and economical production of MK-7 on an industrial scale (Berenjian *et al.*, 2015). Although it has been observed that biofilm formation is a common mode in the bacterial life cycle and MK-7 production shows a liner dependency on biofilm formation (Berenjian *et al.*, 2013), biofilm formation is a key event which leads to mass transfer resistance and costly periodic cleaning which ultimately results in a decrease in bioreactor productivity and higher production costs (Applegate &

Bryers, 1991). Therefore, finding ways to reduce biofilm formation would enhance the performance of the bioreactor.

Besides biofilm formation, another problem in MK-7 production has been attributed to low MK-7 concentration (Berenjian *et al.*, 2015). Even though progress has been made in liquid and solid state fermentation through optimisation of nutrient and operating conditions which led to the improvement of the MK-7 production (Berenjian *et al.*, 2011), the optimum nutrient components and operating conditions also enhanced biofilm formation (Berenjian *et al.*, 2013). Therefore, none of the previous approaches have been able to strike a balance between these two opposing demands. In addition, the presence of a large number of downstream processing steps complicated the production process.

The main purpose of the present study was, therefore, to improve the productivity of the MK-7 production process through developing novel strategies to minimise biofilm formation while maximising the MK-7 production as well as reducing the downstream processing steps involved in the MK-7 production process.

1.2 Overview of the thesis

This thesis is comprised of 10 chapters and is organised as follows: **Chapter 1** contains the introduction and research objectives.

Chapter 2 gives a comprehensive literature review on vitamin K and its health benefits, highlighting the importance of MK-7, an overview of MK-7 production, current problems in the MK-7 production process and novel approaches for addressing these issues. This chapter emphasises the applicability of biocompatible nanoparticles for addressing the problem of biofilm formation, low MK-7 production and many downstream processing steps in addition to milking of MK-7 with biocompatible organic solvents to improve the productivity of the fermentation

process.

Chapter 3 describes the materials and methods applied in this research to provide the reader with a more detailed background.

Chapter 4 describes synthesis and characterisation of iron oxide nanoparticles. In this chapter, synthesis of iron oxide nanoparticles through chemical co-precipitation and post-synthesis surface functionalisation of iron oxide nanoparticles with 3-aminopropyltriethoxysilane (APTES) followed by determination of their structure and magnetic properties are described.

In **Chapter 5** a novel approach to minimise bacterial surface attachment and subsequent biofilm formation through the application of surface functionalised iron oxide nanoparticles is discussed. Reducing bacterial attachment and increasing detachment are two effective strategies that can be applied to mitigate the biofilm formation while maintaining bacterial cell viability which is of utmost importance in the fermentation process. In this chapter, the effect of naked and 3-aminopropyltriethoxysilane coated iron oxide nanoparticles on biofilm formation, growth, and viability of *Bacillus subtilis* cells are discussed. This chapter sheds light on the biocompatibility of APTES coated iron oxide nanoparticles and their ability to reduce bacterial surface attachment and subsequent biofilm formation.

Chapter 6 describes a development of a novel, simplified and accurate method to routinely analyse MK-7 by High-Performance Liquid Chromatography. The general usefulness of the developed method in terms of accuracy, reproducibility, sensitivity and short runtime is demonstrated by the application of the method in the analysis of MK-7 from several *Bacillus* species/strains.

Chapter 7 describes the effect of surface functionalised iron oxide nanoparticles on MK-7 production and identifies the optimum concentration of iron oxide nanoparticles which gives the maximum MK-7 yield. In this chapter, the APTES

coated iron oxide nanoparticles, which significantly reduced biofilm formation described in Chapter 6, were tested for their effect on MK-7 production and the optimum concentration of APTES coated nanoparticles, which would minimise biofilm formation and maximise MK-7 yield is given.

Chapter 8 identifies the optimum medium for *Bacillus subtilis* fermentation which can minimise the biofilm biomass while maximising the MK-7 production. In the first part of this study, a biofilm detachment strategy to reduce biofilm biomass while maximising MK-7 production is explored. In this regard, cellular responses of MK-7 production and biofilm formation to various initial concentrations of the key nutrients which were believed to interfere with the structural integrity of biofilms and their optimum concentrations are assessed for their ability to reduce biofilm formation without compromising the MK-7 production. In this respect, mathematical model fitting with response surface optimisation is demonstrated and validated as a rational approach to identify the effective nutrients and their optimum concentrations. In the second part of this chapter, a combination of a biofilm attachment and a detachment strategy is explored to minimise biofilm formation and maximise MK-7 production. The cell growth, biofilm formation and MK-7 production of *Bacillus subtilis* in this optimum medium are then demonstrated.

Chapter 9 explores further opportunities to enhance total MK-7 production by periodic removal of MK-7 by biocompatible organic solvents from the culture medium and re-use of the biomass for MK-7 production. Hereafter this process is termed as ‘milking’. As menaquinones are said to be involved in feedback inhibition of two key regulatory enzymes in shikimate biosynthesis, it is reported that total MK-7 production can be improved by keeping the MK-7 level below the feedback inhibition threshold. In addition, it is reported that bacteria under metabolically challenged conditions show increased respiration rates which can

result in enhanced MK-7 synthesis. This chapter demonstrates the possibility of improving the total MK-7 production by milking of MK-7 from the culture medium with biocompatible organic solvents. A review of common organic solvents used for MK-7 extraction, changes in bacterial cell viability upon milking of MK-7 with organic solvents, selection of a biocompatible organic solvent for milking MK-7 and the effect of milking MK-7 with biocompatible organic solvents on MK-7 production are discussed in this chapter.

Chapter 10 concludes the significant findings of this thesis and presents some recommendations for future research.

1.3 Publications which have resulted from chapters of this thesis

Peer-reviewed journal publications:

1. Ranmadugala, D., Ebrahiminezhad, A., Manley-Harris, M., Ghasemi, Y., & Berenjian, A. (2017). Iron oxide nanoparticles in modern microbiology and biotechnology. *Critical Reviews in Microbiology, 43*(4), 493–507.

2. Ranmadugala, D., Ebrahiminezhad, A., Manley-Harris, M., Ghasemi, Y., & Berenjian, A. (2017). The effect of iron oxide nanoparticles on *Bacillus subtilis* biofilm, growth and viability. *Process Biochemistry, 62*(1), 231–240.

3. Ranmadugala, D., Ebrahiminezhad, A., Manley-Harris, M., Ghasemi, Y., & Berenjian, A. (2017). Impact of 3–Aminopropyltriethoxysilane-Coated Iron Oxide Nanoparticles on Menaquinone-7 Production Using *Bacillus subtilis*. *Nanomaterials, 7*(11), http://dx.doi.org/10.3390/nano7110350.

4. Ranmadugala, D., Ebrahiminezhad, A., Manley-Harris, M., Ghasemi, Y., & Berenjian, A. (2017). Magnetic immobilization of bacteria using iron oxide nanoparticles. *Biotechnology Letters*, *40*(2), 237–248.

5. Ranmadugala, D., Ebrahiminezhad, A., Manley-Harris, M., Ghasemi, Y., & Berenjian, A. (2017). Reduced biofilm formation in the Menaquinone-7 production process by optimizing the composition of the cultivation medium. *Trends in Pharmaceutical Sciences*, *3*(4), 245–254.

6. Ranmadugala, D., Ebrahiminezhad, A., Manley-Harris, M., Ghasemi, Y., & Berenjian, A. (2018), High Level of Menaquinone-7 Production by Milking Menaquinone-7 with Biocompatible Organic Solvents. *Current Pharmaceutical Biotechnology, 19*(3), 232-239.

7. Ranmadugala, D., Grainger, M., Manley-Harris, M., & Berenjian, A. (2018), Determination of Menaquinone-7 by a Simplified Reversed Phase HPLC Method. *Current Pharmaceutical Biotechnology, 19*(8), 664-673.

Conference presentations:

1. Ranmadugala, D., Ebrahiminezhad, A., Ghasemi, Y., Manley-Harris, M., & Berenjian, A (2017, November), Reduced biofilm formation and enhanced MK-7 production in *Bacillus subtilis* fermentation, presented at the Waikato Young Research Engineers Symposium (WYRES), Hamilton, New Zealand

Chapter 2

Literature Review

This chapter forms the basis for the following publications:

Ranmadugala, D., Ebrahiminezhad, A., Manley-Harris, M., Ghasemi, Y., & Berenjian, A. (2017). Iron oxide nanoparticles in modern microbiology and biotechnology. *Critical Reviews in Microbiology, 43*(4), 493–507.

Ranmadugala, D., Ebrahiminezhad, A., Manley-Harris, M., Ghasemi, Y., & Berenjian, A. (2017). Magnetic immobilization of bacteria using iron oxide nanoparticles. *Biotechnology Letters, 40*(2), 237–248.

2.1 Vitamin K

Vitamin K, an anti-haemorrhagic factor discovered in 1929 by the Danish biochemist Henrik Carl Peter Dam, is capable of correcting dietary induced haemorrhages and spontaneous bleeding (Dam, 1929, as cited in Dam, 1935). The anti-haemorrhagic factor received the letter 'K' as a reference to the first letter of the word 'Koagulation' as spelled in the German and Scandinavian languages (Dam, 1935). The chemical structure of vitamin K was solved by Edward Doisy and his group as 2-methyl-3-phytyl-1,4-naphthoquinone in the late 1930s (MacCorquodale *et al.*, 1939). Both Henrick Dam and Edward Doisy were awarded the Nobel Prize in 1943 for their important roles in discovering vitamin K and elucidation of the chemical structure of vitamin K. The mechanism of action of vitamin K was, however, only disclosed 40 years after Dam reported the bleeding conditions in chickens (Suttie & Nelsestuen, 1980).

Vitamin K is a generic term used for a number of related compounds classified as vitamin K1 (phylloquinone), vitamin K2 (menaquinone) and vitamin K3 (menadione). Phylloquinone (PK) and menaquinones (MK) are the two naturally occurring forms of vitamin K and menadione is the synthetic form of Vitamin K. All forms of vitamin K have the common 2-methyl-1,4-naphthoquinone nucleus but differ in the length and degree of saturation of the side chain at the 3-position (Vermeer & Schurgers, 2000) (Figure 1). The structure of the side chain differs with the number of prenyl units composing the isoprenoid side chain (Dam, 1935) differing from species to species (Fujimoto *et al.*, 2012). Therefore, menaquinones are a series of vitamers having variable side chain lengths of 1–14 repeating isoprene units referred to as MK-*n* where *n* denotes the number of isoprene units (Berenjian *et al.*, 2015; Booth, 2012; Collins & Jones, 1981; Tsukamoto *et al.*, 2001).

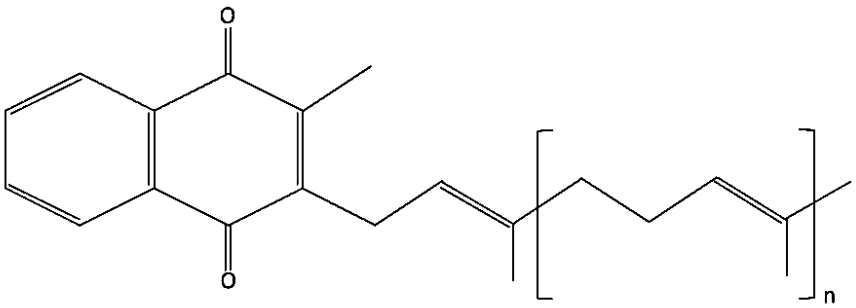

Figure 1 Molecular structure of menaquinone**.**
The letter "n" denotes the number of isoprene units (1-14)

Phylloquinone is commonly found in green leafy parts of plants, and is, therefore, considered as the main dietary form of vitamin K. In contrast, menaquinones are normally synthesised by bacteria (Shearer & Newman, 2008; Suttie, 1995) except menaquinone-4 (MK-4), which is regarded as a short-chain menaquinone produced by the conversion of PK into MK-4 by the intestinal flora in the colon of humans and rodents (Okano *et al.*, 2008). Menaquinones are the most widespread respiratory quinones found as membrane-bound compounds (Fujimoto *et al.*, 2012) in many microorganisms such as archaea (Lübben, 1995) and both gram-positive and gram-negative bacteria (Collins & Jones, 1981). They are also assumed to be evolutionarily the most ancient type of isoprenoid quinones (Lübben, 1995; Nitschke *et al.*, 1995). Menaquinones are known to function mainly as electron carriers in prokaryotic photosynthetic and respiratory electron transport chains (Bentley & Meganathan, 1982; Meganathan, 2001) (Figure 2), whereas phylloquinone functions as an electron receptor during photosynthesis. Thus menaquinones occupy a central role in the electron transport chain and the synthesis of MK is critical for the survival of bacteria (Dhiman *et al.*, 2009).

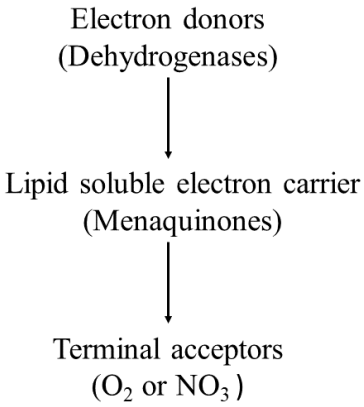

Figure 2 Schematic representation of the gram-positive bacterial electron transport chain.

Taber *et al.* (1981) have extensively studied the mechanism of MK biosynthesis in *Bacillus subtilis.* In MK biosynthesis, the head group precursor 1,4-dihydroxy-2-naphthoate (DHNA) and the side chain are synthesised separately in two distinct independent biosynthetic pathways and the two counterparts are condensed by the enzyme DHNA prenyltransferase before undergoing further modifications by methylation (Nowicka & Kruk, 2010). The biosynthesis of the quinone skeleton is, however, limited by feedback inhibition of aromatic amino acids such as L-tyrosine, L-phenylalanine and L-tryptophan (Tsukamoto *et al.*, 2001). In addition, chorismate and menaquinone (MK-4) are involved in the feedback inhibition of two regulatory enzymes in the shikimate pathway, 3-deoxy-D-arabino-heptulosonate-7-phosphate (DAHP) and shikimate kinase (Taguchi *et al.*) (Figure 3). The intermediates in the pathway have been extensively targeted in the development of mutants with improved MK-7 productivity.

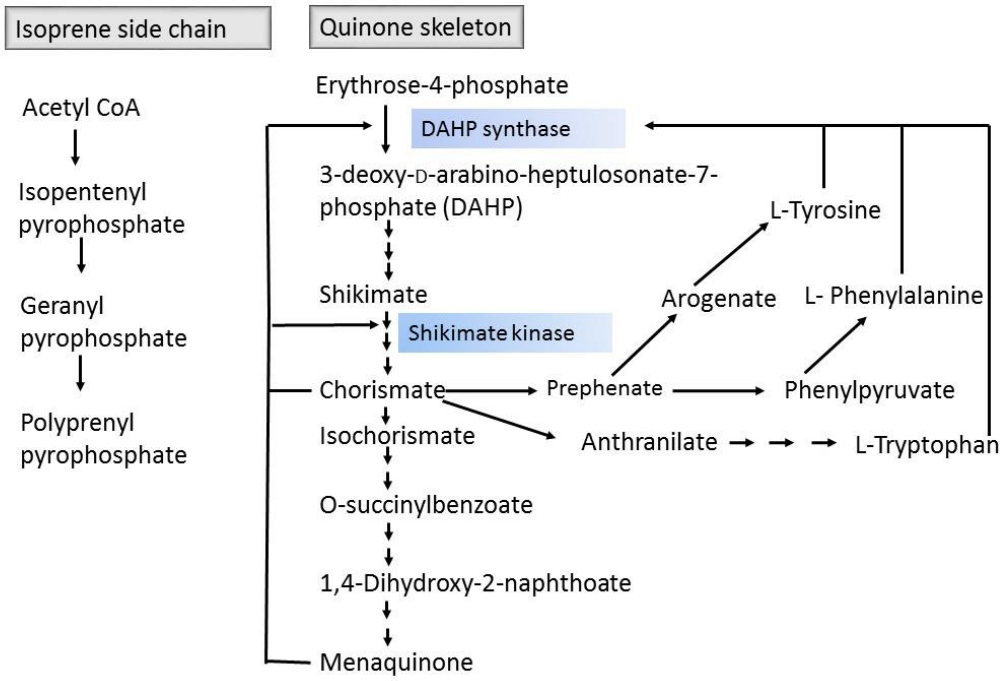

Figure 3 Menaquinone biosynthetic pathway and the regulatory mechanism by feedback inhibition.

2.2 Health benefits of vitamin K

Vitamin K has many health benefits. Beyond the role of normal blood coagulation, vitamin K plays a key role in bone formation (Vermeer, 1990). In mammals, vitamin K acts as a cofactor for ɤ-glutamyl carboxylase enzyme, which converts ɤ- glutamate residues in osteocalcin to ɤ-carboxylase glutamate (Gla) which has calcium binding properties. Gla promotes mineralisation of bone in osteoblasts in bone metabolism (Vermeer, 1990), and therefore it has been suggested that the daily intake of vitamin K would improve bone strength and would prevent osteoporotic fractures (Iwamoto *et al.*, 2006; Shiraki *et al.*, 2000). Deficiency in both phylloquinone and menaquinones have been shown to be connected to low bone mass and femur neck fractures. However, low bone mass and fractures were more closely correlated with MK than with PK. For example, Cockayne *et al.* (2006) report that bone fractures and bone loss are lower in Japanese patients who regularly consume MK. Therefore, in summary, intake of MK is said to be more important

to reduce bone fractures. The intake of MK-7 especially plays a vital role in bone formation (Tsukamoto *et al.*, 2000), reducing bone fractures (Schurgers *et al.*, 2007) and in preventing postmenopausal bone loss by improving bone mineral calcification and the femoral neck width (Knapen *et al.*, 2007). Studies show that MK-7 is more effective in catalysing osteocalcin carboxylation (Schurgers *et al.*, 2007) and thereby can significantly reduce bone fractures. This is due to the long half-life of MK-7 which makes it effectively present in the circulation longer than PK for uptake by extrahepatic tissues (Schurgers *et al.*, 2007).

In addition, a direct link has been seen between MK and cardiovascular health. Beulens *et al.* (2009) have shown that the dietary intake of MK is more important than PK in reducing coronary artery calcification. It has been shown that high dietary intake of MK, especially the long-chain MK (MK-7, MK-8 and MK-9) could protect against cardiovascular disease by preventing coronary artery calcification through the activation of a matrix Gla protein, which is a calcification inhibitor expressed in vascular tissue (Gast *et al.*, 2009; Knapen *et al.*, 2015; Shea & Holden, 2012). Supplementation of MK-7 has especially shown to decrease arterial stiffness in postmenopausal women (Knapen *et al.*, 2015). Therefore, MK-7 is the obvious choice to be included in multivitamin supplements and functional foods for the prevention of these diseases (Cranenburg *et al.*, 2007).

2.3 Dietary intake of vitamin K

When compared to the other vitamins, the dietary intake of vitamin K is very low (Cranenburg *et al.*, 2007). In a typical western diet, especially the intake of MK-7 is less when compared to traditional Asian diets. Further, long-chain MK are limited to certain fermented foods like cheeses (MK-8 and MK-10) and the traditional Japanese soy bean-based product, *natto* (MK-7) (Knapen *et al.*, 2015). According

to Tsukamoto *et al.* (2000), daily intake of *natto* would increase serum levels of MK-7 and ɤ-carboxylated osteocalcin in normal individuals. It is recorded that prolonged intake of *natto* prevents bone loss (Tsukamoto *et al.*, 2000; Yamaguchi *et al.*, 2000). *Natto* is considered as the best source of MK-7. It is a product of fermentation of soybean using *Bacillus subtilis natto* (Booth, 2012; Shea & Holden, 2012). Even though low concentrations of MK-7 can be obtained from certain fermented cheeses and meat products (Song *et al.*, 2014), comparatively *natto* has a high amount of MK-7, typically 800–900 µg per100 g of *natto* (Berenjian *et al.*, 2015; Sakano *et al.*, 1988; Sato *et al.*, 2001b), in addition to MK-8 and PK in moderate concentrations (84 and 35 µg/100g) (Booth, 2012). The concentration of MK-7 in *natto* requires the consumption of 20–22 g *natto*/day to achieve the recommended daily dose of 180 µg/day (Berenjian *et al.*, 2014; Knapen *et al.*, 2015). Further, sufficient consumption is impractical as people have negative feelings towards *natto* due to its texture and smell. Furthermore, *natto* is only popular in certain regions of Japan and is not widely consumed elsewhere (Kamao *et al.*, 2007; Walther *et al.*, 2013). Therefore, quantity production of MK-7 via a bacterial fermentation system is of importance to allow the production of supplements.

2.4 MK-7 production and current challenges

The starter strain used for *natto* production is *Bacillus subtilis* BEST 195 which is thought to have been isolated about 100 years ago (Kubo *et al.*, 2011). Dried rice straw, which is the natural habitat of the spore-forming *Bacillus subtilis*, was used for *natto* fermentation, before the isolation of the starter strain (Kubo *et al.*, 2011). *Natto* gets its sticky texture due to poly ɤ- glutamic acid (PGA) production by BEST 195 via the *pgs* operon (Ashiuchi *et al.*, 1999). *Bacillus subtilis* has been widely investigated as a potential MK-7 producer using both liquid and solid state

fermentation processes (Berenjian *et al.*, 2015). The two bioprocesses mainly differ from each other based on the amount of free liquid in the substrate during fermentation. The water content in the liquid state fermentation (LSF) varies from 90–95% whereas the water content in solid state fermentation (SSF) conceivably varies from 12 wt% up to the maximum water holding capacity of the solid, which in some cases is 80 wt% (Mitchell *et al.*, 2000). Many studies have been carried out to enhance the production of MK-7 using both LSF and SSF. These studies have been focused on optimisation of nutrients and operating conditions (Berenjian *et al.*, 2011; Berenjian *et al.*, 2014; Mahdinia *et al.*, 2017), fed batch addition of nutrients (Berenjian *et al.*, 2012), genetic mutation coupled with optimisation of the fermentation medium (Sato *et al.*, 2001b; Song *et al.*, 2014; Tsukamoto *et al.*, 2001), *in situ* extraction protocols (Berenjian *et al.*, 2014) and magnetic immobilisation of bacteria (Ebrahiminezhad *et al.*, 2016c). In addition, MK-7 production using lactic acid bacteria (Morishita *et al.*, 1999) has also been reported. However, *Bacillus subtilis* is considered as the key microorganism in industrial vitamin K production due to a long history of safe use and the capacity of the bacterium to produce and secrete large quantities of MK-7 (Berenjian *et al.*, 2015; Song *et al.*, 2014).

From the research conducted so far, the highest level of MK-7 that is achievable by LSF fermentation of *Bacillus subtilis natto* in a 3 L fermenter is 226 mg/L (Berenjian *et al.*, 2014) while the highest level from SSF is 140 mg/L (Mahanama *et al.*, 2012). Although *natto* has been traditionally produced via SSF, in comparison with LSF, SSF is difficult to scale up, there is a lack of devices to measure relevant operating variables inside the reactor and it is difficult to remove the large amount of heat that is generated by metabolic activities of microorganisms (Mahanama *et al.*, 2011) which would ultimately affect the growth of the microorganism (Pandey, 2003). There are major concerns with the static mode

fermenters, such as the risk of large oxygen gradients in addition to the temperature gradients when the fermentation progresses (Pandey, 2003). The highest amount of MK-7 production of 140 mg/L through SSF in *Bacillus subtilis* fermentation was therefore achieved using a tray type solid-state fermenter, with an effective cooling system (Mahanama *et al.*, 2012). Further, the space required for the installation of static mode fermenters is comparatively large (Berenjian *et al.*, 2015). Therefore, LSF is a better option for MK-7 production compared to SSF.

Apart from optimising the nutrients, fermentation and operating conditions, mutation studies have also been focused on constructing a strain of *Bacillus subtilis natto* with higher MK-7 productivity. In one of the studies, a combination of chemical *N*-methyl-*N*-nitro-*N*-nitroso-guanidine (NTG) and physical mutation (UV) methods have been used (Tsukamoto *et al.*, 2001). However, the constructed strain with analog resistance to 1-hydroxy-2- naphthoic acid (HNA), *p*-fluoro-D, L-phenylalanine (pFP), *m*-fluoro-D, L-phenylalanine (mFP), and β-2-thienylalanine (βTA) gave only 2-fold increase in MK-7 production compared to that of the commercial strain and the method involved screening of large numbers of mutants (Tsukamoto *et al.*, 2001). While HNA is an analog of DHNA: an intermediate in the biosynthetic pathway of the quinone skeleton, pFP, mFP and βTA are analogs of aromatic amino acids which are involved in a feedback inhibition in the shikimate pathway (Tsukamoto *et al.*, 2001) (Figure 3). Mutation by NTG and low energy beam implantation combined with optimisation of the fermentation medium has been attempted by Song *et al.* (2014); however, the maximum amount of MK-7 production achieved was 3.5 mg/L. A potent, D-phenylamine resistant mutant produced via chemical mutagenesis using NTG has given 60 mg/L of total MK (MK-7 and MK-8) under static fermentation conditions (Sato *et al.*, 2001b), while a menadione-resistant mutant has given 35 mg/L of MK-7 (Sato *et al.*, 2001a). Even

though these studies reported a considerable increase in MK-7 under the optimum conditions with mutant strains of *Bacillus subtilis,* it has been demonstrated that optimisation of nutrient concentrations (Berenjian *et al.*, 2011) and operating conditions (Berenjian *et al.*, 2014) are imperative in increasing MK-7 production. A concentration of 62 mg/L of MK-7 with optimisation of nutrient concentration using central composite face design (CCD) in response surface methodology (RSM) during a static fermentation process, and a concentration of 226 mg/L of MK-7 with aeration and stirring at 40°C in a 3 L fermenter, has been achieved in *Bacillus subtilis natto* fermentation without using any genetic modification. In addition, a new concept of application of nanoparticles for MK-7 biosynthesis was attempted by Ebrahiminezhad *et al.* (2016c). The presence of nanoparticles did not show any negative effect on bacterial cell growth or MK-7 production; however, neither did they cause any significant increase in MK-7 production. An update of the list of studies recorded in Berenjian *et al.* (2015), which used LSF for the production of MK-7 and the resultant concentration, is given in Table 1.

Fermentation of MK-7 at industrial scale, however, is still a complicated process (Berenjian *et al.*, 2015). These complications include biofilm formation (Berenjian *et al.*, 2013), low fermentation yield, and a need for more than 20 different unit operations (Berenjian *et al.*, 2014). As a result, the price of MK-7 in a pure powder form is currently around US$5 million/kg (Berenjian *et al.*, 2015; Ebrahiminezhad *et al.*, 2016b; Wohlgemuth, 2009), signifying the importance of minimising these problems by developing novel bioprocess approaches.

Table 1 List of studies that used LSF for the production of MK-7

Bacteria type	**MK-7 concentration**	**Media composition**	**Shaking speed & aeration**	**Temp (°C)**	**Time (d)**	**Reference**
Lactic acid bacteria	29-123 µg/L	Soymilk; D-glucose 15 g/L	Static	30	2	(Morishita *et al.*, 1999)
Bacillus subtilis natto B.S D200-41	60.1 mg/L	Soybean 100 g/L; Glycerol 50 g/L; Yeast extract 5 g/L; K_2HPO_4 0.5 g/L	120 rpm for one day followed by five days static	37 (shaking) and 45 (static)	6	(Sato *et al.*, 2001a)
Bacillus subtilis natto K3-176	35 mg/L	Soybean extract 100 g/L; Glycerol 50 g/L; Yeast extract 5 g/L	250 rpm 0.5 vvm	37	4	(Sato *et al.*, 2001a)
Bacillus subtilis natto Miyagino	1.4 mg/L	Polypeptone 2 g/L; glycerine 3 g/l	100 rpm	37	2	(Sumi, 2004a)
Bacillus subtilis natto GN13/72	50 mg /L	Soypeptone 12 g/L; yeast extract 0.5 g /L; dextrin 60 g/L; K_2HPO_4 0.05 g/L; NaCl 5 g/L	100 rpm	37	6	(Benedetti et al., 2010, as cited in Berenjian *et al.*, 2015)
Bacillus subtilis natto	62.3 mg/L	Soypeptone 189 g/L; yeast extract 50 g/L; glycerol 50 g/L; K_2HPO_4 0.6 g/L	Static	40	6	(Berenjian *et al.*, 2011)
Bacillus subtilis natto	86 mg/L	Yeast extract 50 g/L; glycerol 50 g/L; K_2HPO_4 0.6 g/L	Static	40	6	(Berenjian *et al.*, 2012)
Bacillus subtilis natto	226 mg/L	Yeast extract 50 g/L; glycerol 50 g/L; Soy peptone 189 g/L; K_2HPO_4 0.6 g/L	1000 rpm 5 vvm	40	5	(Berenjian *et al.*, 2014)
Bacillus subtilis natto mutant BN-2-6	3.5 mg/L	Yeast extract 25 g/L Glycerol 69.6 g/L Peptone 20 g/L Sucrose 34.5g/L K_2HPO_4 4 g/L	150 rpm	37	3	(Song *et al.*, 2014)
Bacillus subtilis (*ATCC 6633*)	11.57 mg/L	Yeast extract 10 g/L Glycerol 50 g/L Soy peptone 15 g/L L-lysine coated iron oxide nanoparticles 100 µg/L	120 rpm	40	5	(Ebrahiminezhad *et al.*, 2016c)
Bacillus natto	35.58 mg/L	Yeast extract 0.6 g/L Glycerol 50 g/L Soypeptone 50 g/L K_2HPO_4 0.3 g/L $CaCl_2$ 0.1 g/L $MgSO_4.7H_2O$ 0.3 g/L	600 rpm 1.5 vvm	37	2.5	(Luo *et al.*, 2016)

2.5 Biofilm formation

Biofilm formation has been used for the production of many value-added products such as organic acids, enzymes, polysaccharides, antibiotics as well as bioenergy (Cheng *et al.*, 2010). In addition, MK-7 production has shown a linear dependency on biofilm formation (Berenjian *et al.*, 2013) and in this regard, biofilm reactors have been used to produce MK-7 (Mahdinia *et al.*, 2017). However, biofilm formation in static mode fermentation by *Bacillus subtilis* has found to be one of the major problems associated with MK-7 production (Berenjian *et al.*, 2013) as it leads to many process complications in industrial fermentation. Most importantly, as biofilms are extremely diffusion limited, oxygen and nutrient deficiency would result in a decrease in bacterial metabolic activity (Stewart & Franklin, 2008). Biofilm cells are also subjected to other stresses, such as high cell density, metabolite accumulation and high osmolarity (Spormann, 2008). Due to the protective nature of biofilm and high survival competence in industry, the formation of biofilms results in costly periodic cleaning in industrial settings (Gibson *et al.*, 1999). Biofilms also cause corrosion of equipment in the industry due to extracellular enzymes active within the biofilm matrix (Beech & Sunner, 2004). Further, endospores produced by genera like *Bacillus* can colonise the process equipment and become a significant source of steady contamination. Countermeasures against biofilms are therefore necessary for good manufacturing practice in order to improve process performance and product quality and quantity and reduce costly periodic cleaning.

Biofilms are architecturally complex, surface-attached communities of microorganisms embedded within a self-produced matrix of extracellular polymeric substances consisting of polysaccharides, proteins and nucleic acids (Kearns *et al.*, 2005; O'Toole *et al.*, 2000). Apart from these, *Bacillus subtilis* is able to produce

poly-ɤ glutamate (PGA) which is an additional matrix component (Chettri *et al.*, 2016; Stanley & Lazazzera, 2005), which, however, makes no significant contribution to the extracellular matrix in the wild strain (Branda *et al.*, 2006). Poly-ɤ -glutamate can enhance biofilm formation by enhancing cell–surface interactions regulated by the loci, DegSU, DegQ, SwrA and the two-component regulator ComPA (Stanley & Lazazzera, 2005). In standing liquid medium, biofilms are formed when cells of *Bacillus subtilis* switch from a highly motile planktonic state to a non-motile state (Kearns *et al.*, 2005) (Figure 4**).** The process of biofilm formation generally can be divided into five distinct stages, each with its own genetic pathway: 1) Initial surface attachment, 2) monolayer formation, 3) formation of multi-layered microcolonies, 4) production of extracellular matrix, and 5) maturation and sporulation taking place from mature biofilm (Lemon *et al.*, 2008; O'Toole *et al.*, 2000). However, there may be variations according to species.

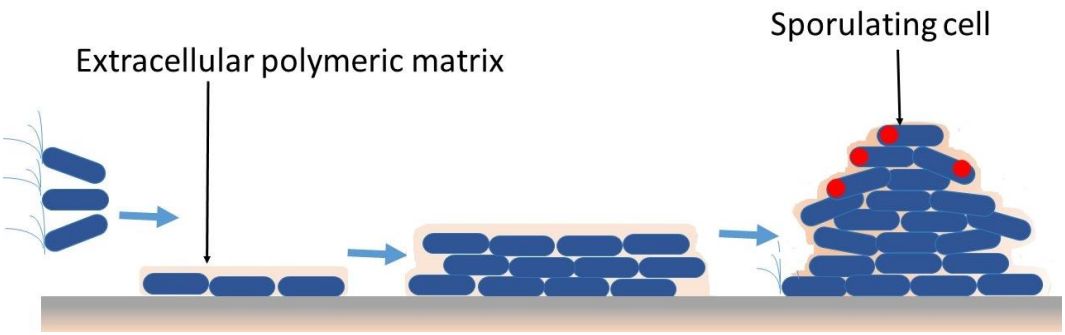

Figure 4 Model of biofilm development.

Varied environmental signals and regulatory pathways control entry into biofilm formation. Environmental signals that trigger the transition from free swimming to sessile form are mainly nutritional content of the medium, temperature, osmolarity, pH, iron and oxygen (O'Toole *et al.*, 2000). These environmental conditions that

trigger biofilm formation, however, vary among organisms as evident by multiple genetic pathways that control biofilm formation. The starvation response pathway is one of the pathways that can be considered as part of the biofilm development cycle (O'Toole *et al.*, 2000).

The key regulatory genes in biofilm development are SinR and SinI (Kearns *et al.*, 2005). SinR is the master regulator that governs the switch of motile cells to nonmotile cells (Kearns *et al.*, 2005). SinR indirectly promotes cell separation and motility by binding to the promoter region of the *eps* operon and repressing the transcription of genes responsible for the production of exopolysaccharides (EPS) (Branda *et al.*, 2006; Kearns *et al.*, 2005). Exopolysaccharides are the primary component of the extracellular matrix (Kearns *et al.*, 2005). The extracellular matrix is responsible for the spatial organisation of *Bacillus subtilis* biofilms (Cairns *et al.*, 2014). In standing liquid cultures, *Bacillus subtilis* form architecturally complex bacterial communities at an air-liquid interface termed pellicles, and sporulation takes place from the aerial structures projecting from the pellicles (Branda *et al.*, 2001; Cairns *et al.*, 2014). Therefore, the extracellular matrix promotes survival of *Bacillus subtilis* in the biofilm by allowing sporulation. Extracellular matrix production and biofilm development take place when the activity of SinR is antagonised by anti-repressor proteins SinI, YlbF and YmcA (Branda *et al.*, 2006; Kearns *et al.*, 2005) (Figure 5). The anti-repression pathway revolving around the transcriptional repressor SinR is triggered by the transcription factor SpoOA (Branda *et al.*, 2001). Phosphorylation and activation of SpoOA (SpoOA~P) are vital to biofilm development (Branda *et al.*, 2001) and this takes place through a signal provided by the Krebs cycle (Ireton *et al.*, 1995). SpoOA is also the key transcriptional regulator that directs entry into sporulation (Cairns *et al.*, 2014).

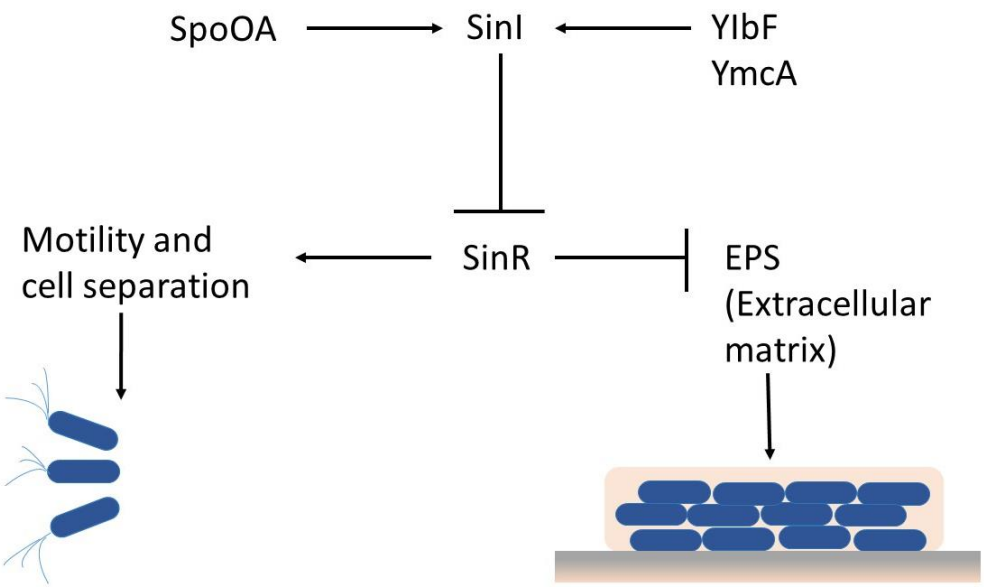

Figure 5 Genetic circuity governing *Bacillus subtilis* lifestyle switch from planktonic to biofilm. Repression of the production of exopolysaccharides and biofilm formation by SinR is shown by the symbol ⊣. SinR indirectly promotes cell separation indicated by an arrow. When conditions are favourable for biofilm formation, SpoOA~P; the key regulatory protein controlling transcription, rises above a threshold limit to initiate biofilm formation. Further, anti-repressor proteins SinI, YIbA and YmcA, antagonize the activity of SinR thereby promoting biofilm formation.

2.6 Biofilm formation and sporulation

Sporulation is a phenomenon closely linked with biofilm formation and is regulated by common regulatory pathways (Tawaba, 2015). The same stimuli of biofilm formation, mainly carbon, nitrogen, or in some instances phosphorus starvation and high population density (Errington, 2003), triggers sporulation in *Bacillus subtilis.* At least three histidine protein kinases (KinA, KinB, and KinC) are said to be involved in the initiation of sporulation (Grossman, 1995; LeDeaux *et al.*, 1995). Even though nutrient deprivation is the primary signal, sporulation is a population density-dependent regulation mediated by extracellularly signalling molecules which regulate SpoOA~P, the key transcription factor that is required for the initiation of sporulation as well as for biofilm development (Grossman, 1995;

Miller & Bassler, 2001). High levels of SpoOA~P triggers sporulation (Branda *et al.*, 2001). Apart from these, a quorum sensing peptide, termed competence stimulating factor, also plays a major role in sporulation (Miller & Bassler, 2001). Further, the activities of Krebs citric acid cycle enzymes are important in sporulation (Ireton *et al.*, 1995). For sporulation to complete, cells need to expend energy, and one of the roles of Krebs citric acid cycle enzymes is to provide energy-yielding compounds and metabolic intermediates necessary for sporulation (Ireton *et al.*, 1995).

In the process of sporulation, dormant environmental resistant spores are formed by an asymmetric cell division that produces a larger mother cell, and a smaller forespore. The forespore matures and develops resistance properties after it is engulfed by the mother cell and the mature spore is released after the mother cell lyses (Grossman, 1995).

2.7 Quorum sensing and microbial biofilms

Biofilm formation and sporulation together with diverse cellular processes are activated by the cell to cell signalling between bacterial cells termed as quorum sensing (QS) (Miller & Bassler, 2001). The large cell densities in biofilms create a local environment suitable for bacterial communication. Bacteria use chemical signals to recognise the cell density and then they respond with appropriate corrective behaviour. *Bacillus subtilis* generally use secreted peptides, which accumulate extracellularly as autoinducers for quorum sensing (Miller & Bassler, 2001). The concentration of autoinducers is correlated with population density (López *et al.*, 2010; Miller & Bassler, 2001). Quorum sensing can influence biofilm formation in different ways. Following starvation, QS signals can increase to initiate biofilm formation and, finally, QS can induce behaviours in biofilm cells,

such as the production of exopolysaccharides and sporulation (Miller & Bassler, 2001). It also plays a major role in controlling the population size in a biofilm, behaviour of biofilm cells and biofilm structure (Spormann, 2008).

For *Bacillus subtilis*, the lipopeptide surfactin has been identified as a quorum-sensing molecule which appears to influence biofilm formation by causing potassium leakage from the cytoplasm (López *et al.*, 2009). Potassium leakage is sensed by a membrane-associated sensor kinase, KinC, which in turn triggers the expression of the genes involved in extracellular matrix production (López *et al.*, 2010). In this species, as discussed earlier, the matrix genes are repressed by the regulator SinR, which is antagonised by SinI. The gene *sin*I is only expressed when KinC-mediated phosphorylation of the transcription factor SpoOA~P rises above a threshold level (Kearns *et al.*, 2005)

As quorum sensing plays a major role in biofilm formation, interference with quorum sensing signalling, through the use of quorum sensing signalling mimics or quorum quenchers, has been a promising approach to combat pathogenic infections of biofilm-forming bacteria (Dong & Zhang, 2005).

2.8 Biofilm formation and sporulation: Implication for MK-7 production

Both biofilm formation and sporulation are closely linked with MK-7 production. However, the information is incomplete and unclear. Farrand and Taber (1974) reported that menaquinones are no longer produced after sporulation is complete. In this context, Sato *et al.* (2001b) showed that static fermentation would result in enhanced MK-7 production as sporulation progresses more slowly within a biofilm in a static culture. In their statement Sato *et al.* (2001b) also referred to the cell density. They concluded that "for enhanced MK production, cells have to be kept

static before cell growth reaches maximum" (Sato *et al.*, 2001b, p. 19). Sporulation is a phenomenon which is dependent on cell density and is mediated by extracellular signalling molecules. Sporulation is inefficient in cells at low population density, even upon starvation (Grossman, 1995; Miller & Bassler, 2001). According to Farrand and Taber (1973), the maximum sporulation can be seen when MK-7 is maximum. A positive correlation between sporulation and MK-7 production has also been demonstrated by Luo *et al.* (2016). However, addressing the relationship between cell density, biofilm formation and MK-7 production, Berenjian *et al.* (2013) claim that high cell density and pellicle formation are not very important for accelerating MK-7 production.

Microorganisms trapped within a biofilm matrix, however, experience limited oxygen and nutrient transfer which would eventually lead to a reduction in the growth rate and cell density (Stewart & Franklin, 2008). Therefore, reducing biofilm formation would be advantageous in the sense that it would address the mass and heat transfer issues that might arise in a large-scale fermentation process and many other process complications in MK-7 production (Berenjian *et al.*, 2013). On the other hand, biofilm fermentation has allowed for efficient product recovery in comparison to the suspended cell systems as there are fewer processing steps in the recovery of MK-7 (Berenjian *et al.*, 2013). Therefore, in industrial MK-7 production, a fermentation system designed to have minimum biofilm formation, maximum MK-7 production and efficient product recovery would offer a greater advantage. Surface functionalised nanoparticles with magnetic properties hold great promise to address all these issues, and the rationale for the use of nanoparticles for biofilm control, enhanced MK-7 production and process intensification are given in the following sections.

2.9 Nanoparticle research

Currently, there is an intense scientific interest in nanoparticle (NP) research. It has a very long history, dating back to the 9th century where NPs were used for generating a glittering effect on the surface of pots by artisans in Mesopotamia (Suganeswari, 2011). The term '*nano*' is derived from the Greek word *'nanos'* for dwarf (Buzea *et al.*, 2007). Although there is no internationally agreed formal definition of nanoparticles, nanoparticles are usually defined as particulate dispersions or solid particles with a size in the range of 10–1000 nm (Suganeswari, 2011) or materials that have structural components smaller than 1000 nm (1µm) in at least one dimension (Buzea *et al.*, 2007). Because the size threshold varies with the type of the material, Buzea *et al.* (2007) argue that the sub-micron level should be taken as the legitimate definition, although some authors limit the upper size limit to 50 nm or 100 nm. Due to distinct properties, such as large surface area and quantum size effects, nanoparticles are considered as a distinct state of matter (Buzea *et al.*, 2007).

A variety of materials, such as proteins, polysaccharides and synthetic polymers, are used to prepare nanoparticles (Suganeswari, 2011). The choice of matrix material for a specific application depends on many factors, including the required size of nanoparticles, surface characteristics, the degree of biocompatibility, the degree of biodegradability and toxicity (Suganeswari, 2011).

Among the nanoparticles, superparamagnetic nanoparticles which can be manipulated by using magnetic field gradients have shown great promise in many fields. Superparamagnetic nanoparticles are single domain particles with all their magnetic moments aligned in the same direction and with a short relaxation time (Benz, 2012). These particles have unique properties, such as the nearly instantaneous charge of magnetisation in the applied magnetic field, which allows

them to be directed towards a target using an external magnetic field and heating in alternating magnetic fields (Ihor *et al.*, 2008). Owing to their unique properties, superparamagnetic nanoparticles have been intensively developed and have found numerous applications, including biomedical, optical and electronic fields, such as biosensing (Miller *et al.*, 2002; Suganeswari, 2011), targeted drug delivery (Neuberger *et al.*, 2005), destruction of cancer tissues through hyperthermia (Laurent *et al.*, 2011), magnetic resonance imaging (Weinstein *et al.*, 2010), jet printing (Tiberto *et al.*, 2013), cell separation, immunoassay and tissue repair (Gupta & Gupta, 2005).

The two main forms of nanoparticles with superparamagnetic properties are magnetite (Fe_3O_4) and its oxidized form maghemite (γ-Fe_2O_3). As the superparamagnetic behaviour of iron oxide nanoparticles strongly depends upon the dimension of the nanoparticles (Laurent *et al.*, 2008), control of uniform size distribution is very important in synthesis. The size and shape of the nanoparticles, however, depend on many factors, such as pH, ionic strength, temperature, nature of the salts and the Fe(II)/Fe(III) concentration ratio (Laurent *et al.*, 2008).

Various procedures have been described to synthesise magnetic nanoparticles, and among these methods, chemical co-precipitation of Fe^{2+} and Fe^{3+} ions by an alkali such as NH_4OH or ammonia in an aqueous solution is the most commonly used solution phase procedure (Gnanaprakash *et al.*, 2007; Martínez-Mera *et al.*, 2007; Song *et al.*, 2014). The chemical reaction is as follows.

$$2Fe^{3+} + Fe^{2+} + 8OH^- \rightarrow FeO.Fe_2O_3 + 4H_2O$$

Nucleation and growth of nanocrystals are the two main steps that are involved in this bottom-up method (Mohapatra *et al.*, 2007). The advantage of the co-precipitation method is that comparatively large quantities of nanoparticles can be prepared (Laurent *et al.*, 2008). Nevertheless, there are several drawbacks in this

method, such as the difficulty in controlling the size distribution (Santoyo Salazar *et al.*, 2011) and the formation of impurities, such as goethite and maghemite (Gnanaprakash *et al.*, 2007).

In co-precipitation, the ideal ratio of Fe^{2+}/ Fe^{3+} is about 1:2 (Berger *et al.*, 1999). When Fe^{2+} ions oxidize to Fe^{3+} ions ($Fe^{2+}+O_2 \rightarrow Fe^{3+}$), the ratio of Fe^{2+}/Fe^{3+} becomes less than 1/2, leading to the formation of nonmagnetic impurities (Gnanaprakash *et al.*, 2007). It is reported that when the particle size of iron oxide nanoparticles is less than 10 nm, increase in surface area /volume ratio results in a large number of surface atoms which would oxidise readily to Fe^{3+} thereby leading to the formation of maghemite on the surface of the magnetic particle (Gnanaprakash *et al.*, 2007). The main factors affecting the formation of impurities during co-precipitation are the initial and final pH of the solution and the reaction temperature (Gnanaprakash *et al.*, 2007). Longer storage periods (6 months) and exposure to high temperatures (>180°C) would also cause the Fe^{2+} ions to oxidise to Fe^{3+} ions, leading to the formation of maghemite (Gnanaprakash *et al.*, 2007). The disadvantage is that the maghemite has slightly less saturation magnetisation than magnetite (Gnanaprakash *et al.*, 2007). However, when it comes to the technological applications of the nanoparticles, both magnetite and maghemite are suitable, as both of them are ferromagnetic in nature with superparamagnetism (Gnanaprakash *et al.*, 2007). In contrast, goethite is antiferromagnetic in nature. The formation of goethite can increase with an increase in pH above 4.7 (Gnanaprakash *et al.*, 2007).

2.10 Impact of nanoparticles on planktonic bacteria

The effect of nanoparticles on different cell lines have been investigated in various studies. However, the impact of nanoparticles on gram-positive bacteria is sparsely researched. Nanoparticle toxicity to bacteria is strain/species-specific (Baek & An,

2011; Hajipour *et al.*, 2012). Some studies show that iron oxide nanoparticles have a growth inhibitory effect on gram-positive and gram-negative bacterial strains such as *P. aeruginosa, S. aureus, E. coli, L. monocytogenes* and *S. marcescens* (Chatterjee *et al.*, 2011; Ebrahiminezhad *et al.*, 2012a; Ismail *et al.*, 2015; Ramteke *et al.*, 2010). Other studies show iron-containing nanoparticles can promote the growth of bacterial cells in a size-dependent manner by acting as an exogenous iron source for bacteria (Borcherding *et al.*, 2014). Therefore, there are still ambiguities with respect to the toxic effects and toxicity mechanisms of nanoparticles (Chang *et al.*, 2012). Cytotoxicity or growth promoting effect of nanoparticles on bacteria depends on the interaction between nanoparticles and bacteria which in turn seems to depend mainly upon the properties of the bacterial cell wall, physicochemical properties of nanoparticles (Laha *et al.*, 2014) as well as the environment/culture conditions (Żur *et al.*, 2016) which are discussed in detail in the following sections.

2.11 The role of bacterial cell wall

The major difference between mammalian cells and bacterial cells in connection with the impact of nanoparticles is the cell wall. The bacterial cell wall is a rigid structure surrounding the cell giving protection to the cell from environmental influences as well as constraining shape. Bacteria are divided into two classes according to the structure of the cell wall, namely gram-positive and gram-negative (Hajipour *et al.*, 2012). The electrostatic attraction or repulsion between nanoparticles, and hence the adhesion of the nanoparticles to bacterial cells, is mainly governed by the surface charge of the bacterial cell wall. Therefore, in order to understand the antibacterial effect of nanoparticles on the gram-positive bacterium *Bacillus subtilis*, it is important to understand the cell wall structure and cell wall interactions with nanoparticles. The cell wall of the gram-positive

bacterium *Bacillus subtilis* contains a thick layer (*i.e.*, 15–30 nm) of peptidoglycan, with teichoic acids and lipoteichoic acids which are unique to the gram-positive cell wall located within and in the latter case also penetrating the cell membrane (Hajipour *et al.*, 2012). Neither outer membrane nor a distinct periplasmic space is present (Scott & Barnett, 2006) **(**Figure 6). The peptidoglycan layer together with teichoic and lipoteichoic acids form a polyanionic matrix with a variety of functions (Scott & Barnett, 2006). Surface components attached to the cell wall contribute to the net negative charge of the cell. Although the nature of the negatively charged groups has not been fully explored, they seem to be mainly carboxyl and phosphate groups (Corpe, 1970). However, the magnitude of the charge can vary from strain to strain (Dickson & Koohmaraie, 1989). Further, if exopolysaccharides, which are produced by many gram-positive bacteria, have a different chemical character from that of the cell wall of the organism, the overall surface charge of the cell will be modified (Corpe, 1970).

Some reports have shown that gram-positive bacteria are more sensitive to iron oxide (Fe_2O_3) nanoparticles than gram-negative bacteria, and these different sensitivities have been attributed to the properties of the cell wall and differences in their cell membrane polarities (Azam *et al.*, 2012; Ismail *et al.*, 2015). The cell wall of gram-negative bacteria is structurally and chemically more complex than that of gram-positive bacteria, with an outer membrane consisting of lipopolysaccharides, phospholipids, and proteins and an underlying thin peptidoglycan layer (Aruguete & Hochella, 2010). It is said that the outer membrane containing lipopolysaccharides in gram-negative bacteria increases the net negative charge of the cell membrane (Hajipour *et al.*, 2012) and would make the cell wall impermeable to lipophilic solutes and would also limit the penetration of negatively charged free radicals (Ismail *et al.*, 2015). Therefore, gram-negative

bacteria are said to be less sensitive to IONs (Ismail *et al.*, 2015). In contrast, the gram-positive bacteria without an outer membrane, having only the peptidoglycan layer, which is not a good permeability barrier, are said to be more sensitive to lower concentrations of IONs (Ismail *et al.*, 2015). However, Baek and An (2011) have reported that the gram-negative bacterium *E. coli* is more susceptible to CuO nanoparticles than gram-positive bacteria (*S. aureus* and *Bacillus subtilis*). Also, Ebrahiminezhad *et al.* (2016a) observed similar results by testing silver nanoparticles against *S. aureus* and *E. coli*. Due to the presence of the thick peptidoglycan layer, gram-positive cells are said to be less subject to the toxicity of nanoparticles (Hajipour *et al.*). Therefore, it is difficult to make generalisations about the sensitivity of bacteria to nanoparticles solely based on bacterial cell wall characteristics. There are other key players, such as the intrinsic properties of the nanoparticles, which play a major role in determining nanotoxicity of IONs.

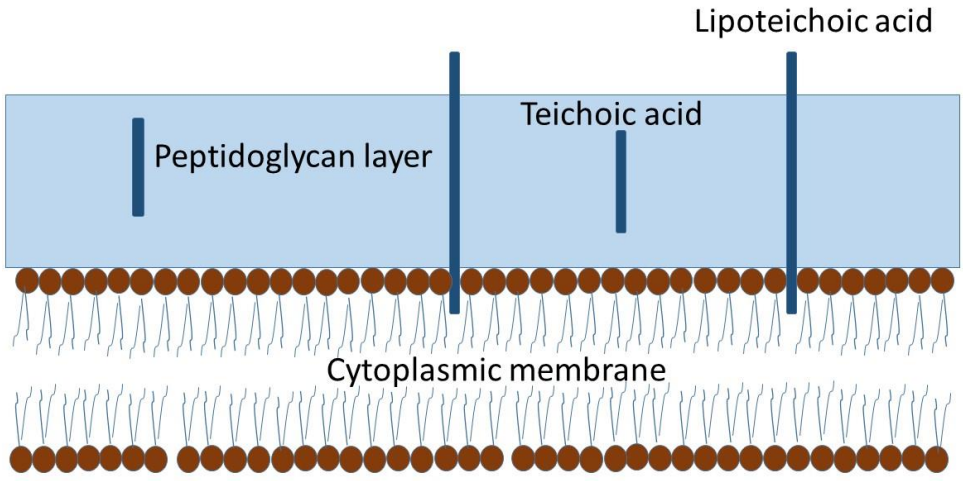

Figure 6 Gram-positive bacterial cell wall structure. The gram-positive cell wall is composed of a thick peptidoglycan layer. Lipoteichoic acid and teichoic acid embedded in the peptidoglycan layer. Lipoteichoic acids extend into the cytoplasmic membrane.

2.12 Antimicrobial effect of nanoparticles

In addition to the structure of the cell wall, the antimicrobial activity of nanoparticles depends on nanoparticle characteristics such as size, stability, shape, surface characteristics, dissolution, chemical composition and concentration of the nanoparticles in the growth medium (Laha *et al.*, 2014; Nel *et al.*, 2006).

Most of the properties of nanoparticles are related to their size (Chang *et al.*, 2012). With their smaller size, nanoparticles have a greater surface area: volume ratio. This allows a greater proportion of its atoms or molecules to be displayed on the surface (Nel *et al.*, 2006), enhancing the reactivity and interaction of nanoparticles with biological molecules. Further, nanoparticles with varying sizes result in different cell uptake rates leading to different levels of toxicity (Baek & An, 2011). Smaller nanoparticles can also play a major role in toxicity by generating more radicals (Applerot *et al.*, 2009), and size can affect the dissolution rate, and hence the release of toxic ions (Liu *et al.*, 2008). Therefore, size is one of the main characteristics that influence the toxic effect of nanoparticles. Generally, for a given mass concentration, smaller nanoparticles have been shown to have a higher antimicrobial activity (Aruguete & Hochella, 2010). However, with iron oxide nanoparticles (IONs), Borcherding *et al.* (2014) reported that the smaller (2 nm) nanoparticles have induced the greatest amount of bacterial cell growth as compared to larger (540 nm) nanoparticles largely owing to enhanced dissolution and increased bioavailability of iron from the smaller particles. A recent study on the antibacterial activity of IONs also shows that the antimicrobial activity of IONs is insignificant against *Bacillus subtilis* when the particle size is less than 50 µM due to electrostatic repulsion between bacteria and IONs with negative surface potential (Arakha *et al.*, 2015). However, at higher concentrations IONs with sizes greater than 50 µM have shown antibacterial activity to some extent (Arakha *et al.*,

2015). Molecular crowding with the increasing concentration of IONs resulting in interactions between IONs and bacteria as well as enhanced production of reactive oxygen species (ROS) are attributed to the observed results (Arakha *et al.*, 2015).

It has also been demonstrated that IONs have an antibacterial effect against *E. coli* and that the activity increases with the increase in the ION concentration (Chatterjee *et al.*, 2011). The concentration of the nanoparticles is thus another parameter that decides toxicity. This concentration-dependent antibacterial activity has been attributed to the production of ROS (Buzea *et al.*, 2007), but the concentration of the nanoparticles can affect particle aggregation as well, and it has been shown that high concentration of nanoparticles would sometimes promote particle aggregation and thereby exert a lower toxic effect (Buzea *et al.*, 2007; Takenaka *et al.*, 2001). Aggregation of nanoparticles further depends on the surface charge, material type and size of nanoparticles (Buzea *et al.*, 2007). Even though agglomeration has frequently been ignored in nanotoxicity studies, nanoparticle aggregation can change the size, surface area, dissolution rate and reactivity of nanoparticles and thereby would alter the potential effect on organisms (Chatterjee *et al.*, 2011; Wiesner *et al.*, 2011).

Toxicity of nanoparticles differs with the shape as well. For example, it is reported that spherical-shaped CuO nanoparticles show more toxicity towards gram-positive bacteria than sheet-shaped CuO nanoparticles (Laha *et al.*, 2014). Further, the shape of the nanoparticles has shown to impact cellular uptake as well (Kolhar *et al.*, 2013). Nevertheless, it is not clear whether the shape of the IONs will affect the nanoparticle toxicity on bacterial cells.

Apart from these factors, the surface characteristics, such as surface charge, play an important role in toxicity**.** Hu *et al.* (2009) studied the relative toxicity of seven metal oxide nanoparticles (ZnO, CuO, Al_2O_3, La_2O_3, Fe_2O_3, SnO_2, TiO_2) with

respect to variation in their surface charge and showed that the cytotoxicity decreases with the increase in the oxidation state of the metal, where TiO_2 with Titanium at +4 is the least toxic and ZnO with Zinc at +2 was the most toxic to bacteria. Thus, the electrovalent attraction of nanoparticles with the bacterial cell wall can contribute to the observed results. The surface negative charge of the bacterial cell can associate with positively charged metal nanoparticles, resulting in electrostatic condensation. A particular bacterial cell could attract more nanoparticles with low cation charge than with high cation charge; thus, the lower valent cations exert greater cytotoxicity (Hu *et al.*, 2009).

Dissolution of metal ions is another factor that affects cell toxicity. It has been shown that the toxic effect of soluble metal/metal oxide nanoparticles is higher than that of the insoluble ones (Brunner *et al.*, 2006). The solubility of nanoparticles is variable in various environmental conditions and the rate of ions released from nanoparticles is commonly related to the pH and temperature of the solution (Chang *et al.*, 2012). However, the role of nanoparticle solubility on nanotoxicity is controversial as Moos *et al.* (2010) showed that the cytotoxicity is independent of the amount of soluble Zn^{2+} in the cell. Moos *et al.* (2010) claim that although nano-sized ZnO is more cytotoxic than micrometre-sized ZnO, soluble Zn^{2+} ions liberated from ZnO nanoparticles are insufficient to promote cytotoxic effects unless the particulate is in contact with the cells. Borcherding *et al.* (2014) report that soluble Fe^{3+} ion released from smaller Fe_2O_3 nanoparticles can increase bacterial growth, while Chatterjee *et al.* (2011) report that Fe_3O_4 nanoparticles exert a toxic effect on bacterial cells (*E.coli*) in a concentration-dependent manner. Therefore, particle solubility and cytotoxicity of IONs on cell cultures show a nanoparticle size and concentration-specific response.

2.13 Key toxicity mechanisms of nanoparticles on planktonic bacteria

Comprehensive understanding of the toxic effect of nanoparticles on bacterial cells is important for the safe use of nanoparticles for MK-7 production using *Bacillus subtilis*. Several mechanisms have been suggested to explain the key toxicity mechanisms of nanoparticles on planktonic bacteria by various authors (Chang *et al.*, 2012; Djurišić *et al.*, 2015; Manke *et al.*, 2013; Nel *et al.*, 2006; Reidy *et al.*, 2013; Saleh *et al.*, 2015). These include:

1. Reactive oxygen species (ROS) mediated oxidative stress, with membrane lipid peroxidation, protein oxidation and DNA damage.
2. The release of metal ions, which react with the cell membrane and other cellular components.
3. Physical disruption of the cell membrane.

However, there is still limited knowledge on the toxicity mechanisms of ION to *Bacillus subtilis*. Reported evidence shows that ROS are the best-developed paradigm for nanoparticle toxicity (Nel *et al.*, 2006). Reactive oxygen species is a term used to describe radical and non-radical forms of high energy molecules containing oxygen such as hydroxyl radical, superoxide anion, singlet oxygen and hydrogen peroxide (Hajipour *et al.*; Saleh *et al.*, 2015). Naked IONs can release free iron II, which can be toxic to the bacterial cells as they catalyse the production of ROS in Fenton's reaction (Equations 1 and 2) (Ebrahiminezhad *et al.*, 2012b; Müller *et al.*, 2007) outside the cell, inside the cell or at the cell membrane (Saleh *et al.*, 2015).

$$Fe^{2+} + H_2O_2 \rightarrow Fe^{3+} + OH^{\bullet} + OH^{-} \quad (1)$$

$$Fe^{3+} + H_2O_2 \rightarrow Fe^{2+} + OOH^{\bullet} + H^{+} \quad (2)$$

Extracellularly ROS can disturb the delicate balance between oxidative stress and antioxidant defence of cells, resulting in membrane lipid peroxidation or protein oxidation leading to membrane leakage (Laha *et al.*, 2014; Müller *et al.*, 2007). Intracellular ROS results in DNA breakage, membrane lipid peroxidation and protein oxidation (Laha *et al.*, 2014; Müller *et al.*, 2007; Sies & Menck, 1992). This would ultimately lead to necrosis and apoptosis of cells (Müller *et al.*, 2007).

Another mechanism which causes nanoparticle toxicity is metal ion release from metal core. Released ions can increase the membrane permeability and induce the leakage of cellular content. Further, uptake of these ions by bacterial cells can result in disruption of DNA replication (Marambio-Jones & Hoek, 2010). The dissolution mechanism of iron oxide nanoparticles depends on their crystal size, crystallinity and crystalline phase (Waychunas *et al.*, 2005) with smaller IONs showing the highest solubility and iron bioavailability (Borcherding *et al.*, 2014). Apart from these, IONs have shown to change the shape of bacterial cells when the bacterial cells are trapped within nanoparticles (Chatterjee *et al.*, 2011).

2.14 Nanoparticles' interaction with bacteria

The interaction pattern between bacterial cells and IONs plays a key role in determining the antimicrobial activity of IONs. Surface attachment of IONs to the bacterial cell surface is mainly governed by electrostatic (Ansari *et al.*, 2009; Huang *et al.*, 2010b) or hydrophobic interactions (Huang *et al.*, 2010b; Li *et al.*, 2009). Naked IONs have a negative surface potential due to the attachment of OH groups to IONs in aqueous solution (Ebrahiminezhad *et al.*, 2012b; Mohapatra *et al.*, 2007). Therefore, the electrostatic repulsion between the negatively charged naked IONs and bacteria with polyanionic cell membranes will hinder the attachment of naked IONs to bacterial cells (Azam *et al.*, 2012) and would not, therefore, elicit

antimicrobial effects at lower concentrations (Chatterjee *et al.*, 2011). However, a higher concentration of IONs would elicit antimicrobial activity to some extent due to molecular crowding resulting in net interaction between IONs and bacteria (Arakha *et al.*, 2015). Further, the zeta potential of IONs can become positive or negative depending on the actual pH of the solution (Dias *et al.*, 2011). As opposed to naked IONs, IONs with positively charged groups will attach more readily to the bacterial surface and stronger interaction will result in enhanced ROS production (Azam *et al.*, 2012). Therefore, surface functionalisation of IONs with biocompatible coatings would change the interaction pattern between IONs and bacterial cells. Electrostatic forces are not the sole force for governing the interaction of IONs, and bacterial cells as IONs can easily attach onto the surfaces of bacterial cells using hydrogen bonds or hydrophobic interactions (Huang *et al.*, 2010b; Larsen *et al.*, 2007) as well as the nano-size effect (Li *et al.*, 2009). Li *et al.* (2009) suggest that IONs adsorbed on the bacterial cells surface do so mainly because of the nano-size effect. Some reports have shown that even surface modified negatively charged IONs could attach to negatively charged bacterial cell surface (Li *et al.*, 2009). On the other hand, bacterial cells are equipped with adhesion factors that mediate the attachment of bacterial cells to various substrates. These factors can also mediate the interactions of the bacterial surface with IONs (Ebrahiminezhad *et al.*, 2014).

Substantial research has been conducted to identify the key nanoparticle attributes related to nanoparticle-cell interaction and associated mechanisms of toxicity for planktonic cells. The relevance of this literature to nanoparticle-biofilm interaction is not well established as the biofilm environment and biofilm themselves are fundamentally different from their planktonic counterparts (Saleh *et al.*, 2015). The key differences between planktonic and biofilm cells are: (1) the planktonic cells

are normally in a homogenous environment (2) biofilm cells are exposed to different microenvironments within the biofilm matrix, and (3) biofilm cells generally produce more exopolysaccharides than the planktonic cells, especially at slow growth rates (Evans *et al.*, 1994; Saleh *et al.*, 2015).

The interaction between biofilms and nanoparticles, however, depends on the electrostatic properties of both nanoparticles and biofilms. This, in turn, may depend on the charge of the biofilm matrix and zeta potential of nanoparticles. The majority of bacteria have a polyanionic biofilm matrix due to the presence of uronic acid or ketal-linked pyruvate with carboxylic acid as functionalities (Hajipour *et al.*, 2012; Sutherland, 2001) and phosphate or rarely sulphate residues (Sutherland, 1990). This polyanionic matrix can potentially bind with positively charged metal ions and organic compounds through electrostatic interactions (Esparza-Soto & Westerhoff, 2003; Selvakumar *et al.*, 2014). Therefore, the exopolysaccharides (EPS) of biofilm matrices contribute directly to the properties of biofilms (Sutherland, 2001) by interacting with a wide range of molecular species (Sutherland, 2001). Production of EPS is governed by nutritional factors. The availability of carbon source and the balance between carbon and other limiting nutrients are said to greatly influence the amount of EPS synthesis within the biofilm (Sutherland, 2001). Nitrogen is said to be the preferred component which stimulates EPS production (Banik *et al.*, 2000). The conformation of many EPS has been elucidated by computer models, and according to these models, the charged groups are all on the exterior of the molecular chains and therefore can interact with ions and other charged molecules (Chandrasekaran & Thailambal, 1990).

The potential for the use of nanoparticles with appropriate size and concentration for controlling biofilm forming pathogens has been demonstrated by few studies. Sathyanarayanan *et al.* (2013) showed that IONs reduce biofilm growth of

Pseudomonas aeruginosa. In contrast, a study by Borcherding *et al.* (2014) has shown that IONs affect biofilm formation in a size-dependent manner where the smaller (2 nm) IONs have been shown to increase growth and biofilm formation significantly due to the release of soluble Fe^{3+} in comparison to larger (540 nm) IONs.

Biofilm formation has a distinct developmental pathway. In the first stage of biofilm formation, microbial cells attach to the surface for their proliferation. It can be speculated that the decoration of bacterial cells with nanoparticles would reduce the accessible functional groups on the microbial cell surface which are important for attachment thereby preventing microbial cells attaching to other surfaces in an aqueous solution and subsequent biofilm formation. The addition of nanoparticles with appropriate size and concentration to the medium would, therefore, affect biofilm formation and the spatiotemporal organisation of the biofilm. Further, the binding of nanoparticles to microbial cells would reduce the proximity to neighbouring cells. The close proximity of bacterial cells facilitates intercellular communication through quorum sensing to initiate biofilm formation and production of EPS. Therefore, binding of nanoparticles to bacterial cells might limit biofilm formation and EPS production by interfering with quorum sensing signalling among the bacterial cells. Nanoparticles can, therefore, be used to reduce biofilm formation as an alternative to existing killing methods that are used to eradicate microbial biofilms. This would be beneficial in fermentation as it would retain bacterial cell viability. However, as toxic effects of naked IONs have been reported on several cell lines (Ebrahiminezhad *et al.*, 2012b; Ebrahiminezhad *et al.*, 2015), surface functionalisation of IONs with biocompatible coatings would be a promising approach to control biofilm formation while maintaining bacterial cell growth and viability in industrial production systems.

2.15 Surface modification of iron oxide nanoparticles

The specific design and synthesis of nanoparticles create particular physicochemical properties which influence their behaviour. There are many problems associated with naked IONs, such as low stability, particle agglomeration as a result of a high surface area of IONs (Dias *et al.*, 2011), rapid biodegradation and alteration of magnetic properties when they are directly exposed to biological systems (Santra *et al.*, 2001). In order to stabilise IONs, prevent undesired particle agglomeration, optimise bio-interactions, to provide biocompatibility and monodispersibility, surface functionalisation of IONs is important. IONs are usually encapsulated in polymeric coatings such as polyethylene glycol (PEG), polyvinyl alcohol (PVA), polyacrylic acid (PAA), polylactide-co-glycolide (PLGA), polyethyleneimine (PEI) (Mahmoudi *et al.*, 2008), silane coupling agents such as 3-aminopropyltriethoxysilane (APTES), *p*-aminophenyltrimethoxysilane (APTS) and mercaptopropyltriethoxysilate (MPTES) (Wu *et al.*, 2008). Further to these, various polysaccharides such as agarose, alginate, carrageenan, chitosan, dextran, heparin, gum Arabic, pullulan and starch (Dias *et al.*, 2011), and non-polymeric substances such as gold, silica, amino acids and lipoamino acids have been used (Ebrahiminezhad *et al.*, 2012b; Gholami *et al.*, 2015; Wang *et al.*, 2015). Recent studies have shown that amine-functionalised nanoparticles have more biological benefits than naked particles due to their biocompatibility, surface activity and chemical simplicity (Ebrahiminezhad *et al.*, 2012b; Ebrahiminezhad *et al.*, 2015). Compounds such as L-lysine, L-arginine and 3-aminopropyltriethoxysilane (APTES), which introduce amine functional groups to the nanoparticles, can be used to coat negatively charged nanoparticles, increasing the chance of nanoparticles binding to the anionic cell membrane without difficulty. While providing active groups for the interaction with the bacterial cell

membrane, amine functionalisation would also stabilise the nanoparticles (Ebrahiminezhad *et al.*, 2015) and would prevent IONs losing magnetism and monodispersibility upon contact with air. Iron oxide nanoparticles coated with L-lysine have already been applied during the fermentation of MK-7 (Ebrahiminezhad *et al.*, 2016c). It has been shown that amino acid coating has no undesirable effect on the properties of IONs but would, however, inhibit the growth of magnetic nanoparticles resulting in smaller sized nanoparticles (Ebrahiminezhad *et al.*, 2016c). Nevertheless, smaller nanoparticles with a high surface area/volume ratio would offer more surface area for attachment on to the bacterial cell surface by electrostatic interactions. It has been reported that the presence of L-lysine coated IONs had no significant inhibitory effect on MK-7 production and cell growth of *Bacillus subtilis* (Ebrahiminezhad *et al.*, 2016c).

In comparison to L-lysine and L-arginine, coating of nanoparticles with APTES would prevent the oxidation of nanoparticles and would provide perfect protection for the crystal structure of nanoparticles (Ebrahiminezhad *et al.*, 2015). APTES is an aminosilane which is a common coupling agent used to functionalise silica surfaces (Asenath Smith & Chen, 2008). In addition, APTES would prevent the agglomeration of superparamagnetic iron oxide nanoparticles through steric repulsion (Sodipo & Aziz, 2014). The silicon shell, as well as the amino groups, would give good solubility and dispersibility for Fe_3O_4 particles in an aqueous medium (Huang *et al.*, 2008). Further, as the isoelectric point of IONs@APTES is above 9 (Bini *et al.*, 2012; Huang *et al.*, 2010b), when the pH of the bacterial culture medium/solution is below the isoelectric point, $-NH_2$ groups of IONs@APTES are protonated to form $–NH^{3+}$ giving a net positive surface charge for IONs@APTES. The presence of high density of cationic amine groups can promote strong electrostatic interaction with negatively charged sites on the bacterial cells (Huang

et al., 2010b). Further, APTES can be used to synthesise smaller IONs which are more sensitive to a magnetic field, fairly quickly (Ebrahiminezhad *et al.*, 2015). Furthermore, bacterial cells decorated with magnetic nanoparticles would offer the advantage of bioprocess intensification through immobilisation of bacterial cells in industrial fermentation.

2.16 Process intensification

Process intensification refers to "any chemical engineering development that leads to a substantially smaller, cleaner, safer and more energy efficient technology"(Stankiewicz & Moulijn, 2000, p. 23). This can be achieved either by decreasing the size of individual equipment or removing the number of operational units (Vaghari *et al.*, 2015). In bioprocesses, the downstream processes are generally involved with a large number of separation steps, and therefore at the industrial scale, the use of bioprocess is limited by size and capital cost. Usually, downstream processing is responsible for about 50–80% of the cost of biomolecules, and therefore, is a critical factor which determines the yield and the cost of production (Sirkar *et al.*, 2006). For a sustainable bioprocess, it is therefore imperative to intensify a process either through equipment intensification or process intensification. Among the many paths for process intensification lies the use of new separation strategies and the integration of reaction and separation (Vaghari *et al.*, 2015).

2.17 Integration of reaction and separation for process intensification

In industrial fermentation of MK-7 using freely dispersed *Bacillus subtilis*, bacterial cells need to be separated from the products after fermentation has taken place.

Typically, the first step of downstream processes is the cell separation step, which is carried out either by filtration or centrifugation (Sirkar *et al.*, 2006) and these steps usually result in loss of viability of cells. In contrast, using the magnetic properties of IONs, the immobilised microbial cells can be easily separated from the fermentation media without the loss of viability of the cells and the cells can then be re-used in the fermentation system (Figure 7). As this reduces the number of downstream processing steps, IONs can be used in bioprocess intensification, which leads to sustainable bioprocesses (Vaghari *et al.*, 2015).

Immobilisation and in situ magnetic separation techniques have been previously applied for dibenzothiophene desulfurizing bacteria. Dibenzothiophene contains a broad range of sulphur heterocyclic compounds that can be desulfurized via the non-invasive biodesulfurization approach under mild conditions (Li *et al.*, 2008). For biodesulfurization using whole cell biotransformation, magnetic separation facilitates the separation of bacteria from the culture medium easily and quickly and provides an alternative to the normal time-consuming and costly separation methods (Ansari *et al.*, 2009; Li *et al.*, 2009). Industrial application of magnetic nanoparticles in designing intensified MK-7 production has been demonstrated recently by Ebrahiminezhad *et al.* (2016b). IONs have shown a promising ability to immobilise *Bacillus subtilis* cells without showing any negative effect on MK-7 production and cell growth. This technology has also facilitated the in situ recovery of cells from the fermentation media with more than 95 % capture efficiency thereby reducing the number of bioprocess steps in MK-7 fermentation (Ebrahiminezhad *et al.*, 2016b). Immobilisation of the cells is, therefore one of the techniques that is used to improve the productivity of bioreactors (Akay *et al.*, 2005). However, as naked IONs have demonstrated antibacterial and bacteriostatic effects in a size and concentration-dependent manner (Arakha *et al.*, 2015; Chatterjee *et*

al., 2011), use of IONs with appropriate coating in industrial fermentation would offer combined advantages of submerged fermentation and re-usability of immobilised bacterial cells as well as enhanced MK-7 production by enhancing membrane permeability and facilitating mass transfer, which is discussed in the following section. This would, in turn, minimise the production cost.

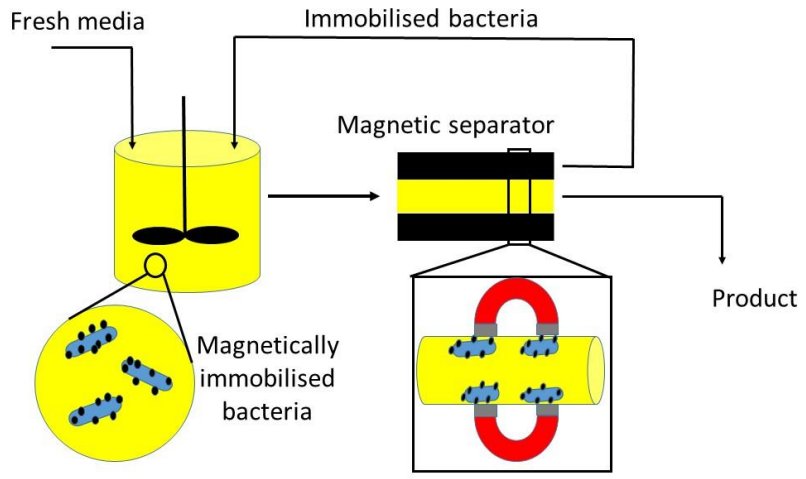

Figure 7 Schematic representation of magnetic immobilisation and separation of bacterial cells using IONs.

2.18 Improving mass transfer and metabolic activity of *Bacillus subtilis*

Maximising the MK-7 production while minimising the biofilm formation is a greater challenge in MK-7 fermentation. As MK-7 is a membrane-bound compound, changes in membrane-associated MK-7 production can be brought about by the modification in membrane structure/composition. In this regard, decoration of bacterial cells with biocompatible nanoparticles can be a promising approach for enhanced synthesis and secretion of MK-7, as the interaction of bacterial cells with nanoparticles can bring about changes in cell membrane permeability leading to improved mass transport and improved metabolic activity (Ansari *et al.*, 2009; Ebrahiminezhad *et al.*, 2016c). For example, in the process of biodesulfurization of

dibenzothiophene by the bacterium, *Rhodococcus erythropolis*, decoration of the bacterial cells with IONs (Fe_3O_4) has increased the dibenzothiophene desulfurization activity possibly by enhancing the membrane permeability and facilitating mass transfer (Ansari *et al.*, 2009). Similarly, in a *Bacillus subtilis natto* fermentation system, bacterial cells decorated with L-lysine coated IONs has found to be beneficial to the MK-7 yield compared to non-decorated bacterial cells possibly through the same mechanism (Ebrahiminezhad *et al.*, 2016c). Therefore, biocompatible and stable IONs can also be used to make the bacterial cells metabolically more efficient in MK-7 bioprocess.

Considering the great demand for MK-7 and low MK-7 yield in bacterial fermentation, magnetic immobilisation of *Bacillus subtilis* cells can also be coupled with novel approaches such as milking of MK-7 from the fermentation medium for further enhancing the production of MK-7. Opportunities for a MK-7 milking process for enhancing productivity is discussed in the next section.

2.19 Milking MK-7 in *Bacillus subtilis* fermentation

It has been recently reported that when bacterial cells are induced to excrete MK (MK-4) to the extracellular medium, the total MK production can be enhanced (Liu *et al.*, 2014). Menaquinones have been found to inhibit two regulatory enzymes, 3-deoxy-D-arabino-heptulosonate-7-phosphate (DAHP) synthase and shikimate kinase of shikimate biosynthesis pathway (Taguchi *et al.*, 1991). Therefore, by inducing the cells to excrete the excessive MK extracellularly, the level can be kept below the level of feedback inhibition of DAHP synthase and shikimate kinase thereby leading to improved total MK concentrations (Liu *et al.*, 2014).

It has also been reported that changes in bacterial cell membrane can result in an increase in oxygen uptake rate/ electron transport activity (Fletcher, 1983)

reflecting an adoptive response from the bacteria (Dhiman *et al.*, 2009; Ingram, 1976) which can, in turn, enhance MK-7 biosynthesis (Farrand & Taber, 1973). Such changes in cell membrane surface components and increased bacterial respiration rate upon treatment with alcohols is reported by Fletcher (1983). In view of the above, induced synthesis and secretion of MK-7 by bacterial cell immobilisation using biocompatible nanoparticles and periodic removal of MK-7 from the culture medium using biocompatible organic solvents can be a promising approach which would allow continuous and enhanced MK-7 production. In addition, periodic removal of MK-7 with biocompatible organic solvents without the need for disruption of the bacterial cells for MK-7 extraction would allow the bacterial cells to be reused for the production of MK-7. This method in which MK-7 is periodically extracted from the bacterial cells using biocompatible organic solvents and reuse of bacterial biomass for MK-7 production is termed 'milking' of *Bacillus subtilis* and is proposed as a novel technique to enhance the total MK-7 production. The term milking was used a par with the Milking of cows which essentially allows the biomass to be continuously reused for milk production, a principle previously used as a novel biotechnological process to milk products from organisms (Frenz *et al.*, 1989; Hejazi *et al.*, 2002; Hejazi *et al.*, 2004; Hejazi & Wijffels, 2004; Sauer & Galinski, 1998).

In the past, several approaches to enhance the MK-7 production has been attempted. However, no published data are available to date on minimising biofilm formation, maximising MK-7 production and at the same time reducing downstream processing steps which would improve the productivity of the system. This thesis provides insights on how best to address all these issues in order to improve the productivity of the system.

Chapter 3

Materials and Methods

3.1 Chemicals

Yeast extract, peptone from soy meal, calcium chloride, urea, absolute ethanol for analysis, 2-propanol, *n*-hexane, crystal violet ACS reagent, ammonium hydroxide, *n*-butanol, diethyl ether, petroleum ether, chloroform, 25% (*v*/*v*) glutaraldehyde solution, sodium cacodylate trihydrate, acetic acid glacial, hydrochloric acid 37% (AR grade), were obtained from Merck (USA). K_2HPO_4 was purchased from Scharlab S.L (Spain) glycerol, ferrous sulphate ($FeSO_4.7H_2O$), ferric chloride ($FeCl_3.6H_2O$) were purchased from Ajax Finechem (New Zealand). Sodium chloride and skim milk were obtained from a domestic supplier. Lipase enzyme was obtained from Novozymes (Denmark). Pure MK-7 standard (97.6%) was purchased from Chromadex (USA) for calibration and HPLC analysis. LIVE/DEAD BacLight assay kit L7012 was purchased from Invitrogen™, Molecular Probes Inc. Nutrient agar plates were obtained from Fort Richard Laboratories, New Zealand.

3.2 Bacterial culture

Bacillus subtilis (ATCC 6633), *Bacillus spheriucs* (NZRM 4381), *Bacillus licheniformes* (ATCC 9789) were obtained from the New Zealand reference culture collection. *Bacillus subtilis natto* was isolated from the commercial *natto* (Japanese fermented soybean).

3.3 Methods

3.3.1 Synthesis of naked iron oxide nanoparticles

IONs were synthesised by co-precipitation of ferric and ferrous ions with ammonium hydroxide under a nitrogen atmosphere as described in Ebrahiminezhad *et al.* (2016b). Briefly, $FeSO_4.7H_2O$ (0.74 g, 2.2 mmol) and $FeCl_3.6H_2O$ (1.17 g,

3.8 mmol) were dissolved in distilled water (50 mL) and the solution was vigorously stirred at 70°C under a nitrogen atmosphere. After 1 hour, ammonium hydroxide solution (5 mL) was injected rapidly into the mixture while stirring was continued. After 1 hour the resultant black precipitate was separated by centrifugation, washed with boiled distilled water, oven dried at 50°C overnight and stored under inert atmosphere (Figure 8).

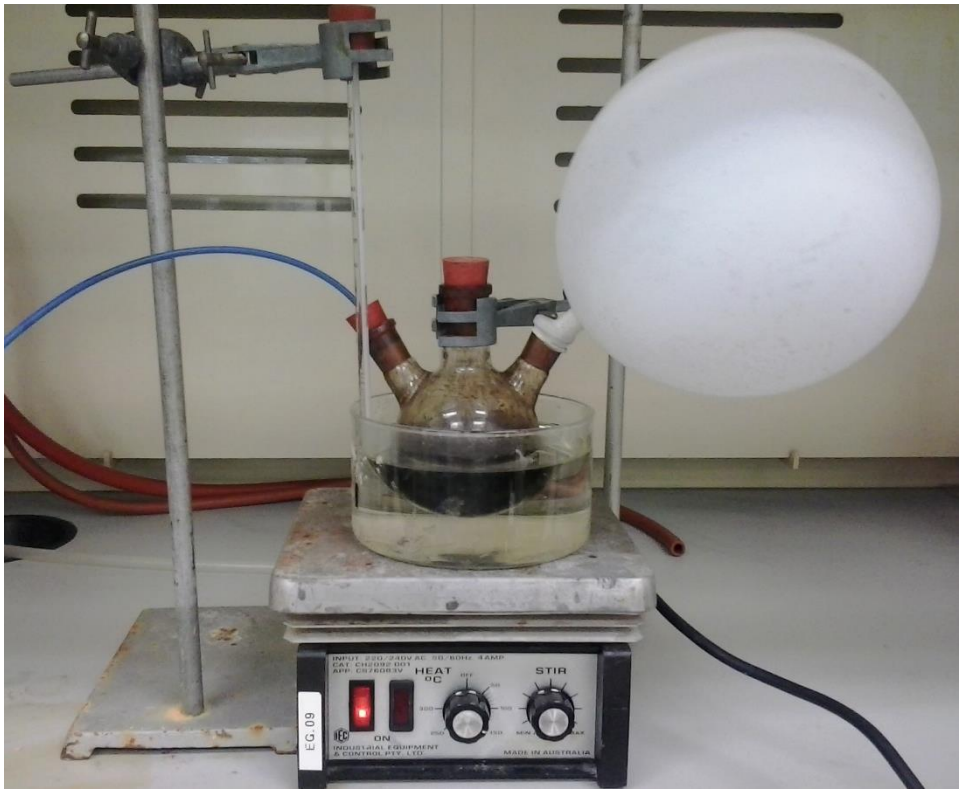

Figure 8 Reactor for the synthesis of superparamagnetic iron oxide nanoparticles.

3.3.2 Synthesis of APTES coated iron oxide nanoparticles

APTES coating was carried out as described in Ebrahiminezhad *et al.* (2015). Naked ION particles (0.7 g) were dissolved in ethanol: water, (1:1, *v/v*, 25 mL) and sonicated for 10 minutes to get a uniform dispersion while cooling in an ice bath. APTES solution (2.8 mL) was injected into the particle dispersion under an N_2 atmosphere while maintaining the temperature of the water bath at 40°C. The

reaction mixture was stirred for 2 hours at 40°C. Finally, the resulting particles were precipitated by centrifugation and washed with absolute ethanol and deionised water and oven dried at 50°C overnight (Figure 9).

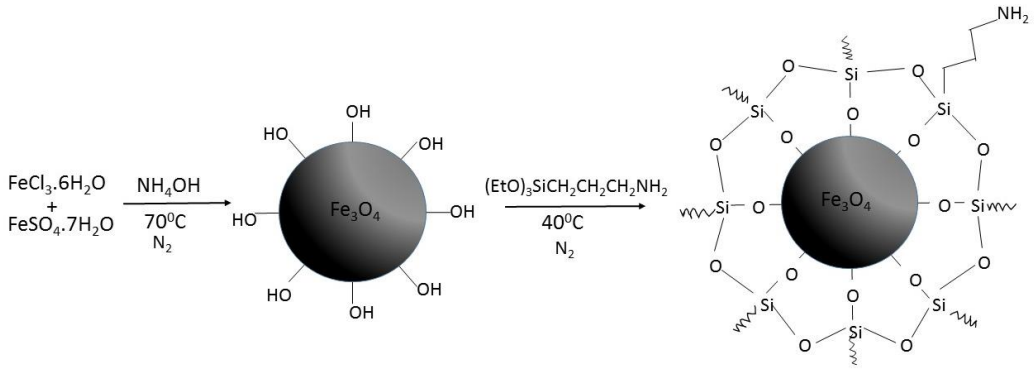

Figure 9 Depiction of IONs@APTES synthesis.

APTES facilitate surface functionalisation of Fe_3O_4 nanoparticles with -NH_2 groups

3.3.3 Characterisation of iron oxide nanoparticles

3.3.3.1 Transmission electron microscopy (TEM)

Particle size distribution and morphology of synthesised nanoparticles were studied by transmission electron microscopy (TEM) as described previously (Ebrahiminezhad *et al.*, 2012b). A drop of nanoparticle dispersion (100 μgmL^{-1} distilled water) was dripped on a carbon-coated copper grid and images of naked IONs and IONs@APTES were taken on a Philips, CM 10; TEM, operated at HT 100 Kv (Philips Electron Optics, Eindhoven, Netherlands).

3.3.3.2 Fourier transformed infrared spectroscopy (FTIR)

Fourier transform infrared (FTIR) spectra were obtained using a Bruker, Vertex 70, FTIR spectrometer Bruker, Kassel, Germany, in the range of 4000 to 400 cm^{-1}. For analysis KBr discs containing 1.5 mg sample and 15 mg of KBr were prepared (Ebrahiminezhad *et al.*, 2012b). Prior to making the KBR disc for infrared analysis, it was ensured that both the sample and KBr were dry. Sample and KBr were ground

in a mortar to form a fine homogenous powder. A compressed KBr disc was prepared using the SPECAC press.

3.3.3.3 X-ray powder diffraction (XRD)

X-Ray powder diffraction patterns were obtained using a Siemens D5000 Vibrating sample magnetometer with 2-Theta ranging between 20° and 90° after the ground sample was packed on a sample holder. Operating conditions include 0.0530° step size, 45 kV voltage, and a 40 mA current (Ebrahiminezhad *et al.*, 2012b).

3.3.3.4 Vibrating sample magnetometer (VSM) analysis

Magnetisation measurements were performed on a known volume of randomly dispersed set of magnetic colloid using a vibrating sample magnetometer (VSM) (Meghnatis Daghigh Kavir Co., Iran) at room temperature in an applied magnetic field sweeping between ± 10000 Oe (Ebrahiminezhad *et al.*, 2012b).

3.3.3.5 Analysis of nanoparticle size

Nanoparticle size analyses were carried out from the corresponding TEM images using ImageJ software version 1.47v, an image analysis software developed by the NIH (http://imagejnihgov/ij/). Particle size and size distribution of 100 particles of IONs@APTES and naked IONs taken randomly were analysed (Ebrahiminezhad *et al.*, 2012a).

3.3.4 The revival of freeze-dried cultures of bacteria and preparation of a stock solution

The outer surface of the ampoule was cleaned with 70% (*v*/*v*) ethanol and allowed to dry. The freeze-dried material was loosened from the glass by tapping the

ampoule gently on the bench. The ampoule was opened by scoring just above the cotton plug with a scissor. The opening of the ampoule was flamed and the cotton plug was removed with forceps. Fifty microlitres of 2% (*w*/*v*) Luria Bertani (LB) was poured into the ampoule and was stirred gently. The content was poured into 250 mL of LB in a shake flask and was incubated for 24 hours at 35°C with shaking at 100 rpm. This culture was taken as inoculum for plate cultures described in section 3.3.5.

In order to prepare stock cultures, the bacterial culture was centrifuged (3000 rpm, 10 minutes) in sterile 50 mL tubes and the cells were separated. Autoclaved glycerol (30%, *v*/*v*) and skim milk (70%, *v*/*v*) were added to the tubes and the tubes were kept in the refrigerator (20 minutes) and in the freezer (-20°C, 24 hours) and stored at -80°C until used.

3.3.5 Microorganism inoculum preparation

*Bacillus subtilis (*ATCC 6633) *Bacillus licheniformes* (ATCC 9789), *Bacillus sphericus* (NZRM 4381) cells were cultured on nutrient agar plates by spreading 100 µL of culture from the stock culture on the plates with an inoculation loop and incubating for 4 days at 37°C. *Bacillus subtilis natto* cells were grown in Luria-Bertani medium for 24 hours before streaking on nutrient agar plates and incubated at 37°C for 4 days for aseptic spore genesis. Plates were scraped after 4 days and a spore suspension was prepared by suspending the cells in 0.9% (*w*/*v*) sodium chloride solution and heating for 30 minutes at 80°C to inactivate the vegetative cells and produce spores. After removing the cell debris by centrifugation at 3,000 rpm a standard spore solution was obtained (Berenjian *et al.*, 2011). The optical density of the spore solution was measured with a UV spectrophotometer (UV-1700 PharmaSpec Shimadzu, Japan) at 600 nm.

3.3.6 Immobilisation of *Bacillus subtilis* (ATCC 6633) cells with naked and IONs@APTES

Naked IONs and IONs@APTES were dissolved in 2% (*w*/*v*) LB medium to obtain a stock solution of 10^5 g/mL and sonicated to get a uniform distribution. The stock solution was used to prepare the desired IONs@APTES (100-400 µg/mL). *Bacillus subtilis* cells were grown in 2% (*w*/*v*) LB medium up to a turbidity of $BaSO_4$ 0.5 McFarland standard (OD_{600} =0.1). McFarland suspension (0.5) was diluted 1:20 with fresh media according to the Clinical Laboratory Standards (Clinical and Laboratory Standards Institute, 2009) and mixed with nanoparticles to get the desired concentration (100-400 µg/mL) and incubated for 60 hours at 37°C with shaking at 120 rpm. Cultures without IONs served as controls. All experiments were conducted in triplicate. (Ebrahiminezhad *et al.*, 2012a).

$BaSO_4$ 0.5 McFarland standard is the turbidity standard for inoculum preparation according to the Clinical and Laboratory Standards Institute. McFarland standards are prepared by adding barium chloride to sulphuric acid in order to obtain a $BaSO_4$ precipitate and used to standardize the quantity of bacteria in a liquid suspension. Turbidity of the bacterial suspension is visually comparted with the turbidity of the McFarland standard and the bacteria are grown until it matches the standard. This protocol eliminates the incubation requirement to estimate the number of bacteria as in plate counting.

3.3.7 Scanning Electron Microscopy (SEM) analysis

Bacterial cultures (*Bacillus subtilis* ATCC 6633) were grown for 60 hours in the presence of varying concentrations of IONs@APTES, naked IONs and in the absence of nanoparticles as described in section 3.3.6. Air dried bacterial smear was heat fixed by passing through the flame of a Bunsen burner and fixed with 2.5%

(*v*/*v*) glutaraldehyde in 0.1M sodium cacodylate buffer with four changes over 30 minutes. Slides were rinsed with normal saline four times over 30 minutes and the cells were dehydrated through a series of alcohol concentrations (50%, 75%, and 95%, *v*/*v*) for one hour in each solution and four changes in absolute ethanol for 20 minutes (Kathi & Khan, 2013). Specimens were subjected to critical point drying (Poloron^{TM}) and the samples were then mounted on aluminium stubs and coated with platinum before examining with a Scanning Electron Microscope (Hitachi S-4700).

Glutaraldehyde (2.5%, *v*/*v*) was made by mixing one part of 25% (*v*/*v*) glutaraldehyde with nine parts of sodium cacodylate buffer. Sodium cacodylate buffer (0.1M) was prepared by dissolving of sodium cacodylate (21.41 g) in distilled water (900 mL), adding HCl (8 mL, 1N) and making up to 1000 mL with distilled water.

3.3.8 Confocal Laser Scanning Microscopy (CLSM) analysis

Biofilms were grown as described previously in 2% (*w*/*v*) LB in the presence of 100 µg/mL of IONs@APTES and in the absence of nanoparticles for 60 hours. Thereafter, biofilms were washed twice with 0.9% (*w*/*v*) NaCl and were stained with LIVE/DEAD staining. Stained biofilms were gently rinsed with 0.9% (*w*/*v*) NaCl. Two independent biofilms were prepared for each condition. Biofilms were observed using a 60 x oil immersion objective (60 x/1.35 O) and images were acquired in an Olympus FluoView FV1000 (Olympus, Lisboa, Portugal) confocal laser microscope. Maximum biofilm thickness was determined after calculating the thickness of 20 different regions from biofilms grown under each condition as described before (Cerca *et al.*, 2012).

3.3.9 Measurement of biofilm

Biofilm formation was evaluated using two methodologies: Crystal violet staining method (CVSM) (O'Toole *et al.*, 2000) and biomass of *Bacillus subtilis* (ATCC 6633) pellicle by weight (g).

3.3.9.1 Crystal violet staining method (CVSM)

In order to test the effect of IONs@APTES and naked IONs on biofilm formation *Bacillus subtilis* (ATCCC 6633) spores were grown up to $BaSO_4$ 0.5 McFarland standard in 2% (*w*/*v*) LB. McFarland suspension (0.5) was diluted 1:20 with fresh media according to the Clinical Laboratory Standards (Clinical and Laboratory Standards Institute, 2009) and mixed with NPs to get the desired concentration (100-400 µg/mL) and incubated at 37°C with shaking at 120 rpm for 60 hours. Cultures without NPs served as controls.

Biofilms were measured at OD 550 after staining with 0.05% (*w*/*v*) crystal violet as described in Robertson *et al.* (2013). Each tube was washed with distilled water several times and then immersed in 0.05% (*w*/*v*) crystal violet solution for 20 minutes. Stained biofilm was rinsed with water and dried. The resulting stained biofilm was immersed in 30% (*v*/*v*) glacial acetic acid solution for 20 minutes to extract the pigments. Titres (125 µL) from each well were transferred to a new microtitre plate and the level (OD) of the crystal violet present in the destaining solution was measured at 550 nm using 30% (*v*/*v*) acetic solution as a blank using Multiskan™ Go microplate spectrophotometer (Thermo scientific). Experiments were conducted in triplicate.

3.3.9.2 Biofilm biomass assay

Bacillus subtilis (ATCC 6633) cultured in 5% (*w*/*v*) yeast extract, 18.9% (*w*/*v*) soy peptone, 5% (*w*/*v*) glycerol and 0.06% (*w*/*v*) K_2HPO_4 were immobilised as described in section 3.3.6. Pellicles were harvested and dried in an oven for five hours at 40°C to constant weight before (5 hours) measuring the dry weight. The dry weight was taken using a 5-figure balance. Experiments were conducted in triplicate. The assay was based on pellicle weight assay as described in Beauregard *et al.* (2013).

3.3.10 Comparison of *Bacillus subtilis* (ATCC 6633) cell growth in the presence of naked IONs and IONs@APTES

In order to compare the effect of IONs@APTES and naked IONs on the growth of *Bacillus subtilis* (ATCC 6633), spores of *Bacillus subtilis* (ATCC 6633) were grown up to $BaSO_4$ 0.5 McFarland standard in 2% (*w*/*v*) LB. McFarland suspension (0.5) was diluted 1:20 with fresh media according to the Clinical Laboratory Standards (Clinical and Laboratory Standards Institute, 2009) and incubated at 37°C with shaking at 120 rpm for 60 hours with varying concentrations of nanoparticles (100-400 µg/mL)**.** Growth was measured at OD 600 nm (Ebrahiminezhad *et al.*, 2012a). *Bacillus subtilis* cultures without nanoparticles served as controls. Experiments were conducted in triplicate.

3.3.11 Live/dead viability assay

Bacterial cultures were grown in the presence of different concentrations of IONs@APTES (100-400 µg/mL) and naked IONs (100-400 µg/mL) for 60 hours as described in section 3.3.6. To reduce background staining bacterial cell pellets were washed with 0.9% (*w*/*v*) NaCl before staining with the LIVE/DEAD BacLight

assay kit L7012 (Invitrogen™, Molecular Probes Inc.) according to the manufacturer's protocol. Briefly, a combined reagent mixture of component A and component B was prepared by adding 30 µl of Component A to 30 µl of Component B. The amount of the dye solution applied to each sample for staining was 1/100 of the sample volume. The mixture was pipetted up and down for several minutes and incubated at room temperature in the dark for 15 minutes. Fluorescence intensity was measured at a wavelength centred at 530 nm (emission 1: green) for each well and with the excitation wavelength still centred at about 485 nm, fluorescence intensity was measured at a wavelength centred at 630 nm (emission 2: red). The ratio between Green/Red was calculated by dividing the fluorescence intensities at emission 1 by emission 2.

3.3.12 Epifluorescence microscopic analysis

Bacterial cultures (*Bacillus subtilis* ATCC 6633) were grown for 60 hours as described in section 3.3.6 and were stained with LIVE/DEAD BacLight stain before being subjected to fluorescence microscopy with a Leica DMRE epifluorescence microscope fitted with Plan Fluotar objectives and a mercury arc lamp. For blue excitation, a Leica I 3 filter set (excitation filter BP450-490 nm), a dichroic mirror (510 nm) and suppression filter LP 515 nm were used. For green excitation BP 515- 560 filter set, a dichroic mirror (580 nm) and a suppression filter LP 590 were used (Leica Microsystems, n.d.).

3.3.13 MK-7 extraction

The procedures for MK-7 extraction and sample purification were modified from previously described methods for quantifying K vitamins (Lambert 1992). Enzymatic hydrolysis of lipids was carried out before extraction by adding 1% (*w*/*v*)

lipase powder to the sample (3 mL), vortex mixing and incubating at 37°C for 45 minutes in a water bath. A mixture of ethanol: water (4:2, *v*/*v*) was added to the reaction mixture to denature proteins before extraction with a mixture of 2-propanol: *n*-hexane (volume ratio of media: 2- propanol: *n*-hexane was 3:2:1) by vigorously vortex-mixing for 1 minute. After vortexing, the mixture was centrifuged for 10 minutes at 3000 rpm and the upper hexane layer was separated into a new vial. One part of the upper *n*-hexane layer was mixed with two parts of 2-propanol (*v/v*) for HPLC analysis. Exposure to direct light was avoided during extraction to prevent the photolysis of MK-7.

3.3.14 Preparation of MK-7 standard

MK-7 standard (10 mg) (Chromadex) was measured and dissolved in a mixture of 2-propanol: *n*-hexane (2:1, *v/v*, 50 mL) in an "A" grade volumetric flask. Standards were stored at -20°C in the dark.

3.3.15 High-performance liquid chromatography (HPLC)

The high-performance liquid chromatography (HPLC) system was comprised of a Waters 2996 photodiode array detector (PDA), Rheodyne 7725i manual sample injector and two Waters 515 HPLC pumps (Waters, Co.UK). A Phenomenex Gemini C 18 column, 250 mm x 4.6 mm, ID 5 µm fitted with a security guard (Phenomenex) was used for separation and eluted with 2-propanol and *n*-hexane (2:1, v/v) at 0.5 ml/min. A 20 µl sample loop was used and the detection was carried out from 200-400 nm and the chromatogram was extracted at a wavelength of 248 nm. The concentration was calculated by peak area, using a standard curve from a serial dilution of a 200 µg/mL standard solution of MK-7 (Chromadex). A serial dilution approach was taken instead of making the separate standard solutions as it

needs a lot of MK-7 as starting material. Care was taken, however, when preparing serial dilutions to avoid an error propagating across succeeding standards. Waters Empower ™ chromatography software was used to control the system

3.3.16 Development and validation of HPLC method

3.3.16.1 Linearity

Linearity was determined by serial dilution of MK-7 standard to concentrations ranging from 200 µg/mL to 0.37 µg/mL (200, 100, 50, 25, 12.5, 6.25, 3.13, 1.56, 0.78, and 0.37 µg/mL) in 2-propanol: *n*-hexane (2:1, *v*/*v*). Analyses were repeated in triplicate (Shabir, 2005). The average peak areas were plotted against concentrations. The linearity of the proposed method was evaluated by using a calibration curve to calculate the coefficient of determination.

3.3.16.2 Accuracy/recovery

The accuracy of the analytical method was expressed by calculating the percent recovery (% R.S.D) of MK-7. The accuracy was evaluated by spiking a known amount of MK-7 (50 µg, 100 µg and 150 µg) to an aliquot of the sample which was conducted in four successive analysis ($n = 4$) (Kayesh *et al.*, 2013). Another aliquot of the same sample was analysed without spiking. Both samples were processed through the entire extraction and HPLC procedure. Percent recovery was calculated as follows:

$$\text{Percent recovery of MK-7} = \frac{\text{Mass of spike recovered}}{\text{Mass of spike added}} \times 100 \qquad (3)$$

3.3.16.3 Precision/reproducibility

In the current method development and validation protocol, the chromatographic precision was determined by five replicate injections each day at the concentration of 150 µg/mL of the standard MK-7 solution on 3 days and expressed as R.S.D % amongst responses using the formula (Kayesh *et al.*, 2013).

$$\text{R.S.D (\%)} = \frac{\text{Standard deviation}}{\text{Mean}} \times 100 \qquad (4)$$

3.3.16.4 HPLC Limit of Detection and Limit of Quantification test procedure

Limit of Detection (LOD) and Limit of Quantification (LOQ) were calculated from the standard deviation of the blank as described in (Shabir, 2005) using the following formula

$$\text{LOQ or LOD} = \frac{\text{F}}{\text{b}} \times \text{S} \qquad (5)$$

F = Factor of 3.3 and10 for LOD and LOQ respectively

SD = Standard deviation of the blank

b= Slope of the regression line

Estimated limits were verified by analysing 6 samples containing the analyte at the corresponding concentrations.

3.3.17 Analysis of MK-7 from bacterial extracts

Spores of *Bacillus subtilis* (ATCC 6633), *Bacillus subtilis natto, B. sphericus and B. licheniformes* were grown up to a turbidity of $BaSO_4$ 0.5 McFarland standard ($OD_{600\ nm}$ = 0.1). The McFarland suspension (0.5) was diluted 1:20 according to the Clinical Laboratory Standards (Clinical and Laboratory Standards Institute, 2009). Liquid state fermentation was carried out in medium consisted of 5% (*w/v*) yeast extract, 18.9% (*w/v*) soy peptone, 5% (*w/v*) glycerol, and 0.06% (*w/v*) K_2HPO_4. Cultures were grown at 37°C at 120 rpm for 60 hours before extraction of MK-7. Accordingly, MK-7 was extracted as described in section 3.3.13 and

analysed by high-performance liquid chromatography as described in section 3.3.15.

3.3.18 Analysis of MK-7 production by *Bacillus subtilis* (ATCC 6633) in the presence of IONs@APTES

Spores of *Bacillus subtilis* (ATCC 6633) were grown up to $BaSO_4$ 0.5 McFarland standard ($OD_{600\ nm}$ = 0.1) in 2% (*w*/*v*) LB. McFarland suspension (0.5) was diluted 1:20 with fresh media according to the Clinical Laboratory Standards (Clinical and Laboratory Standards Institute, 2009) and mixed with varying concentration of IONs@APTES (100-700 µg/mL) in 30 mL universals glass vials and incubated at 37°C with shaking at 120 rpm for 60 hours. Liquid state fermentation was carried out in a medium consisted of 5% (*w/v*) yeast extract, 18.9% (*w/v*) soy peptone, 5% (*w*/*v*) glycerol and 0.06% (*w/v*) K_2HPO_4. MK-7 was extracted by the method described in section 3.3.13 and MK-7 concentration was determined by the method described in section 3.3.15. Growth was measured by the optical density at 600 nm. MK-7 yield was calculated using the following equation:

$$\text{MK-7 yield} = \frac{\text{MK-7 concentration}}{\text{OD 600}} \qquad (6)$$

3.3.19 Time course of *Bacillus subtilis* fermentation in the presence of IONs@APTES

Spores of *Bacillus subtilis* (ATCC 6633) were grown up to $BaSO_4$ 0.5 McFarland standard in 2% (*w*/*v*) LB. McFarland suspension (0.5) was diluted 1:20 with fresh media according to the Clinical Laboratory Standards (Clinical and Laboratory Standards Institute, 2009) and grown in the M1 medium consisting of 5% (*w*/*v*) yeast extract, 18.9% (*w*/*v*) soy peptone, 5% (*w*/*v*) glycerol, 0.06% (*w*/*v*) K_2HPO_4 and 200 µg/mL of IONs@APTES in 30 mL universal glass vials. Cultures were incubated at 37°C with shaking at 120 rpm for 120 hours. Cell growth, pH, biofilm

biomass and MK-7 production were analysed at 12, 24, 36, 48, 60, 72, 84, 108 and 120 hours. Cell growth was measured by the optical density at 600 nm. The pH of the solution was measured by a pH meter. Biofilm biomass was measured by the method described previously in section 3.3.9.2. Extraction and analysis of MK-7 were carried out by the methods described in section 3.3.13 and 3.3.15 respectively. All experiments were carried out in triplicate.

3.3.20 Statistical analysis

The significant difference among the samples was determined through analysis of variance (ANOVA), using IBM SPSS statistics 24, with Dunnet's multiple comparison test to determine the statistical significance between each sample and control. When only two groups were compared, student's t-test was used to identify the statistically significant difference between the two groups. Mean values were considered significantly different at $p < 0.05$.

3.3.21 Experimental design for screening nutrient components which affect biofilm formation and MK-7 production

A full factorial design was used to study the individual and interactive effects of the potent factors on biofilm formation and MK-7 production. Sodium chloride, calcium chloride and urea were selected as potent factors. In all experiments, the growth medium consisted of 5% (*w*/*v*) yeast extract, 18.9% (*w*/*v*) soy peptone, 5% (*w*/*v*) glycerol and 0.06% (*w*/*v*) K_2HPO_4, which is the optimum medium previously described by Berenjian *et al.* (2011) for MK-7 production.

Bacillus subtilis (ATCC 6633) were grown up to $BaSO_4$ 0.5 McFarland standard ($OD_{600\ nm}$=0.1). McFarland suspension (0.5) was diluted 1:20 with fresh media and supplemented with varying concentrations of salts (NaCl and $CaCl_2$) and urea

according to the full factorial design. Cultures were grown at 37°C at 120 rpm for 60 hours before screening for MK-7 production and biofilm biomass.

3.3.22 Response surface optimisation of nutrient components

Response surface optimisation was conducted by a Central Composite Face design (CCD) implemented in MODDE software version 11 (UMetrics). Experimental conditions for the CCD are given in Table 8**.**

3.3.23 Time course of *Bacillus subtilis* fermentation in the presence of $CaCl_2$ and urea

McFarland suspensions of *Bacillus subtilis* (ATCC 6633) were prepared as described previously and incubated at 37°C and shaking at 120 rpm for 120 hours. In all experiments the growth medium consisted of 5% (*w*/*v*) yeast extract, 18.9% (*w*/*v*) soy peptone, 5% (*w*/*v*) glycerol, 0.06% (*w*/*v*) K_2HPO_4, 0.32% (*w*/*v*) $CaCl_2$ and 0.10% (*w*/*v*) urea. This medium is designated as M2. Cell growth, pH, biofilm biomass and MK-7 production were analysed as described previously at 12, 24, 36, 48, 60, 72, 84, 108 and 120 hours.

3.3.24 Time course of *Bacillus subtilis* fermentation in the presence of $CaCl_2$, urea and IONs@APTES

McFarland suspensions of *Bacillus subtilis* were prepared as described previously and incubated at 37°C and shaking at 120 rpm for 120 hours. In all experiments the growth medium consisted of 5% (*w*/*v*) yeast extract, 18.9% (*w*/*v*) soy peptone, 5% (*w*/*v*) glycerol, 0.06% (*w*/*v*) K_2HPO_4, 0.32% (*w*/*v*) $CaCl_2$, 0.10% (*w*/*v*) urea and 200 µg/mL IONs@APTES. This medium is designated as M3. Cell growth, pH biofilm biomass and MK-7 production were analysed at 12, 24, 36, 48, 60, 72, 84,

108, and 120 hours as described previously.

3.3.25 Growth and milking of MK-7 from *Bacillus subtilis* (ATCC 6633) cultures

Bacillus subtilis (ATCC 6633) cells were grown to $BaSO_4$ 0.5 McFarland standard ($OD_{600\ nm}$=0.1) McFarland dilutions (1:20) were grown for 40 hours before milking of MK-7 with organic solvents followed by incubation of the cultures at 37°C with shaking (120 rpm) and periodic extraction of MK-7 at 40, 48, 60, 72 and 84 hours. Fermentation media consisted of 5% (*w*/*v*) yeast extract, 18.9% (*w*/*v*) soy peptone, 5% (*w*/*v*) glycerol, 0.06% (*w*/*v*) K_2HPO_4, 0.32 % (*w*/*v*) $CaCl_2$, 0.1% (*w*/*v*) urea and 200 µg/mL IONs@APTES.

To investigate the effect of milking on MK-7 production, *n*-hexane and a mixture of *n*-butanol: *n*-hexane (1:2, *v*/*v*) were used as organic solvents. Milking of MK-7 from the fermentation medium was carried out by the addition of organic solvent/solvent mixture followed by vortex mixing for 1 minute and centrifuging twice at l000 rpm for 5 minutes for phase separation. The volume ratio of aqueous to organic was 1:1. To determine MK-7 in the organic phase, the upper organic phase was separated and evaporated to dryness under nitrogen gas and re-dissolved in a mixture of 2-propanol: *n*-hexane (2:1, *v*/*v*). MK-7 was analysed by the method described in section 3.3.15.

In the aqueous phase, MK-7 was extracted by the method described previously in 3.3.13 and analysed by HPLC as described in section 3.3.15.

Bacillus subtilis cultures grown under non-milking conditions served as control samples. McFarland dilutions (1:20) were grown for 40, 48, 60, 72 and 84 hours. At each time interval, MK-7 in control samples were determined in the same manner as MK-7 in the aqueous phase. All experiments were conducted in triplicate.

3.3.26 Measurement of bacterial cell viability upon milking with organic solvents

To assess the organic solvent tolerance of *Bacillus subtilis* (ATCC 6633), cells were grown to $BaSO_4$ 0.5 McFarland standard. McFarland suspension (0.5) was diluted with fresh media (1:20). Cultures were grown for 40 hours and were treated (milked) with MK-7 extraction solvents listed in Table 13 and Table 14 by vortex mixing for 1 minute and centrifuging twice at l000 rpm for 5 minutes for phase separation, followed by removal of the supernatant. The change in the viability of the bacterial cells was assessed before and after organic solvent treatment using the LIVE/DEAD assay described in section 3.3.11. All experiments were conducted in triplicate. *Bacillus subtilis* (ATCC 6633) cultures grown under non-milking conditions served as control samples.

Chapter 4

Synthesis and Characterisation of Naked and APTES Coated Iron Oxide Nanoparticles

This chapter forms the basis for the following publications:

Ranmadugala, D., Ebrahiminezhad, A., Manley-Harris, M., Ghasemi, Y., & Berenjian, A. (2017). The effect of iron oxide nanoparticles on *Bacillus subtilis* biofilm, growth and viability. *Process Biochemistry, 62*(1), 231-240.

Ranmadugala, D., Ebrahiminezhad, A., Manley-Harris, M., Ghasemi, Y., & Berenjian, A. (2017). Impact of 3–Aminopropyltriethoxysilane-Coated Iron Oxide Nanoparticles on Menaquinone-7 Production Using *Bacillus subtilis*. *Nanomaterials, 7*(11), http://dx.doi.org/10.3390/nano7110350.

4.1 Introduction

In successful immobilisation of *Bacillus subtilis* in industrial MK-7 production, the use of IONs with appropriate size, shape, concentration and surface functional molecules is of importance to preserve the integrity and viability of *Bacillus subtilis*, while achieving a high immobilisation efficiency. The most common method for the synthesis of superparamagnetic iron oxide nanoparticles is aqueous co-precipitation due to the simplicity of the synthesis and the possibility to obtain large quantities of NPs. This method was first reported by Welo and Baudisch (1925). Naked IONs, are however, recorded to aggregate to micron size clusters in suspension due to attractive Vander Waals (dispersion) forces and this minimises the total surface or interfacial energy (Dias *et al.*, 2011). Particle agglomeration can affect the level of toxicity exerted by IONs on *Bacillus subtilis*, since it changes the size, shape and the sedimentation properties of IONs (Chatterjee *et al.*, 2011). Therefore, post-synthesis modifications of naked IONs are sometimes necessary. It is believed that coating of naked IONs with 3-aminopropyltriethoxysilane (APTES) would protect the magnetic core against oxidation and would maintain the magnetic property of IONs (Mahmoudi *et al.*, 2011). Further, it is believed that APTES coating would sterically stabilise the IONs that would render the particles to be well-dispersed (Tiraferri *et al.*, 2008), which would be useful in industrial MK-7 production. In this regard, in the present work, IONs were first prepared via chemical co-precipitation and subsequently coated with APTES. Then the structure and magnetic properties of synthesised naked IONs and APTES coated iron oxide nanoparticles were investigated using transmission electron microscopy (TEM), Fourier transformed infrared spectroscopy (FTIR), X-ray powder diffraction (XRD) and vibrating sample magnetometry (VSM).

4.2 Results

4.2.1 Synthesis of naked and APTES coated iron oxide nanoparticles

Naked IONs were synthesised by the chemical co-precipitation method described in section 3.3.1 and subsequently coated with APTES as elaborated previously in section 3.3.2.

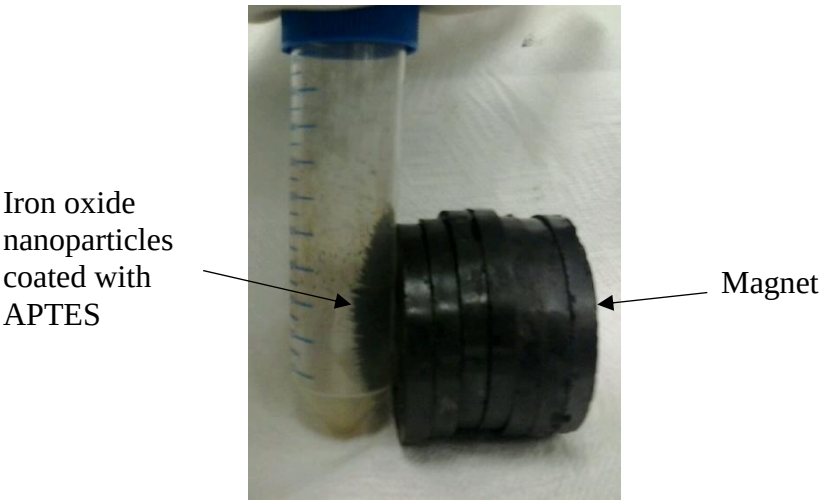

Figure 10 Synthesised IONs@APTES showing magnetic properties in the presence of an external magnetic field.

Chemical co-precipitation resulted in a black precipitate of naked IONs which was separated magnetically and washed with distilled water. The synthesised naked IONs were subsequently coated with APTES. The resultant black precipitate responded well to a permanent magnet indicating good magnetic properties in the presence of an external magnetic field (Figure 10).

4.2.2 Characterisation of naked and APTES coated iron oxide nanoparticles

Characterisation of synthesised IONs (naked IONs and IONs@APTES) was carried out using transmission electron microscopy (TEM), Fourier transform infrared spectroscopy (FTIR), and X-Ray powder diffraction (XRD). Magnetisation measurements were conducted using a vibrating sample magnetometer (VSM).

4.2.2.1 Transmission electron microscopy

The morphology, sizes and the distribution of IONs were determined by TEM by randomly measuring the diameter of 100 particles.

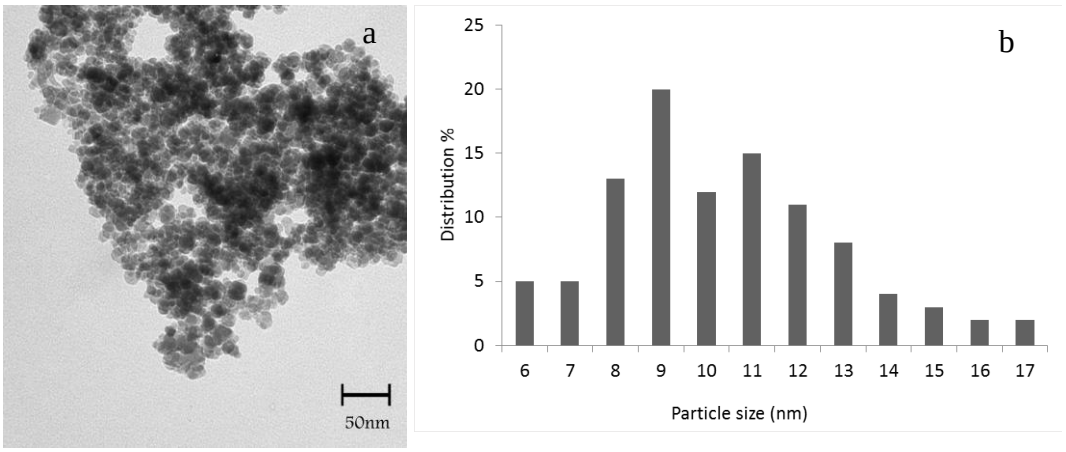

Figure 11 Transmission electron micrograph (a) and particle size histogram (b) of naked IONs.

TEM analysis of naked IONs revealed the production of fairly uniform spherical particles (Figure 11-a) with particle size distribution of naked IONs ranging from 5.728 to17.198 nm. The average particle size was10.37 ± 3.6 nm (Figure 11-b).

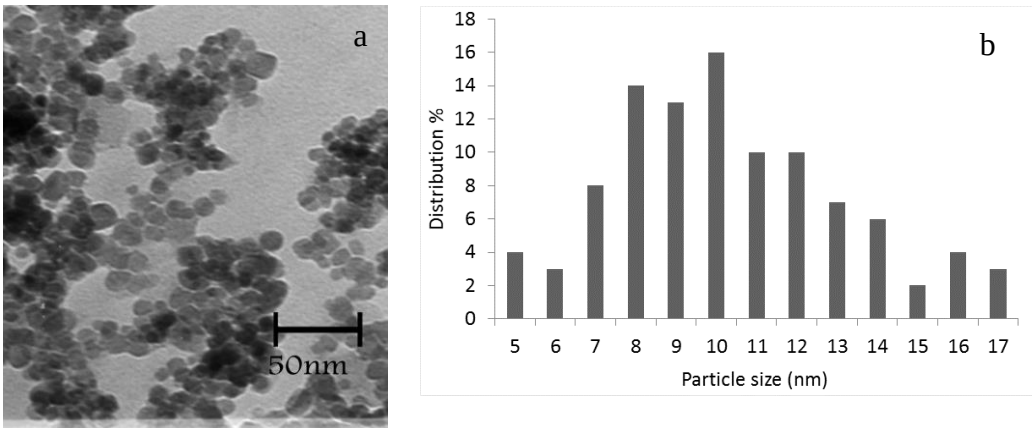

Figure 12 Transmission electron micrograph (a) and particle size histogram (b) of IONs@APTES.

TEM analysis of IONs@APTES also revealed the production of fairly uniform spherical particles (Figure 12-a) with particle size distribution of IONs@APTES

ranging from 4.451 to 17.356 nm and an average size of 10.33 ± 3.9 nm **(**Figure 12-b).

4.2.2.2 Fourier Transform Infrared spectroscopy

In order to find proof for amine functionalisation, FTIR analysis of naked IONs and IONs@APTES was carried out (Figure 13).

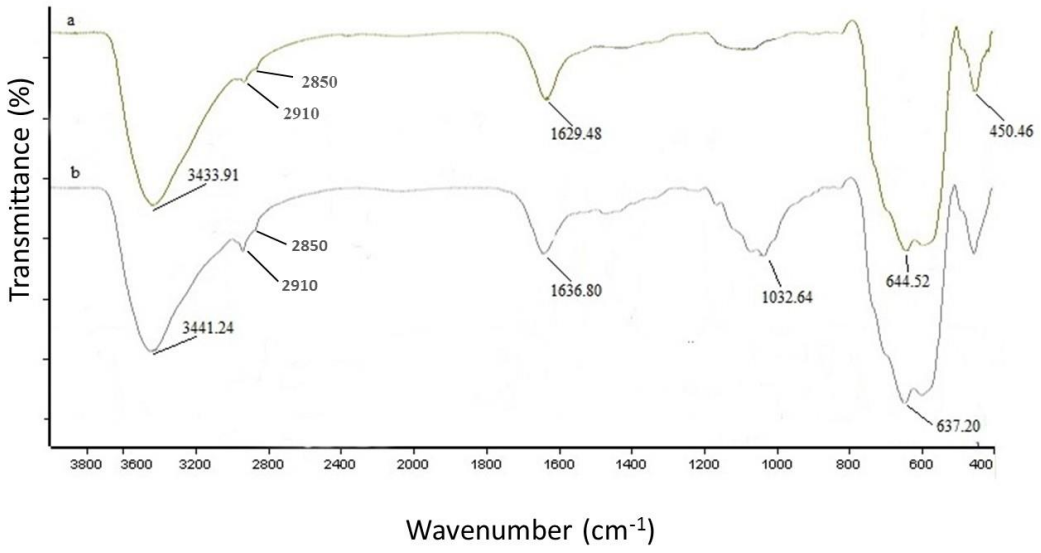

Figure 13 Fourier transform infrared spectroscopy (FTIR) spectra of naked IONs (a) and IONs@APTES (b).

According to FTIR analysis, the Fe-O characteristic peaks of IONs@APTES and naked IONs appeared at ~640 cm^{-1}. In IONs@APTES, the Si-O bond stretching vibration appeared at 1032.64 cm^{-1}. Stretching vibrations of –OH groups appeared at ~3400 cm^{-1} as a broad, characteristic peak, and O-H bending resulted in a peak at ~1630 cm^{-1}. In IONs@APTES, peak at 3441.24 cm^{-1}, corresponds to free amino groups on the IONs@APTES which can be overlapped by O-H stretching vibrations. The peaks at 2910 and 2850 cm^{-1} correspond to the asymmetric and symmetric –C-H stretching vibrations and are indicative of the presence of aliphatic $–CH_2$ groups.

4.2.2.3 Vibrating sample magnetometer

A vibrating sample magnetometer was employed to determine the magnetisation strength of NPs, and saturation magnetisation analysis results are presented in Figure 14.

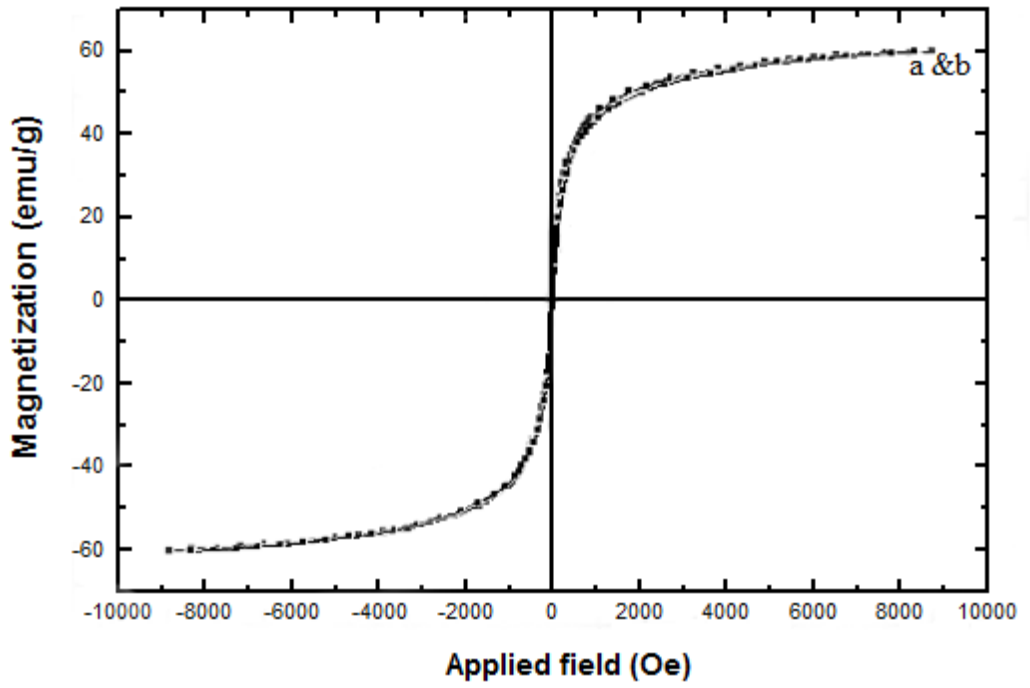

Figure 14 Vibrating sample magnetometer (VSM) diagrams of naked IONs (a) and IONs@APTES (b).

According to the VSM measurements, no hysteresis was seen and magnetisation curves were completely reversible demonstrating the superparamagnetic behaviour of the particles. The saturation magnetisation (Ms) values were found to be 60 emu/g for both naked IONs and IONs@APTES.

4.2.2.4 X-Ray powder diffraction

Powder X-ray diffraction (XRD) studies were performed between 20° and 90° with a Siemens D5000 vibrating sample magnetometer.

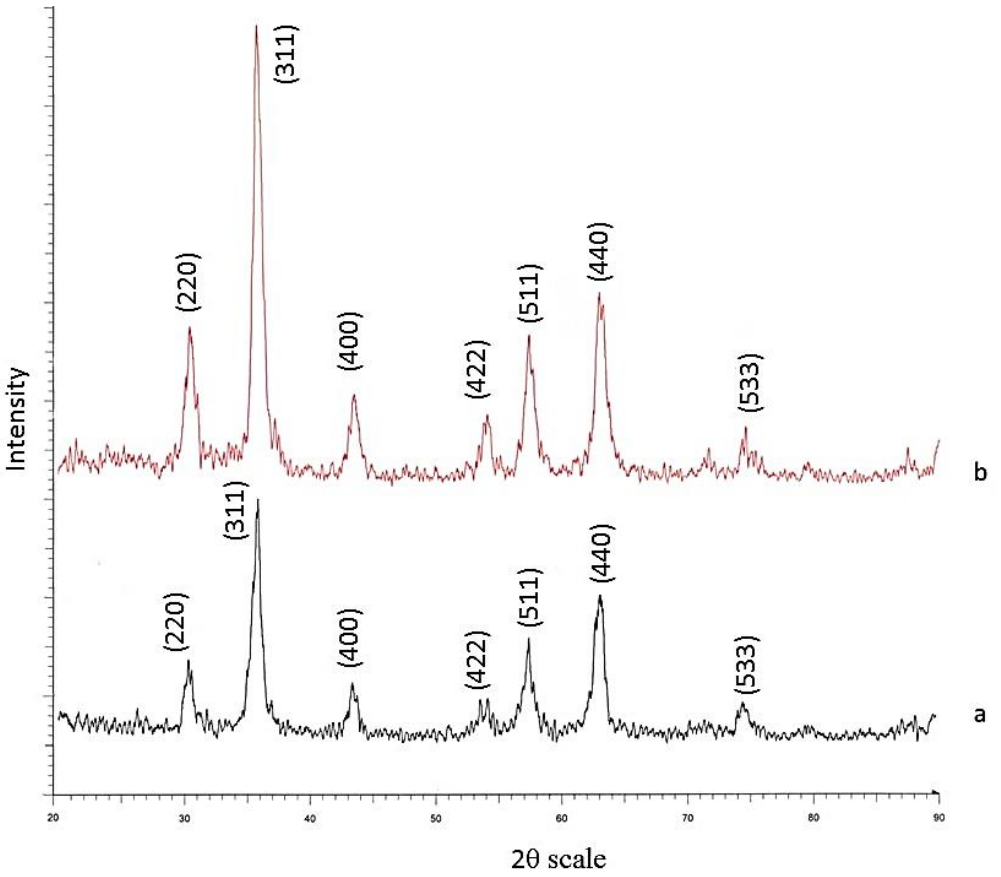

Figure 15 X-ray powder diffraction patterns of naked IONs (a) and IONs@APTES (b).

X-ray powder diffraction patterns of the nanoparticles showed intensity peaks at 2θ degrees of 30°, 35.5°, 43°, 54°, 57° and 63° for both naked IONs and IONs@APTES (Figure 15).

4.3 Discussion

Preparation of surface functionalised IONs has been regarded as a great challenge; however, here we report the synthesis of superparamagnetic Fe_3O_4 NPs with high magnetisation, smaller size and fairly narrow size distribution. Preparation of nanoparticles in this study with chemical co-precipitation method was a simple operation. Naked IONs were prepared by chemical co-precipitation and were subsequently coated with 3-aminopropyltriethoxysilane (APTES) in order to improve the biocompatibility of magnetic IONs, reduce aggregation and reduce

toxicity. Although the co-precipitation method generally results in a wide range of particle size distribution (Dias *et al.*, 2011), making them non-ideal for many applications, the synthesised Fe_3O_4 nanoparticles by co-precipitation by addition of NH_4OH to an aqueous solution of Fe^{2+}/Fe^{3+} in 1:2 stoichiometry under inert atmosphere were of fairly uniform and narrow size distribution with an average size of 10.37 ± 3.6 nm. This is in agreement with the average diameters typically reported by the chemical co-precipitation method which is below 50 nm (Reddy *et al.*, 2012). The mean diameter of synthesised IONs@APTES was 10.33 ± 3.9 nm. According to the results of the present study, the average size of both naked and IONs@APTES were more or less the same. Sundar *et al.* (2014) record an increase in the size of naked IONs upon coating with APTES while Ebrahiminezhad *et al.* (2015) report no size difference upon coating with 3-aminopropyltriethoxysilane. An average size less than 11 nm for both naked and IONs@APTES would, however, enable their better interaction with *Bacillus subtilis* cells.

Any biological application of magnetic nanoparticles requires that these nanoparticles having a high magnetisation value and a smaller size. Based on theoretical calculations, the critical particle size of ferromagnetism of magnetite is said to be ca. 25 nm and a decrease in saturation magnetisation is reported when there is a decrease in particle size of magnetite below 25 nm thereby particles becoming superparamagnetic (Dorniani *et al.*, 2014; Lee *et al.*, 1996; Sato *et al.*, 1987). The magnetite particles synthesised in this study was less than 25 nm and therefore they are expected to be superparamagnetic. This was evident from the VSM measurements, where no hysteresis was seen and magnetisation curves were completely reversible demonstrating the superparamagnetic behaviour of both naked and IONs@APTES. In this study, coating of IONs with APTES did not affect the magnetic properties of iron oxide nanoparticles in agreement with the previous

studies (Can *et al.*, 2009; Ebrahiminezhad *et al.*, 2015). The saturation magnetisation values were found to be 60 emu/g for both naked IONs and IONs@APTES which were lower than that of bulk magnetic particles (92 emu/g) (Sato *et al.*, 1987). Some studies, however, record a small decrease in the saturation magnetisation value when IONs are coated with APTES. For example, Sundar *et al.* (2014) record 56 and 50 emu/g of saturation magnetisation for naked and IONs@APTES, respectively. Similar reduction in saturation magnetisation upon coating of IONs have been reported by few other studies (Ebrahiminezhad *et al.*, 2012b; Huang *et al.*, 2010b; Shen *et al.*, 2004). The reduction in magnetic saturation values are thought to be caused by surface characteristics of nanoparticles, such as the formation of a magnetically inactive layer on the nanoparticle surface (Sato *et al.*, 1987). It has been reported that some of the surface coatings of IONs can contribute as a non-magnetic mass to the total sample volume thereby reducing the saturation magnetisation (Can *et al.*, 2009; Ebrahiminezhad *et al.*, 2012b; Huang *et al.*, 2010b). The degree of the decrease in saturation magnetisation has been related to the density, thickness or the intensity of the inactive layer, with high intensities leading to more reduction in saturation magnetisation (Ebrahiminezhad *et al.*, 2012b; Sato *et al.*, 1987).

X-Ray powder diffraction patterns of naked IONs and IONs@APTES were in agreement with characteristic features of the magnetite showing pure cubic structure (Joint Committee on Powder Diffraction Standards database PDF No. 65-3107) (Ebrahiminezhad *et al.*, 2012b; Grumezescu *et al.*, 2014; Si *et al.*, 2004) with intensity peaks appearing at 2θ degrees of 30°, 35.5°, 43°, 54°, 57° and 63°, indicating the presence of predominantly Fe_3O_4. The presence of intensity peaks at 2θ degrees 30°, 35.5°, 43°, 54°, 57° and 63° in the X-ray powder diffraction pattern of IONs@APTES revealed that the surface coating with APTES did not affect the

crystal structures of magnetite.

FTIR spectroscopy provides valuable information regarding surface modifications of IONs. As shown in Figure 13-a and 13-b, Fe-O stretching vibrations at ~ 640 cm^{-1} for naked IONs and IONs@APTES, O-H stretching vibrations at ~ 3400 cm^{-1} and O-H deformed vibrations ~ 1630 cm^{-1} for both naked and IONs@APTES, suggest that O-H groups coat on the surface of IONs as reported previously (Ebrahiminezhad *et al.*, 2012b; Shen *et al.*, 2004). In IONs@APTES, peak at 3441.24 cm^{-1}, corresponds to the presence of free amino groups which can be overlapped by O-H stretching vibrations (Can *et al.*, 2009; Ebrahiminezhad *et al.*, 2012b; Shen *et al.*, 2004). The peak appearing at 1032.64 cm^{-1} in IONs@APTES corresponding to Si-O stretching vibrations reveals that covalent bond of Fe-O-Si are formed after APTES coating (Ebrahiminezhad *et al.*, 2015; Shen *et al.*, 2004). The results of the FTIR analysis therefore show that the IONs have been successfully coated with APTES. This would allow better dispersion of the IONs in aqueous media and would protect them from leaching in an acidic or basic medium (Huang *et al.*, 2010b). Therefore, APTES coating can be seen as a good candidate for surface modification of magnetite nanoparticles.

4.4 Summary

Uniform spherically shaped superparamagnetic Fe_3O_4 nanoparticles with the high magnetisation of 60 emu/g and fairly narrow size distribution were synthesized and successfully coated with 3-aminopropyltriethoxysilane. Both naked IONs and IONs@APTES exhibited well-defined superparamagnetic behaviour. From the investigations on the particle sizes and magnetisation responses, it can be concluded that chemical co-precipitation by addition of NH_4OH to an aqueous solution of Fe^{2+}/Fe^{3+} in 1:2 stoichiometry under an inert atmosphere is a possible robust method

to synthesise sufficiently small nanoparticles with fairly narrow size distribution and high magnetisation.

These outstanding physicochemical properties of IONs such as superparamagnetism, great surface area to volume ratio and their smaller size would allow good cell adhesion. Therefore, the synthesised nanoparticles can be a promising candidate to immobilise bacteria and study their effect on the growth, viability and biofilm formation in *Bacillus subtilis* fermentation, which will be discussed in the next chapter.

Chapter 5

The Effect of Iron Oxide Nanoparticles on *Bacillus subtilis* Biofilm, Growth and Viability

This chapter forms the basis for the following publication:

Ranmadugala, D., Ebrahiminezhad, A., Manley-Harris, M., Ghasemi, Y., & Berenjian, A. (2017). The effect of iron oxide nanoparticles on *Bacillus subtilis* biofilm, growth and viability. *Process Biochemistry*, *62*(1), 231–240.

5.1 Introduction

One of the major problems with the use of *Bacillus subtilis* in industrial fermentation is the formation of biofilms by this bacterium (Berenjian *et al.*, 2013) which leads to many process and operational complications. Biofilm formation in industrial MK-7 production leads to many process complications, such as limited mass transfer, decreased metabolic activity (Stewart & Franklin, 2008), costly periodic cleaning (Beech & Sunner, 2004) and corrosion of equipment (Gibson *et al.*, 1999). In good manufacturing practice, countermeasures against biofilms are therefore critical in order to improve the process performance. Common strategies for biofilm control are the use of biocides and disinfectants (Simões *et al.*, 2010) which control biofilm formation by killing the microorganisms. However, in industrial production of MK-7, it is of the utmost importance that the removal strategy for biofilm should not affect bacterial cell viability. Bacteria are said to be viable when in the presence of intact and functional nucleic acids as well as in the presence of an intact and polarised cytoplasmic membrane (Hammes *et al.*, 2010). Iron oxide nanoparticles have previously been tested for biofilm control taking into account their antibacterial propensity. However, when IONs are used for biofilm control in the industrial production of MK-7 by *Bacillus subtilis,* the interaction pattern between IONs and *Bacillus subtilis* at the bacterial nanoparticle interface should not affect the growth and viability of bacterial cells. Obviously, the higher the interaction/adsorption of *Bacillus subtilis* onto NPs, the higher the efficiency of immobilisation and the advantages in intensifying downstream processes for industrial MK-7 production. Nevertheless, strong contact of NPs with bacterial cell membrane can sometimes disturb bacterial metabolism (Auffan *et al.*, 2008) mainly due to the induction of oxidative stress by reduced Fe species. On the contrary, there are many other instances where strong adsorption of IONs on to bacterial surface

have not disturbed the integrity of the bacterium, which was further used for intended applications (Ebrahiminezhad *et al.*, 2016c). Further, there are instances where IONs have induced shifts in the biofilm microbial community possibly due to changes in nutrient availability or chemical gradient within the biofilm matrix (Ikuma *et al.*, 2015), making it difficult to generalise the effect of IONs on bacteria. For a particular cell line, therefore IONs can be growth promoting or cytotoxic mainly depending on the concentration, size and surface properties of IONs. Therefore, this chapter aims to evaluate the effect of the synthesised nanoparticles (naked and IONs@APTES) on *Bacillus subtilis* biofilm formation growth and viability in order to open up a new domain for designing an intensified MK-7 production process with reduced biofilm formation.

5.2 Results

5.2.1 Preliminary description of *Bacillus subtilis* (ATCC 6633) biofilm formation

Bacillus subtilis growing in Luria-Bertani (LB) broth produced a biofilm within one day, located at the air-liquid interface with attachment to the vial walls at the meniscus region (Figure 16 a). When grown in the nutrient-rich medium previously described as the optimum media for MK7 production (Berenjian *et al.*, 2011), it produced a biofilm consisting of a large, viscous mass (Figure 16 b).

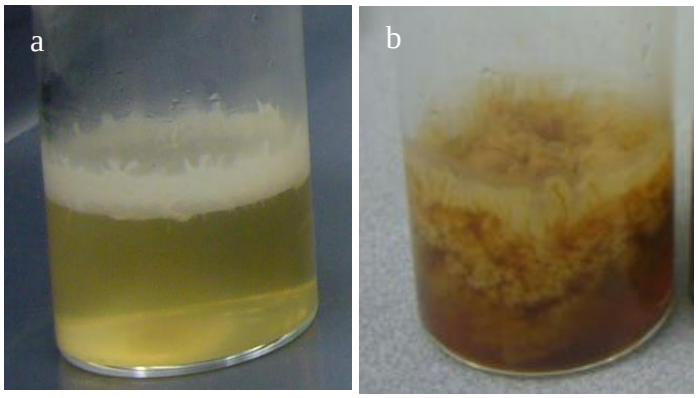

Figure 16 Images of biofilm formation of *Bacillus subtilis* (ATCC 6633) in Luria- Bertani (LB) broth (a) and in the optimum nutrient-medium previously described by Berenjian *et al.* (2011) (b).

5.2.2 Interaction of IONs with *Bacillus subtilis* (ATCC 6633)

In order to study the interactions of IONs with *Bacillus subtilis*, naked IONs and IONs@APTES were prepared as described in section 3.3.1 and 3.3.2. *Bacillus subtilis* (ATCC 6633) cells were immobilised with different concentrations of IONs as described in section 3.3.6. Scanning Electron Microscopy was used to visualise the interaction of IONs with bacteria (section 3.3.7). Figure 17 represents *Bacillus subtilis* cells growing in the presence of IONs@APTES and naked IONs in comparison to *Bacillus subtilis* cells growing in the absence of nanoparticles (control). Both IONs@APTES and naked IONs were found attached to *Bacillus subtilis* cells as shown in Figure 17; however, *Bacillus subtilis* cells were more densely coated with IONs@APTES in comparison to naked IONs. Interaction of NPs with *Bacillus subtilis* did not appear to cause disruptions to the bacterial cell membrane.

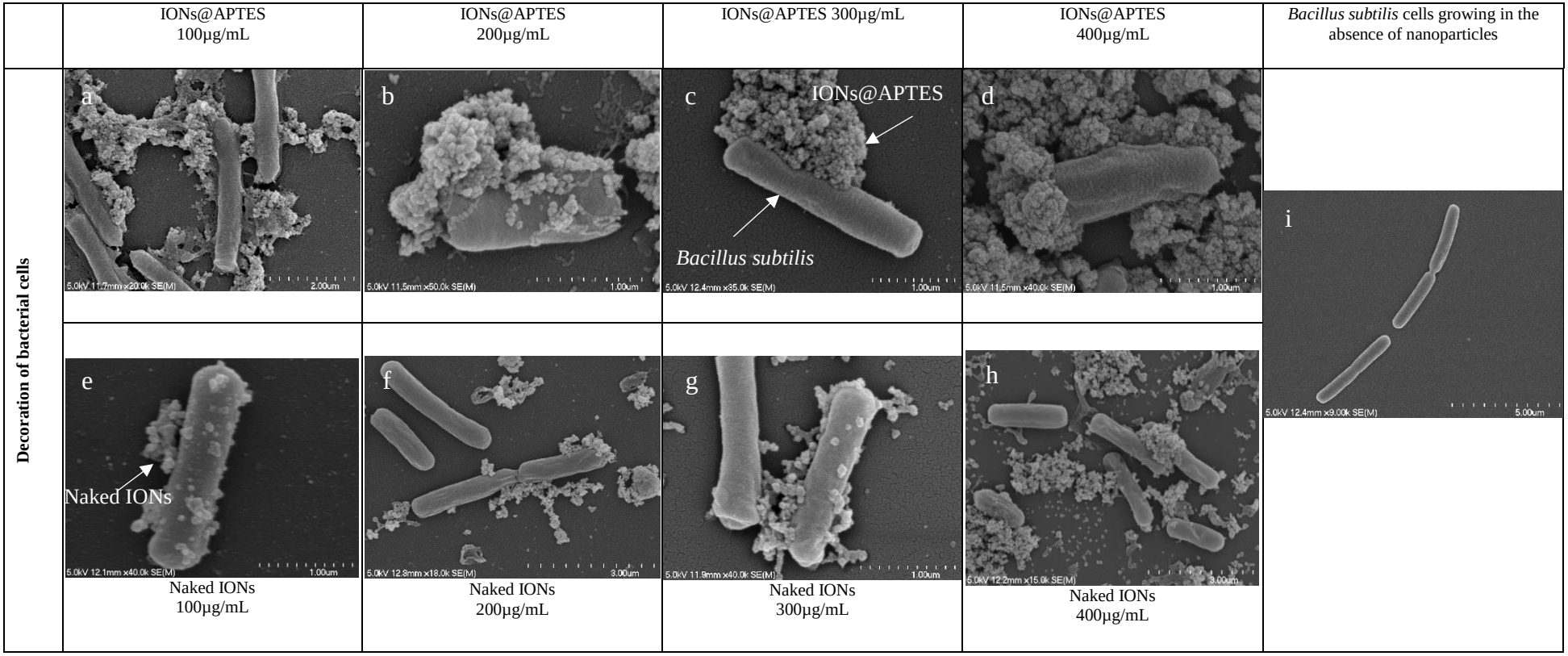

Figure 17 Scanning electron micrographs of *Bacillus subtilis* (ATCC 6633) decorated with IONs@APTES (a-d), naked IONs (e-h) and *Bacillus subtilis* cells growing in the absence of nanoparticles (i) after 60 hours of fermentation. *Bacillus subtilis* cells growing in the absence of nanoparticles are about to undergo division.

However, cultures were found to be heterogeneous in cell morphology. Interestingly, morphological changes, such as increased cell length in some of the cells, were seen in cultures grown in the presence of IONs@APTES and naked IONs as well as in the absence of nanoparticles (Figure 18). Some cells were bent and curved. However, these cells were viable as assessed by fluorescent microscopy. These novel morphs could be readily differentiated from the ancestral short rods of *Bacillus subtilis*. Staining of *Bacillus subtilis* (ATCC 6633) cells with LIVE/DEAD stain revealed that long cells are composed of multiple undissociated cells which are septated (Figure 19).

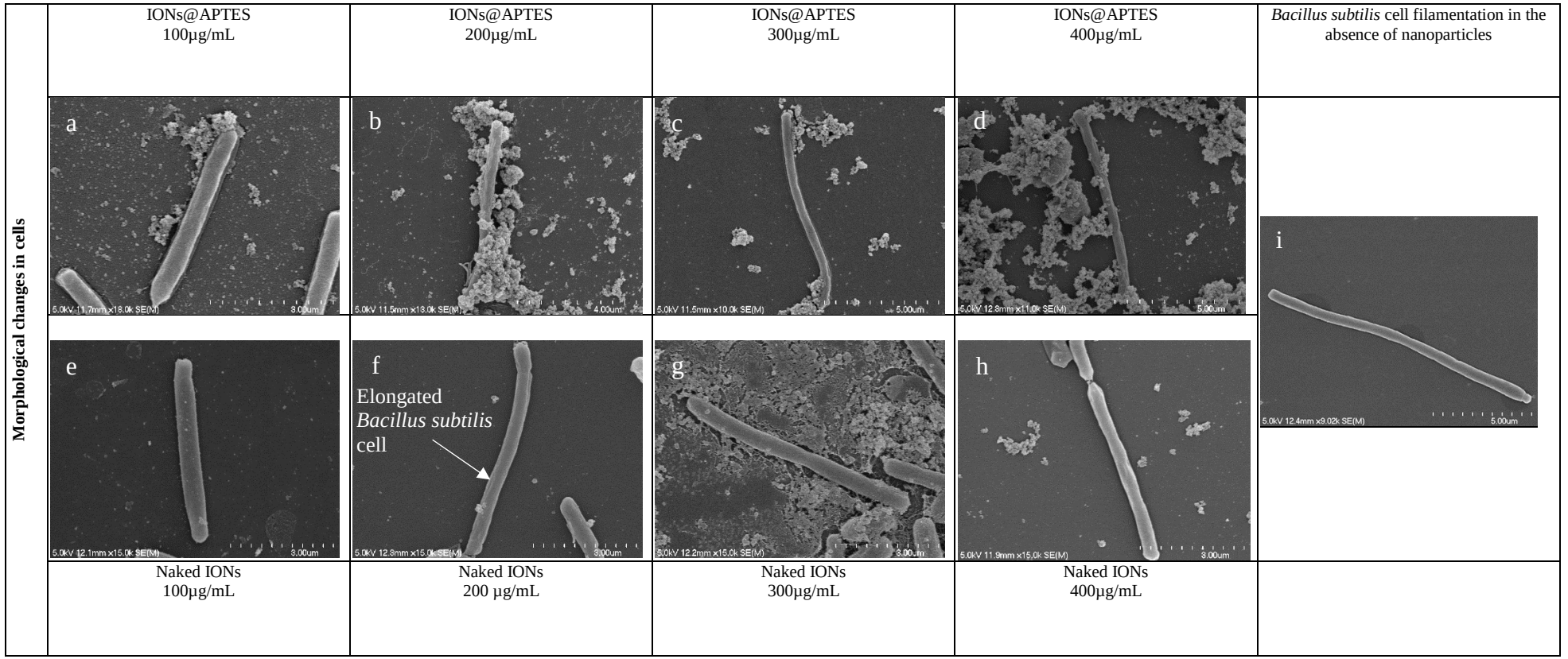

Figure 18 Scanning electron micrographs of *Bacillus subtilis* (ATCC 6633) showing increased cell length in the presence of IONs@APTES (a-d), naked IONs (e-h) and in the absence of nanoparticles (i) after 60 hours of fermentation.

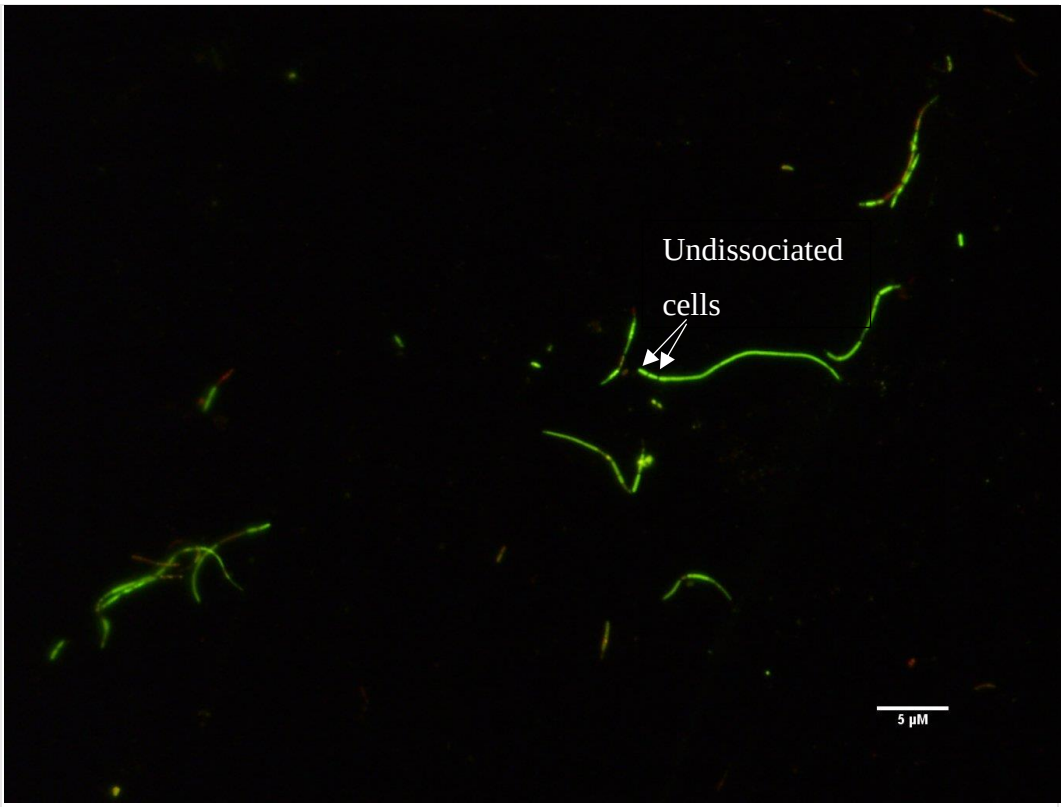

Figure 19 Epifluorescence microscopic image of *Bacillus subtilis* (ATCC 6633) cell filamentation in the absence of nanoparticles after 60 hours of fermentation. Scale bar indicates 5 µM

5.2.3 Effect of IONs on biofilm formation by *Bacillus subtilis* (ATCC 6633)

In order to fully comprehend the effect of IONs@APTES and naked IONs on *Bacillus subtilis* biofilm formation, adherent biofilm biomass and pellicle biofilm biomass were quantified as described in sections 3.3.9.1 and 3.3.9.2 and the results are given in the following sections.

5.2.3.1 *Crystal violet staining method*

Bacillus subtilis cells were immobilised with IONs as described in section 3.3.6. The effect of the nanoparticles' treatments on adherent biofilm biomass is illustrated in Figure 20.

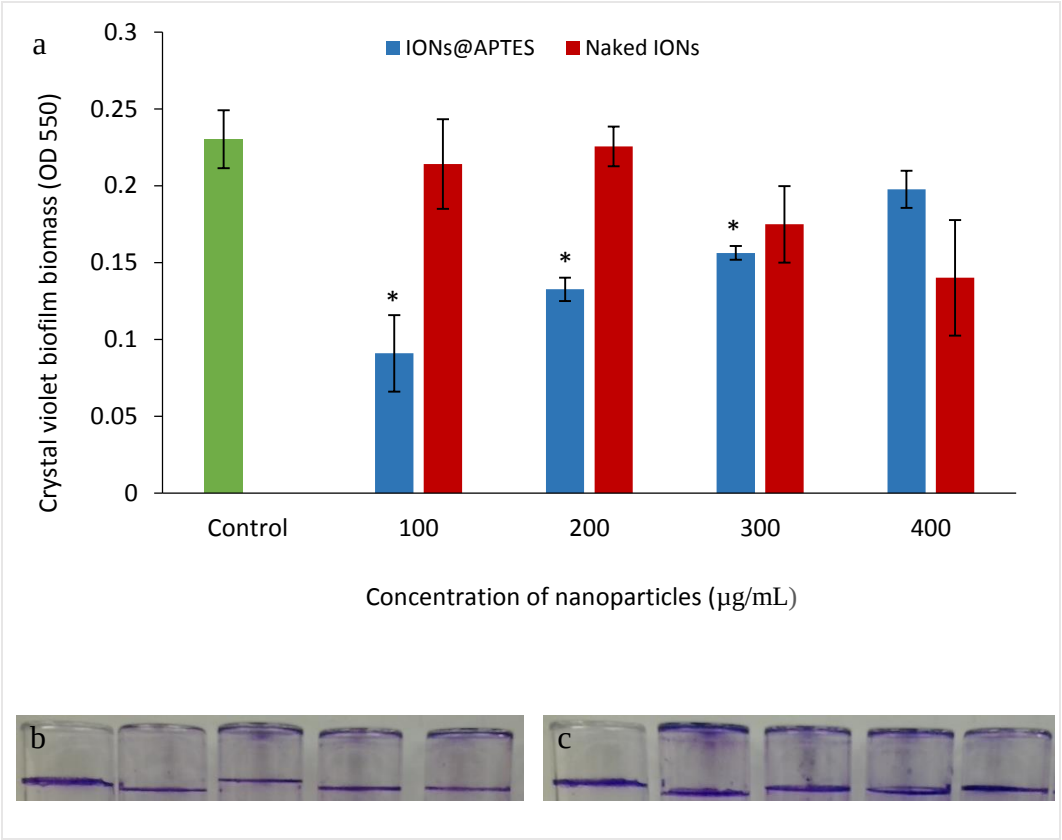

Figure 20 Crystal violet quantification of *Bacillus subtilis* (ATCC 6633) biofilm in the presence of IONs@APTES and naked IONs (a), crystal violet stained biofilms in the presence of IONs@APTES concentrations (from left to right 0-400 µg/mL) (b), crystal violet stained biofilms in the presence of different naked IONs concentrations (from left to right 0-400 µg/mL) (c) after 60 hours of fermentation. Results are expressed as the absorbance measured at 550 nm. Data are the means ± standard error of 3 replicates. An asterisk denotes the significance of difference at $p < 0.05$ compared with the control

The analysis of variance (ANOVA) test showed IONs@APTES significantly reduced the surface adherent biofilm biomass of *Bacillus subtilis* ($p < 0.05$) and that this effect was generally concentration dependent, resulting in 13.93%, 9.76% and 7.39% reduction in biofilm biomass in the presence of 100, 200 and 300 µg/mL IONs@APTES, respectively. Dunnet's multiple comparisons test showed biofilm formation in the presence of 100, 200 and 300 µg/mL of IONs@APTES are significantly lower than the control samples ($p < 0.05$). In contrast, treatment with similar concentrations of naked IONs showed no significant effect on reducing the biofilm formation even at high concentrations of naked IONs (300 and 400 µg/mL) ($p > 0.05$).

5.2.3.2 Pellicle assay and analysis

Measurement of biofilms by crystal violet staining method requires at least 24 to 48 hour-cultures and estimates the adherent biofilm biomass stained after washing to remove non-adherent cells. As the washing steps can significantly affect the final results, the total biofilm biomass was also determined by a pellicle assay. The mass of *Bacillus subtilis* pellicles was ascertained by harvesting and drying the pellicle in an oven (40°C, 5 hours); the dry weight was taken using a 5-figure balance.

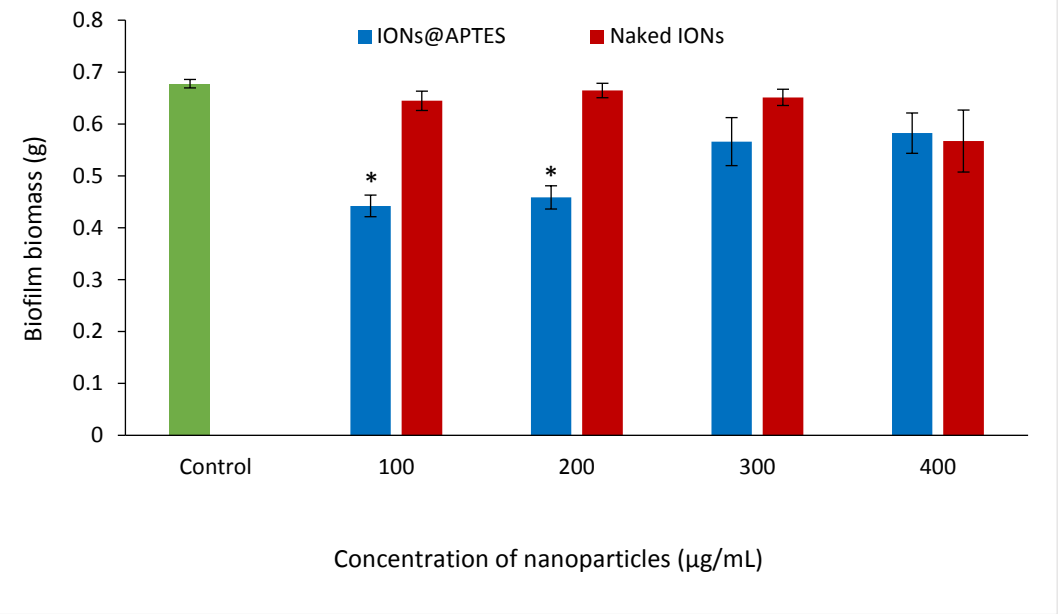

Figure 21 Quantification of *Bacillus subtilis* (ATCC 6633) biofilm pellicle biomass in the presence of IONs@APTES, naked IONs and in the absence of nanoparticles. The formation of a biofilm was measured after 60 hours using the pellicle biomass assay. Results are expressed as dry weight (g). Data are the means ± standard error of 3 replicates. An asterisk denotes the significance of difference at $p < 0.05$ compared with the control

According to ANOVA, IONs@APTES showed a significant reduction in biofilm formation compared to naked IONs ($p < 0.05$) (Figure 21). Post hoc analysis by Dunnet's multiple comparison test showed that biofilm formation in the presence of 100 and 200 µg/mL IONs@APTES were significantly lower than the control ($p < 0.05$). The pellicle assay was consistent with the CVSM showing that 100 and 200 µg/mL IONs@APTES exhibited a comparably significant reduction in biofilm

biomass measured by both methods ($p < 0.05$). However, no significant difference in biofilm formation between the untreated cells and naked ION treated cells were found ($p > 0.05$).

5.2.3.3 Microscopic observations of biofilm formation

In addition to CVSM and pellicle assays, the interaction of IONs@APTES was evaluated using Scanning Electron Microscopy (SEM) and Confocal Laser Scanning Microscopy (CLSM).

5.2.3.3.1 Scanning electron microscopic analysis of biofilm formation

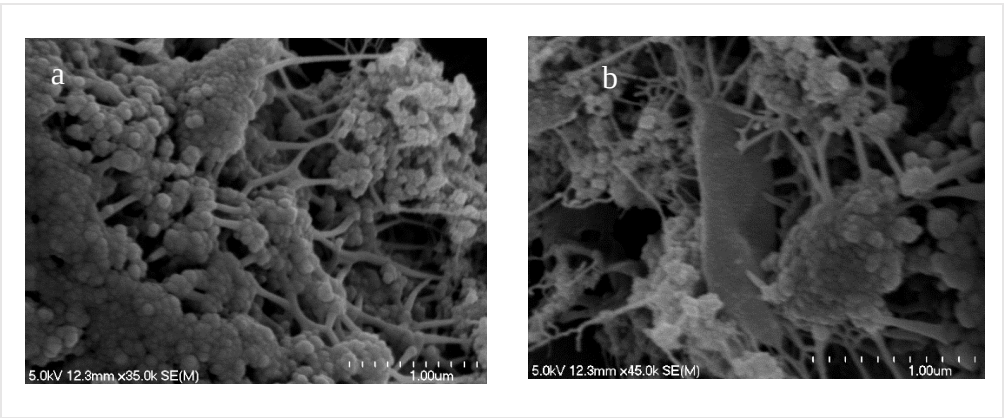

Figure 22 Scanning electron micrographs of *Bacillus subtilis* biofilm matrix in the presence of IONs@APTES (a) and *B subtilis* cell and extracellular polymeric matrix in the presence of IONs@APTES (b) after 60 hours of fermentation.

According to the SEM micrographs, IONs@APTES were seen concentrated and attached to *Bacillus subtilis* cells as well as the extracellular polymeric matrix; a complex network in biofilms, without the need of an external magnetic field (Figure 22). As can be seen from Figure 22-b, binding of IONs@APTES to bacterial cells as well as to the extracellular polymeric matrix would hinder bacterial cell adhesion to other surfaces by acting as a physical barrier.

5.2.3.3.2 Confocal Laser Scanning microscopic analysis

Previous studies showed that the adherence and pellicle biomass was significantly less in the presence of 100 µg/mL IONs@APTES. Therefore, a confocal microscopic analysis was carried out to determine the difference in the maximum biofilm depth in the presence of 100 µg/mL IONs@APTES and in the absence of nanoparticles.

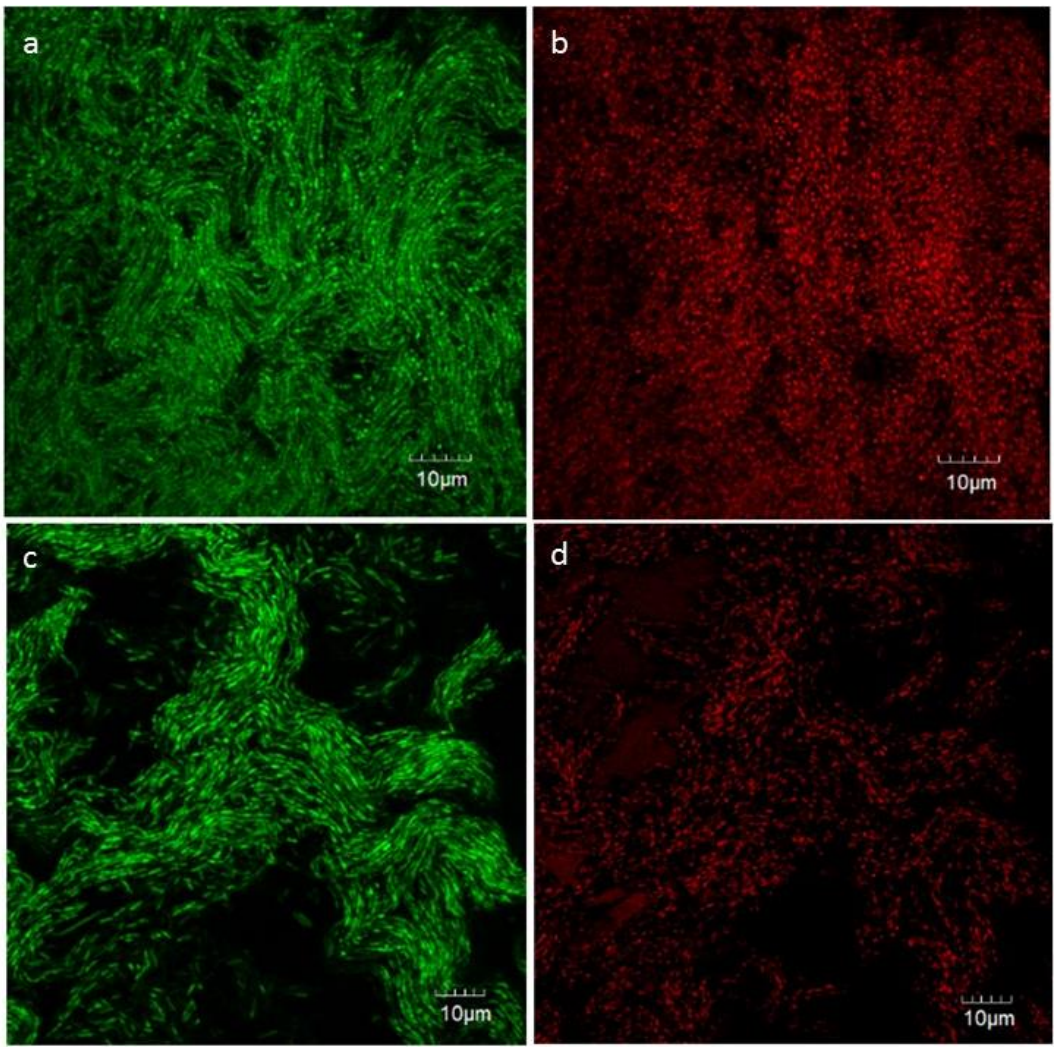

Figure 23 CLSM images of 60 hours *Bacillus subtilis* biofilm in the absence of nanoparticles (a and b) and in the presence of 100 µg/mL IONs@APTES (c and d). Biofilms were stained with LIVE/DEAD. Live cells are stained in green (a and c) dead cells stained in red (b and d)

According to confocal laser scanning micrographs, *Bacillus subtilis* showed a thick biofilm biomass in the absence of IONs@APTES after 60 hours of fermentation in

comparison to biofilm biomass in the presence of IONs@APTES (Figure 23). Biofilm maximum depth was determined after calculating the thickness of 20 different regions from biofilms grown in the presence of 100 µg/mL IONs@APTES and in the absence of nanoparticles (control sample).

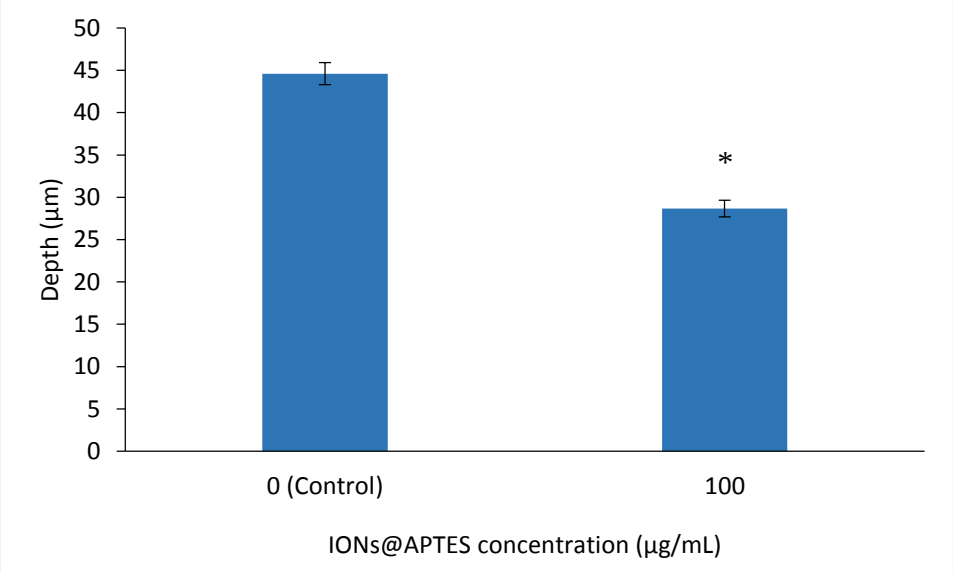

Figure 24 Biofilm maximum depth average obtained by CLSM for *Bacillus subtilis* biofilm in the absence of nanoparticles (control) and in the presence of 100 µg/mL IONs@APTES after 60 hours of fermentation. An asterisk denotes the significance of difference at $p < 0.05$ compared with the control

Confocal microscopic analysis revealed that biofilm maximum depth, which is an indirect measure of the amount of *Bacillus subtilis* biofilm biomass in the presence of 100 µg/mL IONs@APTES, is 28.66 µm in depth which was significantly less than the depth of the biofilm in the absence of IONs@APTES which was 44.60 µm ($p < 0.05$)(Figure 24).

5.2.4 Effect of IONs on the growth of *Bacillus subtilis* (ATCC 6633)

Nanomaterials can be cytotoxic or growth promoting depending on their physicochemical characteristics. In successful cell immobilisation, the immobilised cells, however, need to express their activities, such as growth and metabolic

activities. To this end, we further measured the growth/cell density and viability of *Bacillus subtilis* in the presence of varying concentrations of IONs@APTES, naked IONs and in the absence of these nanoparticles. Biocompatibility studies were carried out when the bacteria are actively growing in the log phase.

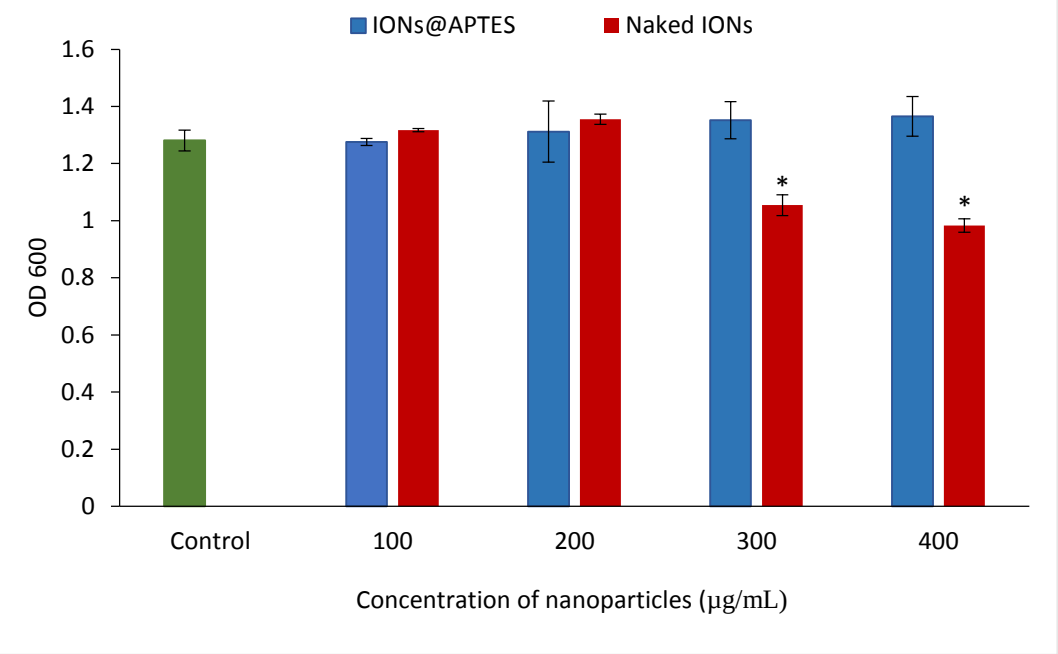

Figure 25 Growth of *Bacillus subtilis* in the presence of IONs@APTES and naked IONs. Data are the means ± standard error of 3 replicates. Optical density was measured at 60 hours. An asterisk denotes the significance of difference at $p < 0.05$ compared with the control

With increasing concentrations of IONs@APTES, an increase of growth/population density was seen after 60 hours as shown in Figure 25**.** However, naked IONS showed a growth promoting effect up to 200 µg/mL and the population density reduced thereafter. A significant reduction in cell density was seen in the presence of high concentrations of naked IONs (300 and 400 µg/mL) ($p < 0.05$). According to the results, IONs@APTES showed more growth promoting effect than the naked IONs.

5.2.5 Effect of IONs on *Bacillus subtilis* (ATCC 6633) cell viability

Optical density values do not distinguish between dead and live cells. Therefore, we further investigated the bacterial cell viability in the presence of naked and IONs@APTES using a LIVE/DEAD assay.

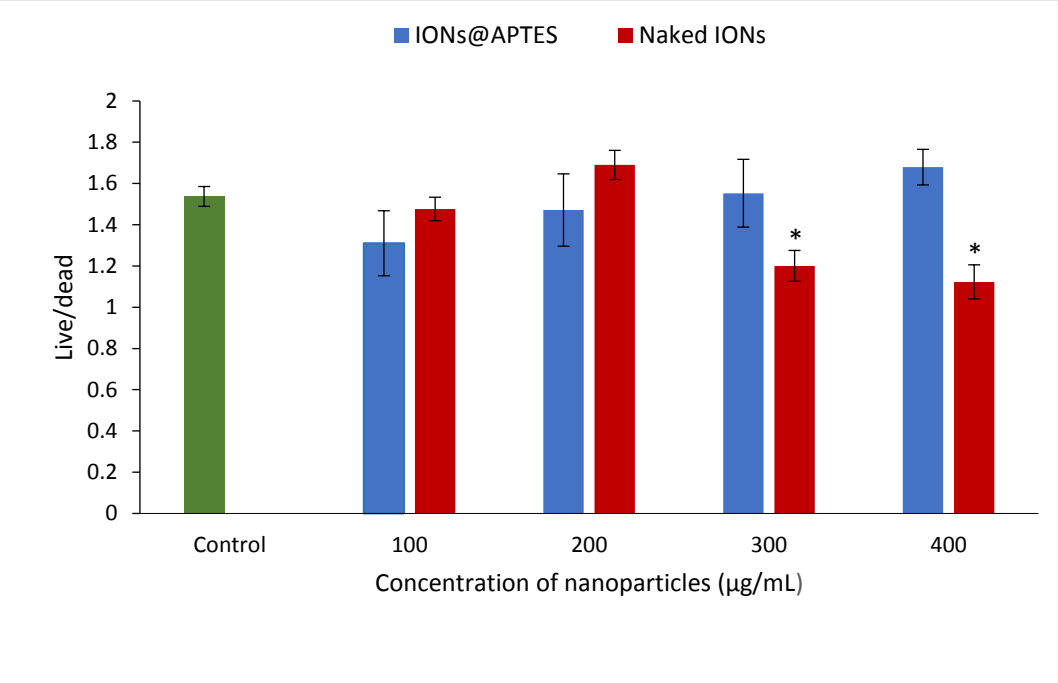

Figure 26 Viability of *Bacillus subtilis* in the presence of IONs@APTES and naked IONs. Data are the means ± standard error of 3 replicates. Viability was measured at 60 hours. An asterisk denotes the significance of difference at $p < 0.05$ compared with the control

As shown in Figure 26, the total cell viability in the presence of 100 and 200 µg/mL IONs@APTES were less than the control conditions by 14% and 4% respectively. However, none of the IONs@APTES concentrations significantly affected the total cell viability of *Bacillus subtilis* ($p > 0.05$). In contrast, the effect of naked IONs on bacterial cell viability was concentration-dependent where the total cell viability of *Bacillus subtilis* was significantly less in the presence of high concentrations of naked IONs (300 and 400 µg/mL) ($p < 0.05$) with a percentage reduction of total cell viability by 22% and 27% respectively.

5.3 Discussion

5.3.1 Interaction of IONs with *Bacillus subtilis* (ATCC 6633)

For successful immobilisation of bacterial cells with magnetic nanoparticles, the interaction of *Bacillus subtilis* cells with nanoparticles is imperative. According to the SEM micrographs, both IONs@APTES and naked IONs were seen attached to *Bacillus subtilis* cells. However, *Bacillus subtilis* cells were densely coated with IONs@APTES in comparison to naked IONs (Figure 17). According to the results, IONs@APTES seem to have provided a perfect platform for the attachment of *Bacillus subtilis*. Computer-derived models have shown that the charged groups of bacterial cells are all on the exterior of the molecular chains (Sutherland, 2001) and therefore would readily interact with charged molecules. In accordance with our study, several other studies show that nanoparticles with positive surface potential would provide unique advantage of attracting bacteria (Azam *et al.*, 2012; Ebrahiminezhad *et al.*, 2016c).

In addition to IONs@APTES, naked IONs were also seen attached to *Bacillus subtilis* cells although the bacterial cells were not densely decorated in comparison with IONs@APTES . Bacterial cell surfaces contain both positively and negatively charged groups. Therefore, the possibility of having islands with various charges to interact with the negatively charged surfaces has been suggested when similar observations of attachment of IONs to bacteria with negative surface potential including *Bacillus subtilis* have been made (Ebrahiminezhad *et al.*, 2016b; Li *et al.*, 2009). Interaction of naked IONs at higher concentrations with bacteria has also been documented and the finding has been rationalised to molecular crowding with an increase in the concentration of naked IONs resulting in net interactive interactions between naked IONs and bacteria (Arakha *et al.*, 2015). In addition, the attachment of naked IONs to *Bacillus subtilis* may also be due to changes in

surface potential of naked IONs with changes with the actual pH of the growth medium (Dias *et al.*, 2011). In aqueous medium, iron oxide is in the form of hydroxyl groups due to the coordination and further dissociation in water (Dias et al., 2011). Therefore, naked IONs can become positively or negatively charged depending on the pH of the culture medium (Dias et al., 2011). Below the isoelectric point of magnetic nanoparticles (around pH 6.8) they can become positively charged due to the formation of Fe-OH^{2+} moieties and above the isoelectric point, they are negatively charged due to the formation of Fe-O^{-} moieties (Dias et al., 2011). Therefore, although it has been hypothesised that the interaction between naked IONs are not strong enough for the NPs to attach to microbial cell surface due to dominant electrostatic repulsion, the above factors may contribute to surface attachment of naked IONs to *Bacillus subtilis*.

It is therefore evident that the interaction of nanoparticles with microbial cells is complex and many factors can come into play. In addition to surface charge, other factors may play a role in successful immobilisation, these include the surface properties of the support/nanoparticles, such as the roughness, porosity, hydrophobicity, superficial charge, toxicity and the type of functional groups present (Żur *et al.*, 2016). Apart from these, the interaction of *Bacillus subtilis* cells with NPs also depends upon the properties of the microbial cell surface as well as environmental conditions. Properties of microbial cells include the presence of extracellular polymeric substances (EPS), the age and physiological state of cells, the presence of cell wall structures, such as pilli and fimbriae, and the presence of surface proteins and glycocalyx (Dickson & Koohmaraie, 1989). Environmental conditions that may affect the efficiency of immobilisation are pH, oxygen concentration, temperature, availability of nutrients, hydrodynamic forces, adhesive forces, antimicrobial agents and the presence of cations/anions (Żur *et al.*,

2016). Grasso *et al.* (1996) demonstrate that there is also a clear impact of the growth state on the cell surface dynamics and adhesion of bacteria onto surfaces even though McEldowney and Fletcher (1986b) report that for some bacterial strains (*P. fluorescens, Chromobacterium* sp., *Flexibacter* sp.) there is no apparent correlation between growth and adhesive properties.

In the present study, it was also apparent that IONs@APTES can readily penetrate and attach to the biofilm matrix. As the majority of bacteria, including *Bacillus subtilis*, have negatively charged biofilm matrix (Hajipour *et al.*, 2012), positively charged IONs@APTES with high surface/volume ratio, which also disperses easily in the aqueous medium, can readily penetrate and bind to the biofilm matrix. Previous studies have also demonstrated that positively charged particles would more easily penetrate negatively charged biofilms (Javanbakht *et al.*, 2016). Apart from the charge, the size of IONs can also impact their diffusion through biofilms (Javanbakht *et al.*, 2016).

Interestingly, morphological changes were visible in *Bacillus subtilis* growing in the presence of IONs@APTES and naked IONs as well as in the absence of nanoparticles. These morphs can be readily differentiated from the ancestral short rods of *Bacillus subtilis.* Changes in cell morphology is a possibility in bacteria-nanoparticle interaction; for example, Chatterjee *et al.* (2011) reported an abrupt increase in cell length of *E.coli* in the presence of iron oxide nanoparticles. However, in this study, the presence of filamentous morphs, even in the absence of nanoparticles, eliminates the possibility of filamentation due to nanoparticle-bacterial interaction and suggests that the presence of filamentous morphs of *Bacillus subtilis* may be due to physiological changes in some cells within the biofilm matrix. Non-motile, long cell chains have been reported previously in *Bacillus subtilis* biofilms (Branda *et al.*, 2006) and in many other

bacteria including *B. cereus*, *E. coli*, *L monocytogenes* and *Salmonella* spp. (Jones *et al.*, 2013) which appears to be a normal aspect of their growth. Cell elongation takes place when cell growth continues in the absence of cell division (Diaz-Visurraga *et al.*, 2010). For many years, filamentous bacteria have been considered to be over-stressed and dying members of the population (Costa *et al.*, 2012). However, on closer examination, cell elongation/changes in morphology have been described as survival mechanisms and confer protection against stressful environmental situations (Costa *et al.*, 2012; Pianetti *et al.*, 2009). Varying morphotypes appear to promote cell survival in adverse conditions and rapid repopulation in the post-stress environment (Pianetti *et al.*, 2009). Under biofilm formation conditions in this study, localised high osmolarity may have arisen due to soluble exopolysaccharides within the biofilm (Sutherland, 2001). Therefore, morphological changes that were visible may be indicators of microbial adaptability to environmental/culture conditions. These morphotypes are regarded as viable because filamentation is a reversible stress response and the cells are able to divide and form new normal cells upon removal of the stress conditions (Jones *et al.*, 2013). This was clearly evident by the division of cells by binary fission and formation of new daughter cells that were seen in the presence of naked and IONs@APTES as well as in the absence of nanoparticles. Based on the results, IONs@APTES could be seen as a better option for decorating *Bacillus subtilis* cells.

5.3.2 Effect of IONs on biofilm formation by *Bacillus subtilis* (ATCC 6633)

Some of the earlier reports have demonstrated the potential for the use of naked IONs with appropriate size and concentration for controlling biofilms

(Sathyanarayanan *et al.*, 2013; Subbiahdoss *et al.*, 2012; Taylor & Webster, 2009; Thukkaram *et al.*, 2014). For example, Sathyanarayanan *et al.* (2013) demonstrated that IONs reduce biofilm growth of *P. aeruginosa* and *S. auereus*. Thukkaram *et al.* (2014) showed IONs in a concentration range of 10 to 100 µg/mL were able to reduce biofilm growth of *S. aureus*, *E.coli* and *P. aeruginosa*. Similarly, Taylor and Webster (2009) have reported a decrease in *S. epidermidis* numbers in a biofilm in the presence of 100 µg/mL of IONs, and Subbiahdoss *et al.* (2012) report the use of IONs to effectively kill biofilm bacteria. It has been suggested that the antibacterial effect of IONs may be either due to the production of reactive oxygen species or membrane damage due to electrostatic interactions or the small size of nanoparticles (Sathyanarayanan *et al.*, 2013). In contrast, Borcherding *et al.* (2014) have shown that naked IONs impact biofilm formation in a size-dependent manner, where the smaller (2 nm) IONs have been shown to increase growth and biofilm formation significantly due to the release of soluble Fe^{3+} in comparison to larger (540 nm) IONs. This study compared the biofilm formation by *Bacillus subtilis* in the presence of IONs@APTES and naked IONs.

According to the results, IONs@APTES at 100 µg/mL and 200 µg/mL significantly reduced the adherence and pellicle biofilm biomass of *Bacillus subtilis* in a concentration-dependent manner ($p < 0.05$) (Figure 20 and Figure 21). In particular, IONs@APTES at 100 µg/mL was the most active concentration since it significantly reduced the total biofilm biomass without affecting the cell viability, suggesting an active role of these IONs@APTES affecting bacterial cell attachment to glass surfaces and pellicle formation. The exact mechanism by which IONs@APTES inhibit the adherence of *Bacillus subtilis* to surfaces and reduces pellicle formation was not investigated in this study. However, bacterial attachment to any surface is related to the surface charge of both substratum and bacteria

(Dickson & Koohmaraie, 1989). Attachment of *Bacillus subtilis* to IONs@APTES is mainly driven by the attractive electrostatic interaction between the positively charged amine functional groups on IONs@APTES and the negatively charged cell surface of bacteria. Therefore, it can be speculated that the significant reduction of biofilm formation in the presence of IONs@APTES may be due to attachment of IONs@APTES on to the negatively charged cell wall of *Bacillus subtilis* thereby changing the surface charge and surface binding potential of cells. Further, once attached to the bacterial cell surface, IONs@APTES can act as a physical barrier for the attachment of bacterial cells to other surfaces and initiation of biofilm formation.

In contrast, treatment with similar concentrations of naked IONs showed no significant effect on reducing the biofilm formation, even at high concentrations of naked IONs (300-400 µg/mL) ($p > 0.05$). Naked IONs might have shown limited use in controlling biofilm formation as they are not well dispersed at higher concentrations; an external magnetic field has sometimes been used to target and penetrate IONs deep into the biofilm and concentrate them therein (Dickson & Koohmaraie, 1989) in order to eliminate preformed biofilms. In this regard, size and physicochemical characteristics of IONs have both played an important role in their diffusion through biofilms and disruption of biofilms (Javanbakht *et al.*, 2016) through the bactericidal effect exerted by the IONs. In contrast, APTES coating seems to stabilise the IONs and maintain them in a dispersed state while specifically interacting with the bacterium and changing the adhesion pattern and subsequent pellicle formation of *Bacillus subtilis.*

However, the effect of IONs@APTES to reduce biofilm formation was masked in the presence of higher concentrations of IONs@APTES. This may be due to the growth promotion effect of IONs@APTES. According to the Derjaguin-Landau-

Verwey-Overbeek (DLVO) model of colloidal stability, electrostatic interactions and Van der Waals interactions are described as the two most important interactions in bacterial cell adhesion (Rijnaarts *et al.*, 1995). However, interactions not included by the DLVO model, such as hydrophobic interactions, can also contribute to bacterial cell adhesion (Grasso *et al.*, 1996; Rijnaarts *et al.*, 1995) which can change with the growth rate. For example, Grasso *et al.* (1996) report that the hydrophobicity of *P. aeruginosa* increased with the increase in the specific growth rate. Further to hydrophobic interactions, surface macromolecules which play a role in surface attachment can also change with the physiological state of the bacterium. Therefore, cell adhesion cannot be attributed to a single factor; it is complex and warrants further study.

In addition to CVSM and pellicle assay, CLSM analysis revealed that biofilm maximum depth, which is an indirect measure of the amount of *Bacillus subtilis* biofilm biomass in the presence of IONs@APTES, was 28.66 µm in depth which was significantly less than the depth of the biofilm in the absence of nanoparticles which was 44.60 µm ($p < 0.05$) (Figure 24). Therefore, IONs@APTES proved to be useful in biofilm control in comparison to naked IONs.

5.3.3 Effect of IONs on the growth of *Bacillus subtilis* (ATCC 6633)

The growth of *Bacillus subtilis* in the presence of naked and IONs@APTES showed that IONs@APTES have more growth promoting effect than the naked IONs. With increasing concentrations of IONs@APTES, an increase in growth/population density was seen (Figure 25). Bacteria surviving and colonising on surfaces functionalised with APTES have been reported previously by Lee *et al.* (1994). It is possible that the binding of IONs@APTES to *Bacillus subtilis* has changed the membrane permeability and has facilitated mass transfer and nutrient absorption in

a concentration-dependent manner. Supporting observations have been reported by Ansari *et al.* (2009) in which coating of bacterial cells with magnetic nanoparticles have resulted in higher desulphurisation activity. It was suggested that this was due to changes in cell membrane permeability which facilitated the entry and exit of reactant and product (Ansari *et al.*, 2009).

The increase in cell density in the presence of varying concentrations of IONs@APTES showed a similar pattern to increase in biofilm biomass. However, the cell density was not significantly less than the control in the presence of 100 and 200 µg/mL of IONs@APTES although the biofilm biomass was significantly less. The results support the idea that IONs@APTES compromise surface adherence of *Bacillus subtilis* to the glass surface and pellicle formation by altering the adhesion pattern of the bacterium without affecting microbial growth.

Naked IONs showed a growth promotion up to 200 µg/mL; however, it was not significantly different from control ($p > 0.05$). Similar observations have been reported previously where IONs have induced growth by acting as an endogenous source of iron for bacteria, and this effect is dependent on the particle size of IONs (Borcherding *et al.*, 2014) as well as the concentration of IONs (Ebrahiminezhad *et al.*, 2015). The population density of *Bacillus subtilis* was significantly reduced in the presence of high concentrations of naked IONs (300 and 400 µg/mL) ($p < 0.05$). However, the reduction in biofilm biomass was not significantly different from the control as described in section 5.3.2, even in the presence of higher concentrations of naked IONs, although the growth /cell density was significantly less ($p < 0.05$). As biofilm bacteria, as well as planktonic bacteria, contribute to the optical density value, it can be speculated that the significant reduction in optical density in the presence of high concentration of naked IONs may be due to the significant antibacterial effect of naked IONs on planktonic bacteria at high concentrations. As

naked IONs are not well dispersed at higher concentrations, the response of biofilm bacteria and planktonic bacteria to IONs may be different. A reduction of *Bacillus subtilis* growth in the presence of naked IONs with an average size of 11 nm, in a concentration and time-dependent manner, has been demonstrated by (Ebrahiminezhad *et al.*, 2016b). Further, (Arakha *et al.*, 2015) reported a reduction in *Bacillus subtilis* growth with increasing concentrations of naked IONs with an estimated particle size of approximately 11± 5 nm; however, the growth inhibition was insignificant for the concentrations of naked IONs studied. Growth inhibitory effect of naked IONs on many other bacterial species, such as *E. coli, L. monocytogenes, S. aureus* and *P. aeruginosa,* in a concentration-dependent manner, have also been reported (Chatterjee *et al.*, 2011; Ebrahiminezhad *et al.*, 2012a; Ebrahiminezhad *et al.*, 2016b; Grumezescu *et al.*, 2010; Ramteke *et al.*, 2010). Growth inhibition has been attributed to the production of ROS resulting in oxidative stress and damage to the cell membrane, protein and DNA (Chatterjee *et al.*, 2011).

Therefore, in comparison to naked IONs, IONs@APTES present a better option for immobilisation of *Bacillus subtilis* and controlling biofilm formation while maintaining bacterial growth.

5.3.4 Effect of IONs on the viability of *Bacillus subtilis* (ATCC 6633)

Previous studies report that the strong interactions of IONs with cell membrane can sometimes disturb the cell membrane integrity, electron and ionic transport chains between the intra and extracellular media and bacterial metabolism (Arakha *et al.*, 2015; Auffan *et al.*, 2008; Javanbakht *et al.*, 2016). One of the criteria to distinguish between dead and viable cells is, therefore, the membrane integrity. While viable cells are assumed to have intact cell membranes, dead cells are considered to have

disrupted cell membranes. Syto 9 fluorescence dye of BacLight™ bacterial viability kit stains bacterial cells with intact cell membranes in green and bacterial cells with damaged cell membranes are stained red with propidium iodide. Among the methods to investigate the bacterial cell viability, backlight assay holds great promise when fast throughput results are required.

In industrial fermentation, biofilm control and growth and viability of the bacterium are equally important; however, previous studies with naked IONs have shown that the reduction in biofilm is due to their antibacterial potential (Sathyanarayanan *et al.*, 2013; Subbiahdoss *et al.*, 2012; Taylor & Webster, 2009; Thukkaram *et al.*, 2014). According to the results of this study, despite the fact that 100 and 200 µg/mL IONs@APTES significantly reduced biofilm formation, none of the IONs@APTES concentrations significantly affected the total cell viability of *Bacillus subtilis* (Figure 26). Similarly, Gottenbos *et al.* (2001) report that positively charged biomaterial surfaces do not affect surface growth nor exert an antimicrobial effect on adhering gram-positive bacteria. The results have been ascribed to the thick and rigid peptidoglycan layer of gram-positive bacteria where it prevents/reduces extensive contact of ammonium groups with the membrane, even under conditions of electrostatic attractions (Gottenbos *et al.*, 2001). Therefore, it is speculated that the reduction in biofilm biomass in the presence of IONs@APTES may be due to the change in surface binding potential or shielding effect of IONs@APTES leading to less adherence and pellicle formation of *Bacillus subtilis*.

In contrast, total cell viability was significantly less at naked IONs concentrations higher than 200 µg/mL, which may be due to the toxic effect exerted by naked IONs. Similarly, (Arakha *et al.*, 2015) reported a 30% reduction in the viability of *Bacillus subtilis* in the presence of 50 µM of naked IONs with an estimated particle size of

approximately 11± 5 nm. Toxic effect of naked IONs on cell lines in a concentration-dependent manner have also been reported by several other studies (Ebrahiminezhad *et al.*, 2015; Javanbakht *et al.*, 2016; Singh *et al.*, 2010; Thukkaram *et al.*, 2014). Therefore, in comparison to naked IONs, IONs@APTES present a better option for immobilising *Bacillus subtilis* and controlling biofilm formation while maintaining bacterial growth. Supporting observations are reported by Ebrahiminezhad *et al.* (2015) where a number of viable HepG2 cells were high in the presence of IONs@APTES than in the presence of naked IONs, although some studies report that positively charged IONs exert strong antimicrobial propensity in comparison to naked IONs (Arakha *et al.*, 2015; Javanbakht *et al.*, 2016), however, only at highest exposure concentrations (Javanbakht *et al.*, 2016).

5.4 Summary

Biofilm formation of *Bacillus subtilis* results in significant operational issues in many fermentation processes. The present study was focused on immobilisation of *Bacillus subtilis* (ATCC 6633) with naked and APTES coated IONs and evaluation of their effects on *Bacillus subtilis* biofilm formation, growth and viability. In comparison to naked IONs, IONs@APTES offered a high density of surface functional groups of $–NH_3^+$ to IONs, promoting strong electrostatic interaction with negatively charged sites on the cell membrane allowing good decoration of cells. IONs@APTES have been demonstrated to be a promising approach to control biofilm formation without the loss of *Bacillus subtilis* cell viability compared to naked IONs. No reduction in viability was seen in the presence higher concentrations of IONs@APTES (300 and 400 µg/mL). Therefore, APTES coated magnetic nanoparticles, at appropriate concentrations, offer a considerable advantage for biofilm control while maintaining the growth and viability of

bacterial cells when designing the next generation of bioprocesses intensification methods in *Bacillus subtilis* fermentation. However, the interaction of IONs@APTES with bacterial cells should not affect the metabolic activity of *Bacillus subtilis*, especially the MK-7 production. It is therefore imperative to study the effect of IONs@APTES on MK-7 production. Due to shortfalls in existing MK-7 analysis protocols, prior to the study of the effect of IONs@APTES on MK-7 production by *Bacillus subtilis*, it is, however, important to have a reliable MK-7 analysis procedure.

Chapter 6

Development of a Novel Approach for MK-7 Analysis

This chapter forms the basis for the following publications:

Ranmadugala, D., Grainger, M., Manley-Harris, M., & Berenjian, A. (2018), Determination of Menaquinone-7 by a Simplified Reversed Phase HPLC method. *Current Pharmaceutical Biotechnology*, *19*(8), 664-673.

6.1 Introduction

MK-7 is a membrane-bound quinone functioning as an electron carrier in the prokaryotic respiratory chain (Fujimoto *et al.*, 2012). With growing interest in MK-7 due to its beneficial role in the blood coagulation process (Suttie, 1995), bone formation (Tsukamoto *et al.*, 2000), reducing bone fractures (Schurgers *et al.*, 2007), preventing postmenopausal bone loss (Knapen *et al.*, 2007) and cardiovascular health (Beulens *et al.*, 2009; Gast *et al.*, 2009; Knapen *et al.*, 2015; Shea & Holden, 2012), the dietary intake of menaquinones are more important than phylloquinone. Therefore, MK-7 can be taken as the obvious choice to be included in multivitamin supplements and functional foods for the prevention of these diseases (Cranenburg *et al.*, 2007). Although HPLC facilitates routine vitamin K analysis, the determination of MK-7 is still a great challenge. One of the reasons for this is the contamination of samples by other lipids, such as esters of fatty aromatic acids (Bentley & Meganathan, 1982). The presence of interfering substances in samples following extraction necessitates an additional sample clean-up with solid phase extraction (Haroon *et al.*, 1982), normal phase HPLC (Canfield *et al.*, 1991), thin layer chromatography (Sakano *et al.*, 1988) or combinations of these methods (Hirauchi *et al.*, 1989) to eliminate interfering substances from the final reversed phase chromatographic system. The use of two chromatographic systems is expensive and time-consuming. Further, several sample manipulation steps increase the risk of experimental errors. Another major problem in MK-7 quantification is the low solubility of MK-7 in polar solvents. The MK-7 analysis is most commonly carried out after evaporation of an MK-7 extract normally in a non-polar solvent and re-solubilisation in polar solvents such as methanol or a mixture of methanol and dichloromethane. However, low polarity lipid soluble MK-7 is often difficult to dissolve in the polar mobile phases usually used for

reversed phase HPLC and this could result in lower quantitation of actual MK- 7 concentration present in the sample.

In addition to the presence of interfering substances and low solubility of MK-7, MK-7 concentration in bacterial fermentation is low. Therefore, a highly sensitive method is required for quantitation. Attempts have been made to determine the level of MK-7 from various sources including, meat, fish, natto (Japanese fermented soybean), milk, cheese, curd and bread (Schurgers & Vermeer, 2000). Although some of these methods have given satisfactory results in terms of sensitivity, the methods have major drawbacks. For example, liquid chromatography-atmospheric pressure chemical ionisation/mass spectrometry (LC-APCI-MS) provides an accurate analysis of menaquinones with high sensitivity (Ahmed & Mahmoud, 2015), however, many laboratories are not equipped with this instrumentation. Therefore, the objective of the present study was to develop a novel, relatively low-cost method for routine MK-7 analysis with greater efficiency and accuracy using HPLC with UV detection.

6.2 Results

6.2.1 Standard calibration curve of MK-7

A standard calibration curve of MK-7 was obtained by plotting analyte concentration against peak area. The retention time of MK-7 was obtained at 7.19 ± 0.1min (Figure 27). The flow rate was 0.5 mL/min. UV detection was from 200-400 nm and the chromatogram was extracted at 248 nm. Figure 27 shows the chromatogram and the absorption spectrum of MK-7 standard.

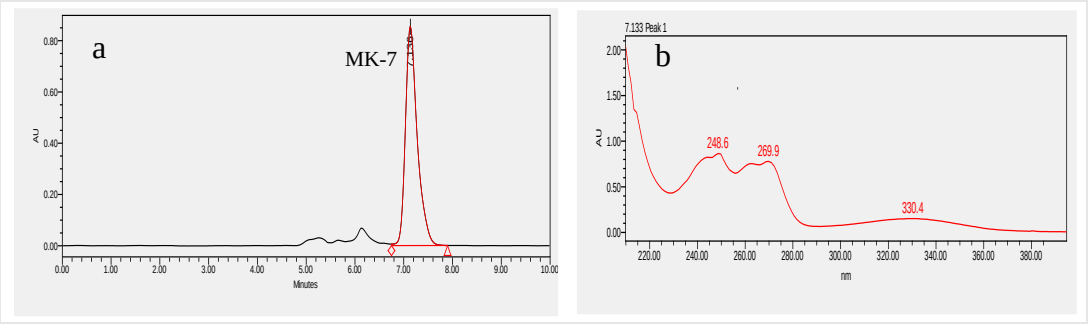

Figure 27 Chromatogram (248 nm) of MK-7 standard 200 µg/mL (a) and extracted UV spectrum of the peak at 7.13 minutes (b).

The UV absorbance spectrum of MK-7 showed four distinct peaks characteristic of the naphthoquinone nucleus between 240 and 280 nm and less sharp absorption at around 320 and 330nm.

6.2.2 Linearity of the method

When linearity was determined for MK-7 following serial dilution of a MK-7 calibration standard ranging from 200 µg/mL to 0.37 µg/mL (200, 100, 50, 25, 12.5, 6.25, 3.13, 1.56, 0.78, and 0.37 µg/mL), a linear relation with good coefficient of determination of 0.9982 was obtained and showed good linear relationship of the newly developed method with the slope (m) of the calibration curve as 83,773.5416 (Figure 28) by using the equation, $y = mx$

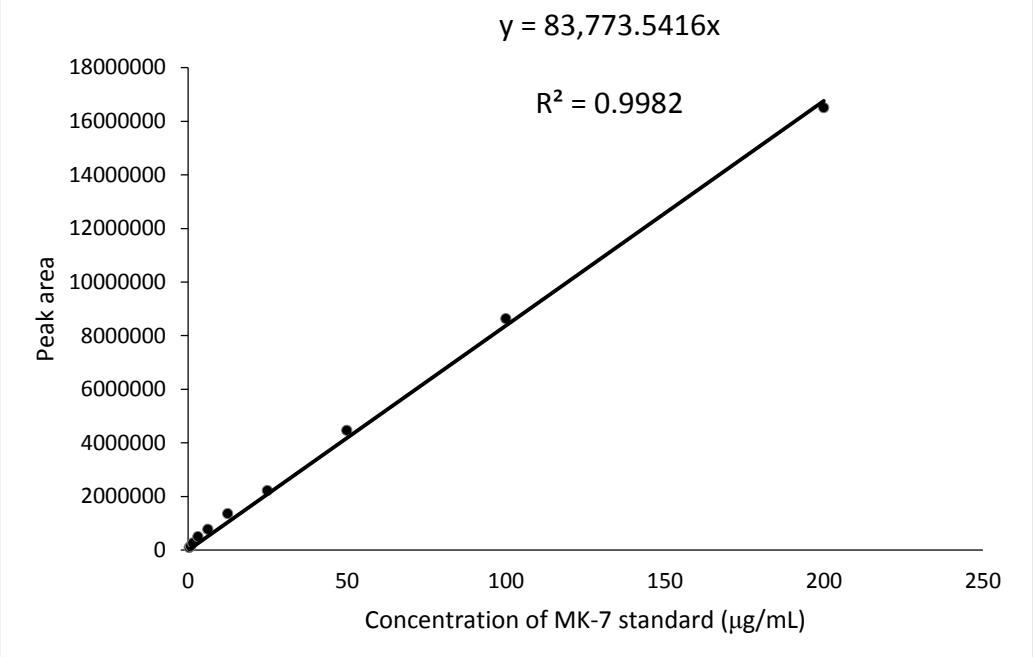

Figure 28 Calibration curve of MK-7 standard.

6.2.3 Accuracy/% recovery studies

The mean percentage of recovery (n=4) from spiked fermented samples was found to be more than 94% (Table 2). Figure 29 shows the HPLC chromatogram of MK-7 with and without a spiked MK-7 standard.

Table 2 Percentage recovery of MK-7 standard

Mass of spike added (µg)	**Mean mass of spike recovered (µg)**	**% recovery**
50.00	49.13 ± 0.0005	98.25 ± 0.95
100.00	95.16 ± 0.0039	95.16 ± 3.91
150.00	141.91 ± 0.0019	94.61 ± 1.28

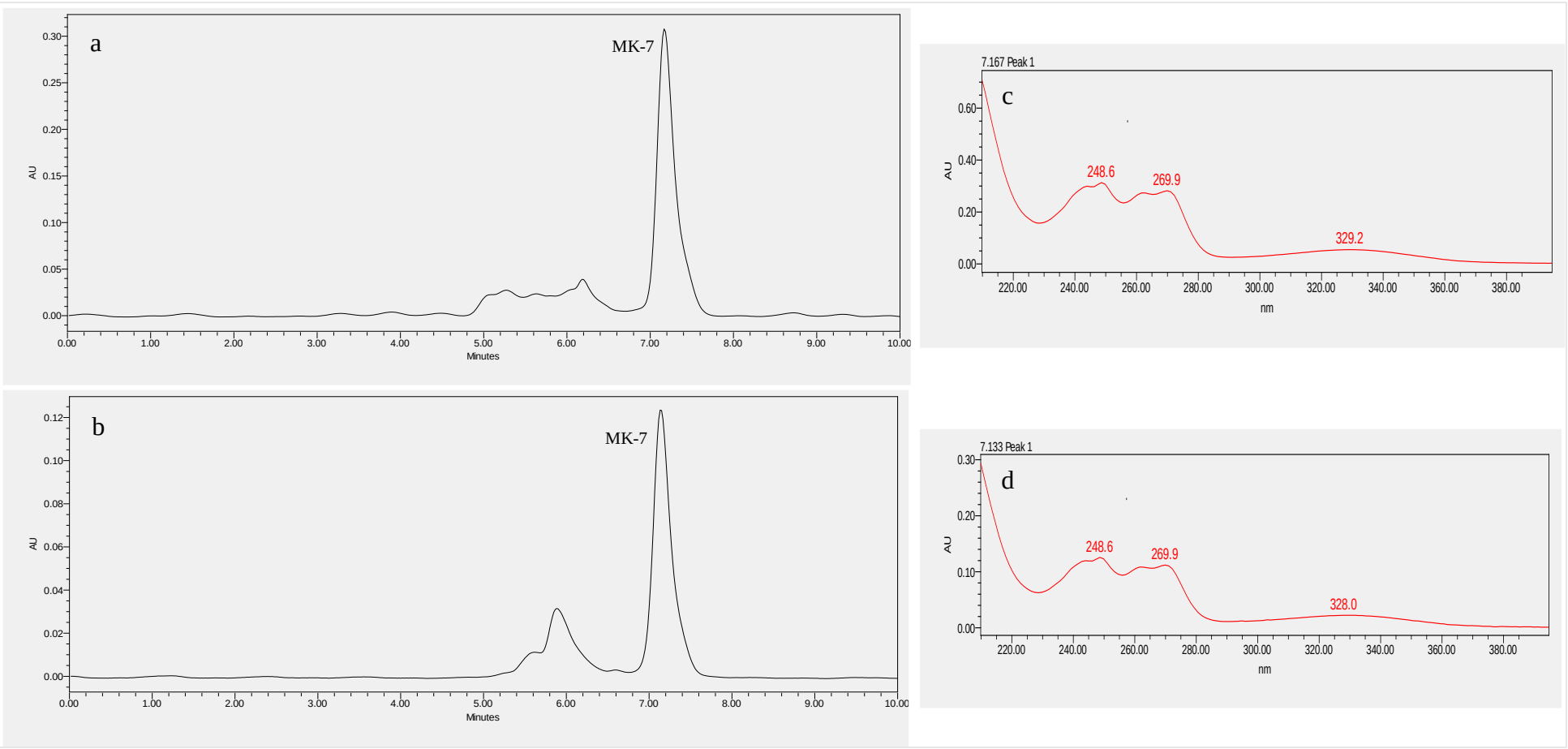

Figure 29 Chromatograms (248 nm) of MK-7 with (a) and without (b) MK-7 spike at 50µg and extracted UV trace of peaks with (c) and without (d) MK-7 spike at 7.19 ± 0.1 minutes.

6.2.4 The precision of the method

The precision was expressed in % RSD and it is less than 2% for both intraday and interday analyses (Table 3 and Table 4).

Table 3 Determination of precision intraday

Day	Injected concentration (µg/mL)	Measured MK-7 concentration (µg/mL)	Mean concentration measured (µg/mL)	SD	%RSD
1	**150.00**	143.96 148.31 146.42 147.47 149.89	147.21	0.0022	1.5054
2	**150.00**	147.63 147.46 142.48 149.19 144.70	146.29	0.0027	1.8274
3	**150.00**	145.96 145.96 146.65 145.77 145.05	145.88	0.0006	0.3925

Table 4 Determination of precision interday

Injected concentration (µg/mL)	Day	Interday Mean concentration measured (µg/mL)	Mean	SD	%RSD
150.00	**Day-1**	147.21	146.46	0.0007	0.4658
	Day-2	146.29			
	Day-3	145.88			

6.2.5 Limit of detection and limit of quantification

High-Performance Liquid Chromatography LOD and LOQ were calculated as described in section 3.3.16.4 and the calculations are shown below. The assay LOD was 0.10 µg/mL and the LOQ was 0.29 µg/mL.

LOD= ((3.3* 2407.89)/ 83,773.5416) =0.10 µg/mL

LOQ= ((10* 2407.89)/ 83,773.5416)=0.29 µg/mL

6.2.6 Preliminary studies on MK-7 extraction and analysis

During this development process, preliminary studies on MK-7 extraction were carried out according to the protocol described by Sato *et al.* (2001b). Briefly, 4 mL of 2- propanol and 8 mL of *n*-hexane was added to 3 mL of bacterial suspension, vigorously shaken and centrifuged to remove the upper *n*-hexane layer. *n*-hexane (20 µL) was directly injected into HPLC column and eluted with 2-propanol: *n*-hexane (2:1, *v*/*v*). However, this procedure resulted in a very high spurious peak co-eluting with MK-7 in the chromatogram, and therefore the MK-7 peak could be poorly detected with UV (Figure 30).

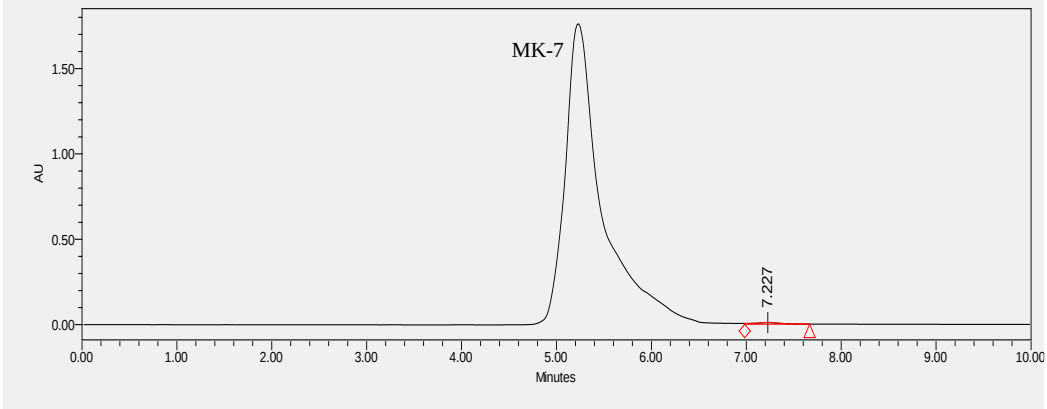

Figure 30 Chromatogram of extracted MK-7 from *Bacillus subtilis* (ATCC 6633) without 1% (*w*/*v*) lipase and ethanol: water (4:2, *v*/*v*) treatment. MK-7 is in *n*-hexane and eluted with a mobile phase solvent mixture of 2- propanol; *n*-hexane (2: 1, *v*/*v*)

Therefore, in the next stage prior to MK-7 extraction from bacterial strains with a mixture of 2-propanol: *n*-hexane (2:1, *v*/*v*), purification of the crude extract was carried out by enzymatic hydrolysis of lipids followed by ethanol precipitation of proteins as described previously by Lambert *et al.* (1992). The mixture was centrifuged and the upper hexane layer was separated into a new vial and directly injected into HPLC.

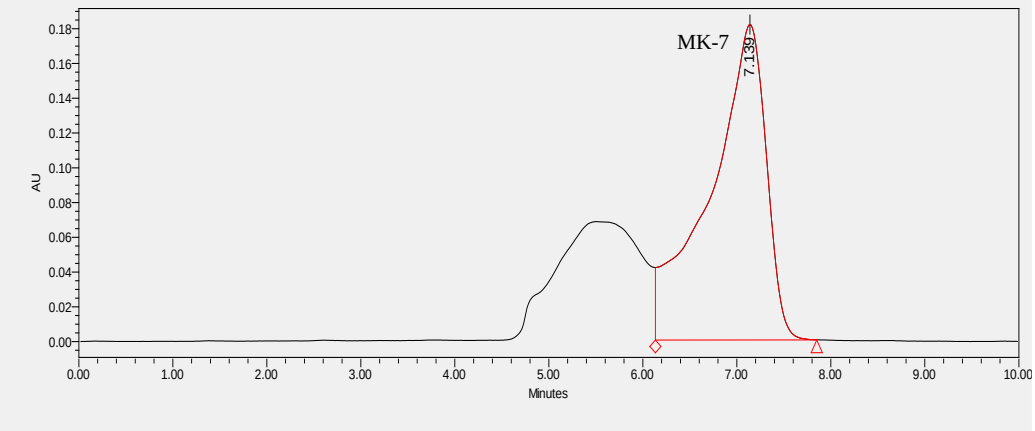

Figure 31 Chromatogram of extracted MK-7 from *Bacillus subtilis* (ATCC 6633) with 1% (*w*/*v*) lipase and ethanol: water (4:2, *v*/*v*) treatment. MK-7 is in *n*-hexane and eluted with a mobile phase solvent mixture of 2- propanol; *n*-hexane (2: 1, *v*/*v*)

Enzymatic hydrolysis with 1% (*w*/*v*) lipase and ethanol-water treatment were able to get rid of the spurious peak and improved the detectability of MK-7 (Figure 31). However, in the resulting chromatogram, the MK-7 peak was poorly resolved (Figure 31). Therefore, instead of directly injecting the *n*-hexane extract to HPLC column, in the next stage, MK-7 extract was reconstituted in a solvent that is the same as the mobile phase by mixing one part of the upper *n*-hexane layer with 2 parts of 2-propanol (*v*/*v*) followed by eluting with the same mobile phase solvent (2-propanol: *n*-hexane, 2:1, *v*/*v*). This procedure improved the peak shape (Figure 32).

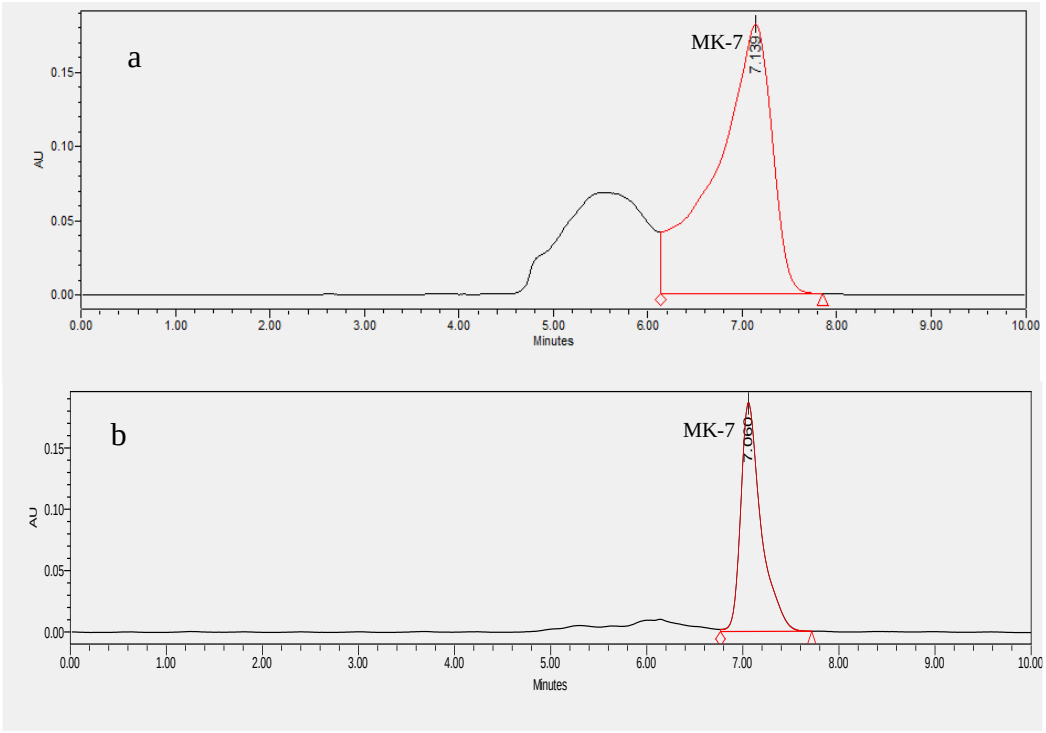

Figure 32 Chromatograms of extracted MK-7 from *Bacillus subtilis* (ATCC 6633) in *n*-hexane (a) in 2- propanol: *n*-hexane (2:1, *v*/*v*) (b) after 1% (*w*/*v*) lipase and ethanol: water (4:2, *v*/*v*) treatment. MK-7 is eluted with a mobile phase solvent mixture of 2- propanol; *n*-hexane (2: 1, *v*/*v*)

The effect of enzymatic hydrolysis and ethanol-water treatment followed by reconstituting the extract in a solvent that is the same as the mobile phase can be clearly seen in Figure 32-b. This protocol would therefore allow accurate quantitative measurement of MK-7 from *Bacillus subtilis* strains.

6.2.7 Determination of MK-7 production by *Bacillus subtilis* species/strains

The accuracy of the proposed method for extraction and analysis of MK-7 from four different *Bacillus* species/strains was studied. MK-7 was identified by comparison of retention time and UV spectrum with a MK-7 standard. MK-7 was extracted as described in 3.3.13 and was analysed by HPLC as described in section 3.3.17. Representative chromatograms and spectra of MK-7 extracted from samples are shown in Figure 33.

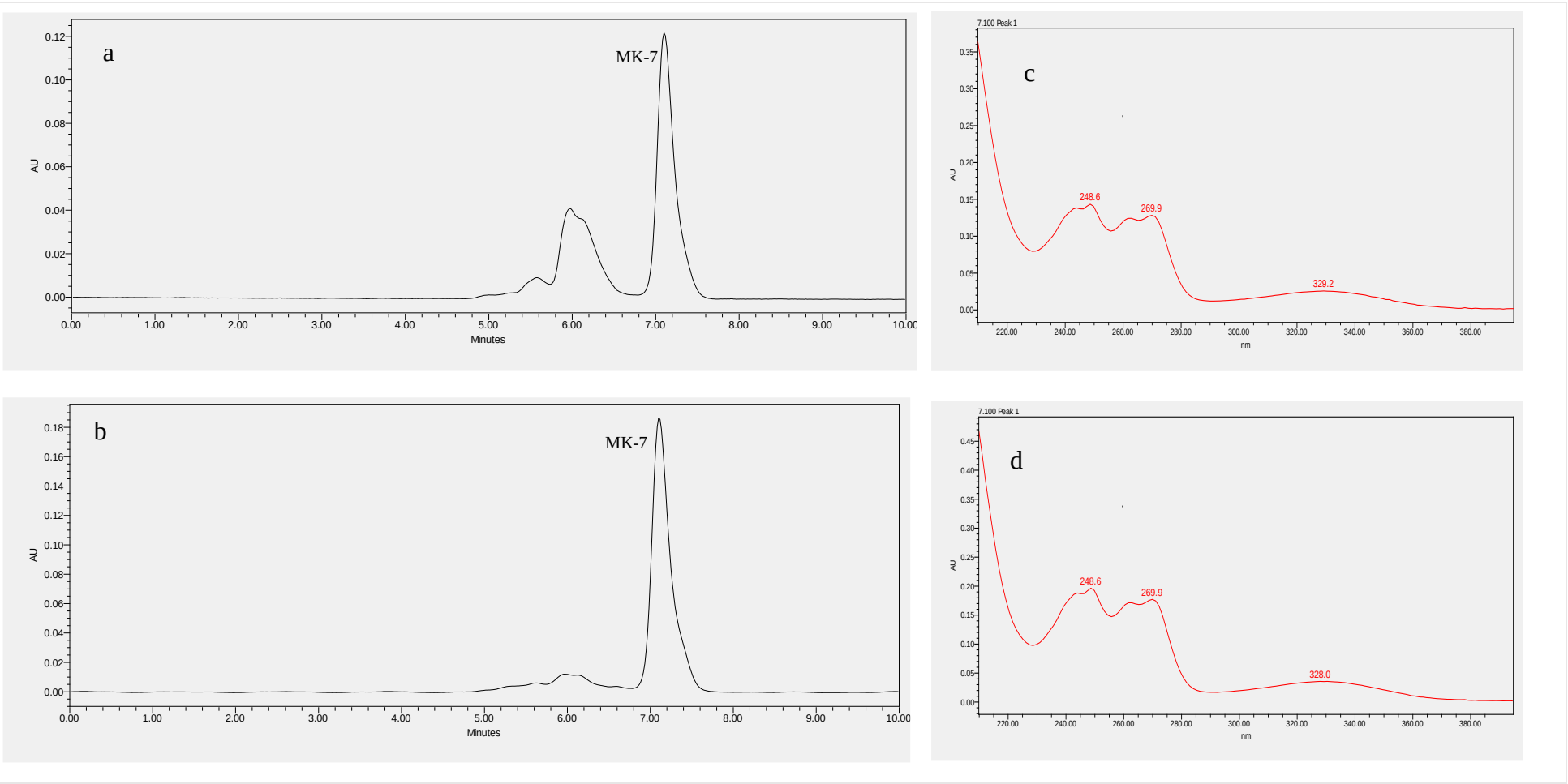

Figure 33 HPLC chromatogram (248 nm) of MK-7 in the culture of *Bacillus subtilis* (ATCC 6633) (a) *Bacillus subtilis natto* (b) and corresponding extracted UV trace of peaks at 7.19 ± 0.1 minutes (c and d)

Analysis of MK-7 from four different *Bacillus* species/strains using the developed method indicated that the highest MK-7 production can be obtained from *Bacillus subtilis natto* followed by *Bacillus subtilis* (ATCC 6633). The amount of MK-7 produced by *Bacillus licheniformes* and *Bacillus sphericus* was much less (Figure 34). The coefficient of variation for the triplicate determination were less than 10% for MK-7 from the four *Bacillus* species/strains.

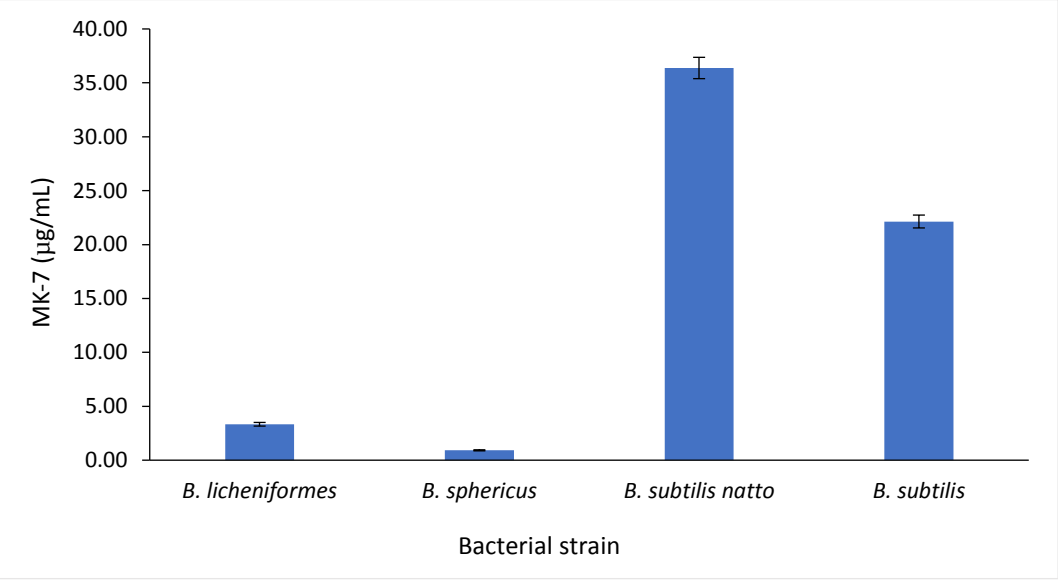

Figure 34 MK-7 production by *B. licheniformes*, *B. sphericus*, *B. subtilis natto* and *B.subtilis* (ATCC 6633) after 60 hours of fermentation. Data are the means ± standard error of three replicates.

6.3 Discussion

The most common choice of analytical method for MK-7 analysis is HPLC (Clejan *et al.*, 1986; Lambert *et al.*, 1992); however, there are still problems relating to extraction and sample clean-up. The aim of this study was to develop a method by which MK-7 can be extracted and quantified from fermented bacterial samples with minimum losses. The procedure combines enzymatic hydrolysis prior to extraction with a mixture of 2-propanol: *n*-hexane (2:1, *v*/*v*) followed by reversed phase HPLC achieved on Gemini 250 mm x 4.6 mm, i.d. 5 µm LC column (Phenomenex) with

UV detection (from 200-400 nm and the chromatogram extracted at 248nm) using an isocratic mobile phase mixture of 2- propanol: *n*-hexane (2:1, *v*/*v*) with a flow rate of 0.5 mL/min. Under these conditions, the retention time was found to be 7.19 ± 0.1 minutes. A linear response was shown by the method with a coefficient of determination (r^2) value of 0.9982. The recoveries of MK-7 were more than 94% and the intraday and interday assay R.S.D values were less than 2%, demonstrating the accuracy of the method. The lower limit of detection (LOD) and the limit of quantification (LOQ) under these conditions were 0.10 µg/mL and 0.29 µg/mL respectively. Although fluorescence detection would give lower LOD and LOQ in comparison to UV detection (Fauler *et al.*, 2000), reduction of the quinone to hydroquinone form is needed in order to measure menaquinones with fluorescence detection and the whole procedure is time-consuming (Jakob & Elmadfa, 1995). In contrast, HPLC-UV is the first choice for routinely measuring the individual forms of vitamin K (Ahmed *et al.*, 2007; Lefevere *et al.*, 1979).

MK-7 levels in fermentation are so low that it is important to eliminate the interfering compounds using sample clean-up methods. Since the reproducibility of the MK-7 profiles is also influenced by the chemical extraction and analysis conditions used to obtain quantitative data, sample clean-up was carried out using enzymatic hydrolysis previously described by Lambert *et al.* (1992) with slight modifications. It is reported that phosphatidyl-glycerol, the major polar lipid content of *Bacillus* species, and diacylglycerols, the major neutral lipid content of *Bacillus* species (Clejan *et al.*, 1986) can be hydrolysed by lipases (Cabot & Gatt, 1978; Verger *et al.*, 1978). The sample preparation in this method is simple in comparison to clean-up using two chromatographic systems. It appeared that enzymatic hydrolysis followed by ethanol precipitation of proteins prior to extraction with a mixture of 2-propanol: *n*-hexane (2:1, *v*/*v*) was very effective to

get rid of contaminants which gave spurious peaks in HPLC while ethanol treatment and centrifugation removed the denatured proteins by the ethanol treatment (Shino, 1988). In comparison to previously used open silica chromatography performed to purify the samples prior to reversed-phase chromatography, the method described here was less time-consuming and yielded good results coupled with the detection system. These treatments are extremely valuable as they can prolong the column life because the lipid contents that are injected into the column is a lot less (Lambert *et al.*, 1992).

Menaquinones are usually extracted with a mixture of a polar solvent and a nonpolar solvent. Commonly used polar solvents are isopropanol (Canfield *et al.*, 1991; Canfield *et al.*, 1990), ethanol (Shino, 1988) and methanol (Hodges *et al.*, 1993). In almost all the studies *n*-hexane has been the choice as a nonpolar solvent (Ahmed *et al.*, 2007; Canfield *et al.*, 1990; Hirauchi *et al.*, 1989; Hodges *et al.*, 1993; Schurgers & Vermeer, 2000; Shino, 1988). The most commonly used extraction solvent to readily extract menaquinones has been a mixture of 2-propanol and *n*-hexane (Hirauchi *et al.*, 1989). In the present study, extraction of MK-7 was therefore carried out with a mixture of 2-propanol and *n*-hexane (2:1, *v*/*v*).

For the purpose of quantification, extracts are normally evaporated and re-dissolved in polar solvents and analysed by reversed-phase chromatography. Each of these additional steps would lead to experimental error and potential loss of sample, and MK-7, which is a non-polar compound (Pennock, 1966), does not dissolve properly in polar solvents which adds to the experimental error. In contrast, the method described in this study does not require evaporation of the non-polar solvent and re-dissolution in a polar solvent. After extraction with a mixture of 2-propanol and *n*-hexane (2:1, *v*/*v*), the upper *n*-hexane layer was separated and mixed with 2-propanol in a volume ratio of 2-propanol: *n*-hexane 2:1 and directly injected into

reversed phase HPLC. MK-7 was eluted with the same mixture of solvents *i.e.* 2-propanol: *n*-hexane (2:1, *v*/*v*). The method described herein, therefore, reduces the number of steps involved in sample preparation for the analysis of MK-7 and eliminates the problem with the solubility of MK-7 leading to accurate quantification of MK-7.

Further, vitamin K homologs are highly lipophilic compounds and on a reversed phase C18 column with a polar solvent have very long retention times. Making the solvent stronger by addition of *n*-hexane speeds up elution/reduces retention. The present study requires a run time of 8 minutes which provides a greater efficiency for quantifying MK-7. The system enabled a high throughput of 7 samples per hour. This would be beneficial in terms of reducing the analytical cost. In addition, the low viscosity of *n*-hexane lowers the instrument back pressure.

The general usefulness of the developed method was demonstrated by its application in the analysis of MK-7 from several microorganisms. Using the above HPLC procedure, MK-7 from four different *Bacillus* species/strains were readily identified. Analysis of MK-7 from several *Bacillus* species/strains gave consistent results with a predominant UV absorbing signal at 248 nm corresponding to MK-7 with a retention time of 7.19 ± 0.1minutes in comparison to an authentic MK-7 standard with a retention time of 7.14 ± 0.02 minutes. The UV spectrum of MK-7 showed four distinct peaks characteristic of the naphthoquinone nucleus between 240 and 280 nm and less sharp absorption at around 320 and 330 nm. The results were consistent with previous records (Sommer & Kofler, 1967; Suttie, 1978). The presence of a single peak in the chromatogram also indicates that the major respiratory quinone present in *Bacillus sp* studied is MK-7. The results are in agreement with previous studies (Watanuki & Aida, 1972). Owing to the satisfactory accuracy, precision, sensitivity and short run time, the proposed HPLC

method can be used for the determination of MK-7 in fermented bacterial samples.

6.4 Summary

As a part of new analytical method development for MK-7 analysis, a rapid and sensitive reversed-phase high performance liquid chromatographic method combined with efficient extraction method was developed and validated with respect to accuracy, precision, specificity and linearity. Herein we describe, to our knowledge, the first HPLC assay to be validated for quantifying MK-7 using the same solvents for extraction and elution of MK-7 in high-performance liquid chromatography, eliminating the requirement to evaporate and re-dissolve extracts in a different mobile phase solvent. Therefore, the method is less time consuming and more accurate. Moreover, the good solubility of MK-7 in a mixture of 2-propanol and *n*-hexane, in comparison to previous mobile phase solvents, such as methanol, gives a more accurate quantification of MK-7 from samples. This method also has added strengths, such as short chromatographic runtime in comparison to previous methods. Therefore, the method described here is simple, efficient, accurate and reproducible, which can be used to routinely analyse bacterially synthesised MK-7. The developed method can, therefore be used to study the effect of IONs@APTES on MK-7 production in *Bacillus subtilis* fermentation which will be the focus of the next chapter.

Chapter 7

Impact of 3-Aminopropyltriethoxysilane-Coated Iron Oxide Nanoparticles on Menaquinone-7 Production Using *Bacillus subtilis*

This chapter forms the basis for the following publication:

Ranmadugala, D., Ebrahiminezhad, A., Manley-Harris, M., Ghasemi, Y., & Berenjian, A. (2017). Impact of 3–Aminopropyltriethoxysilane-Coated Iron Oxide Nanoparticles on Menaquinone-7 Production Using *Bacillus subtilis*. *Nanomaterials, 7*(11), http://dx.doi.org/10.3390/nano7110350.

7.1 Introduction

In terms of human health, the intake of MK-7 plays a vital role in bone formation (Tsukamoto *et al.*, 2000), reducing bone fractures (Cranenburg *et al.*, 2007) and in preventing postmenopausal bone loss by improving bone mineral calcification and the femoral neck width (Knapen *et al.*, 2007). In addition, a direct link has been observed between MK-7 consumption and improved cardiovascular health. Supplementation of MK-7 has especially, shown to decrease arterial stiffness in postmenopausal women (Knapen *et al.*, 2015). Therefore, interest in MK-7 has increased considerably over the past years and can be taken as the obvious choice to be included in multivitamin supplements for the prevention of these diseases (Cranenburg *et al.*, 2007).

MK-7 can only be produced through a fermentation process. Among the bacterial species used in MK-7 production, *Bacillus subtilis* is one of the most studied and recognised MK-7 producers (Sato *et al.*, 2001b). Although many studies on MK-7 production have been published using *Bacillus subtilis*, the fermentation process is still not sustainable enough. One of the complications, other than biofilm formation, is the low fermentation yield (Berenjian *et al.*, 2015).

Currently, nanoparticles are at the forefront of designing intensified bioprocesses with the combined advantages of reducing downstream processing and maximising the production of the target products (Ebrahiminezhad *et al.*, 2016b). In terms of bioprocess intensification, nanoparticles have been used to decorate bacterial cells and magnetically separate and re-use them in the fermentation system, which essentially eliminates the downstream purification steps such as filtration and centrifugation (Ebrahiminezhad *et al.*, 2016b; Sirkar *et al.*, 2006). Stepping towards the designing of an intensified MK-7 production system, recently *Bacillus subtilis* cells have been magnetically immobilised with naked IONs and subsequently

recovered from the fermentation media with a high capture efficiency (Ebrahiminezhad *et al.*, 2016b). In addition to reducing the number of downstream processing steps, magnetic immobilisation of *Bacillus subtilis* have further offered the advantages of good mass transport, catalytic stability (Ansari *et al.*, 2009) and improved metabolic activity (Ebrahiminezhad *et al.*, 2016b). Nevertheless, immobilisation with naked IONs has resulted in less cell densities and metabolic activity (Ebrahiminezhad *et al.*, 2016b). Further, when naked IONs are used in biological systems, many problems are encountered, such as particle agglomeration, low stability, altered magnetic properties (Ranmadugala *et al.*, 2017c) and cytotoxicity (Ranmadugala *et al.*, 2017a). As interaction of bacteria with nanoparticles are governed by the properties of the bacterial cell wall as well as the physicochemical characteristics of the nanoparticles and culture conditions, it is crucial to choose IONs with surface properties which fulfil the fermentation goals, namely, high metabolic activity and biocompatibility.

The current study, together with other previously recorded studies, show that amine-functionalised nanoparticles have more biological benefits than naked particles due to their biocompatibility, surface activity and chemical simplicity (Ebrahiminezhad *et al.*, 2012a; Ebrahiminezhad *et al.*, 2015; Ranmadugala *et al.*, 2017a). Compounds such as L-lysine, L-arginine and 3-aminopropyltriethoxysilane (APTES), which introduces amine functional groups to the nanoparticles, have been used to coat negatively charged nanoparticles, thereby increasing the chance of binding nanoparticles to the anionic cell membrane. Amine functionalised IONs are also reported to be more stable with good magnetic properties (Ebrahiminezhad *et al.*, 2012b; Ranmadugala *et al.*, 2017a). Previously, IONs coated with L-lysine had been reported to result in no significant inhibitory effect on MK-7 production and cell growth (Ebrahiminezhad *et al.*, 2016b). However, it has now been reported that,

in comparison with L-lysine and L-arginine, coating of nanoparticles with APTES prevents the oxidation of nanoparticles and provides perfect protection for the crystal structure of nanoparticles (Ebrahiminezhad *et al.*, 2012b). Therefore, the present study aimed to evaluate the effect of IONs@APTES on MK-7 biosynthesis during *Bacillus subtilis* fermentation.

7.2 Results

7.2.1 Effect of IONs@APTES on MK-7 production

To explore the effect of IONs@APTES on menaquinone production by *Bacillus subtilis*, MK-7 production was compared in the absence and in the presence of varying concentrations of IONs@APTES (100-700 µg/mL). The relationship between IONs@APTES attachment to *Bacillus subtilis* cells and their effect on MK-7 production is shown in Figure 35.

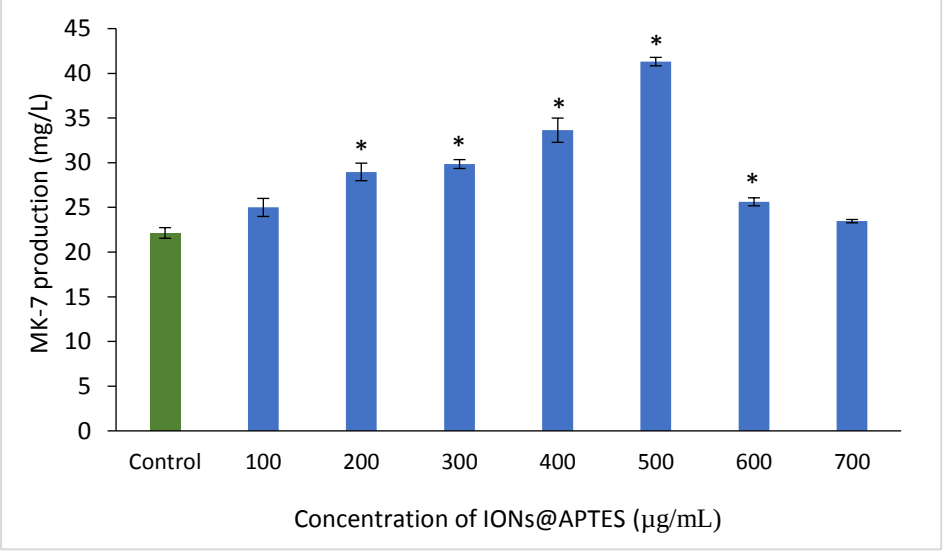

Figure 35 MK-7 production by *Bacillus subtilis* (ATCC 6633) in the presence of varying concentrations of IONs@APTES and in the absence of nanoparticles after 60 hours of fermentation. Values are mean ± standard error of three replicates. An asterisk indicates a significantly different value from the control ($p < 0.05$)

When the concentration of IONs@APTES was increased from 100 µg/ml to 500 µg/ml in the fermentation media, MK-7 production increased from ~22 to ~ 41 mg/L within 60 hours of *Bacillus subtilis* fermentation. However, when the concentration of IONs@APTES was increased beyond 600 µg/mL, the increase in MK-7 production was not significantly different from the control sample ($p > 0.05$). The highest MK-7 production of ~ 41 mg/L was 2-fold higher as compared to untreated bacteria. A typical HPLC chromatogram of MK-7 produced by *Bacillus subtilis* strain (ATCC 6633) in the presence of IONs@APTES (500 µg/mL) after 60 hours of fermentation is shown in Figure 36. These results show the key role played by decorating *Bacillus subtilis* cells with IONs@APTES in enhancing MK-7 biosynthesis.

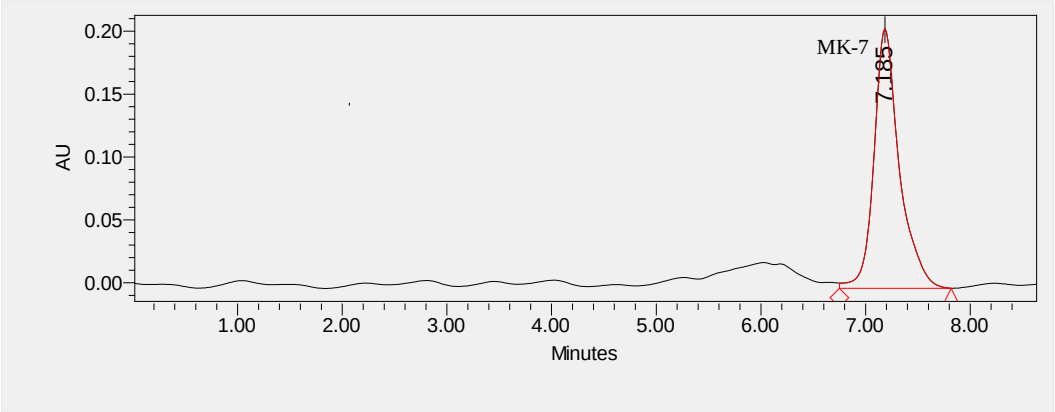

Figure 36 HPLC chromatogram (248 nm) of MK-7 in the culture of *Bacillus subtilis* (ATCC 6633) in the presence of IONs@APTES (500 µg/mL) after 60 hours of fermentation.

7.2.2 Effect of IONs@APTES on the growth of *Bacillus subtilis* (ATCC 6633)

In order to test the hypothesis whether the increased MK-7 production is associated with an increase in cell densities in the presence of IONs@APTES, *Bacillus subtilis* cells were grown for 60 hours in the presence of seven different concentrations of

IONs@APTES (100-700 µg/mL) and in the absence of nanoparticles (Figure 37).

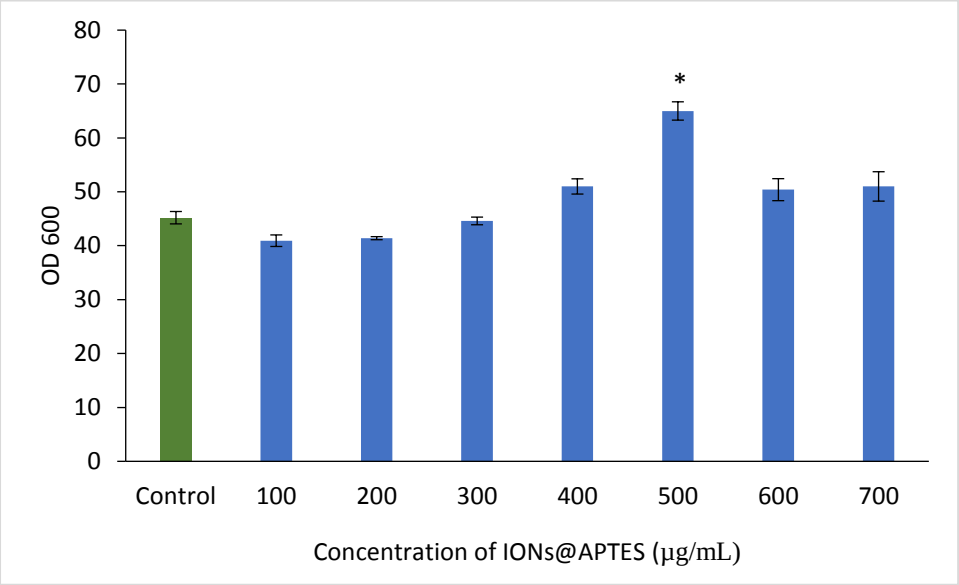

Figure 37 Growth by *Bacillus subtilis* (ATCC 6633) in the presence of varying concentrations of IONs@APTES and in the absence of nanoparticles after 60 hours of fermentation. Values are mean ± standard error of three replicates. An asterisk indicates a significantly different value from the control ($p < 0.05$)

Based on the results, the presence of IONs@APTES showed different effects on *Bacillus subtilis* growth. An increasing trend in *Bacillus subtilis* cell densities was observed with the increase in IONs@APTES concentration up to 500 µg/mL. However, there was no statistically significant difference between the samples decorated with 100-400 µg/mL of IONs@APTES as compared to control samples. A significantly high cell density was observed in the presence of 500 µg/mL of IONs@APTES ($p < 0.05$). Concentrations higher than 500 µg/mL of IONs@APTES led to a decrease in *Bacillus subtilis* cell density.

7.2.3 Effect of IONs@APTES on MK-7 yield

The effect on IONs@APTES concentrations on MK-7 yield was further investigated and the results are shown in Figure 38. MK-7 yield was calculated using the formula; MK-7 yield $= \frac{\text{MK-7concentration}}{\text{OD 600}}$

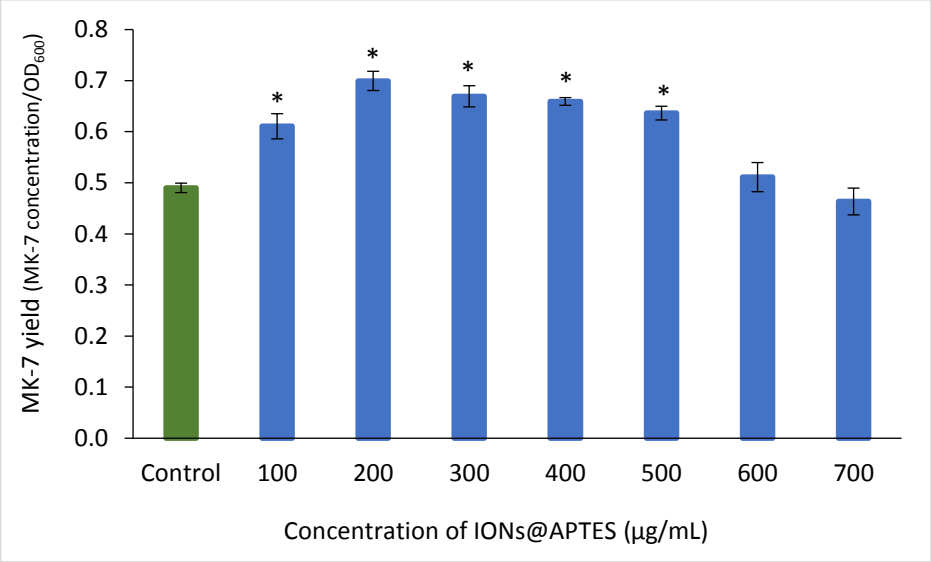

Figure 38 MK-7 yield by *Bacillus subtilis* (ATCC 6633) in the presence of varying concentrations of IONs@APTES and in the absence of nanoparticles after 60 hours of fermentation. Values are mean ± standard error of three replicates. An asterisk indicates a significantly different value from the control ($p < 0.05$)

The MK-7 yield was significantly higher in the presence of IONs@APTES in the range of 100-500 µg/mL as compared to *Bacillus subtilis* cells growing in the absence of nanoparticles ($p < 0.05$). Therefore, decoration of *Bacillus subtilis* cells with IONs@APTES has significantly influenced the MK-7 yield in a concentration-dependent manner. MK-7 fermentation yield increased by approximately 25%, 43%, 37%, 35%, 30% and 4% in the presence of 100-600 µg/mL IONs@APTES. The highest MK-7 yield of 0.70 was obtained when *Bacillus subtilis* cells were grown in the presence of 200 µg/mL of IONs@APTES. The MK-7 yield in the absence of nanoparticles was found to be 0.49. Treatment with 200 µg/mL IONs@APTES increased the *Bacillus subtilis* MK-7 fermentation

yield by approximately 43%. Therefore, 200 µg/mL of IONs@APTES can be taken as the optimum IONs@APTES concentration to obtain a high MK-7 yield during *Bacillus subtilis* (ATCC 6633) fermentation.

7.2.4 Time course of *Bacillus subtilis* fermentation in the presence of IONs@APTES

Time course studies were carried out in order to monitor the cell growth, biofilm biomass, MK-7 production and pH in the medium consisting of 5% (*w*/*v*) yeast extract, 18.9% (*w*/*v*) soy peptone, 5% (*w*/*v*) glycerol, 0.06% (*w*/*v*) K_2HPO_4 and 200 µg/mL IONs@APTES. This medium is designated as M1.

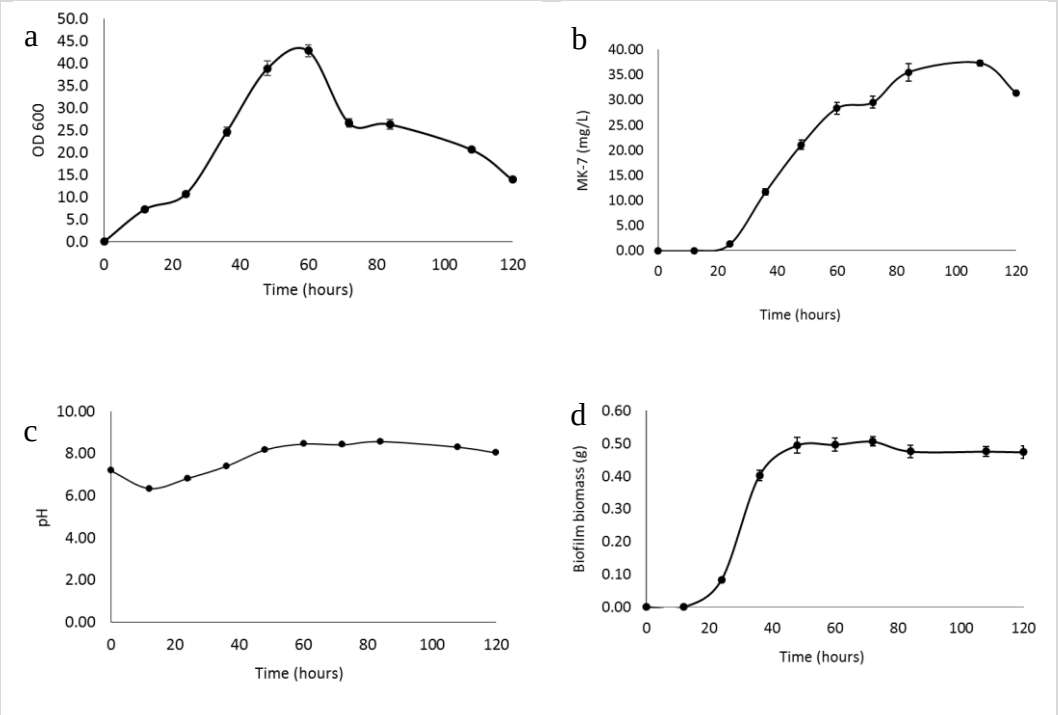

Figure 39 Time course of *Bacillus subtilis* (ATCC 6633) fermentation in the presence of 200 µg/mL IONs@APTES (M1). Error bars indicate standard error of means of triplicate determinations

According to the monitoring results, *Bacillus subtilis* growth increased in a time-dependent manner for about 60 hours and reached a maximum cell density of 42.93 (OD_{600}) (Figure 39-a). Biosynthesis of MK-7 also started after 24 hours of

fermentation and increased during the logarithmic phase (Figure 39-b). MK-7 production still increased after *Bacillus subtilis* growth reached its highest level (Figure 39-a and b). A maximum MK-7 concentration of 37.36 mg/L was observed at 108 hours when the cell growth was already declining. The pH of the medium decreased from 7.19 to 6.34 during the first 12 hours, and increased gradually up to 8.58 after 84 hours, following which it again decreased to 8.04 by the end of fermentation (Figure 39-c). Biofilm biomass increased with increasing cell densities and reached a maximum of 0.50614 g after 72 hours and started decreasing thereafter. Biofilm biomass reached a 0.47387 g at the end of fermentation at 120 hours (Figure 39-d).

7.3 Discussion

In this study, the effect of IONs@APTES on the fermentation yield of MK-7 using *Bacillus subtilis* (ATCC 6633) was investigated. Treatment with different concentrations of IONs@APTES significantly affected the MK-7 production ($p < 0.05$). In comparison to untreated cells, *Bacillus subtilis* cells decorated with IONs@APTES showed a significant increase in both MK-7 production and yield. An approximately twofold increase in menaquinone production (~ 41 mg/L) was observed in the presence of 500 µg/mL of IONs@APTES, as compared to MK-7 production using untreated bacteria after 60 hours of fermentation of *Bacillus subtilis* (ATCC 6633) at 37°C and shaking at 120 rpm. It was, however, apparent that the increase in MK-7 concentration is not merely a reflection on cell density. Binding of IONs@APTES to *Bacillus subtilis* might have changed the state or composition of cell membranes, resulting in enhanced secretion of MK-7 to the fermentation medium as suggested by earlier reports (Ebrahiminezhad *et al.*, 2016c; Liu *et al.*, 2017).

Most importantly, IONs@APTES did not show any negative effect on *Bacillus subtilis* growth within the tested concentrations, indicating that IONs@APTES are clearly compatible with *Bacillus subtilis* cells. The attachment of NPs to bacteria are governed by physicochemical interactions between IONs@APTES and *Bacillus subtilis* cells. While some studies indicate a toxicity effect of positively charged NPs on bacteria, our previous study (Chapter 5.3.4) reports the attachment of NPs without showing any detrimental effect on microorganisms (Ranmadugala *et al.*, 2017a). The interaction of IONs@APTES with *Bacillus subtilis* cells, therefore, provides a brand-new domain for enhancing MK-7 production in *Bacillus subtilis* fermentation without resulting in any harmful effect on bacterial growth. Enhancing the production of MK-7 in *Bacillus subtilis* (ATCC 6633) through the application of nanotechnology has been previously attempted with naked IONs, as well as IONs coated with L-lysine (Ebrahiminezhad *et al.*, 2016b; Ebrahiminezhad *et al.*, 2016c), under the same experimental conditions. However, decoration of *Bacillus subtilis* cells with naked IONs and L-lysine-coated IONs resulted in lower MK-7 concentrations as compared to untreated cells during a 5-day fermentation course (Ebrahiminezhad *et al.*, 2016c). Therefore, in comparison to naked IONs and L-lysine-coated IONs, IONs@APTES provide a perfect platform for enhancing the MK-7 yield of the fermentation system.

According to monitoring studies using 200 µg/mL IONs@APTES, production of MK-7 started after 24 hours and reached its maximum of 37.36 mg/L after 108 hours. The results are in agreement with previous studies (Sato *et al.*, 2001a; Song *et al.*, 2014) indicating that the production of MK-7 is partly growth-associated. Time course fermentation studies showed that the pH of the medium decreased from 7.19 to 6.34 during the first 12 hours, and increased gradually to 8.18 after 48 hours. This increase in pH might be a result of the production of ammonia during

the course of fermentation (Luo *et al.*, 2016). However, the increase in pH showed no negative impact on the MK-7 yield or bacterial growth. It was apparent that the biofilm biomass at 60 hours was 0.49689 g which is in agreement with the results of section 5.2.3.2. The maximum biofilm biomass observed during the course of fermentation was 0.50614 g at 72 hours and the biofilm biomass decreased thereafter. Less biofilm biomass observed in the presence of 200 µg/mL IONs@APTES confirms the findings of the previous study where IONs@APTES might have changed the surface charge and surface binding potential of bacterial cells or act as a physical barrier for the attachment of bacterial cells to other surfaces thereby reducing pellicle biofilm biomass. IONs@APTES, therefore, offers the great advantage of reducing biofilms in *Bacillus subtilis* fermentation which would be advantageous in the sense that it would address the mass and heat transfer issues that might arise in a large-scale fermentation process and many other process complications in MK-7 production (Berenjian *et al.*, 2013), and at the same time enhance MK-7 production in industrial menaquinone production.

7.4 Summary

In this study, IONs@APTES was identified as a promising agent which enhances MK-7 production. Cultivation of *Bacillus subtilis* in the presence of IONs@APTES significantly enhanced the MK-7 production without showing any inhibitory effect on *Bacillus subtilis* growth. The highest percentage increase of 43% was observed upon treatment with 200 µg/mL IONs@APTES. Therefore, 200 µg/mL of IONs@APTES can be taken as the optimum nanoparticle concentration to obtain the highest MK-7 yield during *Bacillus subtilis* fermentation. This study provides a great promise for synthesis and application of IONs@APTES in cell immobilisation in future bioprocess engineering protocols to overcome the low product yield of

MK-7. Therefore, it is of utmost importance to consider the results of the present study for further development of an industrial level production system for MK-7 using IONs@APTES.

In connection with the previous study in Chapter 6 and the monitoring studies, a remarkable observation is that IONs@APTES resulted in a dual activity of reducing biofilm formation while enhancing MK-7 production. IONs@APTES at a concentration level of 200 μg/mL can, therefore, be taken as a promising carrier in the optimisation of the MK-7 fermentation process.

Chapter 8

Reduced Biofilm Formation and Enhanced Menaquinone-7 Production by Medium Optimization

This chapter forms the basis for the following publication:

Ranmadugala, D., Ebrahiminezhad, A., Manley-Harris, M., Ghasemi, Y., & Berenjian, A. (2017). Reduced biofilm formation in Menaquinone-7 production process by optimizing the composition of the cultivation medium. *Trends in Pharmaceutical Sciences*, *3*(4), 245–254.

8.1 Introduction

Nutrients have a marked effect on biofilm formation as well as MK-7 production by *Bacillus subtilis*. Berenjian *et al.* (2011) have previously developed an efficient medium for high MK-7 production. However, it is well documented that the presence of complex nutrients in liquid fermentation media influence bacterial attachment (Mceldowney & Fletcher, 1986a), and as a consequence biofilm formation has posed a major problem in the MK-7 production process (Berenjian *et al.*, 2013). Reduction in biofilm formation would reduce costly periodic cleaning and improve mass transfer. Therefore, biofilm formation is an area worthy of serious attention in the MK-7 production process. Common strategies for biofilm control are the use of biocides and disinfectants which control biofilm formation by killing the microorganisms (Simões *et al.*, 2010). However, in industrial production of MK-7, it is of utmost importance that the removal strategy for biofilm should not affect bacterial cell viability. Furthermore, previous studies have demonstrated a linear dependency of MK-7 production on biofilm formation (Berenjian *et al.*, 2013). Therefore, strategies to optimise the overall productivity of the MK-7 production process with reduced biofilm formation and maximum MK-7 production, while maintaining the biological activity of bacteria, can be achieved either by reducing biofilm attachment as demonstrated by our previous study (Ranmadugala *et al.*, 2017a) or enhancing biofilm detachment (Chen & Stewart, 2000).

In addition to bacterial surface attachment, nutrient conditions in the medium can also greatly influence detachment (Chen, 1998). In this regard, it was hypothesised that the supplementation of the optimum medium for MK-7 production with nutrient components which would promote biofilm detachment might lead to low biofilm biomass and optimum overall productivity in the MK-7 production process.

Experimental evidence from the biofilm research field shows that biofilm detachment resides in the structural integrity of the biofilm (Picioreanu *et al.*, 2001). The structural integrity of biofilms, in turn, results from a combination of forces including van der Waals forces, electrostatic and hydrophobic interactions (Chen & Stewart, 2000). Disruption of these forces can, therefore, bring about biofilm detachment. In recent years the use of monovalent and divalent cations has presented themselves as options for biofilm removal by changing the structure of the biofilm (Chen, 1998; Chen & Stewart, 2002; Chen & Stewart, 2000). Apart from the salts, there are indications that nitrogen source influences the amount and size of exopolysaccharides (Degeest & De Vuyst, 1999), which are a major component of the biofilm matrix. Urea, for example, is a well-known organic nitrogen as well as a carbon source which is said to speed up the growth of bacteria in many instances (Stanbury *et al.*, 2013). While rapid growth rate itself can bring about biofilm biomass loss (Picioreanu *et al.*, 2001), experimental evidence shows that urea can also act as a chaotropic agent which would disrupt the network of hydrogen bonding interactions responsible for biofilm cohesion (Chen & Stewart, 2002; Chen & Stewart, 2000). Therefore, the aim of the present study was to optimise the cultivation medium composition to achieve the lowest possible biofilm biomass with highest possible MK-7 production. Optimisation of the production process was done in two steps. First, the effect of chemical treatment as a biofilm detachment strategy on biofilm formation and MK-7 production was investigated. Secondly, a combination of biofilm attachment and detachment strategies were used where chemical treatment and nanoparticle treatment were combined to see the effect on biofilm biomass and MK-7 production.

8.2 Results

8.2.1 Screening the effect of chemical treatment on biofilm formation and MK-7 production

In order to study the effect of salts and urea on biofilm formation and MK-7 production, *Bacillus subtilis* (ATCC 6633) were grown in the optimum medium previously described by Berenjian *et al.* (2011) with added salts and urea. When selecting parameters that would reduce/remove biofilm formation, the main consideration was the parameters that would reduce/remove biofilm formation without showing any detrimental effect on bacterial growth.

The initial screening process was carried out using Design of Experiment (DOE) methodology with three different variable factors: NaCl, $CaCl_2$, and urea. The three distinct variables were exploited to investigate the most important factors for reducing biofilm biomass and increasing MK-7 production. Experimental range and levels of independent variables used for the full factorial design are presented in Table 5. Concentrations of these variables that were used in the experimental design and the two responses of biofilm formation and MK-7 production are presented in Table 6. Statistical analysis is provided in Table 7 to demonstrate the main effective factors on biofilm formation and MK-7 production. The linear regression coefficient (R^2) was 0.984 and 0.963 for MK-7 production and biofilm biomass, respectively. The R^2 adj values for MK-7 production and biofilm biomass are 0.960 and 0.907 respectively. The data show the validity of the two models, which is visually displayed by the coefficient plots (Figure 40).

Table 5 Nutrient levels for microbial production of MK-7 and biofilm biomass - Full-Factorial design

Variable number	Variable name	Value		
		Low level (-1)	central level (0)	High level (+1)
X_1	NaCl	0	0.5	1
X_2	$CaCl_2$	0	0.5	1
X_3	Urea	0	2.5	5

Table 6 The effect of selective variables on MK-7 production and biofilm biomass of *Bacillus subtilis* (ATCC 6633)

Run	Variable factors [a]			MK-7 production (mg/L)	Biofilm biomass (g)
	NaCl % (*w*/*v*)	$CaCl_2$% (*w*/*v*)	Urea% (*w*/*v*)		
1	0 (-1)	0 (-1)	0 (-1)	22.94	0.76637
2	1 (+1)	0 (-1)	0 (-1)	21.91	0.74428
3	0 (-1)	1 (+1)	0 (-1)	15.81	0.44331
4	1 (+1)	1 (+1)	0 (-1)	12.42	0.42380
5	0 (-1)	0 (-1)	5 (+1)	13.09	0.57875
6	1 (+1)	0 (-1)	5 (+1)	11.17	0.54652
7	0 (-1)	1 (+1)	5 (+1)	12.38	0.38612
8	1 (+1)	1 (+1)	5 (+1)	6.78	0.43780
9	0.5 (0)	0.5 (0)	2.5 (0)	16.36	0.51557
10	0.5 (0)	0.5 (0)	2.5 (0)	14.32	0.48102
11	0.5 (0)	0.5 (0)	2.5 (0)	15.12	0.49195

[a] values are expressed in (% *w*/*v*)

Table 7 Statistical analysis of full factorial design matrix for MK-7 production and biofilm biomass

Term	MK-7 (mg/L) [a]			Biofilm biomass (g) [b]		
	coefficient	Standard error	*P* value	coefficient	Standard error	*P* value
constant	14.7546	0.2780	7.5491e-007	0.5287	0.0115	1.3339e-006
X_1	-1.4946	0.3260	0.0102	-0.0028	0.0135	0.8472
X_2	-2.7133	0.3260	0.0011	-0.1181	0.0135	0.0009
X_3	-3.7080	0.3260	0.0003	-0.0536	0.0135	0.0164
X_1X_2	-0.7551	0.3260	0.0815	0.0108	0.0135	0.4672
X_1 X_3	-0.3876	0.3260	0.3003	0.0076	0.0135	0.6014
X_2 X_3	1.4393	0.3260	0.0116	0.0428	0.0135	0.0337

[a] R^2 = 0.984, R^2 adj 0.960, significance code : $p < 0.05$

[b] R^2 = 0.963, R^2 adj 0.907, significance code : $p < 0.05$

The monovalent salt (NaCl) and the divalent salt ($CaCl_2$) were evaluated to find out the influence on MK-7 production and biofilm formation. As illustrated in Table 7 and Figure 40, the presence of NaCl had no significant impact on biofilm formation by *Bacillus subtilis* ($p > 0.05$). However, the presence of $CaCl_2$ significantly reduced the biofilm biomass ($p < 0.05$). According to the coefficient plots, $CaCl_2$ showed the greatest influence on biofilm biomass. The presence of NaCl and $CaCl_2$ both, however, showed a significant negative effect on MK-7 production ($p < 0.05$). According to the screening results, the presence of urea significantly reduced the biofilm biomass ($p < 0.05$) (Figure 40 and Table 7). Further, the presence of urea showed a negative effect on MK-7 production. However, the presence of urea together with $CaCl_2$ showed a positive effect on MK-7 production. Based on these results, $CaCl_2$ and urea were used as variables for the optimisation of the MK-7 production process.

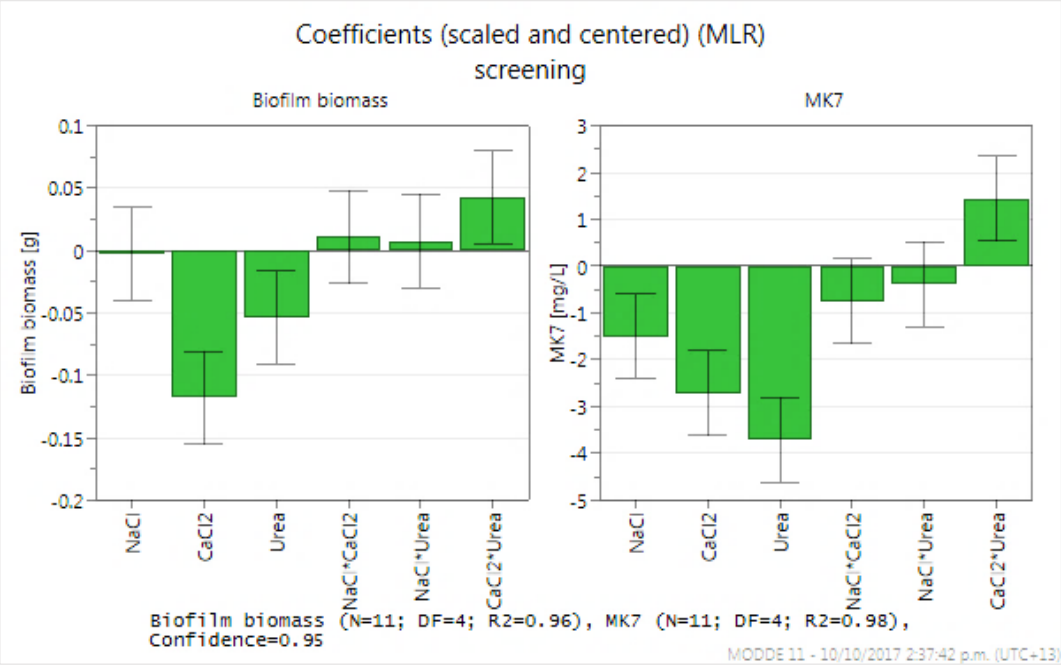

Figure 40 Scaled and centred plots for biofilm biomass and MK-7 production from screening studies.

8.2.2 Optimisation of chemical treatment on biofilm formation and MK-7 production

In the second phase, a full factorial central composite face design (CCD) was applied to optimise the significant effective factors chosen from the screening step. MODDE software version 11 (Umetrics, Sweden) was used for statistical analysis.

8.2.2.1 Statistical analyses and interpretation using Response Surface Methodology (RSM)

The statistical analysis of this research was performed using RSM by a CCD design. Experimental conditions for the central composite face design and responses for MK-7 and biofilm biomass (for both original and scaled factors) are given in Table 8.

Table 8 Experimental conditions for the central composite face design (CCD) and responses for MK-7 and biofilm biomass (for both original and scaled factors)

	$CaCl_2$ (% *w*/*v*)	Urea (% *w*/*v*)	MK-7 observed (mg/L)	MK-7 predicted (mg/L)	Biofilm biomass observed (g)	Biofilm biomass predicted (g)
1	0.1 (-1)	0.1(-1)	23.41	23.06	0.64438	0.65639
2	0.9 (+1)	0.1 (-1)	14.66	14.54	0.47595	0.48801
3	0.1(-1)	4.9 (+1)	14.97	15.36	0.55708	0.55786
4	0.9 (+1)	4.9 (+1)	14.38	14.99	0.50126	0.50209
5	0.1 (-1)	2.5 (0)	21.91	21.88	0.67023	0.65744
6	0.9 (+1)	2.5 (0)	17.94	17.43	0.55824	0.54536
7	0.5 (0)	0.1 (-1)	14.27	14.74	0.47372	0.44965
8	0.5 (0)	4.9 (+1)	12.14	11.13	0.40904	0.40743
9	0.5 (0)	2.5 (0)	15.55	15.60	0.47512	0.47885
10	0.5 (0)	2.5 (0)	14.94	15.60	0.46414	0.47885
11	0.5 (0)	2.5 (0)	15.75	15.60	0.47160	0.47885

Individual factors and their interaction effects on MK-7 production and biofilm formation were determined, and statistical models were created to obtain the optimum conditions to minimise biofilm formation and maximise MK-7 production. Quadratic models are proposed. Statistical analysis of central composite face design experiments and the summary of the ANOVA results of the model fitting is shown in Table 9 and Table 10 respectively.

Table 9 Statistical analysis of the central composite face design experiments

Term	MK-7 production (mg/L) [a]			Biofilm biomass (g) [b]		
	coefficient	Standard error	*p* value	coefficient	Standard error	*p* value
constant	15.598	0.3722	1.4586e-007	0.4788	0.0088	4.0586e-008
X_1	-2.2215	0.2962	0.0007	-0.0560	0.0070	0.0005
X_2	-1.8077	0.2962	0.0017	-0.0211	0.0070	0.0301
X_1^2	4.0560	0.4558	0.0003	0.1225	0.0011	0.0001
X_2^2	-2.6644	0.4558	0.0021	-0.0503	0.0183	0.0056
$X_1 X_2$	2.0392	0.3627	0.0025	0.0282	0.0086	0.0223

X_1 Calcium chloride, X_2 Urea

[a] R^2 = 0.978, R^2 adj 0.955, significance code : $p < 0.05$
[b] R^2 = 0.977, R^2 adj 0.954, significance code : $p < 0.05$

Table 10 Analysis of variance for the quadratic models

Source of variation	Biofilm biomass (g)						MK-7 production (mg/L)					
	DF	SS	MS	SD	F	P	DF	SS	MS	SD	F	P
Total corrected	10	0.0651	0.0065	0.0807	42.806	0.000	10	116.989	11.6989	3.4204	43.457	0.000
Regression	5	0.0636	0.0127	0.1128				114.357	22.8715	4.7824		
Residual	5	0.0015	0.0003	0.0172				2.63148	0.52630	0.7255		
P lack of fit	0.0628						0.0948					
DF lack of fit	3						3					

For both the model equations, F-values of 43.4574 and 42.8068 for MK-7 and biofilm biomass respectively imply that the models are significant. Values of *P* less than 0.05 indicate model terms are significant. In this case, all the model terms *i.e.* X1, X2, $X1^2$, $X2^2$ and X1X2 are significant for MK-7 and biofilm biomass. The empirical relationships between the two responses (MK-7 production and biofilm biomass) and the variables ($CaCl_2$ and urea concentration) were built and are shown by the following regression equations (Equations 7 and 8).

$$Y_1 = 15.598 - 2.2215\,X_1 - 1.80768\,X_2 + 4.05598\,X_1^2 - 2.66436\,X_2^2 + 2.03915\,X_1X_2 \quad (7)$$

$$Y_2 = 0.478847 - 0.05604X_1 - 0.0211117\,X_2 + 0.122548\,X_1^2 - 0.0503071\,X_2^2 + 0.0281525X_1X_2 \quad (8)$$

Y1 and Y2 are the predicted values of MK-7 and biofilm biomass respectively and X1, X2 represents $CaCl_2$ and urea concentration respectively. Figure 41 shows the response contour plots based on Equation (7) and (8) to visualise the influence of the effective variables on biofilm formation and MK-7 production. Correspondingly, the model's equation (7) and (8) assumed that the highest MK-7 production (17.53 mg/L) and lowest biofilm biomass (0.51 g) could be achieved using 0.32% (*w*/*v*) $CaCl_2$ and 0.10% (*w*/*v*) urea, respectively. As can be seen from Figure 41, biofilm biomass decreased with the increase in $CaCl_2$ and urea concentrations. Increasing the percentage of urea in the medium up to 2.25% (*w*/*v*) resulted in higher MK-7 production. However, a further increase in urea

concentration reduced the MK-7 production. Therefore, MK-7 can be improved by adding an optimal amount of urea, which acts as a source of nitrogen in the microbial metabolic pathway. According to the results, $CaCl_2$ and urea were found to be crucial factors to influence both biofilm formation and MK-7 production. Biofilm biomass can be markedly reduced by adding $CaCl_2$ and urea.

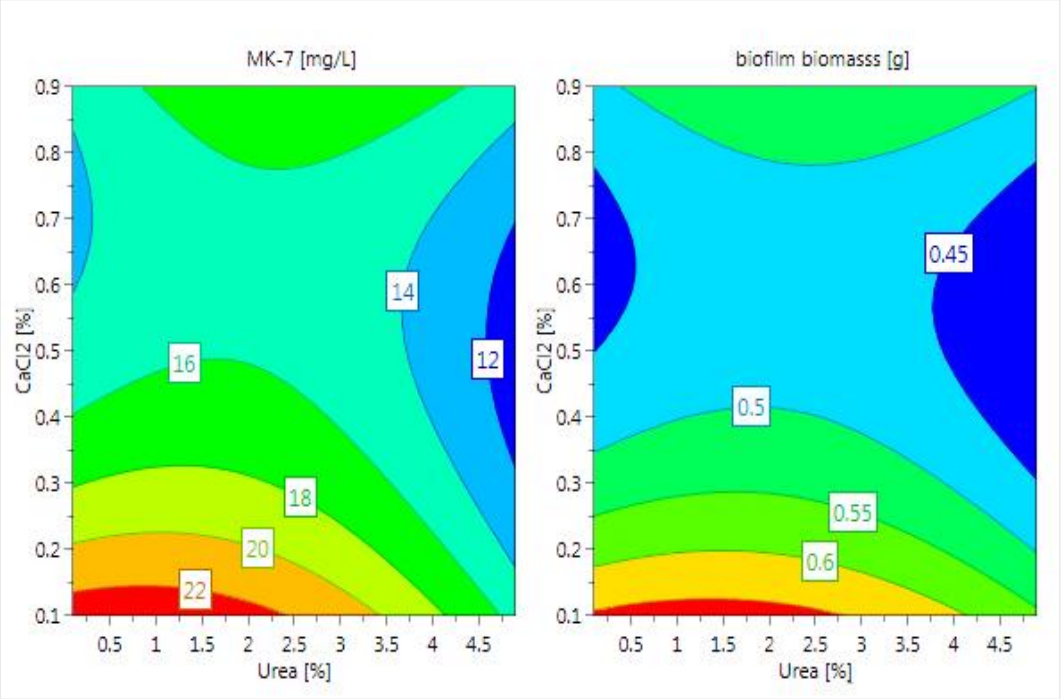

Figure 41 Response contour plots for the biofilm biomass and MK-7 production.

8.2.3 Model validation

In order to evaluate the predicted optimal conditions from the models, a verification test was conducted using the two independent variables: $CaCl_2$ and urea concentrations. The experimental conditions used for the validation experiment are given in Table 11. The test was performed in triplicate.

Table 11 Validation experiment conditions

Experiment	$CaCl_2$ % (*w*/*v*)	Urea % (*w*/*v*)
validation	0.32	0.10

Results of the validation test are given in Table 12. The MK-7 production and biofilm biomass were similar to predicted values from the model with 2% and 8% variation respectively. The outstanding correlation between predicted and measured values verified the model accuracy for these experiments.

Table 12 Percentage variation of biofilm biomass and MK-7 from the predicted values

	Verification test	Predicted values	% variation
Biofilm biomass (g)	0.55 ± 0.02	0.51	8%
MK-7 production (mg/L)	17.98 ± 0.41	17.53	2%

8.2.4 Time course of *Bacillus subtilis* fermentation in the presence of $CaCl_2$ and urea

Based on the results, fermentation experiments were performed for 120 hours to monitor the production of biofilm biomass, MK-7 production, bacterial growth, and pH in the nutrient medium consisting of 5% (*w*/*v*) yeast extract, 18.9% (*w*/*v*) soy peptone, 5% (*w*/*v*) glycerol, 0.06% (*w*/*v*) K_2HPO_4, 0.32% (*w*/*v*) $CaCl_2$ and 0.10% (*w*/*v*) urea. This medium is named as M2.

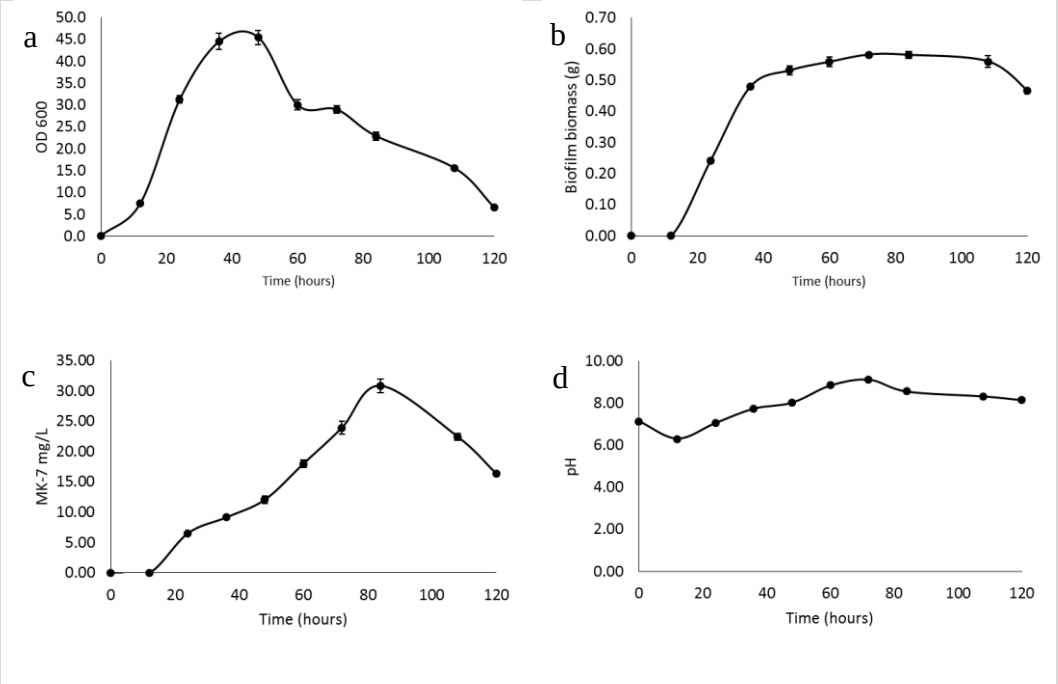

Figure 42 Time course of *Bacillus subtilis* (ATCC 6633) fermentation in the presence of 0.32% (*w*/*v*) $CaCl_2$ and 0.10% (*w*/*v*) urea (M2).

As can be concluded from Figure 42-a, a rapid growth of *Bacillus subtilis* was seen in the presence of $CaCl_2$ (0.3%, *w*/*v*) and 0.10 % (*w*/*v*) urea during the first 48 hours. Cell density reached a maximum of 45.76 ($OD_{600\ nm}$) at 48 hours and started to decline thereafter (Figure 42-a). The rate of accumulation of biofilm biomass was less after 60 hours of fermentation. The maximum biofilm biomass was 0.58163 g at 72 hours of fermentation (Figure 42-b). MK-7 production increased rapidly after the cell density reached its maximum at 48 hours and peaked at 30.83 mg/L after 84 hours of fermentation (Figure 42-c). The pH of the medium decreased from 7.1 to 6.3 during the first 12 hours and gradually increased up to 9.12 thereafter with the increase in cell growth. A slight decrease in pH was seen after the cell growth was at the maximum level (Figure 42-d). A ~27% reduction in biofilm biomass was found in the medium M2 supplemented with 0.32% (*w*/*v*) $CaCl_2$ and 0.10% (*w*/*v*) urea after 60 hours of fermentation. However, a ~22% reduction in MK-7 production was also observed in this medium.

8.2.5 Optimisation of the composition of the cultivation medium for reduced biofilm formation and enhanced MK-7 production

In order to develop an optimum medium with reduced biofilm formation as well as with highest possible MK-7 production, the M2 medium was supplemented with the optimum concentration of IONs@APTES (200 µg/mL). This medium was designated as M3 which consisted of 5% (*w*/*v*) yeast extract, 18.9% (*w*/*v*) soy peptone, 5% (*w*/*v*) glycerol, 0.06% (*w*/*v*) K_2HPO_4, 0.32% (*w*/*v*) $CaCl_2$, 0.10% (*w*/*v*) urea and 200 µg/mL IONs@APTES. All experiments were carried out in triplicate.

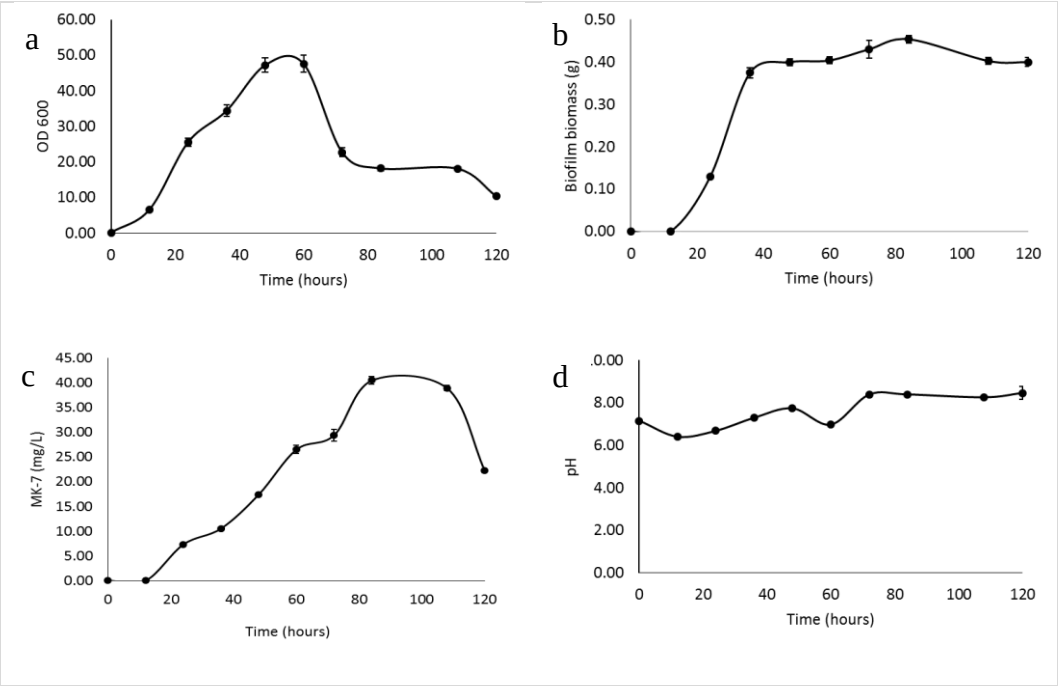

Figure 43 Time course of *Bacillus subtilis* (ATCC 6633) fermentation in the presence of 0.32% (*w*/*v*) $CaCl_2$, 0.10% (*w*/*v*) urea and 200 µg/mL of IONs@APTES (M3).

As can be seen from Figure 43-a, a rapid growth of *Bacillus subtilis* was seen in the presence of 0.32 % (*w*/*v*) $CaCl_2$, 0.10 %, (*w*/*v*) urea and 200 µg/mL IONs@APTES during the first 48 hours. Cell density reached a maximum of 45.6 (OD_{600}) at 60 hours and started to decline thereafter. A rapid increase in biofilm biomass was seen within 40 hours of cultivation (43-b). However, the rate of biomass accumulation was low after 40 hours. The maximum biofilm biomass observed was 0.45392 g at

84 hours of fermentation. MK-7 concentration reached its maximum at 84 hours and peaked at 40.60 mg/L (43-c). The pH of the medium decreased from 7.15 to 6.39 during the first 12 hours and gradually increased up to 7.7 followed by a slight drop in pH to 6.97 at 60 hours after the cell growth was at the maximum level and increased thereafter (43-d). The behaviour of the three culture systems (M1, M2 and M3) are represented in Figure 44.

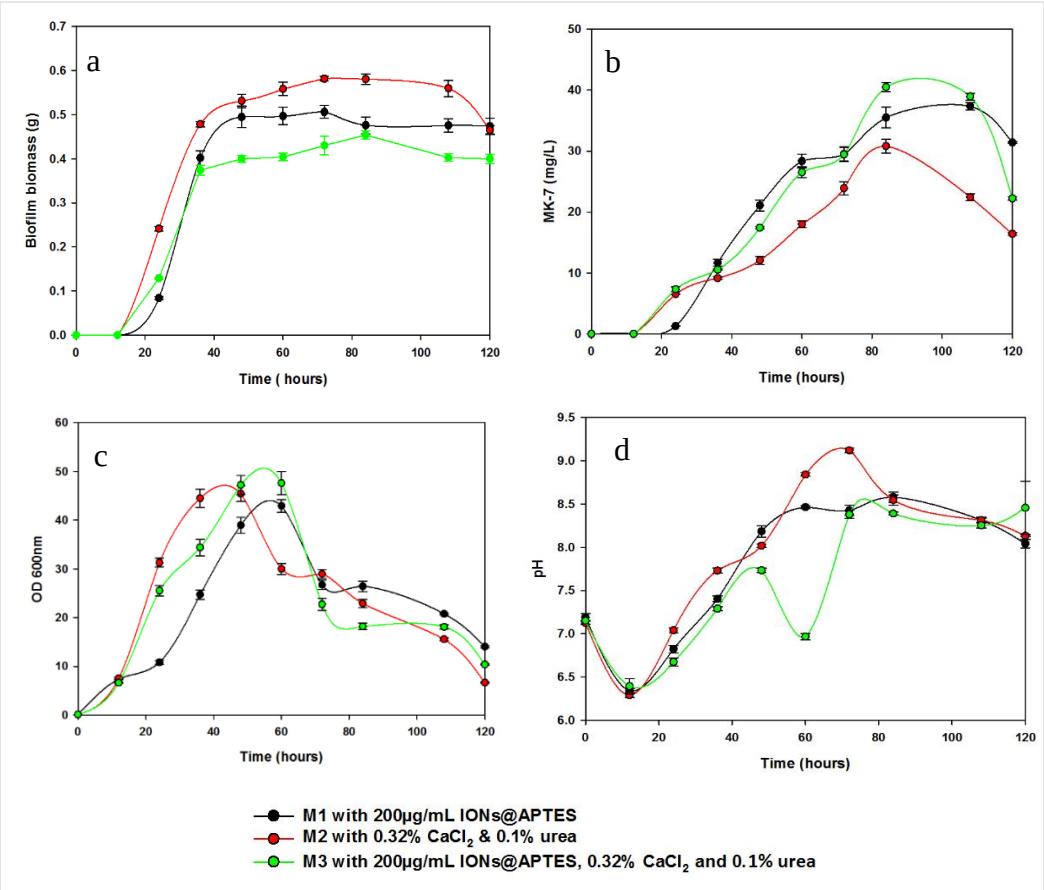

Figure 44 Comparative analysis of biofilm biomass, MK-7 production, cell growth and pH in M1, M2 and M3.

Comparative analysis of biofilm biomass in M1 (medium with IONs@APTES), M2 (medium with $CaCl_2$ and urea) and M3 (medium supplemented with IONs@APTES, $CaCl_2$ and urea), showed a minimum pellicle biofilm biomass in the M3 medium which is supplemented with IONs@APTES, $CaCl_2$ and urea. The maximum biofilm biomass observed in M3 was 0.45392 g which was 0.12771 g less than the

maximum biofilm biomass in M2 and 0.05222 g less than the maximum biofilm biomass in M1 (Figure 44-a.).

Most convincingly, the highest MK-7 production of 40.60 mg/L was seen in the medium supplemented with IONs@APTES, $CaCl_2$ and urea (M3) at 84 hours. This amount was greater than the MK-7 production in M2 (30.83 mg/L) which peaked at 84 hours and in M1 (37.36 mg/L) which peaked at 108 hours of fermentation (Figure 44-b). MK-7 production was significantly less when in the absence of IONs@APTES. In addition, the comparative analysis of the growth of *Bacillus subtilis* in all three media showed that high cell densities could be achieved within 48 hours of fermentation in the medium supplemented with IONs@APTES, $CaCl_2$ and urea (M3) (Figure 44-c). A significant drop in the pH was observed during the first 12 hours of fermentation in all three media. In the M3 medium with $CaCl_2$, urea and IONs@APTES, a drop in pH was observed again at 60 hours whereas the pH increased at 72 hours in the medium supplemented with $CaCl_2$, urea (Figure 44-d). The results indicated that M3 is the optimum medium which can result in the lowest biofilm formation and the highest MK-7 production.

In comparison with controlled conditions without added $CaCl_2$, urea and IONs@APTES, the medium M3 supplemented with 0.32% (*w*/*v*) $CaCl_2$, 0.10% (*w*/*v*) urea and 200 µg/mL IONs@APTES showed approximately 47% reduction in biofilm biomass and most importantly, ~ 16% increase in MK-7 production after 60 hours of fermentation in comparison to medium without added $CaCl_2$, urea and IONs@APTES.

A typical HPLC chromatogram of MK-7 produced by *Bacillus subtilis* strain (ATCC 6633) in the optimum medium (M3) is shown in Figure 45.

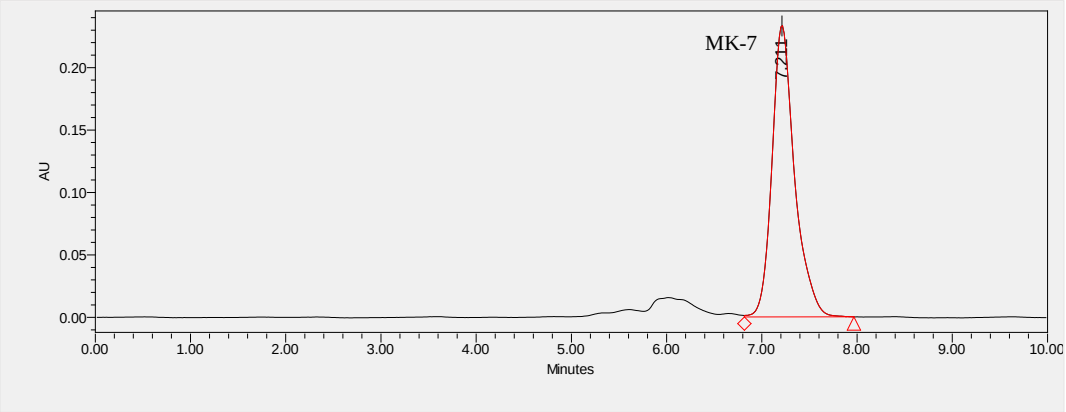

Figure 45 HPLC Chromatogram of MK-7 in the culture of *Bacillus subtilis* in the optimum medium designed in this study after 60 hours of fermentation. HPLC conditions are described in the section on materials and methods.

8.3 Discussion

Biofilm formation and MK-7 production by *Bacillus subtilis* can be greatly influenced by medium components. In *Bacillus subtilis* fermentation, main consideration was therefore given to the parameters which would reduce biofilm biomass without killing the bacteria. In this regard, the first phase of the study was geared towards developing a biofilm detachment strategy by changing the biofilm structure/interfering with biofilm crosslinking forces. Therefore, in the initial screening study, salts (monovalent cationic salts, divalent cationic salts) and urea were selected as variables based on their ability to interfere with the structural integrity of biofilms without affecting the viability of the bacterial cells. The effect of three types of variables *i.e.* two types of salts namely NaCl, and $CaCl_2$, and urea on biofilm formation and MK-7 production were investigated. Prior to the screening study, a preliminary study was carried out to have a rough estimation of parameter ranges.

Disruption of the forces that maintain the structural integrity of biofilms, such as the electrostatic and hydrophobic interactions, is said to bring about biofilm detachment (Chen & Stewart, 2000). The results of the present study indicated that

the presence of $CaCl_2$ significantly reduces the biofilm biomass. These findings were similar to the previous studies where $CaCl_2$ is said to reduce the biofilm by disrupting biofilm crosslinking forces such as electrostatic interactions and destroying structural biofilm components (Chen, 1998; Chen & Stewart, 2000). There are other reports showing that calcium can increase bacterial adhesion in a concentration-dependent manner (Turakhia *et al.*, 1983). However, Das *et al.* (2014) report that Ca^{2+} can increase biofilm biomass only in the presence of eDNA (Das *et al.*, 2014), and the response could vary depending on the bacterial strain (Larsen *et al.*, 2007) and their growth stage (Tian *et al.*, 2012).

The presence of urea also contributed to less biofilm biomass in this study. Apart from the electrostatic interactions, hydrogen bonding is also regarded as a major cohesive force which plays a major role in maintaining the integrity of the biofilm structure. The results of this study are in agreement with the findings of Chen and Stewart, who demonstrated that treatment with 2M Urea reduces biofilm viscosity by 46% by disrupting the hydrogen bonding network between water molecules (Chen & Stewart, 2002; Chen & Stewart, 2000). The presence of urea might have also influenced the amount and size of exopolysaccharides, which are a major component of the biofilm matrix which biofilm bacteria are being held as described previously by Degeest and De Vuyst (1999). In addition to the contribution towards reducing biofilm biomass, urea might have also acted as a carbon and an organic nitrogen source which speed up the growth (Stanbury *et al.*, 2013). However, the effect of urea on the growth of *Bacillus subtilis* is concentration dependent. It has been reported that concentrations of urea above 4% (*w*/*v*) would lead to no growth or cell division (Valentine & Bradfield, 1954).

According to our study, NaCl was not effective as a nutrient to reduce biofilm biomass although earlier reports suggested that NaCl promotes biofilm detachment

(Chen & Stewart, 2002; Chen & Stewart, 2000) as well as reduces bacterial gel strength of extracellular polymeric substances (Gordon *et al.*, 1991). In terms of MK-7 production, it was apparent that the interaction of urea with $CaCl_2$ had a significantly positive impact on MK-7 production ($p < 0.05$).

In this study, the optimum conditions to minimise biofilm formation while maximising MK-7 production was predicted by response surface methodology successfully. The models assumed the lowest biofilm biomass (0.51 g) and highest MK-7 production (17.96 mg/L) could be achieved at 0.32% (*w*/*v*) $CaCl_2$ and 0.10% (*w*/*v*) urea. The predicted values were justified by a verification test. According to the results, biofilm detachment might have been brought about by 1) loss of biofilm strength or loosening of biofilm structure, or 2) change in the texture of the biofilm. These results are in agreement with the studies which reported that bacterial detachment can be manipulated using monovalent and divalent cations and urea (Chen, 1998; Chen & Stewart, 2002; Chen & Stewart, 2000).

In the second phase of the study, the optimum nutrient medium was supplemented with the optimum IONs@APTES (200 µg/mL) and the behaviour of the culture system was monitored. The optimum medium supplemented with IONs@APTES showed elevated levels of MK-7 with minimum biofilm formation. Comparative studies showed that although the biofilm developed faster at the early stages in the optimum medium (M3), the biofilm biomass was less and it showed higher instability after 36 hours. These results are in agreement with previous studies where it has been shown that microbial detachment depends on microbial growth rate and high microbial growth rates would lead to instability in biofilm accumulation and would trigger biomass loss (Picioreanu *et al.*, 2001). It is evident that the presence of IONs@APTES has also contributed to the lower biofilm biomass in agreement with our previous observations (section 5.2.3) where

IONs@APTES can reduce bacterial attachment by changing the surface binding potential of *Bacillus subtilis* and also by acting as a physical barrier for surface attachment (Ranmadugala *et al.*, 2017a).

In addition, previous reports suggest that changes in pH can also influence the biofilm structure. For example, a slight decrease in pH was seen after the cell growth was at the maximum level, a possible explanation for which is the conversion of organic substances to volatile fatty acids and poorly-soluble gases, both weakening the biofilm structure (Applegate & Bryers, 1991). Further, it has also been shown that oxygen limited biofilms with higher Ca^{2+} concentration exhibit shear removal rates (Applegate & Bryers, 1991). Although the chemical basis is unknown, it was evident that the presence of monovalent and divalent salts together with urea and IONs@APTES have changed the attachment and detachment properties of *Bacillus subtilis* biofilm biomass.

It was evident that the presence of $CaCl_2$ and urea together had a positive effect on MK-7 production. It can, therefore, be speculated that these nutrients might have boosted up bacterial metabolism. Elevated levels of MK-7 were observed in the optimum medium (M3) which confirms the results of our previous study (section 7.2.1) where IONs@APTES might have changed the state/composition of the bacterial cell membrane resulting in enhanced synthesis and secretion of MK-7 (Ebrahiminezhad *et al.*, 2016c; Liu *et al.*, 2017; Ranmadugala *et al.*, 2017b).

The feasibility of reducing biofilm formation and maximising MK-7 production using $CaCl_2$, urea and IONs@APTES was confirmed in the present study. This chapter has an important outcome since the approach presented here can be applied to biofilm control in any type of bioreactor in order to reach the optimal desirable properties for different applications.

8.4 Summary

In the present study, the culture medium was optimised to address the problem of biofilm formation while maximising the MK-7 production. Calcium chloride and urea were found to be effective in influencing both biofilm formation and MK-7 production. It was evident that $CaCl_2$ and urea significantly reduced biofilm biomass while these two nutrients together had a positive effect on MK-7 production. The presence of 200 µg/mL of IONs@APTES in addition to $CaCl_2$ and urea in the medium (M3) showed elevated levels of MK-7, which confirms that the presence of IONs@APTES in the optimum medium may have changed the state of the cell membrane leading to enhanced synthesis and secretion of MK-7. The optimum medium, which would result in minimum biofilm formation and maximum MK-7 production, consisted of 5% (*w*/*v*) yeast extract, 18.9% (*w*/*v*) soy peptone, 5% (*w*/*v*) glycerol, 0.05% (*w*/*v*) K_2HPO_4, 0.32% (*w*/*v*) $CaCl_2$, 0.10% (*w*/*v*) urea and 200 µg/mL IONs@APTES. Approximately ~ 47% reduction in biofilm biomass and ~ 16% increase in MK-7 production was observed after 60 hours of fermentation in comparison to the medium without added $CaCl_2$, urea and IONs@APTES. The feasibility of reducing biofilm formation and maximising MK-7 production in *Bacillus subtilis* fermentation while maintaining the growth of the bacterium in the optimum medium supplemented with $CaCl_2$, urea and IONs@APTES was confirmed in this study. The proposed treatments generally can, therefore, be applied to minimise biofilm formation while maximizing the MK-7 production in the *Bacillus subtilis* fermentative system. Using this medium, the feasibility of designing a milking process in the MK-7 fermentation system is assessed in the next chapter.

Chapter 9

The Effect of Milking Process on MK-7 Production from *Bacillus subtilis* (ATCC 6633)

This chapter forms the basis for the following publication:

Ranmadugala, D., Ebrahiminezhad, A., Manley-Harris, M., Ghasemi, Y., & Berenjian, A (2018), High level of Menaquinone-7 Production by Milking Menaquinone-7 with Biocompatible Organic Solvents. *Current Pharmaceutical Biotechnology*, *19*(3), 232-239.

9.1 Introduction

Menaquinone (vitamin K2) comprise a class of therapeutic agents that significantly improve the treatment options for a variety of diseases in addition to their role in blood clotting. MK-7 especially is important for the treatment and prevention of coronary heart diseases (Beulens *et al.*, 2009; Gast *et al.*, 2009; Knapen *et al.*, 2015), rheumatoid arthritis (Abdel-Rahman *et al.*, 2015) osteoporosis (Shiraki *et al.*, 2000; Yamaguchi *et al.*, 2000) and cancer (Shi *et al.*, 2018). MK-7 can be mainly produced via fermentation process of *Bacillus subtilis* at very low concentrations. In this regard, a number of different approaches have been taken to enhance the MK-7 production. As MK-7 is a membrane compound, MK-7 enhancing strategies are currently centred towards changing membrane permeability or membrane composition (Ebrahiminezhad *et al.*, 2016c; Liu *et al.*, 2017; Ranmadugala *et al.*, 2017b). In Chapter 7, a nanobiotechnological approach was taken to enhance MK-7 production where *Bacillus subtilis* cells were immobilised with 3-aminopropyltriethoxysilane coated iron oxide nanoparticles to enhance MK-7 production while maintaining the growth of bacterial cells (Ranmadugala *et al.*, 2017b).

Menaquinones are synthesised through the shikimate pathway (Taguchi *et al.*, 1991) and known to be a major component in the photochemical electron-transport system. Therefore, the synthesis of MK-7 is essential for the survival of bacteria. Menaquinone productivity is, however, restricted by the intracellularly level of MK, causing metabolic repression of menaquinone biosynthesis as MK is involved in the feedback inhibition of 3-deoxy- D-arabino-heptulosonate-7-phosphate (DAHP) synthase and shikimate kinase, the regulatory enzymes of the shikimate pathway (Taguchi *et al.*, 1991). It was recently reported that when bacterial cells are induced to secrete excessive menaquinone (MK-4) extracellularly, the MK can be kept

below the level of feedback inhibition of DAHP synthase (Taguchi *et al.*, 1991), leading to improvement in total menaquinones (Liu *et al.*, 2014). Although a feedback inhibition by MK-7 on DAHP synthase is not recorded, it is possible that that MK-7 production could be enhanced in a similar manner by removing the excess MK-7 by milking with biocompatible organic solvents. In addition, it is reported that bacteria are under metabolically challenged conditions upon treatment with organic solvents, leading to increased oxygen uptake/respiration rate due to modifications in cell physiology and/or surface characteristics as an adaptive response (Fletcher, 1983). In either case, it was hypothesised that bacteria should produce more MK-7 to compensate the loss of electron transport activity upon milking of MK-7 with biocompatible organic solvents from the fermentation medium.

Milking of cows essentially allows the biomass to be continuously reused for milk production. This principle has been used as a novel biotechnological process to milk products from microorganisms where cells have been reused continuously, without the need for harvesting, concentrating and destroying the cells to extract the products (Frenz *et al.*, 1989; Hejazi *et al.*, 2002; Hejazi *et al.*, 2004; Hejazi & Wijffels, 2004; Sauer & Galinski, 1998). The objective of the present study was, therefore, to investigate whether milking of MK-7 with biocompatible organic solvents would allow the continuous biosynthesis of MK-7 at maximum production levels without showing any detrimental effects on microbial growth and metabolism. The study was conducted in two stages. The objective of the first stage was to find a biocompatible solvent/s which can be used to extract MK-7 while maintaining the viability of the bacterial cells. In the second stage, MK-7 production was evaluated upon milking of MK-7 with the selected biocompatible

organic solvents. All experiments were performed at 37°C and shaking at 120 rpm in the optimum medium previously described in section 8.2.5.

9.2 Results

9.2.1 Common vitamin K extraction solvents

Solvents commonly used for vitamin K extraction were reviewed and listed in Table 13. It was apparent that in most cases, a polar solvent together with a non-polar solvent has been used for MK-7 extraction to facilitate good recoveries.

Table 13 Common vitamin K extraction solvents

Type of vitamin K	Solvents	Proportion (*v*/*v*)	Reference
MK-7	Sample: (mixture of 2-propanol: *n*-hexane)	1: 3(3:2)	(Canfield *et al.*, 1991; Canfield *et al.*, 1990)
PK and MK-6	Sample: 2-propanol: *n*-hexane	6.5:1:2	(Langenberg *et al.*, 1986)
PK and MK	Sample: 2-propanol: *n*-hexane	1:5:6	(Hirauchi *et al.*, 1989)
MK-4 to MK-10	Sample: ethanol: *n*-hexane: diethyl ether	(1:1:3:3)	(Shino, 1988)
Lipoquinones	Sample: methanol: *n*-hexane	(1:2:1)	(Tindall *et al.*, 1989)
MK	Sample: (methanol: aqueous NaCl): petroleum ether (60-80°C)	1:4 (10:1):4	(Athalye *et al.*, 1984; Minnikin *et al.*, 1984; Saddler *et al.*, 1986)
MK (MK-4 to MK-9)	Sample: ethanol: *n*-hexane	1:4:8	(Marinova *et al.*, 2011; Schurgers & Vermeer, 2000)
PK, MK (MK-6, MK-7 and MK-8)	Sample: (chloroform: methanol): *n*-hexane	0.5:40(3:1):15	(Hodges *et al.*, 1993)
MK	Sample: methanol-light petroleum mixture: light petroleum	0.5:3(3:2):1	(Křivánková & Dadák, 1980)
MK-7	Sample: 2-propanol: *n*-hexane	3:4:8	(Sato *et al.*, 2001a)
MK-7	Sample: ethanol: water: NH_4OH: *n*-hexane	1:4:2:0.2:7.5	(Lambert *et al.*, 1992)
MK	Sample: water: (2-propanol: *n*-hexane)	0.2:10:15 (3:2)	(Karl *et al.*, 2014)
PK and MK	Sample: *n*-hexane	1:1	(Jakob & Elmadfa, 1996, 2000; Song *et al.*, 2014)
Isoprenoid quinones	Sample: petroleum ether (60-80°C)	1:1	(Bentley & Meganathan, 1982)

Review of commonly used MK-7 extraction solvents shows that almost all the studies have used either 2-propanol, methanol or ethanol as a polar solvent in the extraction solvent mixture. In most of the studies *n*-hexane has been the choice as a non-polar solvent whereas, in few studies, petroleum ether has been used as a non-polar solvent.

9.2.2 Effect of milking on the viability of *Bacillus subtilis*

In order to find out biocompatible organic solvent/s for milking MK-7, organic solvent tolerance of *Bacillus subtilis* was determined on the basis of the change in Live/dead ratio of bacterial cells upon periodic milking with organic solvent/s. The change in the viability of bacteria was determined after milking with organic solvents at 40 and 48 hours. Experiments were performed in two phases. In phase one, organic solvent mixtures which have been used previously for MK-7 extraction were evaluated for their ability to retain the viability of *Bacillus subtilis* cells upon milking for MK-7. In the second phase, modified solvent mixtures were used to test their toxicity to bacterial cells. Milking was then continued for a cultivation period of 84 hours with the selected biocompatible solvents and the change in *Bacillus subtilis* viability was investigated.

Phase I

Change in the viability *of Bacillus subtilis* (ATCC 6633) upon milking with solvent mixtures previously used for MK-7 extraction

Milking of MK-7 from the fermentation medium at 40 hours with previously recorded MK-7 extraction solvents resulted in a loss of *Bacillus subtilis* cell viability other than when milking was carried out with a mixture of ethanol: *n*-hexane: diethyl ether (1:3:3, *v*/*v*), and *n*-hexane alone. However, subsequent incubation of the cultures following milking at 37°C with shaking at 120 rpm for 8

hours and milking again with the solvent systems at 48 hours, resulted in a significant reduction in *Bacillus subtilis* viability ($p < 0.05$) when a mixture of ethanol: *n*-hexane: diethyl ether (1:3:3, *v*/*v*) was used. Nevertheless, no significant changes to the viability were apparent upon milking with *n*-hexane alone.

Phase II

Change in the viability *of Bacillus subtilis* (ATCC 6633) upon milking with modified solvent mixtures

In the second phase modified solvent mixtures along with *n*-hexane were used for milking MK-7 and their effect on the bacterial cell viability was assessed. Solvent mixtures used in the second phase are listed in Table 14. Bacterial cell viability after milking with organic solvents are given in Figure 46.

Table 14 Modified solvent mixtures and the ratios used for milking MK-7

	Volume ratio
1	Sample: *n*-butanol:*n*-hexane (3:2:1)
2	Sample: *n*-butanol: *n*-hexane :diethylether (1:1:3:3)
3	Sample: *n*-hexane (1:1)
4	Sample: *n*-butanol:*n*-hexane (3:1:2)

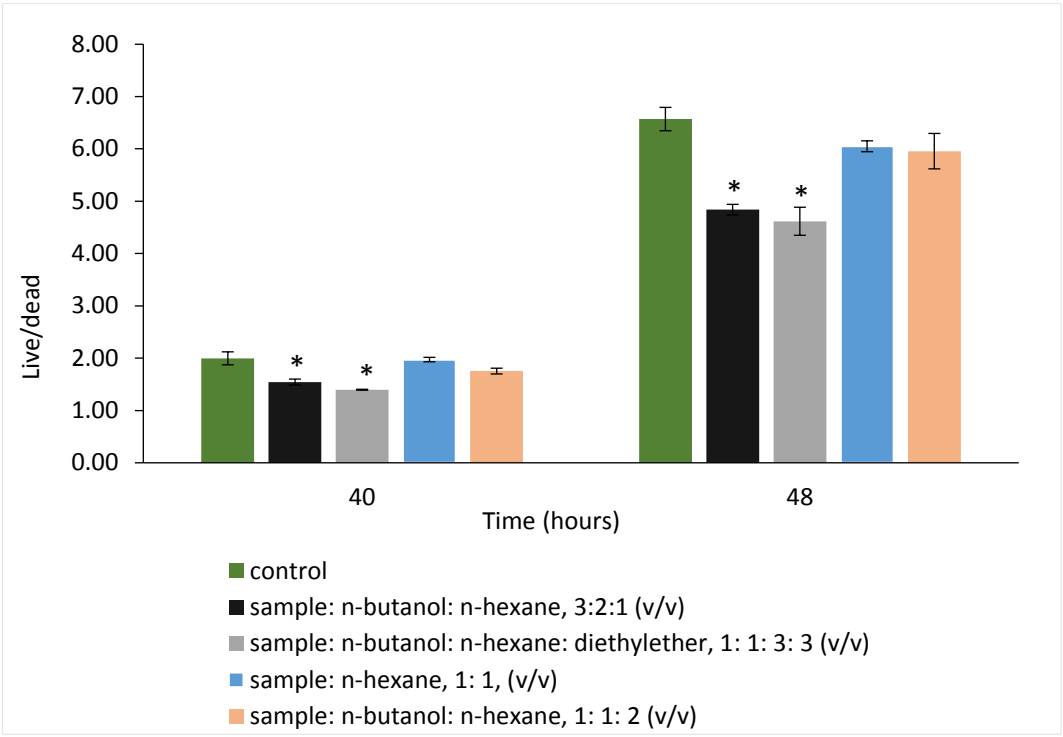

Figure 46 Change in the viability *of Bacillus subtilis* (ATCC 6633) upon milking with modified MK-7 extraction solvents in comparison to non-milking conditions (control). Data are the means ± standard error of three replicates. An asterisk indicates a significantly different value from the control ($p < 0.05$)

The results indicated that a mixture of *n*-butanol:*n*-hexane (1:2, *v*/*v*) and *n*-hexane alone can be used for milking MK-7 without any significant reduction in bacterial cell viability ($p > 0.05$), while the other two solvent mixtures reduced the viability of *Bacillus subtilis* cells upon periodic milking of MK-7 from the bacterial cultures ($p < 0.05$). Therefore, milking was continued with a mixture of *n*-butanol: *n*-hexane (1:2, *v*/*v*) and *n*-hexane over a cultivation period of 84 hours and the change in *Bacillus subtilis* viability was measured.

Change in *Bacillus subtilis* viability upon milking of MK-7 with *n*-hexane and a mixture of *n*-butanol: *n*-hexane (1:2, *v*/*v*) over a cultivation period of 84 hours

Change in the cellular viability of *Bacillus subtilis* (ATCC 6633) over a cultivation period of 84 hours assessed by a LIVE/DEAD viability assay is given in Figure 47.

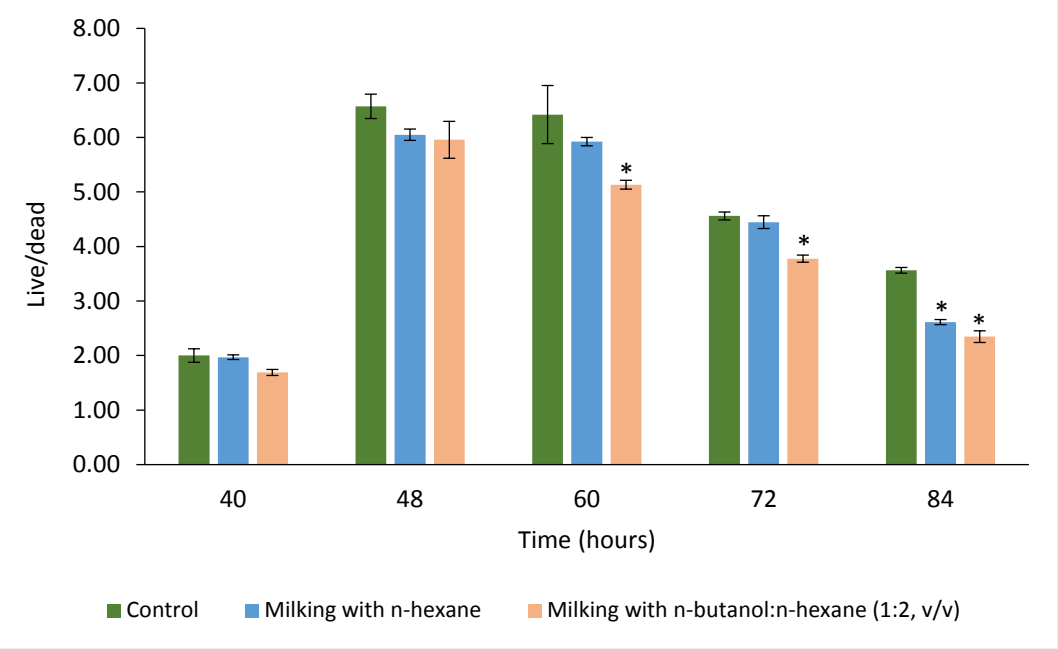

Figure 47 Change in the viability of *Bacillus subtilis* upon milking with *n*-hexane and a mixture of *n*-butanol: *n*-hexane (1:2, *v*/*v*) in comparison to non-milking conditions (control). Data are the means ± standard error of three replicates. An asterisk indicates a significantly different value from the control ($p < 0.05$)

According to the results, periodic milking with *n*-hexane did not show any detrimental effect on the viability of *Bacillus subtilis* up to 84 hours. Milking with a mixture of *n*-butanol: *n*-hexane (1:2, *v*/*v*) did not change the viability of *Bacillus subtilis* initially; however, periodic milking of MK-7 with a mixture of *n*-butanol: *n*-hexane (1:2, *v*/*v*) significantly influenced the viability of *Bacillus subtilis* after 48 hours.

9.2.3 Effect of milking on MK-7 production

In the next stage, MK-7 production upon milking with the two solvent systems *i.e.* a mixture of *n*-butanol: *n*-hexane (1:2, *v*/*v*) and *n*-hexane over a cultivation period of 84 hours were compared with MK-7 production under controlled conditions.

9.2.3.1 MK-7 production by *Bacillus subtilis* upon milking with *n*-hexane

Figure 48 shows the changes in MK-7 concentration in the organic and the aqueous phase upon milking with *n*-hexane in comparison to non-milking conditions (control).

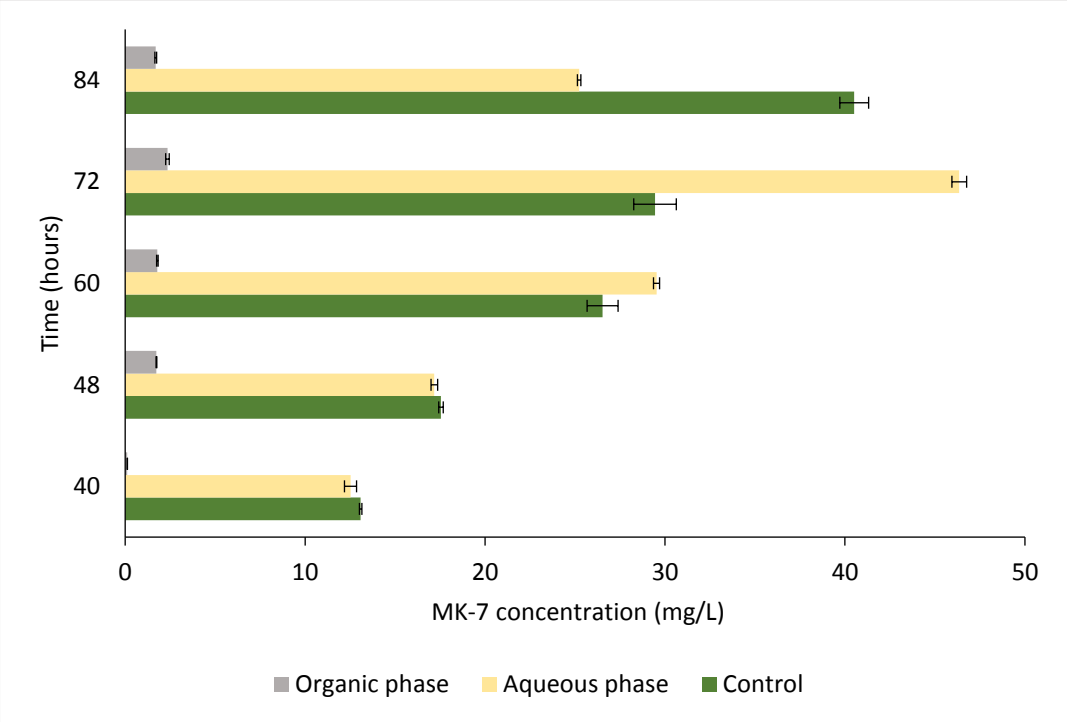

Figure 48 Change in MK-7 concentration in the aqueous and organic phase upon milking with *n*-hexane in comparison to non-milking conditions (control). Data are the means ± standard error of three replicates.

Analysis of MK-7 concentration in the aqueous and organic phase upon milking with *n*-hexane over a cultivation period of 84 hours showed that the MK-7 concentration in the aqueous phase and the organic phase increases upon periodic milking, in a time-dependent manner. MK-7 concentration in the aqueous phase

increased rapidly during the first 72 hours and the concentration reached its highest level of 46.35 mg/L at 72 hours. On the other hand, MK-7 concentration in the organic phase was hardly detected at 40 hours and increased relatively slowly compared to that of the aqueous phase. Maximum MK-7 concentration in the organic phase was 2.35 mg/L at 72 hours. A typical HPLC chromatogram of MK-7 in the aqueous phase of *Bacillus subtilis* (ATCC 6633) culture upon milking with *n*-hexane at 72 hours is shown in Figure 49.

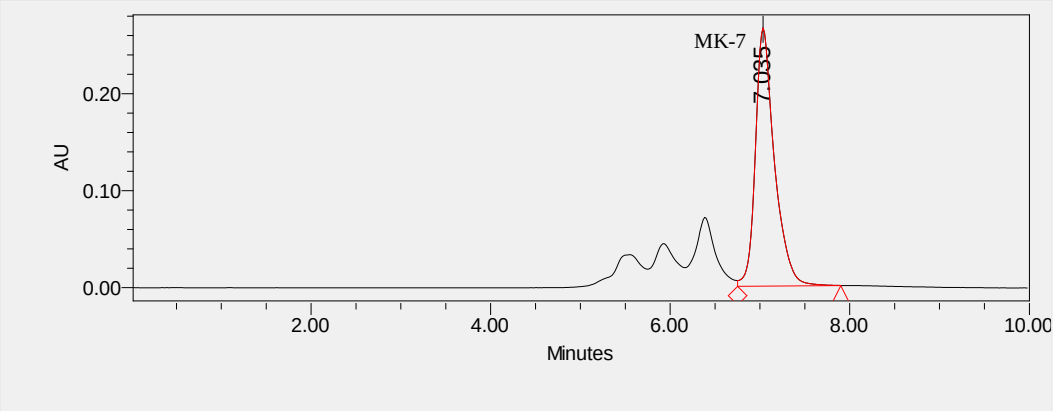

Figure 49 HPLC chromatogram of MK-7 in the aqueous phase of *Bacillus subtilis* culture upon milking with *n*-hexane at 72 hours.

In addition, total MK-7 production upon milking with *n*-hexane was compared with the MK-7 production in batch fermentation under non-milking conditions (control). Figure 50 shows a schematic representation of how the total MK-7 concentration upon periodic milking at each time interval was analysed.

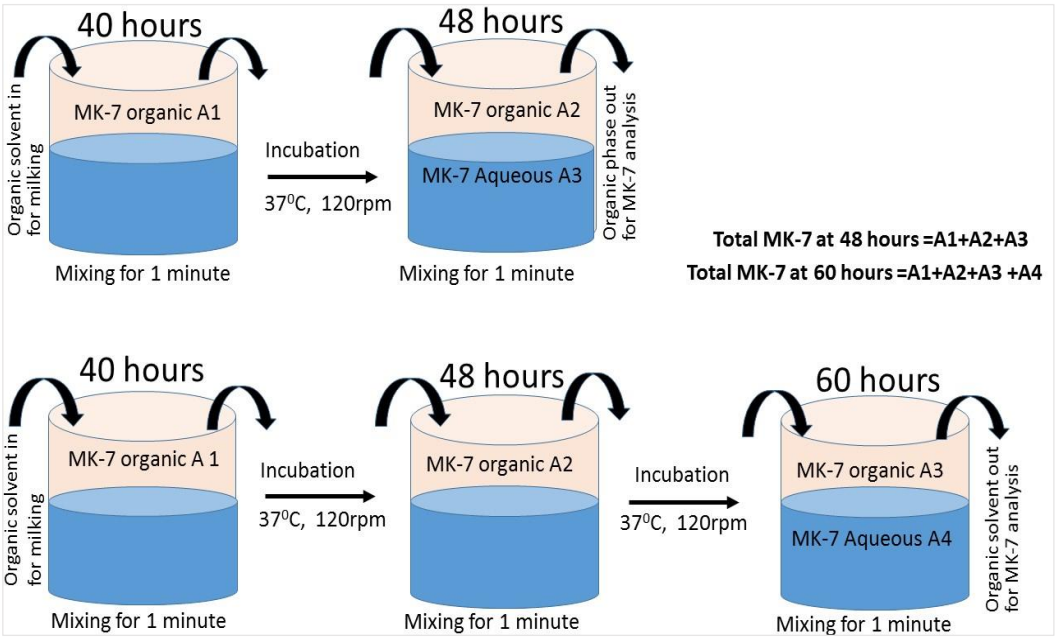

Figure 50 Schematic representation of analysis of total MK-7 upon periodic milking with organic solvents.

According to the results, the maximum total MK-7 concentration that could be achieved upon milking with *n*-hexane in comparison to non-milking conditions are depicted in Figure 51**.**

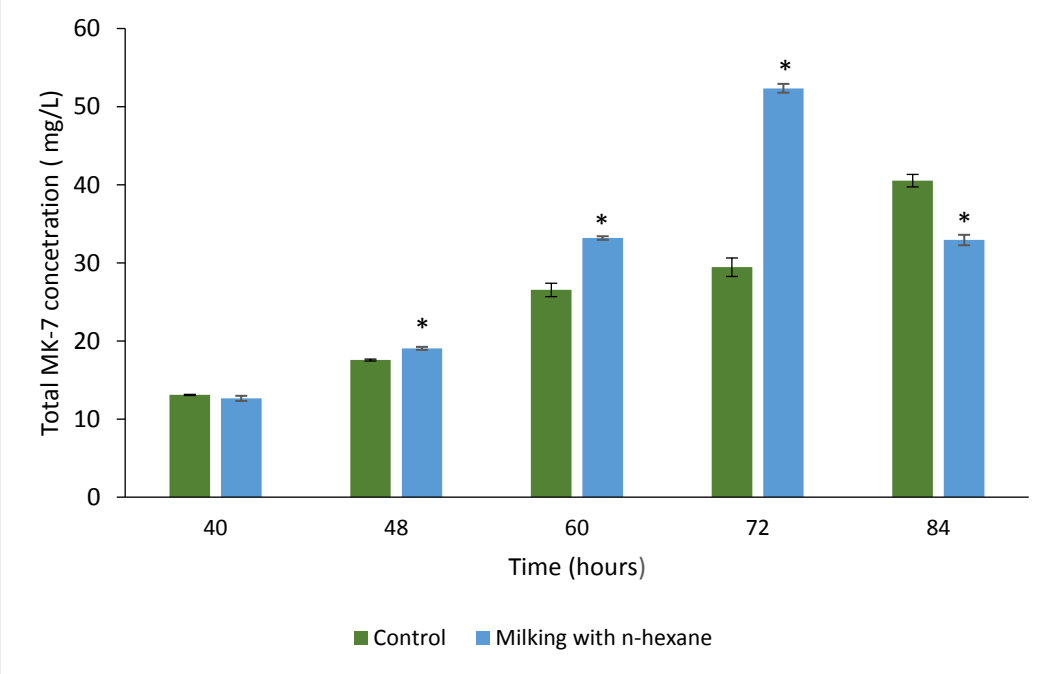

Figure 51 Total MK-7 production over time upon milking with *n*-hexane in comparison to non-milking conditions (control). Data are the means ± standard error of three replicates. An asterisk indicates a significantly different value from the control ($p < 0.05$)

The maximum total MK-7 concentration that could be achieved upon periodic milking with *n*-hexane was 52.34 mg/L and this could be achieved within 72 hours of fermentation. In contrast, only 40.52 mg/L of MK-7 concentration could be achieved even after 84 hours of batch fermentation under non-milking conditions (control). This data clearly indicates that milking with *n*-hexane can effectively enhance the total MK-7 concentration and thus the productivity of the fermentation system.

9.2.3.2 MK-7 production by *Bacillus subtilis* upon milking with a mixture of *n*-butanol and *n*-hexane (1:2, *v*/*v*)

As the amount of MK-7 which could be removed by milking with *n*-hexane alone was significantly low, milking of MK-7 was also attempted with a mixture of *n*-butanol: *n*-hexane (1:2, *v*/*v*) and the effect of milking on MK-7 production was re-investigated. Figure 52 shows the changes in MK-7 production with or without milking with a mixture of *n*-butanol: *n*-hexane (1:2, *v*/*v*).

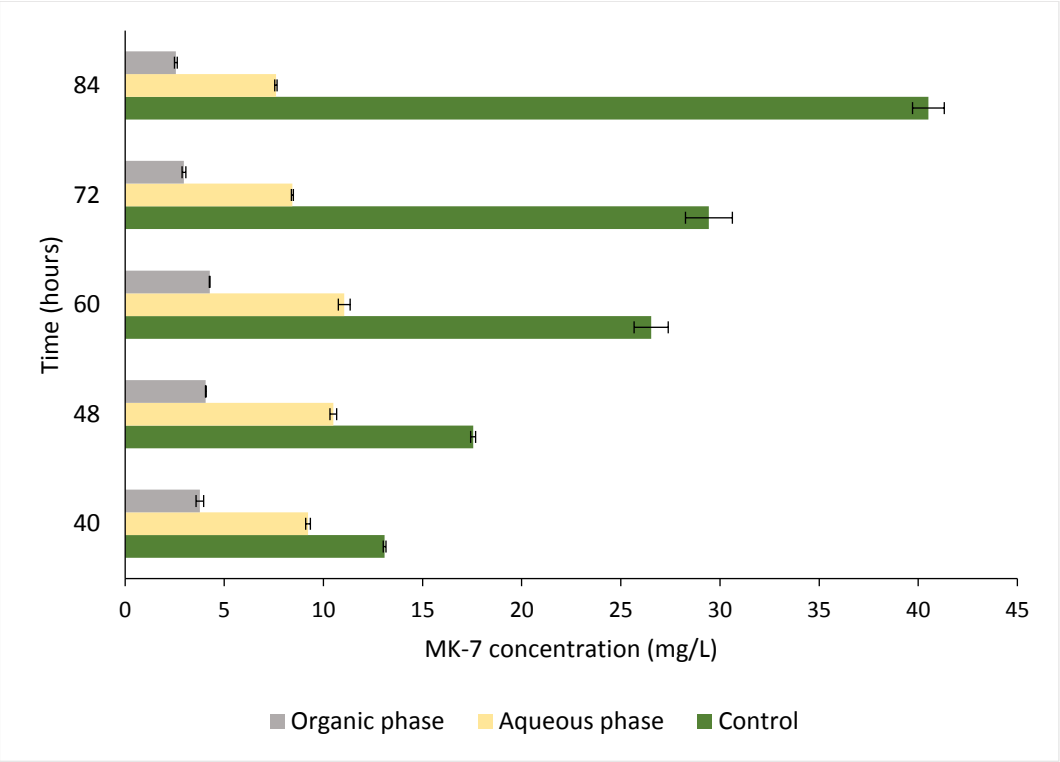

Figure 52 Change in MK-7 concentration in the aqueous and organic phase upon milking with a mixture of *n*-butanol: *n*-hexane (1:2, *v*/*v*) and non-milking conditions (control). Data are the means ± standard error of three replicates

According to the results, MK-7 concentration in the organic phase as well as in the aqueous phase increased over a period of 60 hours. The MK-7 concentration in the organic phase was greater when a mixture of *n*-butanol: *n*-hexane (1:2, *v*/*v*) was used in comparison to the concentration of MK-7 which could be extracted only with *n*-hexane. However, no significant gain in MK-7 concentration could be achieved upon milking with a mixture of *n*-butanol: *n*-hexane (1:2, *v*/*v*) in comparison to non-milking conditions. MK-7 concentration in both the organic and aqueous phase decreased significantly after 60 hours ($p < 0.05$) (Figure 52).

As described previously, the total MK-7 concentration that could be realised upon milking with a mixture of *n*-butanol: *n*-hexane (1:2, *v*/*v*) in comparison to non-milking conditions were also evaluated and depicted in Figure 53.

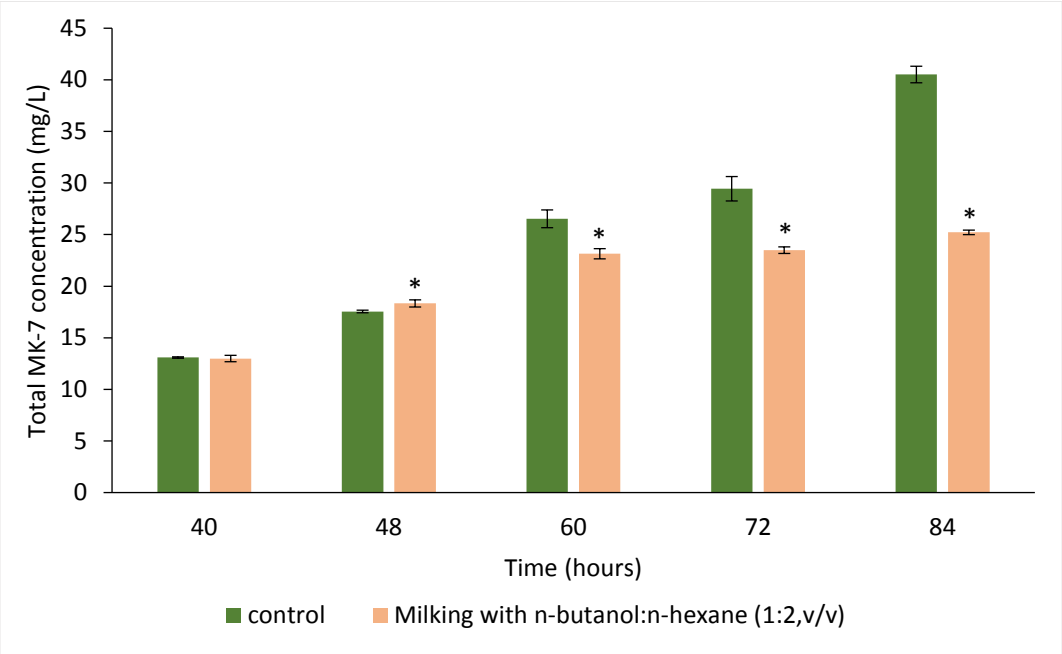

Figure 53 Total MK-7 production over time upon milking with a mixture of *n*-butanol: *n*-hexane (1:2, *v*/*v*) in comparison to non-milking conditions (control). Data are the means ± standard error of three replicates. An asterisk indicates a significantly different value from the control ($p < 0.05$)

Analysis of total MK-7 production upon milking with a mixture of *n*-butanol: *n*-hexane (1:2, *v*/*v*) showed that at 48 hours, the total MK-7 concentration that could be obtained upon periodic milking with a mixture of *n*-butanol: *n*-hexane (1:2, *v*/*v*) was significantly higher compared to non-milking conditions ($p < 0.05$). This indicates that milking of MK-7 is beneficial for enhancing MK-7 production. However, after 48 hours, the total MK-7 concentration which could be obtained upon periodic milking with the mixture of *n*-butanol: *n*-hexane (1:2, *v*/*v*) was significantly decreased in comparison to MK-7 concentration under non-milking conditions ($p < 0.05$). This observation clearly demonstrates the poor biocompatibility of *n*-butanol: *n*-hexane (1:2, *v*/*v*) with *Bacillus subtilis* cells (Figure 53).

9.3 Discussion

9.3.1 Solvents used for MK-7 extraction

In order to design a milking process for MK-7, first, different organic solvents commonly used for the extraction of MK in the aqueous-organic system were reviewed and summarised in Table 13.

The extraction of MK-7 is usually by means of a liquid-liquid extraction process prior to the determination (Sommer & Kofler, 1967). Common lipid extraction methods have been employed for extracting vitamin K compounds from various sources. As MK-7 is bound to cell membranes, most commonly a polar solvent together with a non-polar solvent has been used in MK-7 extraction to facilitate the extraction. The most commonly used extraction solvent has been a mixture of 2-propanol and *n*-hexane. However, according to Langenberg *et al.* (1986), vitamin K is said to be more stable in *n*-hexane than in more polar solvents such as methanol.

9.3.2 Effect of milking MK-7 with organic solvents on the viability of *Bacillus subtilis*

The selection of an appropriate organic phase is a critical step for the success of designing a milking process for MK-7. The choice of organic phase mainly depends on the organic solvent tolerance of bacteria which may depend on the choice of the organic phase. Therefore, to study the effect of the milking process, detailed studies were carried out to find out a biocompatible organic solvent for milking MK-7. In the first phase, common extraction solvents that were previously reported for MK-7 extraction were evaluated for their ability to retain the bacterial cell viability upon milking MK-7 from the fermentation medium. It was evident that none of the previously described vitamin K extraction solvents other than *n*-hexane alone can maintain the viability of *Bacillus subtilis* cells upon periodic milking for MK-7 as

almost all the solvent mixtures contained a polar solvent together with a non-polar solvent. The presence of alcohols in the extraction solvent in these instances might have inhibited the growth of bacteria in a concentration-dependent manner possibly by damaging the cell membrane (Ingram, 1976). In addition, the miscibility of the polar solvents with the aqueous layer made them unsuitable for the process of milking. Therefore, in the second stage, the change in bacterial cell viability upon treatment with *n*-hexane and three other modified solvent mixtures were assessed. The modified solvent mixtures contained different proportions of *n*-butanol together with *n*-hexane. The reason for choosing *n*-butanol is because the carbon chain of *n*-butanol, which is non-polar, decreases its solubility in water, although *n*-butanol is polar. According to the results, no apparent growth inhibition was found in *Bacillus subtilis* cells as assessed by the LIVE/DEAD assay upon milking MK-7 with *n*-hexane and a mixture of *n*-butanol: *n*-hexane (1:2, *v*/*v*) initially. However, the viability of *Bacillus subtilis* cells was significantly influenced by periodic milking with the mixture of *n*-butanol: *n*-hexane (1:2, *v*/*v*) starting at 60 hours. This apparent toxicity of *n*-butanol can be due to traces of *n*-butanol remaining in the fermentation medium, inhibiting the growth of the bacterium (Huang *et al.*, 2010a). However, results showed that periodic milking with *n*-hexane did not have any detrimental effect on the viability of *Bacillus subtilis* up to 84 hours. It is therefore apparent that *n*-hexane has a delayed toxicity compared to the *n*-hexane/*n*-butanol mixture. Less cytotoxic properties of *n*-hexane can be accounted by its low solubility in the fermentation medium and a log P_{ow} of 3.6. Less polar solvents with a greater log P_{ow} values are reported to be less toxic to bacteria as they would not reach high membrane concentration due to low water solubility (Sardessai & Bhosle, 2004). Several bacterial species such as *E. coli* and *Bacillus subtilis* which are tolerant to *n*-hexane have been recorded previously

(Aono & Kobayashi, 1997; Sardessai & Bhosle, 2004). The intrinsic tolerance level of each organism is, however, said to be strain specific and is determined genetically. In addition, environment/culture conditions and exposure time can also influence the tolerance level. In this study, cultivations were performed at 37°C and shaking at 120 rpm in the optimum medium developed earlier in Chapter 8 which consist of 5% (*w*/*v*) yeast extract, 18.9% (*w*/*v*) soy peptone, 5% (*w*/*v*) glycerol, 0.06% (*w*/*v*) K_2HPO_4, 0.32 % (*w*/*v*) $CaCl_2$, 0.10% (*w*/*v*) urea and 200 µg/mL IONs@APTES. According to the literature, ions such as Ca^{2+} is said to stabilise the organisation of the bacterial cell membrane (Lăzăroaie, 2009). Thus, it is possible that the presence of $CaCl_2$ in the cultivation medium may have also contributed to the solvent tolerant ability of *Bacillus subtilis* (Aono & Kobayashi, 1997) and delayed their death (Postgate & Hunter, 1962).

Little information is available on the mechanism of *n*-hexane tolerance of *Bacillus subtilis*; however, this may be linked to the peptidoglycan layer present in the gram-positive bacterium, protection rendered by endospores or induction of general stress response (Sardessai & Bhosle, 2004). Therefore, *n*-hexane was found to be a promising solvent for the MK-7 milking process which can retain the viability of *Bacillus subtilis* upon periodic milking of MK-7.

9.3.3 Effect of milking process on MK-7 production

Comparison of MK-7 production upon milking of MK-7 from the culture media by biocompatible organic solvent mixtures showed that the total MK-7 production can be significantly improved by periodic milking of MK-7 with *n*-hexane during *Bacillus subtilis* fermentation. Further, a total MK-7 production of 52.34 mg/L of MK-7 could be achieved within 72 hours of *Bacillus subtilis* cultivation which was

~ 1.7 fold higher than the control samples. Most importantly, this high MK-7 concentration could be achieved within a shorter fermentation time.

Menaquinones are the predominant lipoquinone of gram-positive bacteria and the gram-positive aerobe *Bacillus subtilis* contains only MK-7 which is essential for their survival (Dairi, 2009). Menaquinones, especially MK-7, occupies a central role in the electron transport chain as an electron carrier in cellular respiration. Therefore, bacteria should produce more MK-7 to compensate the loss of electron transport activity upon milking of MK-7 with organic solvents. Further, upon treatment with organic solvents, bacteria are under metabolically challenged conditions, where the oxygen uptake/respiration rate can increase as an adaptive response. An increase in respiration rate upon organic solvent treatment has been previously reported by Fletcher (1983) due to modifications in cell physiology and/or surface characteristics. An increase in respiration rate can, therefore, lead to enhanced MK-7 production.

In addition, it was recently reported that when bacterial cells are induced to secrete excessive MK (MK-4) extracellularly, the MK are kept below the level of feedback inhibition of DAHP synthase (Taguchi *et al.*, 1991), the first regulatory enzyme in the shikimate pathway leading to improvement in total MK (Liu *et al.*, 2014). Although a feedback inhibition by MK-7 on DAHP synthase is not recorded, a similar mechanism might be promoting the MK-7 production when excess MK-7 is removed by milking with organic solvents. Further experimental evidence on the mechanism would, however, expand and refine the application of the milking process. However, when a mixture of *n*-butanol: *n*-hexane (1:2, *v/v*) was used for milking MK-7, the total MK-7 production decreased over time in comparison to non-milking conditions. This can be attributed to the poor biocompatibility of *n*-butanol: *n*-hexane (1:2, *v*/*v*) with *Bacillus subtilis* due to traces of *n*-butanol

remaining in the fermented medium inhibiting microbial growth (Huang *et al.*, 2010a).

The amount of MK-7 which could be extracted from the culture medium with *n*-hexane alone was lower than when milking was carried out with a mixture of *n*-butanol: *n*-hexane (1:2, *v*/*v*). This is largely attributed to the fact that MK-7 is tightly bound to the bacterial cell membrane (Minnikin *et al.*, 1984) and the occurrence of MK-7 usually at lower concentrations. It is reported that the non-disruptive extraction of MK-7 with pure organic solvents is poor (Luo *et al.*, 2016). Therefore, in many cases, the extraction of MK-7 has been facilitated substantially by cell wall destruction either by ultrasonication, freeze-thawing, steam explosion, acid-heating, alkaline hydrolysis and homogenisation (Luo *et al.*, 2016). Destruction of bacterial cells, however, make it impossible for the cells to be reutilised. In contrast, in this study, the culture medium was supplemented with 200 µg/mL IONs@APTES which previously proved to be a promising carrier to change the state or composition of cell membrane resulting in enhanced synthesis and secretion of MK-7 to the fermentation medium without affecting bacterial growth and viability (Ebrahiminezhad *et al.*, 2016c; Liu *et al.*, 2017; Ranmadugala *et al.*, 2017b). In addition, the presence of $CaCl_2$ in the medium may have facilitated the recovery of MK-7 by acting as a salting-out mediator (Ahmed & Mahmoud, 2015). A combination of strategies thus has proved useful in enhancing the productivity of the MK-7 production system.

9.4 Summary

In this study, applying a milking process was shown to be an effective strategy to enhance the total MK-7 production. Among the organic solvents studied for milking MK-7, *n*-hexane was the most suitable extraction solvent for milking MK-7,

without compromising the bacterial cell viability. It was evident that the total MK-7 production can be significantly enhanced by ~ 1.7 fold upon milking with *n*-hexane within 72 hours of *Bacillus subtilis* fermentation. Therefore, the MK-7 milking process described here is a promising approach that can be employed to enhance the total MK-7 production and continuously re-use *Bacillus subtilis* biomass for fermentation. Most importantly, it works with intact bacterial cells without affecting their viability and high titres could be achieved within a shorter cultivation period.

Chapter 10

Conclusions and Future Directions

10.1 Overview

This thesis has mainly examined the topic of biofilm formation and MK-7 production by *Bacillus subtilis* and explored how to minimise biofilm formation while maximising MK-7 production. This chapter summarises the key findings of the thesis and aims to make recommendations for future investigations. By adopting a more holistic multidisciplinary approach (nanotechnology, biotechnology and chemistry), the research has sought to develop strategies to combat biofilm formation, increase MK-7 production and reduce downstream processing steps in the MK-7 production process. The remainder of this chapter summarises the key findings of each research chapter and provides recommendations for future research from the knowledge derived from this study.

10.2 Key findings

At the beginning of this thesis, no information was available on how to enhance the productivity of the MK-7 production process through optimising the major influencing factors in MK-7 production; *i.e.* biofilm formation, low MK-7 concentration and a large number of downstream processing steps, all in one go. Developing strategies to address all these issues remained a greater challenge.

The conventional practices for biofilm control have been through physical cleaning and the use of antimicrobials or antibiotics. These conventional practices are, however, aimed at eradicating or killing the bacteria. In *Bacillus subtilis* fermentation, it was of utmost importance that the biofilm controlling strategies would not interfere with the growth of bacteria. As a result of this, finding a non-

antibiotic antifouling strategy to permit the growth and viability of bacterial cells in the fermentation process posed a greater challenge.

In terms of enhancing the MK-7 production, a number of studies have focused on optimisation of the cultivation medium, selection of different microorganisms or chemical mutagenesis. Very few studies have, however, concentrated on bacterial cell membrane as a primary target to enhance MK-7 productivity. A few studies have also attempted to reduce the many numbers of downstream processing steps in order to increase the productivity of the system. However, none of the studies have considered strategies to combat all these issues in a single production process. To accomplish this, functionalised iron oxide nanoparticles with APTES were successfully fabricated. The synthesised nanoparticles by chemical co-precipitation method were sufficiently small and exhibited well-defined superparamagnetic behaviour. IONs@APTES with the smaller size and larger surface area, in addition to their charge, showed great promise in decorating bacterial cells. Although the presence of coatings can sometimes negatively affect the magnetic properties of IONs, coating with APTES did not affect the magnetic properties of IONs as discussed in **Chapter 4**.

In addition, biofilm formation in MK-7 production by *Bacillus subtilis* was successfully addressed using a nanobiotechnological approach for the first time in this study. This was the main focus of **Chapter 5**. Superparamagnetic IONs (naked and IONs@APTES) were explored as potential candidates for reducing biofilm formation. IONs@APTES showed good solubility and dispersibility in the culture media in comparison to naked IONs. In this circumstance, the IONs@APTES were able to maintain the growth and the viability of *Bacillus subtilis* cells while reducing biofilm formation. Further, IONs@APTES were able to penetrate the extracellular polymeric matrix without an external magnetic field. Taken together,

IONs@APTES were identified as promising agents that can be used to reduce biofilm formation without compromising the growth and viability of *Bacillus subtilis.*

Further, in the present work, a new, simple, accurate, fast and sensitive method for routine analysis of MK-7 was developed as discussed in **Chapter 6**. As the reproducibility of MK-7 production is influenced by analysis conditions, this study was designed to establish a reproducible analytical protocol for MK-7 analysis. A simple, efficient, accurate and reproducible reversed phase high performance liquid chromatographic method combined with efficient extraction method was developed and validated with respect to accuracy, precision, specificity and linearity. In this protocol, the use of the same solvents to extract MK-7 and to elute MK-7 in high-performance liquid chromatography eliminated the requirement to evaporate and re-dissolve extracts in a separate mobile phase solvent which allowed accurate quantification while improving the efficiency. In addition, the good solubility of MK-7 in a mixture of 2-propanol and *n*-hexane contributed to the accuracy in the quantification of MK-7 from samples. This method also had the advantage of short runtime with throughput of 7 samples per hour. Therefore, the major breakthrough, as discussed in Chapter 6, is the development of a simple, efficient, accurate and reproducible HPLC method to routinely analyse bacterially synthesised MK-7. The development of a valid HPLC protocol added strength to the thesis in contrast to previous studies with bacterial MK-7 where HPLC methods have not been validated before MK-7 has been measured.

In **Chapter 7**, a better framework was put forward for enhancing MK-7 production using IONs@APTES which previously proved to be a promising carrier for controlling biofilm formation in *Bacillus subtilis* without exhibiting cellular toxicity and growth. As magnetic immobilisation is also an effective strategy for

the separation and re-use of bacteria in the system thereby reducing downstream processing steps, the innovation brought by immobilisation of *Bacillus subtilis* cells with IONs@APTES in this particular instance was tripled. This chapter sought to highlight that decoration of *Bacillus subtilis* cells with IONs@APTES can significantly increase MK-7 production and MK-7 yield. The chapter also identified the optimum IONs@APTES concentration to maximise MK-7 yield.

In addition to the use of IONs@APTES to reduce surface attachment and biofilm formation, medium components were optimised to enhance biofilm detachment through treatment with salts and urea. The production process was optimised by a combined approach of reducing surface attachment and enhancing detachment to combat biofilm formation while maximising the MK-7 production as described in **Chapter 8**. Elevated levels of MK-7 (~16%) and reduction in biofilm biomass (~47%) was observed in the optimum medium (M3) which consist of 5% (*w*/*v*) yeast extract, 18.9% (*w*/*v*) soy peptone, 5% (*w*/*v*) glycerol, 0.05% (*w*/*v*) K_2HPO_4, 0.32% (*w*/*v*) $CaCl_2$, 0.10% (*w*/*v*) urea and 200 µg/mL IONs@APTES after 60 hours of fermentation in comparison to controlled medium. The proposed medium can, therefore, be applied to minimise biofilm formation while maximising MK-7 production in *Bacillus subtilis* fermentation.

Finally, an innovative fundamentally unique approach to enhance MK-7 production termed as milking process was introduced in **Chapter 9**. Overall, this chapter demonstrated that MK-7 productivity can be enhanced by periodic milking of MK-7 from the culture medium with biocompatible organic solvents. The organic solvent *n*-hexane served well for this purpose since it showed delayed toxicity to *Bacillus subtilis* (ATCC 6633). This provided a promising platform for achieving high concentrations of MK-7 within a shorter fermentation time without compromising the viability of the microbial cells and found to be a promising approach to achieve

high MK-7 concentration in comparison to non-milking conditions. In addition, milking with organic solvents further reduced biofilm biomass and also gives a cleaner trace in HPLC analysis as it would extract only the non-polar compounds. Therefore, in conclusion, the milking of MK-7 from the fermentative medium can sustain a stable operation to increase the productivity of MK-7. Current findings will open up a new production system for MK-7 fermentation with high productivity for industrial application.

10.3 Future work

Magnetic IONs proved to be an important group of nanomaterials in bacterial cell immobilisation. It is important to highlight that the use of IONs@APTES had intrinsic advantages over conventional antifouling methods where they proved to maintain the growth and viability of microbial cells. In addition, they offered enhanced MK-7 production and reduced downstream processing due to facilitated cell recovery and reusability. The research presented in the thesis have however raised more questions and there are several lines of research which can be pursued in the future as presented below.

- The preponderance of evidence indicates that the bacterial cell membrane can be the primary target when it comes to biofilm control and manipulation of MK-7 production. However, there remain major questions ahead: a) the exact mechanism behind reduce biofilm attachment associated with IONs@APTES b) the exact mechanism of enhanced MK-7 production associated with IONs@APTES, and c) the exact mechanism behind enhanced MK-7 production upon milking MK-7. The findings of this research have opened the field to many underlying questions which are, however, difficult to assess from chemical

engineering data alone, but which can be addressed with molecular microbiology.

- With further understanding of bacterial-IONs@APTES interactions, bacterial cell immobilisation processes employing magnetic IONs@APTES described will, therefore, find its widest applications in many sectors. The progress in this area can be supported by the further development of automated systems for magnetic cell separation coupled with computer technology, which enables the detection and quantification of microbial cell capture efficiency.
- The thesis also covers a novel method by which MK-7 can be extracted and quantified with minimum losses. Although extraction and analysis of MK-7 from four different *Bacillus subtilis* species/strains were regarded as adequate at this stage, the method can be employed for quantification of MK-7 from various sources.
- In the present study, lipase treatment prior to extraction of MK-7 with a mixture of 2-propanol: *n*-hexane (1:2, *v*/*v*) was observed to be useful. When MK-7 is extracted and analysed from matrices with high-fat content, optimisation of all the reaction conditions for hydrolysis by lipase can be carried out.
- In the present study, *Bacillus subtilis* (ATCC 6633) was used as the reference strain from ATCC, which is the premier source for validly described type cultures in order to get reproducible results. Most of the previous studies of MK-7 production from *Bacillus subtilis* records the preparation of inoculum from bacteria isolated from *natto*, the traditional Japanese fermented soybean (Berenjian *et al.*, 2013; Berenjian *et al.*, 2011; Berenjian *et al.*, 2012; Berenjian *et al.*, 2014). However, only three validly described genomic sequences of *Bacillus subtilis natto* strains are deposited in NCBI, and out of these only one strain related to MK-7 production is published recently by Luo *et al.* (2016)

using 16SrDNA. In the present study, *Bacillus subtilis* (ATCC 6633), which was previously used by Ebrahiminezhad *et al.* (2016b) on magnetic immobilisation of bacteria for menaquinone production, was used. However, it was noted that *Bacillus subtilis natto* would give high MK-7 production. Therefore, in future research, deposition of genomic sequences in NCBI together with the deposition of type strains of validly named *Bacillus subtilis natto* can be implemented as part of the MK-7 analysis process.

- While this work has many breakthroughs, such as reduced biofilm formation, increased MK-7 production, reduced downstream processing as well as a novel method for MK-7 analysis, it has also paved the way for an important step towards improving the MK-7 concentration through milking. This work is also crucial in providing a foundation and direction towards large-scale cost-effective fermentation process/industrial production of MK-7. The methodologies employed could be used as a critical initial step and could be upgraded to industrial scale. In this regard, further analyses of oxygen uptake rate, bacterial membrane fluidity and changes in membrane fatty acid compositions, use of visualisation techniques and studying the kinetics of MK-7 release from the cells to unravel the mechanism behind the improvement in MK-7 production upon milking with biocompatible organic solvents would be an added advantage.
- In addition, to fully comprehend the effect of milking on bacterial cell viability and MK-7 production, optimum conditions for milking could be determined through response surface methodology. The starting time for milking, pH, mixing time, the volume of organic solvent can be taken as variables.
- Further studies could also be carried out to find out what other *Bacillus subtilis* strains can be milked.

- These findings can ultimately be used to calculate the kinetic parameters and for the designing of a MK-7 fermentation system possible with Fed- batch addition of nutrients. Continuous fermentation with the addition of fresh media is not however recommended. This is due to the fact that MK-7 production seems to follow a mixed- mode where majority of MK-7 is produced after the bacterial cell density reached its maximum. An economic analysis of the process is also recommended.
- Results of organic solvent tolerance of *Bacillus subtilis* also brings in to questioning whether cell immobilisation has offered high resistance to environmental stresses. It is well documented that biofilm bacteria are resistant to many antimicrobials. In the same manner, artificial immobilisation might offer high resistance to stressful environmental conditions. If this phenomenon can be tested, biocompatible nanomaterials such as IONs@APTES can present enormous potential for industrial production of high titres of fermentative biofuels such as *n*-butanol.

References

Abdel-Rahman, M. S., Alkady, E. A., & Ahmed, S. (2015). Menaquinone-7 as a novel pharmacological therapy in the treatment of rheumatoid arthritis: A clinical study. *European Journal of Pharmacology, 761*, 273-278.

Ahmed, S., Kishikawa, N., Nakashima, K., & Kuroda, N. (2007). Determination of vitamin K homologues by high-performance liquid chromatography with on-line photoreactor and peroxyoxalate chemiluminescence detection. *Analytica Chimica Acta, 591*(2), 148-154.

Ahmed, S., & Mahmoud, A. M. (2015). A novel salting-out assisted extraction coupled with HPLC-fluorescence detection for trace determination of vitamin K homologues in human plasma. *Talanta, 144*, 480-487.

Akay, G., Erhan, E., & Keskinler, B. (2005). Bioprocess intensification in flow‐through monolithic microbioreactors with immobilized bacteria. *Biotechnology and Bioengineering, 90*(2), 180-190.

Ansari, F., Grigoriev, P., Libor, S., Tothill, I. E., & Ramsden, J. J. (2009). DBT degradation enhancement by decorating *Rhodococcus erythropolis* IGST8 with magnetic Fe_3O_4 nanoparticles. *Biotechnology and Bioengineering, 102*(5), 1505-1512.

Aono, R., & Kobayashi, H. (1997). Cell surface properties of organic solvent-tolerant mutants of *Escherichia coli* K-12. *Applied and Environmental Microbiology, 63*(9), 3637-3642.

Applegate, D. H., & Bryers, J. D. (1991). Effects of carbon and oxygen limitations and calcium concentrations on biofilm removal processes. *Biotechnology and Bioengineering, 37*(1), 17-25.

Applerot, G., Lipovsky, A., Dror, R., Perkas, N., Nitzan, Y., Lubart, R., & Gedanken, A. (2009). Enhanced antibacterial activity of nanocrystalline ZnO due to increased ROS‐mediated cell injury. *Advanced Functional Materials, 19*(6), 842-852.

Arai, S. (2007). Global view on functional foods: Asian perspectives. *British Journal of Nutrition, 88*(Suppl. 2), S139-S143.

Arakha, M., Pal, S., Samantarrai, D., Panigrahi, T. K., Mallick, B. C., Pramanik, K., Mallick, B., & Jha, S. (2015). Antimicrobial activity of iron oxide nanoparticle upon modulation of nanoparticle-bacteria interface. *Scientific Reports, 5:14813* doi:10.1038/srep14813.

Aruguete, D. M., & Hochella, M. F. (2010). Bacteria–nanoparticle interactions and their environmental implications. *Environmental Chemistry, 7*(1), 3-9.

Asenath Smith, E., & Chen, W. (2008). How to prevent the loss of surface functionality derived from aminosilanes. *Langmuir, 24*(21), 12405-12409.

Ashiuchi, M., Soda, K., & Misono, H. (1999). A poly-γ-glutamate synthetic system of *Bacillus subtilis* IFO 3336: gene cloning and biochemical analysis of poly-γ-glutamate produced by *Escherichia coli* clone cells. *Biochemical and Biophysical Research Communications, 263*(1), 6-12.

Athalye, M., Goodfellow, M., & Minnikin, D. (1984). Menaquinone composition in the classification of *Actinomadura* and related taxa. *Microbiology, 130*(4), 817-823.

Auffan, M. l., Achouak, W., Rose, J. r., Roncato, M.-A., Chanéac, C., Waite, D. T., Mason, A., Woicik, J. C., Wiesner, M. R., & Bottero, J.-Y. (2008). Relation between the redox state of iron-based nanoparticles and their cytotoxicity toward *Escherichia coli*. *Environmental Science & Technology, 42*(17), 6730-6735.

Azam, A., Ahmed, A. S., Oves, M., Khan, M. S., Habib, S. S., & Memic, A. (2012). Antimicrobial activity of metal oxide nanoparticles against Gram-positive and Gram-negative bacteria: a comparative study. *International Journal of Nanomedicine, 7*(7), 6003-6009.

Baek, Y.-W., & An, Y.-J. (2011). Microbial toxicity of metal oxide nanoparticles (CuO, NiO, ZnO, and Sb_2O_3) to *Escherichia coli*, *Bacillus subtilis*, and *Streptococcus aureus*. *Science of the Total Environment, 409*(8), 1603-1608.

Banik, R., Kanari, B., & Upadhyay, S. (2000). Exopolysaccharide of the gellan family: prospects and potential. *World Journal of Microbiology and Biotechnology, 16*(5), 407-414.

Beauregard, P. B., Chai, Y., Vlamakis, H., Losick, R., & Kolter, R. (2013). *Bacillus subtilis* biofilm induction by plant polysaccharides. *Proceedings of the National Academy of Sciences, 110*(17), E1621-E1630.

Beech, I. B., & Sunner, J. (2004). Biocorrosion: towards understanding interactions between biofilms and metals. *Current Opinion in Biotechnology, 15*(3), 181-186.

Bentley, R., & Meganathan, R. (1982). Biosynthesis of vitamin K (menaquinone) in bacteria. *Microbiological Reviews, 46*(3), 241-280.

Benz, M. (2012). Superparamagnetism: theory and applications. *Discussion*.

Berenjian, A., Chan, N. L.-C., Mahanama, R., Talbot, A., Regtop, H., Kavanagh, J., & Dehghani, F. (2013). Effect of biofilm formation by *Bacillus subtilis natto* on menaquinone-7 biosynthesis. *Molecular Biotechnology, 54*(2), 371-378.

Berenjian, A., Mahanama, R., Kavanagh, J., & Dehghani, F. (2015). Vitamin K series: current status and future prospects. *Critical Reviews in Biotechnology, 35*(2), 199-208.

Berenjian, A., Mahanama, R., Talbot, A., Biffin, R., Regtop, H., Valtchev, P., Kavanagh, J., & Dehghani, F. (2011). Efficient media for high

menaquinone-7 production: response surface methodology approach. *New Biotechnology, 28*(6), 665-672.

Berenjian, A., Mahanama, R., Talbot, A., Regtop, H., Kavanagh, J., & Dehghani, F. (2012). Advances in menaquinone-7 production by *Bacillus subtilis natto*: fed-batch glycerol addition. *American Journal of Biochemistry and Biotechnology, 8*, 105-110.

Berenjian, A., Mahanama, R., Talbot, A., Regtop, H., Kavanagh, J., & Dehghani, F. (2014). Designing of an intensification process for biosynthesis and recovery of menaquinone-7. *Applied Biochemistry and Biotechnology, 172*(3), 1347-1357.

Berger, P., Adelman, N. B., Beckman, K. J., Campbell, D. J., Ellis, A. B., & Lisensky, G. C. (1999). Preparation and properties of an aqueous ferrofluid. *Journal of Chemical Education, 76*(7), 943-948.

Beulens, J. W., Bots, M. L., Atsma, F., Bartelink, M.-L. E., Prokop, M., Geleijnse, J. M., Witteman, J. C., Grobbee, D. E., & van der Schouw, Y. T. (2009). High dietary menaquinone intake is associated with reduced coronary calcification. *Atherosclerosis, 203*(2), 489-493.

Bini, R. A., Marques, R. F. C., Santos, F. J., Chaker, J. A., & Jafelicci Jr, M. (2012). Synthesis and functionalization of magnetite nanoparticles with different amino-functional alkoxysilanes. *Journal of Magnetism and Magnetic Materials, 324*(4), 534-539.

Booth, S. L. (2012). Vitamin K: food composition and dietary intakes. *Food & Nutrition Research, 56*, 1-5.

Borcherding, J., Baltrusaitis, J., Chen, H., Stebounova, L., Wu, C.-M., Rubasinghege, G., Mudunkotuwa, I. A., Caraballo, J. C., Zabner, J., & Grassian, V. H. (2014). Iron oxide nanoparticles induce *Pseudomonas aeruginosa* growth, induce biofilm formation, and inhibit antimicrobial peptide function. *Environmental Science: Nano, 1*(2), 123-132.

Branda, S. S., Chu, F., Kearns, D. B., Losick, R., & Kolter, R. (2006). A major protein component of the *Bacillus subtilis* biofilm matrix. *Molecular Microbiology, 59*(4), 1229-1238.

Branda, S. S., González-Pastor, J. E., Ben-Yehuda, S., Losick, R., & Kolter, R. (2001). Fruiting body formation by *Bacillus subtilis*. *Proceedings of the National Academy of Sciences, 98*(20), 11621-11626.

Brunner, T. J., Wick, P., Manser, P., Spohn, P., Grass, R. N., Limbach, L. K., Bruinink, A., & Stark, W. J. (2006). In vitro cytotoxicity of oxide nanoparticles: comparison to asbestos, silica, and the effect of particle solubility. *Environmental Science & Technology, 40*(14), 4374-4381.

Buzea, C., Pacheco, I. I., & Robbie, K. (2007). Nanomaterials and nanoparticles: sources and toxicity. *Biointerphases 2*(4), http//dx.doi:10.1116/1.2815690.

Cabot, M. C., & Gatt, S. (1978). The hydrolysis of triacylglycerol and diacylglycerol by a rat brain microsomal lipase with an acidic pH

optimum. *Biochimica et Biophysica Acta-Lipids and Lipid Metabolism 530*(3), 508-512.

Cairns, L. S., Hobley, L., & Stanley‐Wall, N. R. (2014). Biofilm formation by *Bacillus subtilis*: new insights into regulatory strategies and assembly mechanisms. *Molecular Microbiology, 93*(4), 587-598.

Can, K., Ozmen, M., & Ersoz, M. (2009). Immobilization of albumin on aminosilane modified superparamagnetic magnetite nanoparticles and its characterization. *Colloids and Surfaces B: Biointerfaces, 71*(1), 154-159.

Canfield, L., Hopkinson, J., Lima, A., Silva, B., & Garza, C. (1991). Vitamin K in colostrum and mature human milk over the lactation period-a cross-sectional study. *The American Journal of Clinical Nutrition, 53*(3), 730-735.

Canfield, L. M., Hopkinson, J. M., Lima, A. F., Martin, G. S., Sugimoto, K., Burr, J., Clark, L., & McGee, D. L. (1990). Quantitation of vitamin K in human milk. *Lipids, 25*(7), 406-411.

Cerca, N., Gomes, F., Pereira, S., Teixeira, P., & Oliveira, R. (2012). Confocal laser scanning microscopy analysis of *S. epidermidis* biofilms exposed to farnesol, vancomycin and rifampicin. *BMC Research Notes, 5*(1), 244.

Chandrasekaran, R., & Thailambal, V. (1990). The influence of calcium ions, acetate and L-glycerate groups on the gellan double-helix. *Carbohydrate Polymers, 12*(4), 431-442.

Chang, Y.-N., Zhang, M., Xia, L., Zhang, J., & Xing, G. (2012). The toxic effects and mechanisms of CuO and ZnO nanoparticles. *Materials, 5*(12), 2850-2871.

Chatterjee, S., Bandyopadhyay, A., & Sarkar, K. (2011). Effect of iron oxide and gold nanoparticles on bacterial growth leading towards biological application. *Journal of Nanobiotechnology 9*(34), 1-7.

Chen, X. (1998). *Chemically Induced Biofilm Detachment.* PhD thesis, Montana State University, Bozeman, MT.

Chen, X., & Stewart, P. (2002). Role of electrostatic interactions in cohesion of bacterial biofilms. *Applied Microbiology and Biotechnology, 59*(6), 718-720.

Chen, X., & Stewart, P. S. (2000). Biofilm removal caused by chemical treatments. *Water Research, 34*(17), 4229-4233.

Cheng, K.-C., Demirci, A., & Catchmark, J. M. (2010). Advances in biofilm reactors for production of value-added products. *Applied Microbiology and Biotechnology, 87*(2), 445-456.

Chettri, R., Bhutia, M. O., & Tamang, J. P. (2016). Poly-γ-glutamic acid (PGA)-producing *Bacillus* species isolated from Kinema, Indian fermented soybean food. *Frontiers in Microbiology, 7*(971), https://doi.org/10.3389/fmicb.2016.00971.

Clejan, S., Krulwich, T., Mondrus, K., & Seto-Young, D. (1986). Membrane lipid composition of obligately and facultatively alkalophilic strains of *Bacillus spp*. *Journal of Bacteriology, 168*(1), 334-340.

Clinical and Laboratory Standards Institute. (2009). *Methods for dilution antimicrobial susceptibility tests for bacteria that grow aerobically: Approved standard, 8th ed.* Retrieved March, 2016, from http://simpleshowoflove.weebly.com/uploads/1/4/0/7/14073276/agar_dilution_assay.pdf.

Cockayne, S., Adamson, J., Lanham-New, S., Shearer, M. J., Gilbody, S., & Torgerson, D. J. (2006). Vitamin K and the prevention of fractures: systematic review and meta-analysis of randomized controlled trials. *Archives of Internal Medicine, 166*(12), 1256-1261.

Collins, M., & Jones, D. (1981). Distribution of isoprenoid quinone structural types in bacteria and their taxonomic implication. *Microbiological Reviews, 45*(2), 316-354.

Corpe, W. A. (1970). Attachment of marine bacteria to solid surfaces. In R. S. Manly (Ed.), *Adhesion in Biological Systems* (pp. 73-87). Academic Press, New York.

Costa, S. B., Campos, A. C. C., Pereira, A. C. M., de Mattos-Guaraldi, A. L., Júnior, R. H., Rosa, A. C. P., & Asad, L. M. (2012). The role of DNA base excision repair in filamentation in *Escherichia coli* K-12 adhered to epithelial HEp-2 cells. *Antonie van Leeuwenhoek, 101*(2), 423-431.

Cranenburg, E. C., Schurgers, L. J., & Vermeer, C. (2007). Vitamin K: the coagulation vitamin that became omnipotent. *Thrombosis and Haemostasis, 98*(1), 120-125.

Dairi, T. (2009). An alternative menaquinone biosynthetic pathway operating in microorganisms: an attractive target for drug discovery to pathogenic *Helicobacter* and *Chlamydia* strains. *The Journal of Antibiotics, 62*(7), 347-352.

Dam, H. (1935). The antihaemorrhagic vitamin of the chick. *Biochemical Journal, 29*(6), 1273-1285.

Das, T., Sehar, S., Koop, L., Wong, Y. K., Ahmed, S., Siddiqui, K. S., & Manefield, M. (2014). Influence of calcium in extracellular DNA mediated bacterial aggregation and biofilm formation. *PloS One, 9*(3), http://dx.doi.org/10.1371/journal.pone.0091935.

Degeest, B., & De Vuyst, L. (1999). Indication that the nitrogen source influences both amount and size of exopolysaccharides produced by *Streptococcus thermophilus* LY03 and modelling of the bacterial growth and exopolysaccharide production in a complex medium. *Applied and Environmental Microbiology, 65*(7), 2863-2870.

Dhiman, R. K., Mahapatra, S., Slayden, R. A., Boyne, M. E., Lenaerts, A., Hinshaw, J. C., Angala, S. K., Chatterjee, D., Biswas, K., & Narayanasamy, P. (2009). Menaquinone synthesis is critical for

maintaining mycobacterial viability during exponential growth and recovery from non‐replicating persistence. *Molecular Microbiology, 72*(1), 85-97.

Dias, A., Hussain, A., Marcos, A., & Roque, A. (2011). A biotechnological perspective on the application of iron oxide magnetic colloids modified with polysaccharides. *Biotechnology Advances, 29*(1), 142-155.

Diaz-Visurraga, J., Garcia, A., & Cardenas, G. (2010). Morphological changes induced in bacteria as evaluated by electron microscopy. *Scientific Reports, 6*(307-315), http://dx.doi.org/10.1038/srep24929.

Dickson, J. S., & Koohmaraie, M. (1989). Cell surface charge characteristics and their relationship to bacterial attachment to meat surfaces. *Applied and Environmental Microbiology, 55*(4), 832-836.

Djurišić, A. B., Leung, Y. H., Ng, A., Xu, X. Y., Lee, P. K., & Degger, N. (2015). Toxicity of metal oxide nanoparticles: mechanisms, characterization, and avoiding experimental artefacts. *Small, 11*(1), 26-44.

Dong, Y.-H., & Zhang, L.-H. (2005). Quorum sensing and quorum-quenching enzymes. *The Journal of Microbiology, 43*(1), 101-109.

Dorniani, D., Kura, A. U., Hussein-Al-Ali, S. H., Bin Hussein, M. Z., Fakurazi, S., Shaari, A. H., & Ahmad, Z. (2014). In Vitro Sustained Release Study of Gallic Acid Coated with Magnetite-PEG and Magnetite-PVA for Drug Delivery System. *Scientific World Journal, 2014*(Article ID 416354), http://dx.doi.org/10.1155/2014/416354.

Ebrahiminezhad, A., Bagheri, M., Taghizadeh, S.-M., Berenjian, A., & Ghasemi, Y. (2016a). Biomimetic synthesis of silver nanoparticles using microalgal secretory carbohydrates as a novel anticancer and antimicrobial. *Advances in Natural Sciences: Nanoscience and Nanotechnology, 7*(1), 015018.

Ebrahiminezhad, A., Davaran, S., Rasoul-Amini, S., Barar, J., Moghadam, M., & Ghasemi, Y. (2012a). Synthesis, characterization and anti-*Listeria monocytogenes* effect of amino acid coated magnetite nanoparticles. *Current Nanoscience, 8*(6), 868-874.

Ebrahiminezhad, A., Ghasemi, Y., Rasoul-Amini, S., Barar, J., & Davaran, S. (2012b). Impact of amino-acid coating on the synthesis and characteristics of iron-oxide nanoparticles (IONs). *Bulletin of the Korean Chemical Society, 33*(12), 3957-3962.

Ebrahiminezhad, A., Rasoul-Amini, S., Davaran, S., Barar, J., & Ghasemi, Y. (2014). Impacts of iron oxide nanoparticles on the invasion power of *Listeria monocytogenes*. *Current Nanoscience, 10*(3), 382-388.

Ebrahiminezhad, A., Rasoul-Amini, S., Kouhpayeh, A., Davaran, S., Barar, J., & Ghasemi, Y. (2015). Impacts of amine functionalized iron oxide nanoparticles on HepG2 cell line. *Current Nanoscience, 11*(1), 113-119.

Ebrahiminezhad, A., Varma, V., Yang, S., & Berenjian, A. (2016b). Magnetic immobilization of *Bacillus subtilis natto* cells for menaquinone-7 fermentation. *Applied Microbiology and Biotechnology, 100*(1), 173-180.

Ebrahiminezhad, A., Varma, V., Yang, S., Ghasemi, Y., & Berenjian, A. (2016c). Synthesis and Application of Amine Functionalized Iron Oxide Nanoparticles on Menaquinone-7 Fermentation: A Step towards Process Intensification. *Nanomaterials, 6*(1), 1-9.

Errington, J. (2003). Regulation of endospore formation in *Bacillus subtilis*. *Nature Reviews Microbiology, 1*(2), 117-126.

Esparza-Soto, M., & Westerhoff, P. (2003). Biosorption of humic and fulvic acids to live activated sludge biomass. *Water Research, 37*(10), 2301-2310.

Evans, E., Brown, M. R., & Gilbert, P. (1994). Iron chelator, exopolysaccharide and protease production in *Staphylococcus epidermidis*: a comparative study of the effects of specific growth rate in biofilm and planktonic culture. *Microbiology, 140*(1), 153-157.

Farrand, S., & Taber, H. (1973). Physiological effects of menaquinone deficiency in *Bacillus subtilis*. *Journal of Bacteriology, 115*(3), 1035-1044.

Farrand, S., & Taber, H. (1974). Changes in menaquinone concentration during growth and early sporulation in *Bacillus subtilis*. *Journal of Bacteriology, 117*(1), 324-326.

Fauler, G., Muntean, W., & Leis, H. J. (2000). Vitamin K. In A. P. De Leenheer, W. E. Lambert & J. F. Van Bocxlaer (Eds.), *Modern Chromatographic Analysis of Vitamins* (Chapter 4, pp. 240-281). New York: Marcel Dekker.

Fletcher, M. (1983). The effects of methanol, ethanol, propanol and butanol on bacterial attachment to surfaces. *Microbiology, 129*(3), 633-641.

Frenz, J., Largeau, C., & Casadevall, E. (1989). Hydrocarbon recovery by extraction with a biocompatible solvent from free and immobilized cultures of *Botryococcus braunii*. *Enzyme and Microbial Technology, 11*(11), 717-724.

Fujimoto, N., Yamada, M., & Kosaka, T. (2012). Menaquinone as well as ubiquinone as a crucial component in the *Escherichia coli* respiratory chain. In D. Ekinci (Ed.), *Chemical Biology* (Chapter 10, pp. 188-208). Japan: Intech Open Science.

Gast, G.-C. M., de Roos, N. M., Sluijs, I., Bots, M. L., Beulens, J. W., Geleijnse, J. M., Witteman, J. C., Grobbee, D. E., Peeters, P. H., & van der Schouw, Y. T. (2009). A high menaquinone intake reduces the incidence of coronary heart disease. *Nutrition, Metabolism and Cardiovascular Diseases, 19*(7), 504-510.

Gholami, A., Rasoul-amini, S., Ebrahiminezhad, A., Seradj, S. H., & Ghasemi, Y. (2015). Lipoamino acid coated superparamagnetic iron oxide nanoparticles concentration and time dependently enhanced growth of human hepatocarcinoma cell line (Hep-G2). *Journal of Nanomaterials, 2015*, 150.

Gibson, H., Taylor, J. H., Hall, K. E., & Holah, J. T. (1999). Effectiveness of cleaning techniques used in the food industry in terms of the removal of bacterial biofilms. *Journal of Applied Microbiology, 87*(1), 41-48.

Global Market Insights. (2018). *Vitamin K Market Size, Share-Industry Statistics Report 2017-2024 (Report ID: GMI1481)*. Retrieved 6 December, 2017, from https://www.gminsights.com/industry-analysis/vitamin-k-market.

Gnanaprakash, G., Mahadevan, S., Jayakumar, T., Kalyanasundaram, P., Philip, J., & Raj, B. (2007). Effect of initial pH and temperature of iron salt solutions on formation of magnetite nanoparticles. *Materials Chemistry and Physics, 103*(1), 168-175.

Gordon, C. A., Hodges, N. A., & Marriott, C. (1991). Use of slime dispersants to promote antibiotic penetration through the extracellular polysaccharide of mucoid *Pseudomonas aeruginosa*. *Antimicrobial Agents and Chemotherapy, 35*(6), 1258-1260.

Gottenbos, B., Grijpma, D. W., van der Mei, H. C., Feijen, J., & Busscher, H. J. (2001). Antimicrobial effects of positively charged surfaces on adhering Gram-positive and Gram-negative bacteria. *Journal of Antimicrobial Chemotherapy, 48*(1), 7-13.

Grasso, D., Smets, B., Strevett, K., Machinist, B., Van Oss, C., Giese, R., & Wu, W. (1996). Impact of physiological state on surface thermodynamics and adhesion of *Pseudomonas aeruginosa*. *Environmental Science & Technology, 30*(12), 3604-3608.

Grossman, A. D. (1995). Genetic networks controlling the initiation of sporulation and the development of genetic competence in *Bacillus subtilis*. *Annual Review of Genetics, 29*(1), 477-508.

Grumezescu, A., Mihaiescu, D., Mogoşanu, D., Chifiriuc, M., Lazar, V., Lazar, V., Calugarescu, I., & Traistaru, V. (2010). In vitro assay of the antimicrobial activity of Fe_3O_4 and $CoFe_2O_4$/oleic acid-core/shell on clinical isolates of bacterial and fungal strains. *Optoelectronics and Advanced Materials, 4*(11), 1798-1801.

Grumezescu, A. M., Gestal, M. C., Holban, A. M., Grumezescu, V., Vasile, B. Ş., Mogoantă, L., Iordache, F., Bleotu, C., & Mogoşanu, G. D. (2014). Biocompatible Fe_3O_4 increases the efficacy of amoxicillin delivery against Gram-positive and Gram-negative bacteria. *Molecules, 19*(4), 5013-5027.

Gupta, A. K., & Gupta, M. (2005). Cytotoxicity suppression and cellular uptake enhancement of surface modified magnetic nanoparticles. *Biomaterials, 26*(13), 1565-1573.

Hajipour, M. J., Fromm, K. M., Akbar Ashkarran, A., Jimenez de Aberasturi, D., Larramendi, I. R. d., Rojo, T., Serpooshan, V., Parak, W. J., & Mahmoudi, M. (2012). Antibacterial properties of nanoparticles. *Trends in Biotechnology, 30*(10), 499-511.

Hammes, F., Berney, M., & Egli, T. (2010). Cultivation-independent assessment of bacterial viability. In S. Müller & T. Bley (Eds.), *High Resolution*

Microbial Single Cell Analytics (Vol. 124, pp. 123-150). Berlin, Germany: Springer.

Haroon, Y., Shearer, M. J., Rahim, S., Gunn, W. G., McEnery, G., & Barkhan, P. (1982). The content of phylloquinone (vitamin K1) in human milk, cows' milk and infant formula foods determined by high-performance liquid chromatography. *The Journal of Nutrition, 112*(6), 1105-1117.

Hejazi, M., De Lamarliere, C., Rocha, J., Vermue, M., Tramper, J., & Wijffels, R. (2002). Selective extraction of carotenoids from the microalga *Dunaliella salina* with retention of viability. *Biotechnology and Bioengineering, 79*(1), 29-36.

Hejazi, M., Holwerda, E., & Wijffels, R. (2004). Milking microalga *Dunaliella salina* for β - carotene production in two - phase bioreactors. *Biotechnology and bioengineering, 85*(5), 475-481.

Hejazi, M. A., & Wijffels, R. H. (2004). Milking of microalgae. *Trends in Biotechnology, 22*(4), 189-194.

Hirauchi, K., Sakano, T., Notsumoto, S., Morimoto, A., Fujimoto, K., Masuda, S., & Suzuki, Y. (1989). Measurement of K vitamins in animal tissues by high-performance liquid chromatography with fluorimetric detection. *Journal of Chromatography. B, Biomedical Sciences and Applications, 497*, 131-137.

Hodges, S., Bejui, J., Leclercq, M., & Delmas, P. (1993). Detection and measurement of vitamins K1 and K2 in human cortical and trabecular bone. *Journal of Bone and Mineral Research, 8*(8), 1005-1008.

Hu, X., Cook, S., Wang, P., & Hwang, H. (2009). In vitro evaluation of cytotoxicity of engineered metal oxide nanoparticles. *Science of the Total Environment, 407*(8), 3070-3072.

Huang, H., Liu, H., & Gan, Y.-R. (2010a). Genetic modification of critical enzymes and involved genes in butanol biosynthesis from biomass. *Biotechnology Advances, 28*(5), 651-657.

Huang, Y.-F., Wang, Y.-F., & Yan, X.-P. (2010b). Amine-functionalized magnetic nanoparticles for rapid capture and removal of bacterial pathogens. *Environmental Science & Technology, 44*(20), 7908-7913.

Huang, Z., Zheng, X., Yan, D., Yin, G., Liao, X., Kang, Y., Yao, Y., Huang, D., & Hao, B. (2008). Toxicological effect of ZnO nanoparticles based on bacteria. *Langmuir, 24*(8), 4140-4144.

Ihor, T., Sergiy, M., Mikhail, M., & Yuri, R. (2008). Colloidal Systems on the Nanometer Length Scale. In *Handbook of Surface and Colloid Chemistry, Third Edition* (pp. 131-154). CRC Press.

Ikuma, K., Decho, A. W., & Lau, B. L. T. (2015). When nanoparticles meet biofilms—interactions guiding the environmental fate and accumulation of nanoparticles. *Frontiers in Microbiology, 6*(Article ID 591), http://dx.doi.org/10.3389/fmicb.2015.00591.

Ingram, L. (1976). Adaptation of membrane lipids to alcohols. *Journal of Bacteriology, 125*(2), 670-678.

Ireton, K., Jin, S., Grossman, A. D., & Sonenshein, A. L. (1995). Krebs cycle function is required for activation of the Spo0A transcription factor in *Bacillus subtilis*. *Proceedings of the National Academy of Sciences, 92*(7), 2845-2849.

Ismail, R. A., Sulaiman, G. M., Abdulrahman, S. A., & Marzoog, T. R. (2015). Antibacterial activity of magnetic iron oxide nanoparticles synthesized by laser ablation in liquid. *Materials Science and Engineering C 53*, 286-297.

Iwamoto, J., Takeda, T., & Sato, Y. (2006). Role of vitamin K2 in the treatment of postmenopausal osteoporosis. *Current Drug Safety, 1*(1), 87-97.

Jakob, E., & Elmadfa, I. (1995). Rapid HPLC assay for the assessment of vitamin K1, A, E and beta-carotene status in children (7-19 years). *International Journal for Vitamin and Nutrition Research. , 65*(1), 31-35.

Jakob, E., & Elmadfa, I. (1996). Application of a simplified HPLC assay for the determination of phylloquinone (vitamin K1) in animal and plant food items. *Food Chemistry, 56*(1), 87-91.

Jakob, E., & Elmadfa, I. (2000). Rapid and simple HPLC analysis of vitamin K in food, tissues and blood. *Food Chemistry, 68*(2), 219-221.

Javanbakht, T., Laurent, S., Stanicki, D., & Wilkinson, K. J. (2016). Relating the Surface Properties of Superparamagnetic Iron Oxide Nanoparticles (SPIONs) to Their Bactericidal Effect towards a Biofilm of *Streptococcus mutans*. *PloS One, 11*(4), http://dx.doi.org/10.1371/journal.pone.0154445.

Jones, T. H., Vail, K. M., & McMullen, L. M. (2013). Filament formation by foodborne bacteria under sublethal stress. *International Journal of Food Microbiology, 165*(2), 97-110.

Kamao, M., Suhara, Y., Tsugawa, N., Uwano, M., Yamaguchi, N., Uenishi, K., Ishida, H., Sasaki, S., & Okano, T. (2007). Vitamin K content of foods and dietary vitamin K intake in Japanese young women. *Journal of Nutritional Science and Vitaminology, 53*(6), 464-470.

Karl, J. P., Fu, X., Dolnikowski, G. G., Saltzman, E., & Booth, S. L. (2014). Quantification of phylloquinone and menaquinones in feces, serum, and food by high-performance liquid chromatography–mass spectrometry. *Journal of Chromatography B, 963*, 128-133.

Kathi, S., & Khan, A. (2013). Enrichment, isolation and identification of polycyclic aromatic hydrocarbon degrading *Rhodococcus ruber* from sediments. *International Journal of Scientific Research and Publications, 3*(2), 1-7.

Kayesh, R., Sultan, M., Rahman, A., Uddin, M., Aktar, F., & Rashid, M. (2013). Development and validation of a RP-HPLC method for the quantification of omeprazole in pharmaceutical dosage form. *Journal of Scientific Research, 5*(2), 335-342.

Kearns, D. B., Chu, F., Branda, S. S., Kolter, R., & Losick, R. (2005). A master regulator for biofilm formation by *Bacillus subtilis*. *Molecular Microbiology, 55*(3), 739-749.

Knapen, M., Braam, L. A., Drummen, N. E., Bekers, O., Hoeks, A., & Vermeer, C. (2015). Menaquinone-7 supplementation improves arterial stiffness in healthy postmenopausal women: double-blind randomized clinical trial. *Thrombosis and Haemostasis, 113*(5), 1135-44.

Knapen, M., Schurgers, L., & Vermeer, C. (2007). Vitamin K2 supplementation improves hip bone geometry and bone strength indices in postmenopausal women. *Osteoporosis International, 18*(7), 963-972.

Kolhar, P., Anselmo, A. C., Gupta, V., Pant, K., Prabhakarpandian, B., Ruoslahti, E., & Mitragotri, S. (2013). Using shape effects to target antibody-coated nanoparticles to lung and brain endothelium. *Proceedings of the National Academy of Sciences, 110*(26), 10753-10758.

Křivánková, L., & Dadák, V. (1980). Semimicro extraction of ubiquinone and menaquinone from bacteria. *Methods in Enzymology, 67*, 111-114.

Kubo, Y., Rooney, A. P., Tsukakoshi, Y., Nakagawa, R., Hasegawa, H., & Kimura, K. (2011). Phylogenetic analysis of *Bacillus subtilis* strains applicable to natto (fermented soybean) production. *Applied and Environmental Microbiology, 77*(18), 6463-6469.

Laha, D., Pramanik, A., Laskar, A., Jana, M., Pramanik, P., & Karmakar, P. (2014). Shape-dependent bactericidal activity of copper oxide nanoparticle mediated by DNA and membrane damage. *Materials Research Bulletin, 59*, 185-191.

Lambert, W., Vanneste, L., & De Leenheer, A. (1992). Enzymatic sample hydrolysis and HPLC in a study of phylloquinone concentration in human milk. *Clinical Chemistry, 38*(9), 1743-1748.

Langenberg, J., Tjaden, U., DEVOGEL, E., & Langerak, D. I. (1986). Determination of phylloquinone (vitaminK1) in raw and processed vegetables using reversed phase HPLC with electrofluorometric detection. *Acta Alimentaria, 15*(3), 187-198.

Larsen, N., Nissen, P., & Willats, W. G. (2007). The effect of calcium ions on adhesion and competitive exclusion of *Lactobacillus sp*. and *E. col*i O138. *International Journal of Food Microbiology, 114*(1), 113-119.

Laurent, S., Dutz, S., Häfeli, U. O., & Mahmoudi, M. (2011). Magnetic fluid hyperthermia: focus on superparamagnetic iron oxide nanoparticles. *Advances in Colloid and Interface Science, 166*(1), 8-23.

Laurent, S., Forge, D., Port, M., Roch, A., Robic, C., Vander Elst, L., & Muller, R. N. (2008). Magnetic iron oxide nanoparticles: synthesis, stabilization, vectorization, physicochemical characterizations, and biological applications. *Chemical Reviews, 108*(6), 2064-2110.

Lăzăroaie, M. (2009). Mechanisms involved in organic solvent resistance in Gram-negative bacteria. *World Academy of Science Engineering and Technology, 30*, 643-653.

LeDeaux, J. R., Yu, N., & Grossman, A. D. (1995). Different roles for KinA, KinB, and KinC in the initiation of sporulation in *Bacillus subtilis*. *Journal of Bacteriology, 177*(3), 861-863.

Lee, J., Isobe, T., & Senna, M. (1996). Preparation of Ultrafine Fe_3O_4Particles by Precipitation in the Presence of PVA at High pH. *Journal of Colloid and Interface Science, 177*(2), 490-494.

Lee, J. H., Jung, H. W., Kang, I.-K., & Lee, H. B. (1994). Cell behaviour on polymer surfaces with different functional groups. *Biomaterials, 15*(9), 705-711.

Lefevere, M., De Leenheer, A., & Claeys, A. (1979). High-performance liquid chromatographic assay of vitamin K in human serum. *Journal of Chromatography A, 186*, 749-762.

Leica Microsystems. (n.d.). Retrieved 18th September, 2016, from https://www.meyerinst.com/html/leica/filter/wavelengthranges.pdf.

Lemon, K. P., Earl, A. M., Vlamakis, H. C., Aguilar, C., & Kolter, R. (2008). Biofilm Development with an Emphasis on *Bacillus subtilis*. *Current topics in Microbiology and Immunology, 322*, 1-16.

Li, G.-q., Li, S.-s., Zhang, M.-l., Wang, J., Zhu, L., Liang, F.-l., Liu, R.-l., & Ma, T. (2008). Genetic rearrangement strategy for optimizing the dibenzothiophene biodesulfurization pathway in *Rhodococcus erythropolis*. *Applied and Environmental microbiology, 74*(4), 971-976.

Li, Y.-G., Gao, H.-S., Li, W.-L., Xing, J.-M., & Liu, H.-Z. (2009). In situ magnetic separation and immobilization of dibenzothiophene-desulfurizing bacteria. *Bioresource Technology, 100*(21), 5092-5096.

Liu, J., Aruguete, D. M., Jinschek, J. R., Rimstidt, J. D., & Hochella, M. F. (2008). The non-oxidative dissolution of galena nanocrystals: Insights into mineral dissolution rates as a function of grain size, shape, and aggregation state. *Geochimica et Cosmochimica Acta, 72*(24), 5984-5996.

Liu, Y., Ding, X.-m., Xue, Z.-l., Hu, L.-x., Zhang, N.-j., Wang, Z., Yang, J.-w., Cheng, Q., Chen, M.-h., & Zhang, Z.-z. (2017). The change of the state of cell membrane can enhance the synthesis of menaquinone in *Escherichia coli*. *World Journal of Microbiology and Biotechnology, 33*(3), 52.

Liu, Y., Zheng, Z.-M., Qiu, H.-W., Zhao, G.-H., Wang, P., Liu, H., Wang, L., Li, Z.-M., Wu, H.-F., & Liu, H.-X. (2014). Surfactant supplementation to enhance the production of vitamin K2 metabolites in shake flask cultures using *Escherichia sp.* mutant FM3-1709. *Food Technology and Biotechnology, 52*(3), 269-275.

López, D., Fischbach, M. A., Chu, F., Losick, R., & Kolter, R. (2009). Structurally diverse natural products that cause potassium leakage trigger

multicellularity in *Bacillus subtilis*. *Proceedings of the National Academy of Sciences, 106*(1), 280-285.

López, D., Vlamakis, H., & Kolter, R. (2010). Biofilms. *Cold Spring Harbor perspectives in biology, 2*(Article ID. a000398), http://dx.doi.org/10.1101/cshperspect.a000398.

Lübben, M. (1995). Cytochromes of archaeal electron transfer chains. *Biochimica et Biophysica Acta (BBA)-Bioenergetics, 1229*(1), 1-22.

Luo, M.-m., Ren, L.-j., Chen, S.-l., Ji, X.-j., & Huang, H. (2016). Effect of media components and morphology of *Bacillus natto* on menaquinone-7 synthesis in submerged fermentation. *Biotechnology and Bioprocess Engineering, 21*(6), 777-786.

MacCorquodale, D., Binkley, S., Thayer, S., & Doisy, E. (1939). On the constitution of Vitamin K1. *Journal of the American Chemical Society, 61*(7), 1928-1929.

Mahanama, R., Berenjian, A., Dehghani, F., & Kavanagh, J. M. (2011). *Solid-substrate fermentation of menaquinone -7 with Bacillus subtilis: comparison of continuous rotation with stationary bed fermentation at different initial moisture levels.* School of Chemical and Biomolecular Engineering, The University of Sydney, Sydney, Australia. 10p.

Mahanama, R., Berenjian, A., Regtop, H., Talbot, A., Dehghani, F., & Kavanagh, J. M. (2012). Modeling Menaquinone-7 production in tray type solid state fermenter. *ANZIAM Journal, 53*, 354-372.

Mahdinia, E., Demirci, A., & Berenjian, A. (2017). Optimization of *Bacillus subtilis natto* growth parameters in glycerol-based medium for vitamin K (Menaquinone-7) production in biofilm reactors. *Bioprocess and Biosystems Engineering, 41*, 195-204.

Mahmoudi, M., Sant, S., Wang, B., Laurent, S., & Sen, T. (2011). Superparamagnetic iron oxide nanoparticles (SPIONs): development, surface modification and applications in chemotherapy. *Advanced Drug Delivery Reviews, 63*(1), 24-46.

Mahmoudi, M., Simchi, A., Imani, M., Milani, A. S., & Stroeve, P. (2008). Optimal design and characterization of superparamagnetic iron oxide nanoparticles coated with polyvinyl alcohol for targeted delivery and imaging. *The Journal of Physical Chemistry B, 112*(46), 14470-14481.

Manke, A., Wang, L., & Rojanasakul, Y. (2013). Mechanisms of nanoparticle-induced oxidative stress and toxicity. *BioMed Research International, 2013*(Article ID 942916), http://dx.doi.org/10.1155/2013/942916.

Marambio-Jones, C., & Hoek, E. M. (2010). A review of the antibacterial effects of silver nanomaterials and potential implications for human health and the environment. *Journal of Nanoparticle Research, 12*(5), 1531-1551.

Marinova, M., Lütjohann, D., Westhofen, P., Watzka, M., Breuer, O., & Oldenburg, J. (2011). A Validated HPLC Method for the Determination of

Vitamin K in Human Serum–First Application in a Pharmacological Study. *The Open Clinical Chemistry Journal, 4*, 17-27.

Martínez-Mera, I., Espinosa-Pesqueira, M., Pérez-Hernández, R., & Arenas-Alatorre, J. (2007). Synthesis of magnetite (Fe_3O_4) nanoparticles without surfactants at room temperature. *Materials Letters, 61*(23), 4447-4451.

Mceldowney, S., & Fletcher, M. (1986a). Effect of growth conditions and surface characteristics of aquatic bacteria on their attachment to solid surfaces. *Microbiology, 132*(2), 513-523.

McEldowney, S., & Fletcher, M. (1986b). Variability of the influence of physicochemical factors affecting bacterial adhesion to polystyrene substrata. *Applied and Environmental Microbiology, 52*(3), 460-465.

Meganathan, R. (2001). Ubiquinone biosynthesis in microorganisms. *FEMS Microbiology Letters, 203*(2), 131-139.

Miller, M., Prinz, G., Cheng, S.-F., & Bounnak, S. (2002). Detection of a micron-sized magnetic sphere using a ring-shaped anisotropic magnetoresistance-based sensor: a model for a magnetoresistance-based biosensor. *Applied Physics Letters, 81*(12), 2211-2213.

Miller, M. B., & Bassler, B. L. (2001). Quorum sensing in bacteria. *Annual Reviews in Microbiology, 55*(1), 165-199.

Minnikin, D., O'donnell, A., Goodfellow, M., Alderson, G., Athalye, M., Schaal, A., & Parlett, J. (1984). An integrated procedure for the extraction of bacterial isoprenoid quinones and polar lipids. *Journal of Microbiological Methods, 2*(5), 233-241.

Mitchell, D. A., Berovic, M., & Krieger, N. (2000). Biochemical engineering aspects of solid state bioprocessing. In Th.Scheper (Ed.), *Advances in Biochemical Engineering/Biotechnology* (Vol. 68, Chapter New Products and New Areas of Bioprocess Engineering, pp. 61-138). Berlin Heidelberg: Springer.

Mohapatra, S., Pramanik, N., Mukherjee, S., Ghosh, S. K., & Pramanik, P. (2007). A simple synthesis of amine-derivatised superparamagnetic iron oxide nanoparticles for bioapplications. *Journal of Materials Science, 42*(17), 7566-7574.

Moos, P. J., Chung, K., Woessner, D., Honeggar, M., Cutler, N. S., & Veranth, J. M. (2010). ZnO particulate matter requires cell contact for toxicity in human colon cancer cells. *Chemical Research in Toxicology, 23*(4), 733-739.

Morishita, T., Tamura, N., Makino, T., & Kudo, S. (1999). Production of menaquinones by lactic acid bacteria. *Journal of Dairy Science, 82*(9), 1897-1903.

Müller, K., Skepper, J. N., Posfai, M., Trivedi, R., Howarth, S., Corot, C., Lancelot, E., Thompson, P. W., Brown, A. P., & Gillard, J. H. (2007). Effect of ultrasmall superparamagnetic iron oxide nanoparticles

(Ferumoxtran-10) on human monocyte-macrophages in vitro. *Biomaterials, 28*(9), 1629-1642.

Nel, A., Xia, T., Mädler, L., & Li, N. (2006). Toxic potential of materials at the nanolevel. *Science, 311*(5761), 622-627.

Neuberger, T., Schöpf, B., Hofmann, H., Hofmann, M., & Von Rechenberg, B. (2005). Superparamagnetic nanoparticles for biomedical applications: possibilities and limitations of a new drug delivery system. *Journal of Magnetism and Magnetic Materials, 293*(1), 483-496.

Nitschke, W., Kramer, D., Riedel, A., & Liebl, U. (1995). From naphtho-to benzoquinones-(r) evolutionary reorganizations of electron transfer chains. In P. Mathis (Ed.), *Photosynthesis: from Light to Biosphere* (Vol. 1, pp. 945-950). Dordrecht Kluwer Academic Publishers.

Nowicka, B., & Kruk, J. (2010). Occurrence, biosynthesis and function of isoprenoid quinones. *Biochimica et Biophysica Acta (BBA)-Bioenergetics, 1797*(9), 1587-1605.

O'Toole, G., Kaplan, H. B., & Kolter, R. (2000). Biofilm formation as microbial development. *Annual Reviews in Microbiology, 54*(1), 49-79.

Okano, T., Shimomura, Y., Yamane, M., Suhara, Y., Kamao, M., Sugiura, M., & Nakagawa, K. (2008). Conversion of Phylloquinone (Vitamin K1) into Menaquinone-4 (Vitamin K2) in mice two possible routes for menaquinone-4 accumulation in cerebra of mice. *Journal of Biological Chemistry*, *283*(17), 11270-11279.

Pandey, A. (2003). Solid-state fermentation. *Biochemical Engineering Journal, 13*(2), 81-84.

Pennock, J. F. (1966). Occurence of Vitamins K and Related Quinones. In R. Harris, I. G. Wool, J. A. Loraine, G. F. Marrian & K. V. Thimann (Eds.), *Vitamins and Hormones* (Vol. 24, pp. 307-330). New York: Elsevier.

Pianetti, A., Battistelli, M., Citterio, B., Parlani, C., Falcieri, E., & Bruscolini, F. (2009). Morphological changes of *Aeromonas hydrophila* in response to osmotic stress. *Micron, 40*(4), 426-433.

Picioreanu, C., Van Loosdrecht, M. C., & Heijnen, J. J. (2001). Two-dimensional model of biofilm detachment caused by internal stress from liquid flow. *Biotechnology & Bioengineering, 72*(2), 205-218.

Postgate, J. R., & Hunter, J. R. (1962). The survival of starved bacteria. *Microbiology*, *29*(2), 233-263.

Ramteke, C., Ketan Sarangi, B., Chakrabarti, T., Mudliar, S., Satpute, D., & Avatar Pandey, R. (2010). Synthesis and broad spectrum antibacterial activity of magnetite ferrofluid. *Current Nanoscience, 6*(6), 587-591.

Ranmadugala, D., Ebrahiminezhad, A., Manley-Harris, M., Ghasemi, Y., & Berenjian, A. (2017a). The effect of iron oxide nanoparticles on *Bacillus subtilis* biofilm, growth and viability. *Process Biochemistry, 62*, 231-240.

Ranmadugala, D., Ebrahiminezhad, A., Manley-Harris, M., Ghasemi, Y., & Berenjian, A. (2017b). Impact of 3–Aminopropyltriethoxysilane-Coated Iron Oxide Nanoparticles on Menaquinone-7 Production Using *B. subtilis*. *Nanomaterials, 7*(11), http://dx.doi.org/10.3390/nano7110350.

Ranmadugala, D., Ebrahiminezhad, A., Manley-Harris, M., Ghasemi, Y., & Berenjian, A. (2017c). Iron oxide nanoparticles in modern microbiology and biotechnology. *Critical Reviews in Microbiology, 43*(4), 493-507.

Reddy, L. H., Arias, J. L., Nicolas, J., & Couvreur, P. (2012). Magnetic nanoparticles: design and characterization, toxicity and biocompatibility, pharmaceutical and biomedical applications. *Chemical Reviews, 112*(11), 5818-5878.

Reidy, B., Haase, A., Luch, A., Dawson, K. A., & Lynch, I. (2013). Mechanisms of silver nanoparticle release, transformation and toxicity: a critical review of current knowledge and recommendations for future studies and applications. *Materials, 6*(6), 2295-2350.

Rijnaarts, H. H., Norde, W., Bouwer, E. J., Lyklema, J., & Zehnder, A. J. (1995). Reversibility and mechanism of bacterial adhesion. *Colloids and Surfaces B: Biointerfaces, 4*(1), 5-22.

Robertson, M., Hapca, S. M., Moshynets, O., & Spiers, A. J. (2013). Air–liquid interface biofilm formation by psychrotrophic pseudomonads recovered from spoilt meat. *Antonie Van Leeuwenhoek, 103*(1), 251-259.

Saddler, G., Goodfellow, M., Minnikin, D., & O'Donnell, A. (1986). Influence of the growth cycle on the fatty acid and menaquinone composition of *Streptomyces cyaneus* NCIB 9616. *Journal of Applied Microbiology, 60*(1), 51-56.

Sakano, T., Notsumoto, S., Nagaoka, T., Morimoto, A., Fujimoto, K., Masuda, S., Suzuki, Y., & Hirauchi, K. (1988). Measurement of K vitamins in food by high-performance liquid chromatography with fluorometric detection. *Vitamins 62*(8), 393-398.

Saleh, N. B., Chambers, B., Aich, N., Plazas-Tuttle, J., Phung-Ngoc, H. N., & Kirisits, M. J. (2015). Mechanistic Lessons Learned from Studies of Planktonic Bacteria with Metallic Nanomaterials: Implications for Interactions between Nanomaterials and Biofilm Bacteria. *Frontiers in Microbiology, 6*(Article ID 677), http://dx.doi.org/10.3389/fmicb.2015.00677.

Santoyo Salazar, J., Perez, L., de Abril, O., Truong Phuoc, L., Ihiawakrim, D., Vazquez, M., Greneche, J.-M., Begin-Colin, S., & Pourroy, G. (2011). Magnetic iron oxide nanoparticles in 10− 40 nm range: Composition in terms of magnetite/maghemite ratio and effect on the magnetic properties. *Chemistry of Materials, 23*(6), 1379-1386.

Santra, S., Tapec, R., Theodoropoulou, N., Dobson, J., Hebard, A., & Tan, W. (2001). Synthesis and characterization of silica-coated iron oxide nanoparticles in microemulsion: the effect of nonionic surfactants. *Langmuir, 17*(10), 2900-2906.

Sardessai, Y. N., & Bhosle, S. (2004). Industrial potential of organic solvent tolerant bacteria. *Biotechnology Progress, 20*(3), 655-660.

Sathyanarayanan, M. B., Balachandranath, R., Genji Srinivasulu, Y., Kannaiyan, S. K., & Subbiahdoss, G. (2013). The effect of gold and iron-oxide nanoparticles on biofilm-forming pathogens. *ISRN Microbiology, 2013*(Article ID 272086), http://dx.doi.org/10.1155/2013/272086.

Sato, T., Iijima, T., Seki, M., & Inagaki, N. (1987). Magnetic properties of ultrafine ferrite particles. *Journal of Magnetism and Magnetic Materials, 65*(2-3), 252-256.

Sato, T., Yamada, Y., Ohtani, Y., Mitsui, N., Murasawa, H., & Araki, S. (2001a). Efficient production of menaquinone (vitamin K2) by a menadione-resistant mutant of *Bacillus subtilis*. *Journal of Industrial Microbiology and Biotechnology, 26*(3), 115-120.

Sato, T., Yamada, Y., Ohtani, Y., Mitsui, N., Murasawa, H., & Araki, S. (2001b). Production of menaquinone (vitamin K 2)-7 by *Bacillus subtilis*. *Journal of Bioscience and Bioengineering, 91*(1), 16-20.

Sauer, T., & Galinski, E. A. (1998). Bacterial milking: a novel bioprocess for production of compatible solutes. *Biotechnology and Bioengineering, 57*(3), 306-313.

Schurgers, L. J., Teunissen, K. J., Hamulyák, K., Knapen, M. H., Vik, H., & Vermeer, C. (2007). Vitamin K–containing dietary supplements: comparison of synthetic vitamin K1 and natto-derived menaquinone-7. *Blood, 109*(8), 3279-3283.

Schurgers, L. J., & Vermeer, C. (2000). Determination of phylloquinone and menaquinones in food. *Pathophysiology of Haemostasis and Thrombosis, 30*(6), 298-307.

Scott, J. R., & Barnett, T. C. (2006). Surface proteins of gram-positive bacteria and how they get there. *Annual Review of Microbiology, 60*, 397-423.

Selvakumar, R., Aravindh, S., Ashok, A. M., & Balachandran, Y. L. (2014). A facile synthesis of silver nanoparticle with SERS and antimicrobial activity using *Bacillus subtilis* exopolysaccharides. *Journal of Experimental Nanoscience, 9*(10), 1075-1087.

Shabir, G. A. (2005). Step-by-step analytical methods validation and protocol in the quality system compliance industry. *Journal of validation technology, 10*, 314-325.

Shea, M. K., & Holden, R. M. (2012). Vitamin K status and vascular calcification: evidence from observational and clinical studies. *Advances in Nutrition, 3*(2), 158-165.

Shearer, M. J., & Newman, P. (2008). Metabolism and cell biology of vitamin K. *Thrombosis and Haemostasis, 100*(4), 530-547.

Shen, X.-C., Fang, X.-Z., Zhou, Y.-H., & Liang, H. (2004). Synthesis and characterization of 3-aminopropyltriethoxysilane-modified superparamagnetic magnetite nanoparticles. *Chemistry Letters, 33*(11), 1468-1469.

Shi, J., Zhou, S., Kang, L., Ling, H., Chen, J., Duan, L., Song, Y., & Deng, Y. (2018). Evaluation of the antitumor effects of vitamin K2 (menaquinone-7) nanoemulsions modified with sialic acid-cholesterol conjugate. *Drug Delivery and Translational Research, 8*(1), 1-11.

Shino, M. (1988). Determination of endogenous vitamin K (phylloquinone and menaquinone-n) in plasma by high-performance liquid chromatography using platinum oxide catalyst reduction and fluorescence detection. *Analyst, 113*(3), 393-397.

Shiraki, M., Shiraki, Y., Aoki, C., & Miura, M. (2000). Vitamin K2 (menatetrenone) effectively prevents fractures and sustains lumbar bone mineral density in osteoporosis. *Journal of Bone and Mineral Research, 15*(3), 515-521.

Si, S., Kotal, A., Mandal, T. K., Giri, S., Nakamura, H., & Kohara, T. (2004). Size-controlled synthesis of magnetite nanoparticles in the presence of polyelectrolytes. *Chemistry of Materials, 16*(18), 3489-3496.

Sies, H., & Menck, C. F. (1992). Singlet oxygen induced DNA damage. *Mutation Research, 275*(3-6), 367-375.

Simões, M., Simoes, L. C., & Vieira, M. J. (2010). A review of current and emergent biofilm control strategies. *LWT-Food Science and Technology, 43*(4), 573-583.

Singh, N., Jenkins, G. S., Asadi, R., & Doak, S. (2010). Potential toxicity of superparamagnetic iron oxide nanoparticles (SPION). *Nano Reviews, 1*(1), https://doi.org/10.3402/nano.v1i0.5358.

Sirkar, K. K., Luo, R. G., Xu, Y., & Dai, X.-P. (2006). Patent No. US 6,986,847 B2. Method and apparatus for isolation and purification of biomolecules.

Sodipo, B. K., & Aziz, A. A. (2014). A sonochemical approach to the direct surface functionalization of superparamagnetic iron oxide nanoparticles with (3-aminopropyl) triethoxysilane. *Beilstein Journal of Nanotechnology, 5*(1), 1472-1476.

Sommer, P., & Kofler, M. (1967). Physicochemical properties and methods of analysis of phylloquinones, menaquinones, ubiquinones, plastoquinones, menadione, and related compounds. *Vitamins and Hormones, 24*, 349-399.

Song, J., Liu, H., Wang, L., Dai, J., Liu, Y., Liu, H., Zhao, G., Wang, P., & Zheng, Z. (2014). Enhanced Production of Vitamin K2 from *Bacillus subtilis* (*natto*) by Mutation and Optimization of the Fermentation Medium. *Brazilian Archives of Biology and Technology, 57*(4), 606-612.

Spormann, A. M. (2008). Physiology of Microbes in Biofilms. In T. Romeo (Ed.), *Bacterial Biofilms* (pp. 17-36). Berlin, Heidelberg: Springer Berlin Heidelberg.

Stanbury, P. F., Whitaker, A., & Hall, S. J. (2013). *Principles of Fermentation Technology*. Elsevier.

Stankiewicz, A. I., & Moulijn, J. A. (2000). Process intensification: transforming chemical engineering. *Chemical Engineering Progress, 96*(1), 22-34.

Stanley, N. R., & Lazazzera, B. A. (2005). Defining the genetic differences between wild and domestic strains of *Bacillus subtilis* that affect poly - γ - DL - glutamic acid production and biofilm formation. *Molecular Microbiology, 57*(4), 1143-1158.

Stewart, P. S., & Franklin, M. J. (2008). Physiological heterogeneity in biofilms. *Nature Reviews Microbiology, 6*(3), 199-210.

Subbiahdoss, G., Sharifi, S., Grijpma, D. W., Laurent, S., van der Mei, H. C., Mahmoudi, M., & Busscher, H. J. (2012). Magnetic targeting of surface-modified superparamagnetic iron oxide nanoparticles yields antibacterial efficacy against biofilms of gentamicin-resistant *staphylococci*. *Acta Biomaterialia, 8*(6), 2047-2055.

Suganeswari, M. (2011). Nano particles: a novel system in current century. *international Journal of Pharmaceutical & Biological Archive, 2*(3), 847-854.

Sumi, H. (2004a). Patent No. US6677141B2. Edible compositions of *Bacillus subtilis natto* cells containing water-soluble vitamin K.

Sumi, H. (2004b). Patent No. US6, 677,143 B2. Method for culturing *Bacillus subtilis natto* to produce water-soluble vitamin K and food product, beverage, or feed containing the cultured microorganism or the vitamin K derivative.

Sundar, S., Mariappan, R., & Piraman, S. (2014). Synthesis and characterization of amine modified magnetite nanoparticles as carriers of curcumin-anticancer drug. *Powder Technology, 266*, 321-328.

Sutherland, I. W. (1990). *Biotechnology of Microbial Exopolysaccharides*. Cambridge Studies in Biotechnology 9. Cambridge, UK: Cambridge University Press.

Sutherland, I. W. (2001). Biofilm exopolysaccharides: a strong and sticky framework. *Microbiology, 147*(1), 3-9.

Suttie, J. (1995). The importance of menaquinones in human nutrition. *Annual Review of Nutrition, 15*(1), 399-417.

Suttie, J., & Nelsestuen, G. L. (1980). Mechanism Of Action Of Vitamin K: Synthesis Of γ-Carboxyglutamic Acid. *CRC Critical Reviews in Biochemistry, 8*(2), 191-223.

Suttie, J. W. (1978). The Fat-Soluble Vitamins. In H. F. DeLuca (Ed.), *Handbook of Lipid Research 2* (pp. 211-265). New York and London: Plenum Publishing Corporation.

Taber, H. W., Dellers, E. A., & Lombardo, L. R. (1981). Menaquinone biosynthesis in *Bacillus subtilis*: isolation of men mutants and evidence for clustering of men genes. *Journal of Bacteriology, 145*(1), 321-327.

Taguchi, H., Kita, S., & Tani, Y. (1991). Enzymatic alteration in the shikimate pathway during derivation of menaquinone-4-producing mutants of *Flavobacterium* sp. 238-7. *Agricultural and Biological Chemistry, 55*(3), 769-773.

Takenaka, S., Karg, E., Roth, C., Schulz, H., Ziesenis, A., Heinzmann, U., Schramel, P., & Heyder, J. (2001). Pulmonary and systemic distribution of inhaled ultrafine silver particles in rats. *Environmental Health Perspectives, 109*(Suppl 4), 547-551.

Tawaba, J.-C. B. (2015). *Design of a single-species biofilm reactor based on metal structured packing for the production of high added value biomolecules.* PhD thesis, University of Liège, Belgium.

Taylor, E. N., & Webster, T. J. (2009). The use of superparamagnetic nanoparticles for prosthetic biofilm prevention. *International Journal of Nanomedicine, 4*, 145-152.

Thukkaram, M., Sitaram, S., & Subbiahdoss, G. (2014). Antibacterial efficacy of iron-oxide nanoparticles against biofilms on different biomaterial surfaces. *International Journal of Biomaterials, 2014*(Article ID 716080), http://dx.doi.org/10.1155/2014/716080.

Tian, L., Chen, X. D., Yang, Q. P., Chen, J. C., Shi, L., & Li, Q. (2012). Effect of calcium ions on the evolution of biofouling by *Bacillus subtilis* in plate heat exchangers simulating the heat pump system used with treated sewage in the 2008 Olympic Village. *Colloids and Surfaces B: Biointerfaces, 94*, 309-316.

Tiberto, P., Barrera, G., Celegato, F., Coïsson, M., Chiolerio, A., Martino, P., Pandolfi, P., & Allia, P. (2013). Magnetic properties of jet-printer inks containing dispersed magnetite nanoparticles. *The European Physical Journal B, 86*(4), 1-6.

Tindall, B., Stetter, K., & Collins, M. (1989). A novel, fully saturated menaquinone from the thermophilic, sulphate-reducing archaebacterium *Archaeoglobus fulgidus*. *Microbiology, 135*(3), 693-696.

Tiraferri, A., Chen, K. L., Sethi, R., & Elimelech, M. (2008). Reduced aggregation and sedimentation of zero-valent iron nanoparticles in the presence of guar gum. *Journal of Colloid and Interface Science, 324*(1), 71-79.

Tsukamoto, Y., Ichise, H., Kakuda, H., & Yamaguchi, M. (2000). Intake of fermented soybean (natto) increases circulating vitamin K2 (menaquinone-

7) and γ-carboxylated osteocalcin concentration in normal individuals. *Journal of Bone and Mineral Metabolism, 18*(4), 216-222.

Tsukamoto, Y., Kasai, M., & Kakuda, H. (2001). Construction of a *Bacillus subtilis* (*natto*) with high productivity of vitamin K2 (menaquinone-7) by analog resistance. *Bioscience, Biotechnology, and Biochemistry, 65*(9), 2007-2015.

Turakhia, M., Cooksey, K., & Characklis, W. (1983). Influence of a calcium-specific chelant on biofilm removal. *Applied and Environmental Microbiology, 46*(5), 1236-1238.

Vaghari, H., Eskandari, M., Sobhani, V., Berenjian, A., Song, Y., & Jafarizadeh-Malmiri, H. (2015). Process intensification for production and recovery of biological products. *American Journal of Biochemistry and Biotechnology, 11*(1), 37.

Valentine, R., & Bradfield, J. (1954). The urea method for bacterial viability counts with the electron microscope and its relation to other viability counting methods. *Microbiology, 11*(3), 349-357.

Verger, R., Rietsch, J., Pattus, F., Ferato, F., Pieroni, G., De Hass, G. H., & Desnuelle, P. (1978). Studies of lipase and phospholipase A2 acting on lipid monolayers. In S. Gatt, L. Freysz & P. Mandel (Eds.), *Enzymes of Lipid Metabolism - Advances in Experimental Medicine and Biology* (Vol. 101, pp. 79-94). New York: Plenum Press.

Vermeer, C. (1990). Gamma-carboxyglutamate-containing proteins and the vitamin K-dependent carboxylase. *Biochemical Journal, 266*(3), 625-636.

Vermeer, C., & Schurgers, L. J. (2000). A comprehensive review of vitamin K and vitamin K antagonists. *Hematology/Oncology Clinics of North America, 14*(2), 339-353.

Walther, B., Karl, J. P., Booth, S. L., & Boyaval, P. (2013). Menaquinones, bacteria, and the food supply: the relevance of dairy and fermented food products to vitamin K requirements. *Advances in Nutrition: An International Review Journal, 4*(4), 463-473.

Wang, L., Cole, M., Li, J., Zheng, Y., Chen, Y. P., Miller, K. P., Decho, A. W., & Benicewicz, B. C. (2015). Polymer grafted recyclable magnetic nanoparticles. *Polymer Chemistry, 6*(2), 248-255.

Watanuki, M., & Aida, K. (1972). Significance of quinones in the classification of bacteria. *The Journal of General and Applied Microbiology, 18*(6), 469-472.

Waychunas, G. A., Kim, C. S., & Banfield, J. F. (2005). Nanoparticulate iron oxide minerals in soils and sediments: unique properties and contaminant scavenging mechanisms. *Journal of Nanoparticle Research, 7*(4-5), 409-433.

Weinstein, J. S., Varallyay, C. G., Dosa, E., Gahramanov, S., Hamilton, B., Rooney, W. D., Muldoon, L. L., & Neuwelt, E. A. (2010).

Superparamagnetic iron oxide nanoparticles: diagnostic magnetic resonance imaging and potential therapeutic applications in neurooncology and central nervous system inflammatory pathologies, a review. *Journal of Cerebral Blood Flow & Metabolism, 30*(1), 15-35.

Welo, L. A., & Baudisch, O. (1925). XXXIX. The two-staye transformation of magnetite into hematite. *The London, Edinburgh, and Dublin Philosophical Magazine and Journal of Science, 50*(296), 399-408.

Wiesner, M. R., Lowry, G. V., Casman, E., Bertsch, P. M., Matson, C. W., Di Giulio, R. T., Liu, J., & Hochella Jr, M. F. (2011). Meditations on the ubiquity and mutability of nano-sized materials in the environment. *Acs Nano, 5*(11), 8466-8470.

Wohlgemuth, R. (2009). The locks and keys to industrial biotechnology. *New Biotechnology, 25*(4), 204-213.

Wu, W., He, Q., & Jiang, C. (2008). Magnetic Iron Oxide Nanoparticles: Synthesis and Surface Functionalization Strategies. *Nanoscale Research Letters, 3*(11), 397-415.

Yamaguchi, M., Kakuda, H., Gao, Y. H., & Tsukamoto, Y. (2000). Prolonged intake of fermented soybean (natto) diets containing vitamin K2 (menaquinone-7) prevents bone loss in ovariectomized rats. *Journal of Bone and Mineral Metabolism, 18*(2), 71-76.

Żur, J., Wojcieszyńska, D., & Guzik, U. (2016). Metabolic Responses of Bacterial Cells to Immobilization. *Molecules, 21*(Article ID 21070958), http://dx.doi.org/10.3390/molecules21070958.